JOHANNES GUTENBERG UNIVERSITÄT MAINZ

JG|U

Build and release of molecular strain as a tool in organic synthesis

Dissertation
for the degree of "Doctor of Natural Sciences"
in the doctoral subject chemistry

at the Faculty of Chemistry, Pharmaceutical Sciences,
Geography and Geosciences
of the Johannes Gutenberg University Mainz

Henning Maag
[redacted]

Mainz, October 2024

1. Examiner: [redacted]

2. Examiner: [redacted]

Day of the oral exam: [redacted]

Acknowledgements

[redacted]

[redacted]

Table of contents

Summary

Over the course of this work, the build and release of molecular strain was used as a tool in organic synthesis.

In the first research project, a proof-of-concept for the synthesis of *O*-heterocycles from photochemically generated strained intermediates was provided. *α*-Aminoacetophenones were identified as a versatile platform for the systematic investigation of the light-driven Norrish-Yang cyclisation. The influence of protecting groups on the heteroatom and the influence of sterically demanding substituents on the success of the cyclisation were investigated. Consecutively, the synthesis of several 3-azetidinols and a 3-oxetanol was demonstrated. Use of an electron-deficient trifluoroacetophenone enabled the formation of stable hemi ketals from the synthesised heterocycles. The increased acidity of the formed hemi ketals enabled the ring-opening reaction of 3-azetidinols towards dioxolanes without the need for external activation. Transformation of 3-oxetanols into dioxolanes was efficiently realised in a cobalt catalysed dynamic kinetic resolution, providing high degrees of diastereo- and enantioselectivity.

During the second research project, the build and release of molecular strain was used not for the generation of molecular complexity, but for the storage of light energy in chemical bonds. The previous investigation of the Norrish-Yang cyclisation inspired the use of structurally rigid systems, which resulted in the development of an isomer pair *ortho*-methylacetophenone ⇄ benzocyclobutenol. A unique beneficial effect of a trifluoromethyl group on the photocyclisation was asserted and the mechanism of the transformation was elucidated. The overall robustness of the reaction was confirmed, merely a detrimental influence of oxygen onto the reaction was found. All formed side and degradation products were unambiguously identified. Comparison of several previously unknown benzocyclobutenols resulted in the emergence of an isomer-pair with several benefits compared to literature known reference systems for the chemical storage of light energy. By addition of catalytic amounts of organic base, the stored energy was found to be releasable under ambient conditions and an immobilised base was utilised to showcase the cyclability of the system. Finally, the successful charging of the system with solar light was demonstrated, underlining its applicability.

Zusammenfassung

Im Rahmen der vorliegenden Arbeit wurden der Auf- und Abbau von Ringspannung als Werkzeug der Organischen Chemie gezeigt.
Im Laufe des ersten Projektes wurde die Realisierbarkeit der Synthese von *O*-Heterozyklen ausgehend von photochemisch erzeugten gespannten Ringen bewiesen. α-Aminoacetophenone wurden als eine vielseitige Plattform für eine systematische Untersuchung der photochemischen Norrish-Yang Zyklisierung identifiziert. Der Einfluss der Schutzgruppe am Heteroatom sowie der Einfluss sterisch anspruchsvoller Reste auf den Erfolg der Zyklisierung wurden untersucht. Anschließend konnte die Synthese einiger 3-Azetidinole und eines 3-Oxetanols gezeigt werden. Unter Reaktion mit einem elektronenarmen Trifluoroacetophenon wurden stabile Halbketale aus den hergestellten Heterozyklen gebildet. Eine erhöhte Azidität der Halbketale erlaubte eine unkatalysierte Ringöffnung von 3-Azetidinolen zu Dioxolanen, während 3-Oxetanole unter Cobaltkatalyse in einer dynamischen kinetischen Racematspaltung mit hoher Diastereo- und Enantioselektivität zu Dioxolanen umgesetzt werden konnten.
Im Laufe des zweiten Projektes konnte der Auf- und Abbau von Ringspannung nicht wie zuvor zur Erzeugung von molekularer Komplexität, sondern zur Speicherung von Lichtenergie in chemischen Bindungen genutzt werden. Die vorhergehende Untersuchung der Norrish-Yang Zyklisierung inspirierte die Nutzung starrerer molekularer Strukturen und das Isomerenpaar *ortho*-Methylacetophenon ⇄ Benzocyclobutenol wurde entwickelt. Ein einzigartiger, positiver Effekt einer Trifluoromethylgruppe auf die Zyklisierung wurde erörtert. Die generelle Robustheit der Reaktion konnte gezeigt werden, jedoch wurde ebenso ein negativer Effekt der Sauerstoffkonzentration auf den Erfolg der Reaktion deutlich. Alle gebildeten Neben- und Zerfallsprodukte konnten eindeutig identifiziert werden. Der Vergleich mehrerer zuvor unbekannter Benzocyclobutenole stellte ein Isomerenpaar heraus, welches einige Vorteile im Vergleich zu bekannten Literatursystem zur chemischen Speicherung von Lichtenergie bietet. Unter Zugabe katalytischer Mengen organischer Base erfolgte die kontrollierte Freisetzung der gespeicherten Energie und eine immobilisierte Base konnte benutzt werden, um die Zyklisierbarkeit des Systems zu zeigen. Zuletzt konnte das Aufladen des Systems mit Sonnenlicht demonstriert werden, wodurch eine tatsächliche Anwendbarkeit untermauert werden konnte.

Publications

Parts of this work have been published in peer reviewed journals:

- Dynamic kinetic resolution of transient hemiketals: a strategy for the desymmetrisation of prochiral oxetanols
  A. Sandvoß,* H. Maag, C. G. Daniliuc, D. Schollmeyer, J. M. Wahl,*
  Chem. Sci. **2022**, *13*, 6297-6302.
  *Corresponding Authors
- Ring Opening of Photogenerated Azetidinols as a Strategy for the Synthesis of Aminodioxolanes
  H. Maag, D. J. Lemcke, J. M. Wahl, *
  Beilstein J. Org. Chem. **2024,** *20*, 1671-1676.
  *Corresponding Author

Poster presentations

Parts of this work have been presented at the following scientific conferences/workshops:

- Thinking out of the ring. Present and future of small cyclic compounds; Lorentz Center Leiden, The Netherlands; 05/2024
  Ring-opening of Photogenerated Azetidinols as a Strategy for the Synthesis of Amino-dioxolanes
  H. Maag, D. J. Lemcke, J. M. Wahl.
- ORCHEM 2022 – 22nd Lecture Conference; Münster, Germany; 09/2022
  Dynamic Kinetic Resolution of Transient Hemiketals: A Strategy for the Desymmetrisation of Prochiral Oxetanols
  A. Sandvoß, H. Maag, C. G. Daniliuc, D. Schollmeyer, J. M. Wahl.

Declaration oft the work of others included herein

Over the course of the research projects entailed in this thesis, other individuals contributed to the work described herein. Below, a detailed overview of the contributions of each collaborator can be found.

Contributions to the first research project (*cf.* chapter 2) were made by [redacted], [redacted] and [redacted]. [redacted] prepared the azetidinol **2.69**, which was further purified as part of this work. [redacted] synthesised the starting materials for the envisioned synthesis of azetidinols **2.78**, **2.79** and **2.80** (acetophenone **2.123**). [redacted] helped in the purification of hydrate **2.51** and synthesised the oxetanol **2.61**, which was used in the synthesis of dioxolane **2.106**. As part of his own work, [redacted] contributed to the ring-opening of 3-oxetanols (*cf.* chapter 2.5). He identified the electron deficient ketone **2.52** as a source of stable hemi ketals. Furthermore, he identified *Katsuki* type Co^{II}·salen complexes as suitable catalysts for the transformation of 3-oxetanols to 1,3-dioxolanes. An excerpt of his optimisation is shown in Table 2. Further contributions by [redacted] included the initial scope of the reaction, which consisted of sp^2 substituted cyclobutanols and includes the synthesis of dioxolanes **2.113** and **2.115**. At last, the mechanistic proposal for the mechanism of the investigated transformation was provided by [redacted].

In the second research project, [redacted] contributed to the synthesis and characterisation of tricycle **3.46** (*cf.* chapter 3.4.3). [redacted] performed the set-up of the second robustness screening, while the development of the experiment and the analysis of the data was part of this work. Additionally, an experiment in the determination of the thermal half-life was conducted by [redacted] at 503.15 K (*cf.* chapter 3.6.1). Furthermore, [redacted] contributed to the mechanistic investigation by measuring the quantum yield for the transformation of acetophenone **3.8** to benzocyclobutenol **3.26** at different temperatures and all UV-spectra were measured in collaboration with him. The X-ray measurement and structure refinement of samples from the molecules **3.26**, **3.28**, **3.30, 3.42** and **3.46** was performed by [redacted].

Index of abbreviations

Ad	adamantyl
Ar	aryl
atm.	atmosphere
BINOL	1,1′-bi-2-naph-thol
BTPP	*tert*-butylimino-tri(pyrrolidino)phosphorane
Bzh	benzhydryl
cod	cycloocta-1,5-diene
CW	cool-white
CyH	cyclohexane
DBU	1,8-diazabicyclo(5.4.0)undec-7-ene
DKR	dynamic kinetic resolution
DMA	*N*,*N*-dimethylacetamide
DMF	*N*,*N*-dimethylformamide
dr	diastereomeric ratio
DSC	dynamic scanning calorimetry
E-azo	*E*-azobenzene
EC	electrocyclisation
EDG	electron donating group
ELN	electronic lab notebook
eq.	equivalents
er	enantiomeric ratio
EtOAc	ethyl acetate
EWG	*elec*tron withdrawing group
FC	flash chromatography
GP	general procedure
HAT	hydrogen atom transfer
HFIP	1,1,1,3,3,3-hexafluoroisopropanol
HRMS	high resolution mass spectrometry
I	Intensity
IR	infrared
ISC	intersystem crossing
LG	leaving group
m.p.	melting point
MOST	molecular solar thermal
Ms	methanesulfonyl, mesyl
NBD	norbornadiene
N-Me-TBD	7-methyl-1,5,7-triazabicyclo[4.4.0]dec-5-ene
NMR	nuclear magnetic resonance
NOESY	nuclear *Overhauser* effect spectroscopy
Nph	naphthyl, naphthyl
OTf	trifluoromethanesulfonate
Piv	pivalate
ppm	parts per million
PS-TBD	polystyrene supported TBD
QC	quadricyclane
RP-MPLC	reversed phase medium pressure liquid chromatography
rt	room temperature

T	temperature
TBD	1,5,7-triazabicyclo[4.4.0]dec-5-ene
TPP	tetraphenylporphyrin
Ts	tosyl
UV	ultraviolet
vis	visible
Z-azo	*Z*-azobenzene

1 Introduction

Photochemical processes on earth precede organic life itself.[1] Once developed, life adapted to a strong constant irradiation with energetic light, ultimately learning to harness its power.[2] Plants emerged over the millennia, tirelessly combining the simplest building blocks CO_2 and water into complex natural scaffolds and oxygen, thus enabling the formation of higher life.[3] From a chemists perspective, photosynthesis is a generally inefficient process, with an overall efficiency of 0.2–0.3% in nature.[4] Yet, photosynthesis achieves the conversion of light energy into chemical energy.

As *Ciamician* wisely pointed out in his visionary speech "The Photochemistry of the Future" in 1912, chemists needs to unravel and conquer the photochemical processes of nature.[5] Each hour, the sun delivers an amount of energy to the earths surface, that satisfies humanities demand for a whole year.[6] According to *Ciamician*, developments were made in the artificial photosynthesis, copying natures strategy to incorporate the energy into chemical bonds.[7] Evidently, efficient processes for the storage of the light energy need to be further improved. Nonetheless, the subsequent access to this stored chemical energy apart from combustion remains an additional challenge. Hence, chemists continue to search for alternative substances with high chemical energy. An exceedingly elegant way to overcome both challenges at once would be the realisation of a photochemical build and release approach, which builds up highly energetic strained molecules and uses them for subsequent transformations.

1.1 Build and release of molecular strain

Molecular strain can be viewed as energy storage within chemical bonds, providing spring-loaded precursors for the realisation of chemical transformations.[8] In this regard, the release of molecular strain is becoming more relevant as a facile tool for driving chemical reactions and generating molecular complexity.[9] Harnessing the intrinsic high reactivity of strained molecules has allowed chemists to broaden chemical space and equipped medicinal chemists with powerful tools for elaborate late-stage functionalisation.[10] The increased energy of small saturated carbocycles compared to their linear analogues can be partially explained by deviations of the bond-angles from the optimal 109.5° of a sp^3 centre, a fact already

recognised by *Baeyer* in 1885.[11] The aforementioned effect increases with decreasing ring size from cyclohexane to cyclopropane. Generally, an increase in strain energy is observed in that row, which is not only reasoned by said *Baeyer* strain but also by further contribution from torsional strain in the *C–C–C–C* bond angles (*Pitzer* strain).[12] Including bi- and tricyclic compounds, this trend is culminating in [1.1.1]propellane **1.1**, where the bridgehead carbons are actually inverted in their geometry. The connection of three small rings forces all four bonds of the bridgehead carbons to point towards the same direction, which in turn increases the strain energy contained in this molecule (Figure 1).[13] Interestingly, when medium and larger ring systems are considered, transannular nonbonding interactions are becoming noticeably relevant, thus introducing strain to the molecule (*Prelog* strain).[12]

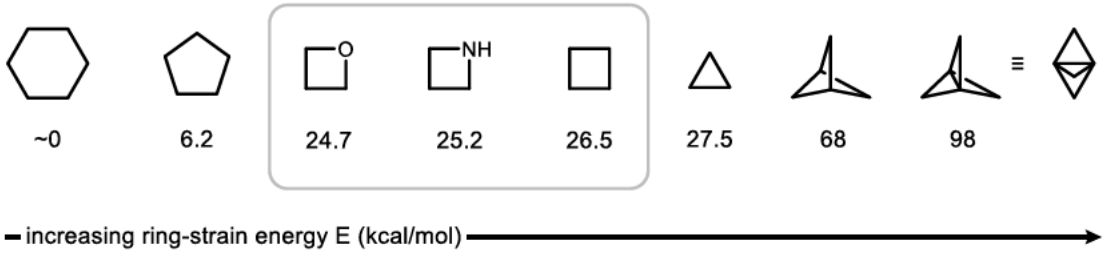

Figure 1: Strain energies for selected cycloalkanes and heterocycles in kcal/mol.[14]

Accessing increasingly strained structures often necessitates the use of harsh reaction conditions.[15] At the same time, the obtained molecules feature a high thermodynamic driving force to relieve their intrinsic strain, challenging chemist with the appropriate storage and isolation already in the initial syntheses of such strained structures.[16]

Scheme 1: Spontaneous polymerisation of [1.1.1]propellane 1.1 towards staffane 1.2.[17]

This can be noticed in the spontaneous or radical induced polymerisation of [1.1.1]propellane **1.1** towards staffane **1.2** under release of its ring-strain energy.[17] All transformations that lead to a complete or partial release of strain energy through minimisation of the above-described components of ring-strain, are summarised as strain-release reactions while popular examples display ring-expansion or -opening reactions. No direct correlation exists between the amount of ring-strain energy and the observed reactivity of a compound in strain-release reaction, which is exemplified by comparing the reactivity of four- and three-

membered rings.[18] While cyclobutane, oxetane and azetidine possess a similar strain energy compared to their three-membered analogues, they are considerably more stable.[19] The discrepancy between ring-strain energy and the observed reactivity has been attributed to several effects, from electronic interactions (bonding interactions)[20] to the difference in overall release of *Baeyer* strain,[18] but no definite model for the prediction of reaction rates from strain energies is generally accepted, yet.[21]

Another approach to access the reactivity of highly energetic intermediates can be found in the use of photochemical methods. The precise delivery of photon energy enables endergonic transformations under mild conditions, converting light energy into chemical energy and storing it as ring strain in reactive intermediates ready for further functionalisation or transformation.[22] If combined appropriately with a subsequent reaction, such a 'build and release approach' provides products in unprecedented precision and efficiency, enabling the venture into previously unchartered chemical space (Scheme 2).

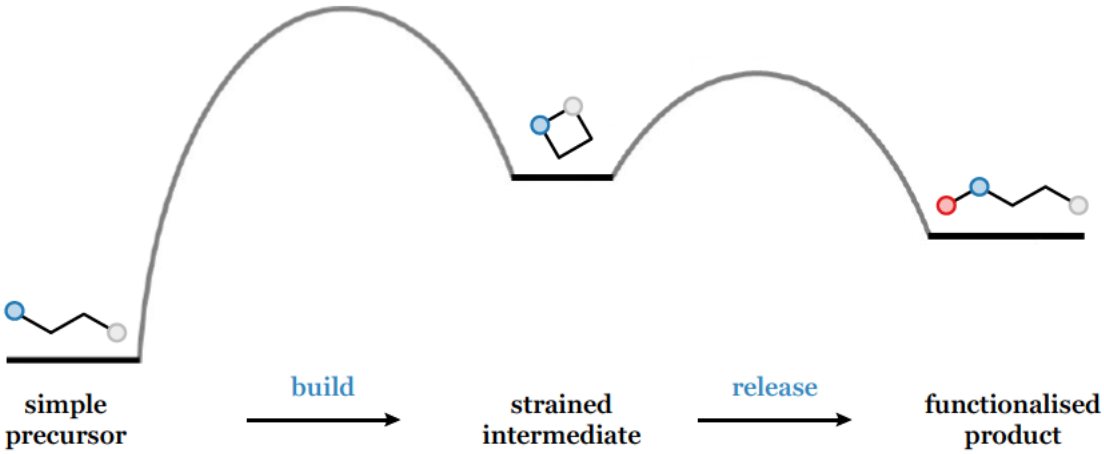

Scheme 2: Graphical representation of a build and release strategy.

However, both reactions must be balanced with great care with respect to the activation energy needed, and careful optimisation of the reaction conditions is often mandatory. An excellent example is the generation of the above-mentioned [1.1.1]propellane **1.1** and its subsequent transformation towards bicyclo[1.1.1]pentanes, which are prominent aryl isosteres.[23] The initial synthesis of **1.1** was first reported in 1982 by *Wiberg*,[24] but most modern approaches still rely on the synthesis strategy of *Szeimies* and coworkers from 1989.[25] They later developed a protocol for the rapid functionalisation of this archetypical strained intermediate (Scheme 3).[26]

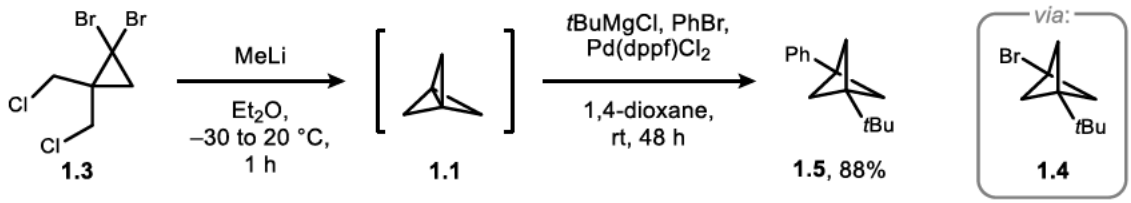

Scheme 3: Synthesis and functionalisation of [1.1.1]propellane by *Szeimies* and coworkers.[26]

Methyl lithium is added to the typical precursor **1.3**, which leads to lithium-halogen exchange and subsequent intramolecular nucleophilic substitution of both chlorine atoms to form **1.1**. The immensely strained nature of the tricyclic system prevents its isolation, nonetheless, storage of **1.1** is possible in ethereal solution at lower temperatures. After nucleophilic addition of a Grignard reagent, the resulting bromobicyclo[1.1.1]pentane **1.4** is cross-coupled with an aryl halide to give **1.5**. The reaction conditions in the first step remain harsh, yet *Baran* and coworkers were able to successfully demonstrate the synthesis of **1.1** in multigram scale.[10d] While the reactivity of [1.1.1]propellane and related multicyclic compounds sparked great interest over the recent years,[10a] monocyclic strained compounds are equally harnessed for chemical transformations.[16,27]

A prominent example is the stereospecific ring expansion from orthocylophane **1.6** to metacylophane **1.7** by *Murakami* and coworkers, [28] which is an overall endergonic and atom-economic[29] transformation. Here, the central benzocyclobutenol intermediate **1.8** is formed in an energetically uphill photocyclisation, and the relief of the ring strain energy fuels the rhodium catalysed ring expansion.

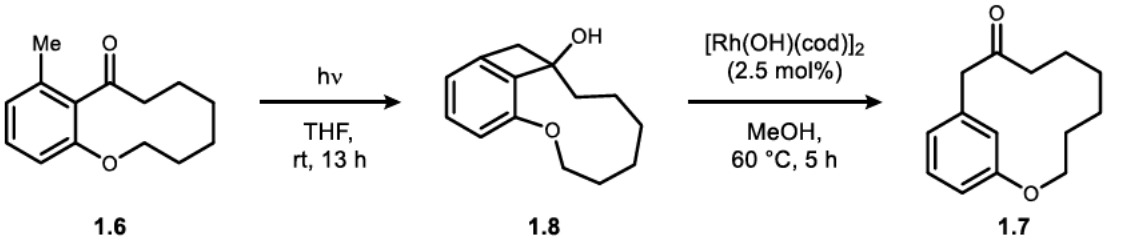

Scheme 4: Stereospecific ring expansion of a photochemically generated cyclobutanol by *Murakami* and coworkers.[28]

Another very recent example of the use of a 'build and release approach' was published by *Sandvoß* and *Wahl* in 2023 (Scheme 5).[30]

Sandvoß and *Wahl*, 2023:

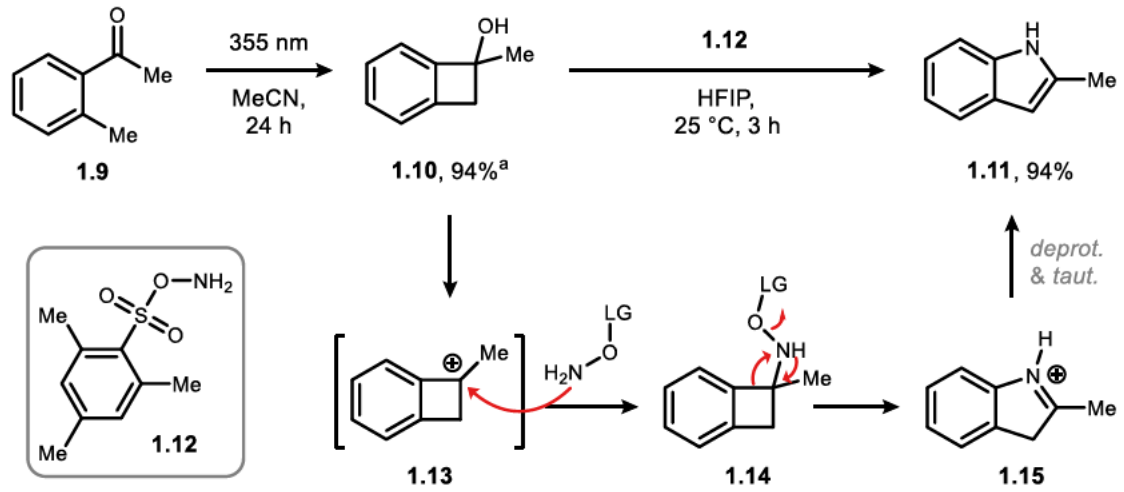

Scheme 5: Build and release strategy for the synthesis of 2-methylindole by *Sandvoß* and *Wahl*.[30] HFIP = 1,1,1,3,3,3-hexafluoroisopropanol, LG = leaving group. [a]Yield based on recovered starting material.

By irradiation of *ortho*-methylacetophenone **1.9**, a strained arylcylobutanol **1.10** was accessed, which was further functionalised in a nitrogen insertion reaction to yield indole **1.11** in 88% yield over two steps. The authors propose an activation of the substrate in presence of the fluorinated solvent, leading to a nucleophilic substitution of the alcohol with the amination reagent **1.12** *via* intermediate **1.13** to give the tetrahedral intermediate **1.14**. The tetrahedral intermediate subsequently rearranges to form **1.15**, which is deprotonated and tautomerises to form the stable indole **1.11**.

2 Construction and ring-opening of four-membered heterocycles

2.1 Introduction

2.1.1 Norrish-Yang cyclisation

Reliable photochemical reactions with a predictable outcome are essential for the realisation of a build and release strategy. The [2+2] cycloaddition reaction for the synthesis of cyclobutane[31] or the Paterno-Büchi reaction for the generation of oxetanes[32] are excellent examples for well-developed and frequently employed methods in the generation of four-membered rings. The photochemical synthesis of azetidines is less explored, although it has been known for 50 years *via* the Norrish-Yang cyclisation.

The Norrish-Yang cyclisation was discovered in 1958 by *Yang* and *Yang*, as an unusual side reaction of a Norrish type II reaction of ketones in solution.[33] Upon irradiation of 2-pentanone **2.1** in cyclohexane (CyH) with ultraviolet (UV) light, a mixture of cyclobutanol **2.2**, acetone **2.3** and ethene **2.4** was obtained (Figure 2, top).

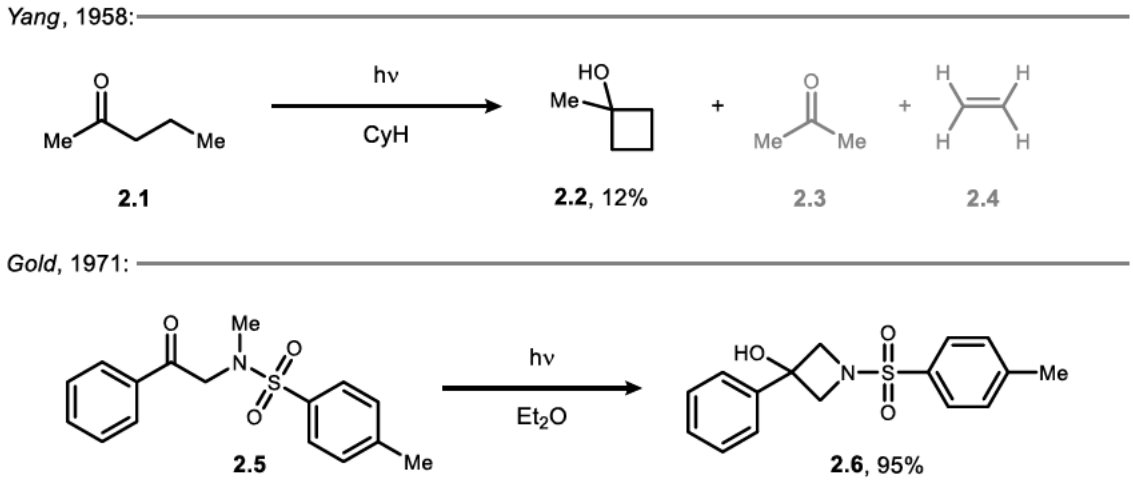

Figure 2: Top: Selected example of the initial experiments performed by *Yang*. Bottom: First example of the synthesis of an azetidine *via* Norrish-Yang cyclisation by *Gold*.

The first example of the formation of azetidines *via* Norrish-Yang cyclisation was published by *Gold* in 1971.[34] Irradiation of *N*-tosyl (Ts) protected *α*-aminoacetophenone **2.5** in ether, gave azetidinol **2.6** in impressive 95% yield without detection of the Norrish type II fragmentation product. Since then, several reports

deciphered the mechanism in detail, which will be briefly described in the following for an *α*-aminoketone **2.7** (Scheme 6).[35] Upon irradiation with visible light (vis), ketone **2.7** is excited to the first singlet state in an n-π* transition, from which intersystem crossing (ISC) occurs to the triplet state of molecule ^{3}**2.7**. Subsequently, a *γ*-hydrogen is abstracted in a 1,5-hydrogen atom transfer (1,5-HAT) and the triplet biradical ^{3}**2.8** is formed. Now, three different pathways are competing after ISC: the unproductive backreaction *via* HAT towards **2.7**, the productive recombination to give cyclobutanol **2.9** and the *β*-cleavage towards fragmentation products **2.10** and **2.11**. Depending on the geometry in the transition state ^{3}**2.8** and the initial conformation of the molecule **2.7** in the ground state, different pathways might be more or less efficient, which is reflected in the ratio of cyclisation to fragmentation after the reaction.[36]

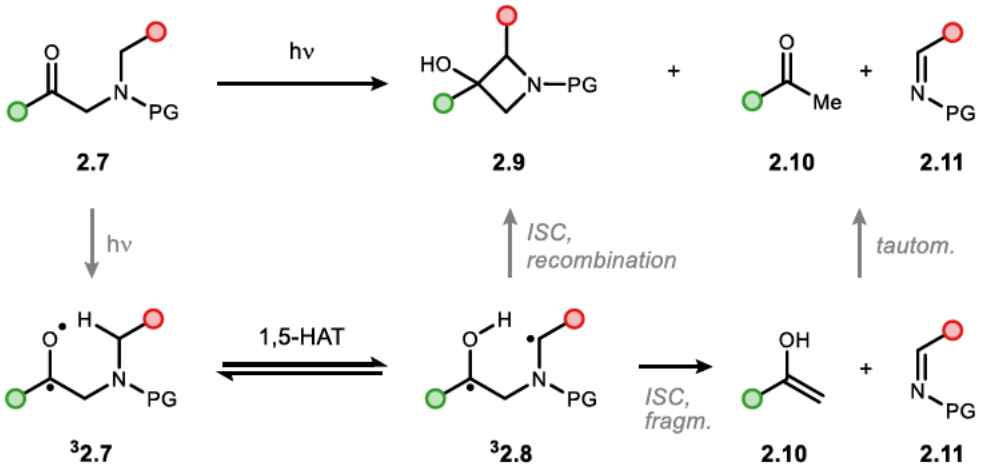

Scheme 6: Mechanism of the Norrish-Yang cyclisation.

The reaction is therefore very sensitive to the employed solvent[35b] and other factors influencing the ground state and transition state geometry, like the restriction of conformational freedom through sterically demanding substituents,[37] rigid molecular structures[38] or intramolecular hydrogen bonds.[39] This dependency on external influences can be considered as a major drawback, still several groups were able to utilise it for synthetic benefit. By limiting the molecular freedom, stereoselective syntheses were achieved, first in solid-state[40] and later also in solution.[41] This also enabled *Scheffer* and coworkers to determine the optimal geometric parameters for successful hydrogen abstraction by irradiation of solid-state crystals. They were able to modify their conditions to achieve enantioselective products by providing a chiral surrounding during excitation. Regarding the initial abstraction, a six-membered transition state provides the optimal geometry for flexible molecules. The distance between the carbonyl

oxygen and the γ-hydrogen was found to be the most important factor, whereas the trajectory of the abstraction was found to be less relevant (Scheme 7).[42]

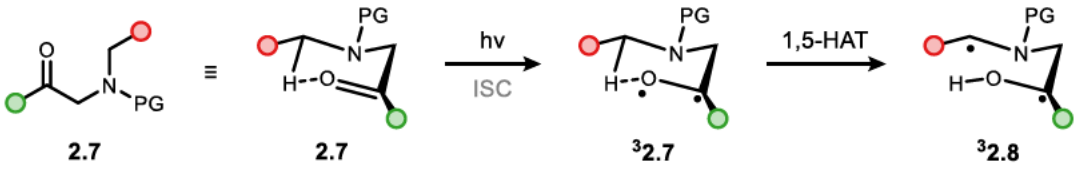

Scheme 7: Optimal geometry for 1,5-HAT *via* a 6-membered transition state.

Several other examples of stereoselective syntheses in solution are known today, for example the use of hydrogen-bonds, [43] host-guest interactions[44] and ionic auxiliaries.[45] In recent years, some groups have spotted the synthetic use of the Norrish-Yang cyclisation. The effectiveness of the transformation from α-amino-acetophenone **2.5** to 3-azetidinol **2.6** inspired *Murakami* and coworkers to use azetidinol **2.6** as a cornerstone in a seminal publication, where they simultaneously harnessed solar photon energy to construct a strained intermediate and incorporated CO_2 in a one-pot reaction to form carbonate **2.12** (Scheme 8, top).[46]

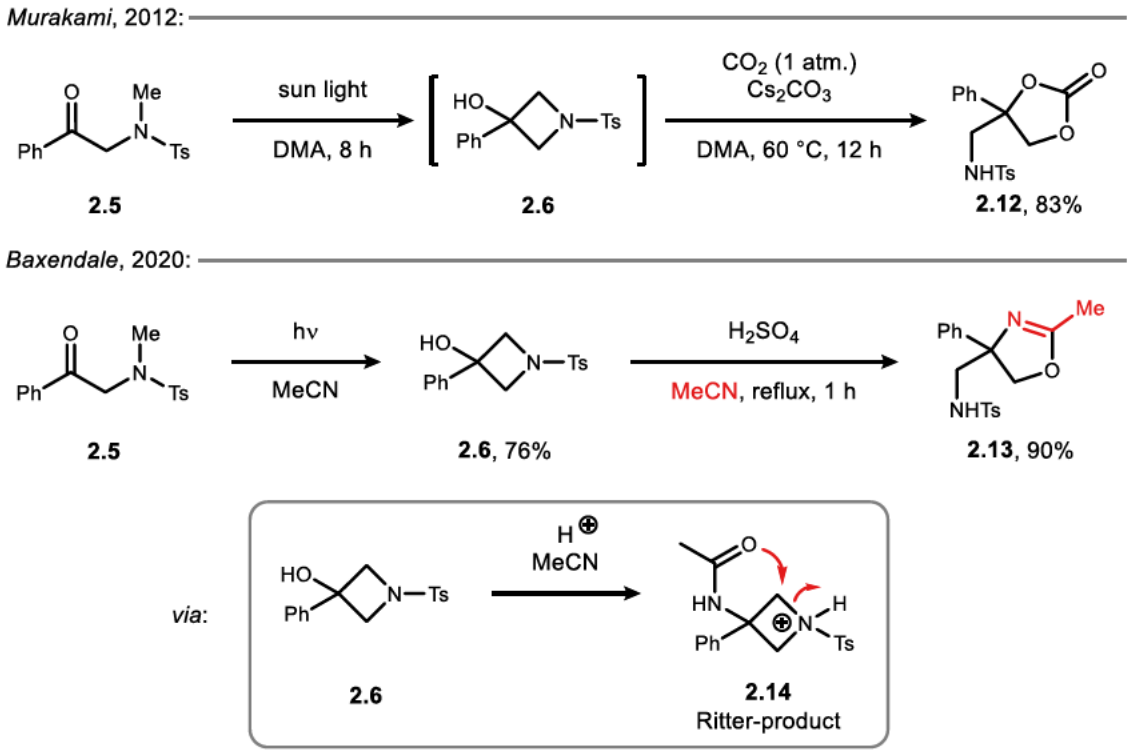

Scheme 8: Build and release approaches leveraging azetidines. Top: Incorporation of CO_2 using sun light by *Murakami*.[46] Bottom: Formation of 2-oxazolines by *Baxendale*.[47] DMA = *N*,*N*-dimethylacetamide, atm. = atmosphere.

Baxendale and coworkers later developed a flow synthesis, which gave access to the four-membered ring **2.6** in gram-scale (Scheme 8, bottom).[47] They intended to further functionalise azetidinol **2.6** in a Ritter reaction, however, their isolated product was found to be oxazoline **2.13**. The authors propose a cascade

sequence, where the amide of the protonated expected product **2.14** attacks the activated azetidine, resulting in a ring-opening reaction and the formation of the 2-oxazoline **2.13**.

Despite all advancements in the recent years, the Norrish-Yang cyclisation remains relatively underutilised compared to the Paterno-Büchi reaction or [2+2] cycloadditions and the range of products, as well as the predictability of the reaction outcome remain a limiting factor. For example, generation of oxetanes *via* the Norrish-Yang cyclisation is still considered to be challenging.[48]

2.1.2 Ring opening of 4-membered cyclic alcohols

Several studies concerning the opening of oxetanes[49], azetidines[50] and cyclobutanols[51,19c] were published over the recent years. Although four-membered rings possess high ring-strain energies, they are much more stable than their three-membered counterparts and usually need activation to perform ring opening reactions at lower temperatures.[19] With a constant strive for the generation of enantiopure material for medicine and biology,[52] desymmetrisation of prochiral four-membered rings has proven to be an efficient synthesis strategy.[53] Depending on the substrate, this might involve the catalytic use of *Brønsted* acids or bases, *Lewis* acids, transition metals or enzymes. Still, exothermic ring-strain release acts as a driving force for all these transformations. In the following, selected examples from the plethora of ring-opening reactions will be discussed, each of which will present a structural element featured in this work.

For their seminal publication on oxetanes, *Jacobsen* and coworker were inspired by the enantioselective opening of epoxides and developed Co^{III}·salen complex **2.15**, that efficiently activate oxetanes towards nucleophilic intramolecular ring-opening reactions yielding enantioenriched tetrahydrofuranes (Scheme 9, top).[54] They were able to synthesise several prochiral 3-substituted oxetanes containing a tethered oxygen nucleophile and demonstrated the opening of 3,3-disubstituted quaternary oxetane **2.16** towards tetrahydrofuran **2.17** in excellent enantiomeric ratios (*er*). Mechanistically, a bimetallic activation was proposed, with simultaneous activation of nucleophile and oxetane. The assumption was supported by the successful use of an oligomeric catalyst, which led to enhanced enantioselectivities. Using a similar tethering approach, *Houk* and *Sun* were able to demonstrate the enantioselective intramolecular attack of oxetane **2.18** to give tetrahydrothiophenes **2.19** under *Brønsted* acid catalysis using

chiral phosphoric acid **2.20** (Scheme 9, bottom).[55] Since then, *Sun* and several other groups successfully achieved the ring-opening of oxetanes employing inter- and intramolecular reactions using oxygen-[56], sulphur-[57], nitrogen-[58], halogen-[59], or carbon-based[60] nucleophiles, which will not be discussed further in this work.

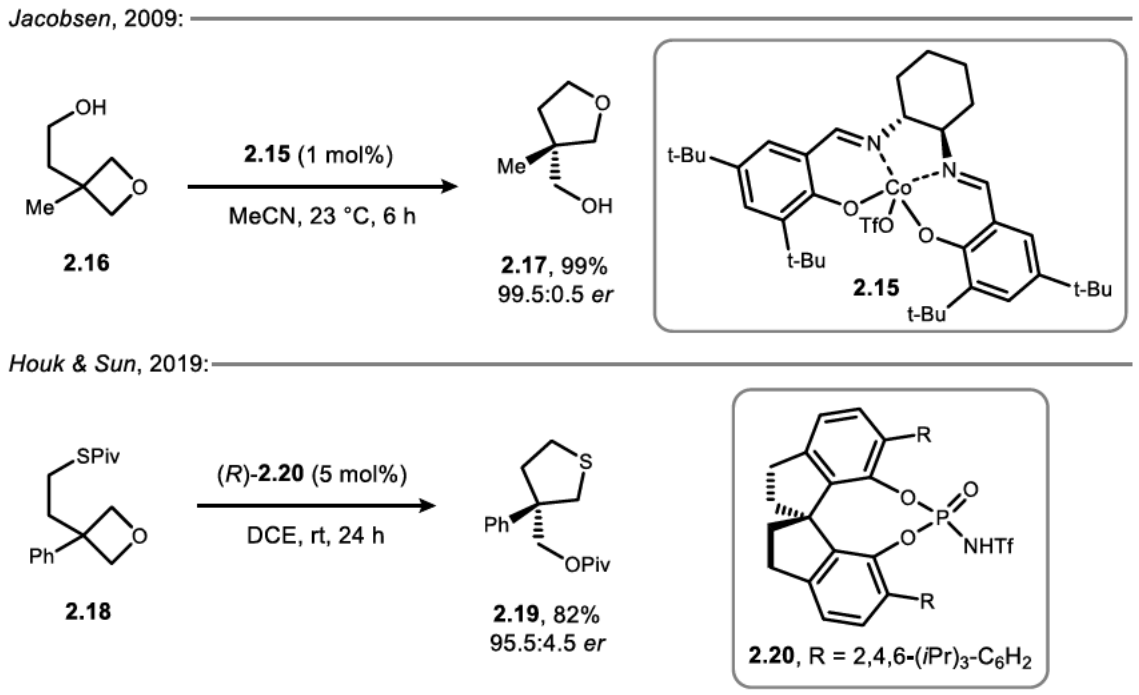

Scheme 9: Top: Cobalt catalysed enantioselective intramolecular ring opening of oxetanes by *Jacobsen*.[54] Bottom: *Brønsted* acid catalysed asymmetric ring opening of oxetanes by *Sun*.[55] OTf = trifluoromethanesulfonate, Piv = pivalate.

Regarding the asymmetric ring opening of azetidines, two seminal studies were published by the *Sun* group (Scheme 10), with both utilising the intermolecular nucleophilic attack of a sulphur nucleophile **2.21** under *Brønsted* acid catalysis. In their first publication, the authors hypothesize a dimeric hydrogen-bonding interaction between the engaging nucleophile **2.21** and the phosphor acid catalyst **2.22**, ultimately leading to a better asymmetric induction upon acidic activation of the substrate **2.23**. Hence, chiral ring-opening product **2.24** is generated in high yield and enantioselectivity (Scheme 10, top). In a later publication, alkylation generated the activated azetidinium **2.25**, which was insoluble in the used unpolar solvent and essentially created a biphasic system. By formation of a chiral ion pair between the azetidinium salt and the catalyst **2.26** under the reaction conditions, the solubility of the previously insoluble azetidinium **2.25** was increased and hence reaction under asymmetric control could proceed. This eliminated uncatalysed background reactions between the nucleophile and the activated azetidine and delivered **2.27** in excellent enantioselectivities (Scheme 10,

bottom). Again, other ring opening reactions of azetidines were published, under use of alkyl halides,[50a] sulphur nucleophiles,[61] cyanides[62] and other carbon nucleophiles,[63] which will not be discussed here.

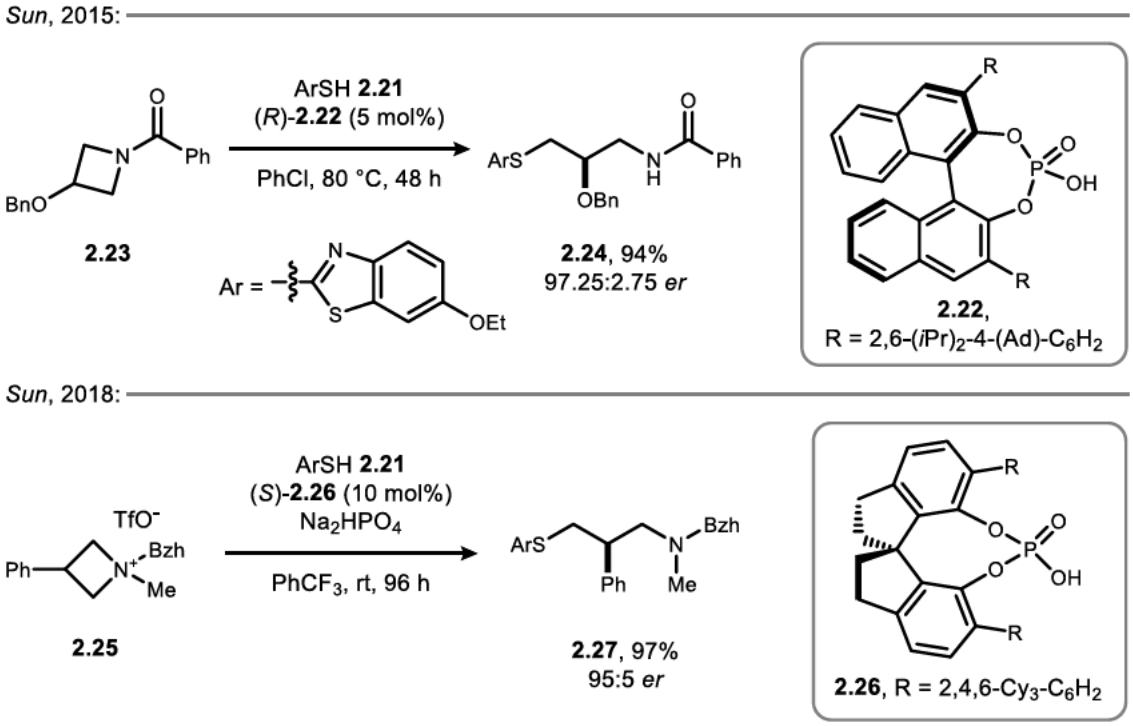

Scheme 10: Top: First catalytic asymmetric intermolecular desymmetrisation of azetidines.[64] Bottom: Counter-ion induced asymmetric ring opening of azetidinium ions.[65] Ar = aryl, Ad = adamantyl, Bzh = benzhydryl.

The ring opening of cyclobutanols provides its own challenges, as the cyclobutene core consists of inert *C*–*C* bonds, which are not polarised and thermodynamically stable.[66] Fortunately, the hydroxyl group can act as a handle to induce reactivity, releasing the ring strain and allowing for the generation of quaternary stereogenic centres in desymmetrisation reactions. Transition metal catalysed or radical mediated ring opening reactions are known, and usually proceed *via* a metal alkoxide that undergoes *β*-carbon elimination or an alkoxyl radical that undergoes *β*-scission.[67,66,19c] In a series of publications, *Uemura* and coworkers showed the catalytic arylation of cyclobutanols, and were able to develop an asymmetric variant using ligand **2.28** with high yields and enantioselectivity, transforming cyclobutanol **2.29** into the chiral ketone **2.30** (Scheme 11, top).[68]

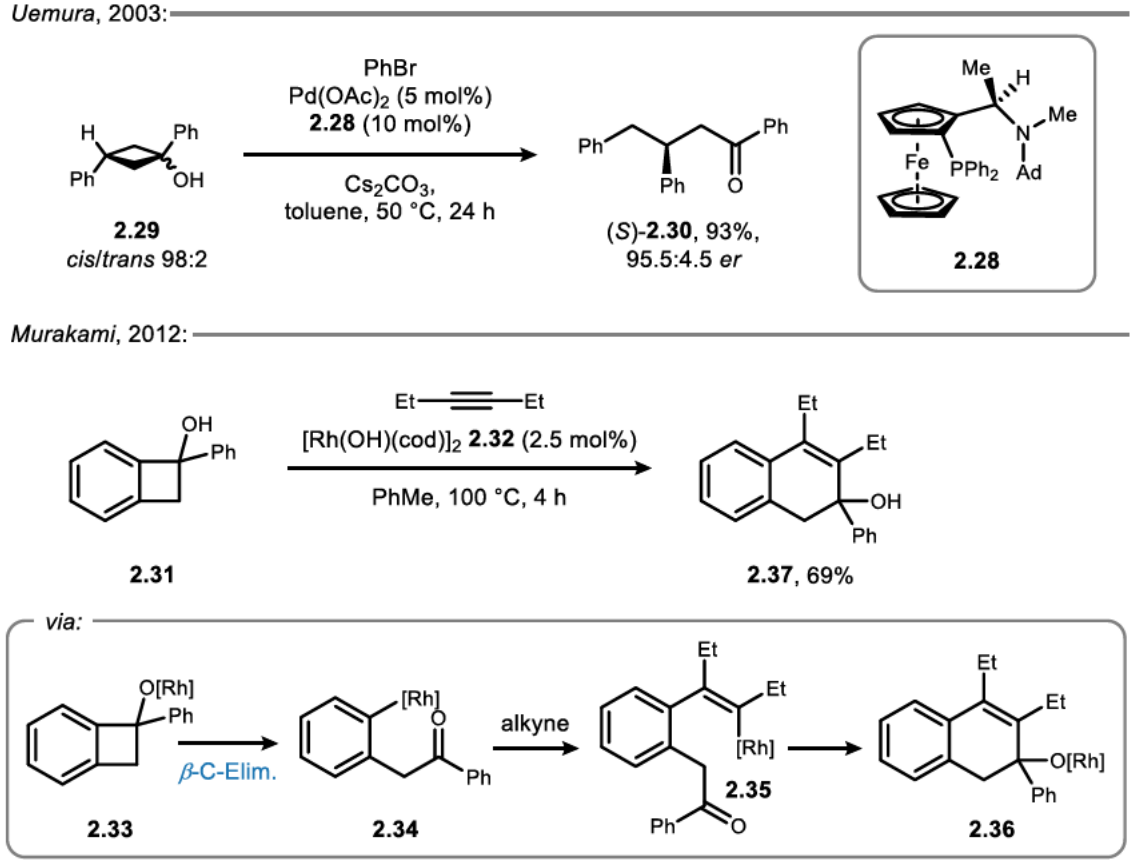

Scheme 11: Top: Palladium catalysed asymmetric arylation by *Uemura*.[68a] Bottom: Site-selective ring-opening of benzocyclobutenols under rhodium catalysis by *Murakami*.[69] cod = cycloocta-1,5-diene.

The *Murakami* group used the reactivity of benzocyclobutenols in a site selective ring opening of benzocyclobutenol **2.31** with a rhodium catalyst **2.32**. Following deprotonation of **2.31** by the catalyst, a Rh^{I}-benzocylobutenolate **2.33** is formed, and undergoes β-carbon elimination to **2.34**. This aryl metalate is then trapped by the alkyne as **2.35**, and the alkenylrhodium adds back into the carbonyl group. The alkoxyrhodium **2.36** can then be proto-demetallated by another starting material, ultimately closing the redox-neutral catalytic cycle and giving dihydronaphthalene **2.37** as the product.

2.1.3 Motivation and aim

The construction and ring-opening of four-membered heterocycles was sought to be investigated in the context of build and release reactions. A division of the overall project into three parts is proposed. In the first part, the photochemical synthesis of azetidinols and oxetanes *via* the Norrish-Yang reaction will be investigated. The second part concerns the ring-opening of azetidinols, whereas the third part will investigate the desymmetrisation of oxetanols.

Although many groups were able to decipher the mechanism of the Norrish-Yang reaction, the influence of substituents is not fully understood yet. Furthermore, comparative studies under similar reaction conditions are lacking. Therefore, the first part of this project will consist of a systematic investigation of substitution patterns on the reaction of α-aminoacetophenones, and a proof-of-concept for the formation of oxetanols is envisioned. In order to perform this study, an easy access to substituted derivatives is needed. Here, a building-block based approach guarantees flexibility, with enhanced ability to quickly incorporate molecular changes from commercially available or easy attainable starting materials and hence an easy tuning of the system (Scheme 12). Different substitution on nitrogen is postulated to influence the success of the Norrish-Yang-cyclisation and different protecting group and the effect of radical stabilising substituents will be investigated. The strategic disconnection between α-bromoacetophenones and double functionalised amines was identified as a feasible approach for the synthesis of a library of starting materials.

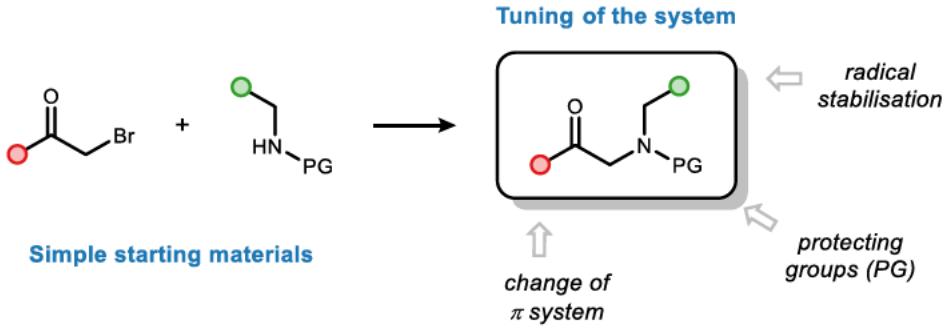

Scheme 12: Rapid access to a library of α-aminoacetophenones.

As the second and third part of this project, the ring-opening reaction of 3-azetidinols and 3-oxetanols will be investigated (Scheme 13). The ring-strain of these four-membered heterocycles represents a thermodynamic driving force for the rapid generation of molecular complexity. Attack of an intramolecular oxygen nucleophile generates oxygen rich heterocycles, as discussed above (*cf.*

chapter 2.1.2). Transient hemi-ketals are identified as central intermediates, as they possess a nucleophilic hydroxy functionality and can be generated in-situ from reaction of alcohols with electron deficient ketones.

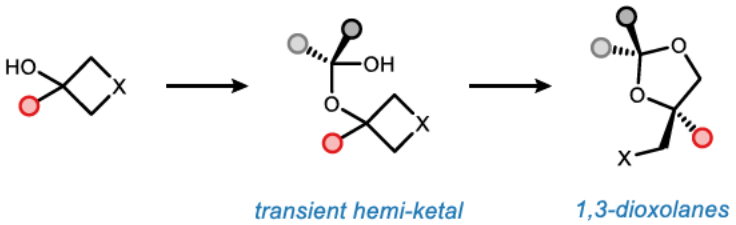

Scheme 13: Synthesis of 1,3-dioxolanes *via* a transient hemi-ketal.

Therefore, during the second part of the project, the ring-opening of photochemically generated 3-azetidinols will be tested. Thirdly, the ring-opening of prochiral 3-oxetanols using transient hemi-ketals in a dynamic kinetic resolution (DKR) will be investigated. This part was conducted in collaboration with [redacted], who demonstrated the enantioselective ring-opening of aryl-substituted 3-oxetanols as part of his own work. A DKR using transient hemi-ketals relies on the existence of a fast dynamic equilibrium in the first reaction step (Scheme 14). The interaction with a chiral catalyst renders one enantiomer more reactive than the other, which leads to constant consumption of one enantiomer from the rapid equilibrium. Thereby, high enantioselectivities can be achieved.

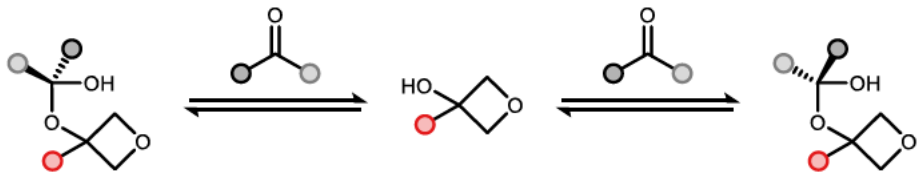

Scheme 14: Dynamic equilibrium of the formation of the transient hemi-ketal.

In this collaboration, the investigation of the hemi ketal formation and optimisation of reaction conditions will be conducted by [redacted]. As part of this work, contributions in the improvement of the additional catalysts were aimed for. Furthermore, the use of alkynyl- and alkyl-substituted oxetanols in the desired ring-opening reaction and substitution of the previously employed electron deficient ketone was envisioned. Again, the combination of the photochemical synthesis of 3-oxetanols from part one of the project *via* the Norrish-Yang cyclisation with a ring-opening reaction (part three) is believed to increase the overall synthetic value of the desired build and release transformation.

With the knowledge gained from both parts of this conceptionally intertwined project, the use of 3-azetidinols and 3-oxetanols as central strained intermediates

in a build and release approach using transient hemi-ketals will be evaluated (Scheme 15).

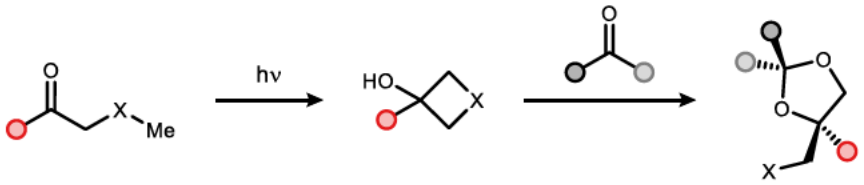

Scheme 15: Build and release approach using photogenerated four-membered heterocycles.

2.2 Synthesis of starting materials

2.2.1 Synthesis of *α*-substituted acetophenones

A library of different *α*-aminoacetophenones was synthesised to evaluate their performance in the Norrish-Yang cyclisation (Scheme 16). Substrates **2.5** and **2.38** to **2.44** were prepared in an adapted literature procedure from 2-bromoacetophenone and the respective secondary amines in a nucleophilic substitution.[46] Substrate **2.45** was synthesised from 2-bromo-2'-acetonaphthone and *N*-methyl-*p*-toluenesulfonamide. Secondary amines were either commercially available or were prepared from primary amine sources by protection with tosyl or mesyl chloride (Ms).

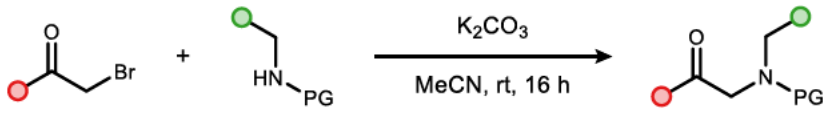

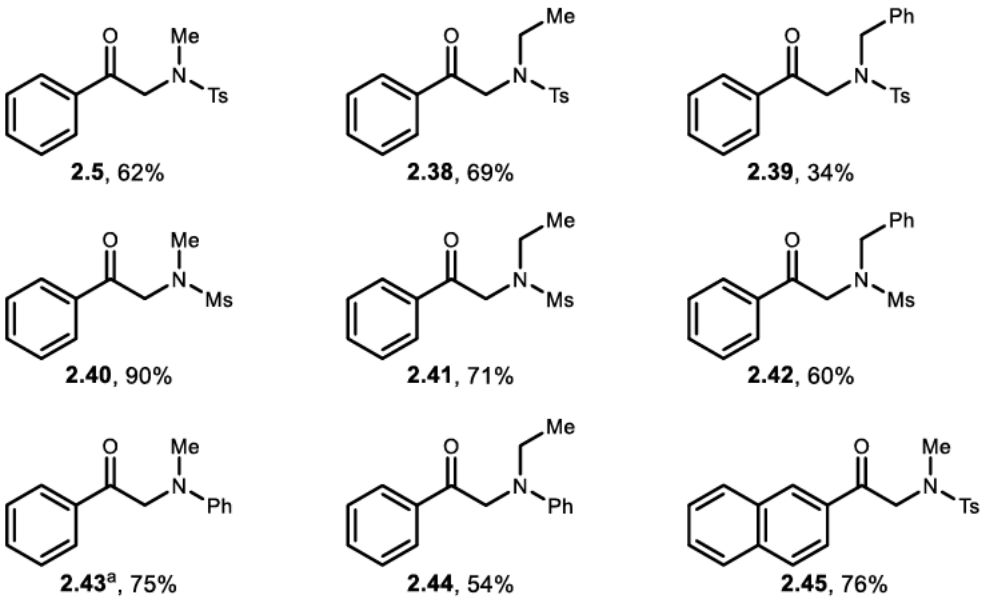

Scheme 16: *α*-Aminoacetophenones synthesised during this project. [a]Synthesis performed at 70 °C.

Overall, the approach to synthesise a variety of different substrates based on the same methodology proved effective, with yields exceeding 60% for most substrates. Only substrates **2.39** and **2.44**, which are derived from sterically demanding secondary amines, were formed in lower yield and degraded when stored under air at room temperature (rt). Therefore, they were stored at –20 °C, where they were found to be stable for months. Similarly, an *α*-methoxyacetophenone was synthesised through nucleophilic substitution from 2-bromo-1-(o-tolyl)ethanone **2.46** and sodium methanolate, yielding *α*-methoxyacetophenone **2.47** in 23% yield after column chromatography and bulb-to-bulb distillation (Scheme 17).

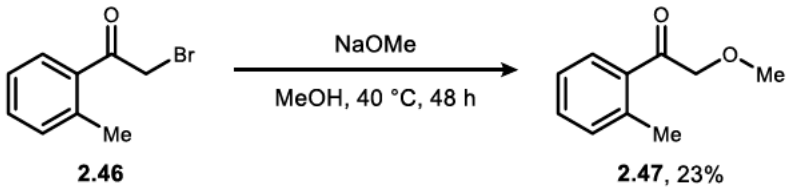

Scheme 17: Preparation of *α*-methoxyacetophenone 2.55.

2.2.2 Synthesis of 3,5-dinitroacetophenones

Electron deficient 3,5-dinitroacetophenones were prepared in collaboration with [redacted] for the envisioned implementation of transient hemi ketals in the

ring-opening step of the build and release approach (*vide supra,* Scheme 13 and following chapters 2.4 and 2.5). Acetophenones **2.48** and **2.49** were subjected to a mixture of concentrated nitric acid and sulfuric acid at elevated temperatures, where double nitration was achieved. The substrates were found to be highly hygroscopic, therefore purification by standard column chromatography or distillation was found to be challenging.

Under the aqueous work-up conditions hydrates where formed, which could be recrystallised from water. Hydrate **2.50** was delivered as a colourless solid in analytical purity. Hydrate **2.51** was obtained after recrystallisation from water and further purified by [redacted] *via* column chromatography. The hydrates were dehydrated in an azeotropic distillation with toluene in a *Dean-Stark* apparatus, yielding the ketones **2.52** and **2.53** quantitatively.

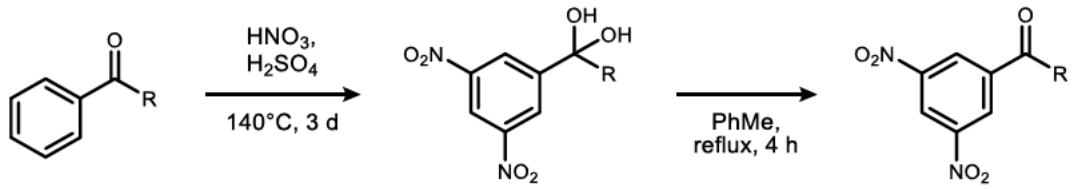

2.48 R = CF_3
2.49 R = CF_2Cl

2.50 R = CF_3, 53%
2.51[a] R = CF_2Cl, 23%

2.52 R = CF_3, *quant.*
2.53 R = CF_2Cl, *quant.*

Scheme 18: Synthesise of the 3,5-dinitroacetophenones *via* the respective hydrates. [a] Column chromatography performed by [redacted].

2.2.3 Synthesis of 3-substituted oxetanes

Over the course of this study, several 3-oxetanols were synthesised to probe their reactivity in ring-opening reactions. By nucleophilic addition of organolithium reagents to 3-oxetanone **2.54**, 3-oxetanols **2.55** to **2.60** were accessed (Scheme 19). In the case of 3-oxetanol **2.55**, the lithiated precursor was generated through lithium-halogen exchange, whereas simple deprotonation of the alkynes with *n*-butyl lithium was successful for substrates **2.56-2.60**. Synthesis of the alkylated 3-oxetanol **2.61** was performed by [redacted] from 3-oxetanone and commercially available *n*-butyl lithium.

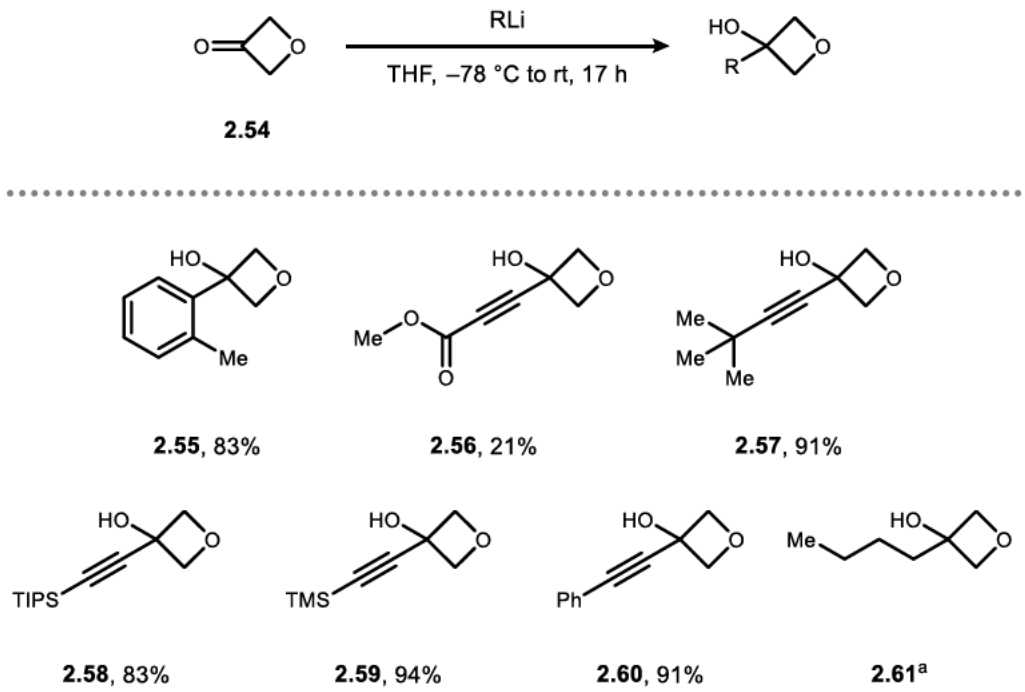

Scheme 19: 3-Oxetanols synthesised *via* addition of carbon nucleophiles. [a] Synthesis performed by [redacted].

Additionally, 3-oxetanamine **2.62** was prepared *via* reductive amination from 3-oxetanone **2.54** and aniline. Sodium triacetoxyborohydride was employed as a very mild reductant, since it is unreactive towards the ketone under the reaction conditions.[70]

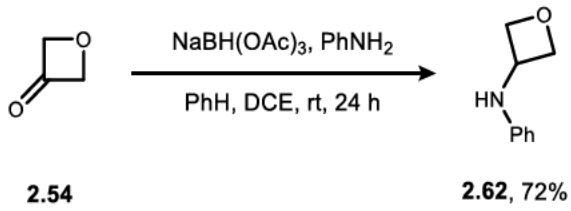

Scheme 20: Synthesis of 2.62 *via* reductive amination, DCE = 1,2-dichloroethane.

2.2.4 Synthesis of catalysts

Over the course of this work, three metal complexes were prepared to be tested in the ring-opening of 3-oxetanols. An optimisation by [redacted] revealed Co^{II} complexes with bulky salen ligands as suitable catalysts for the desired transformation (*cf.* chapter 2.5). Therefore, the *Katsuki* type salen ligands **2.63** and **2.64** were synthesised (Scheme 21).

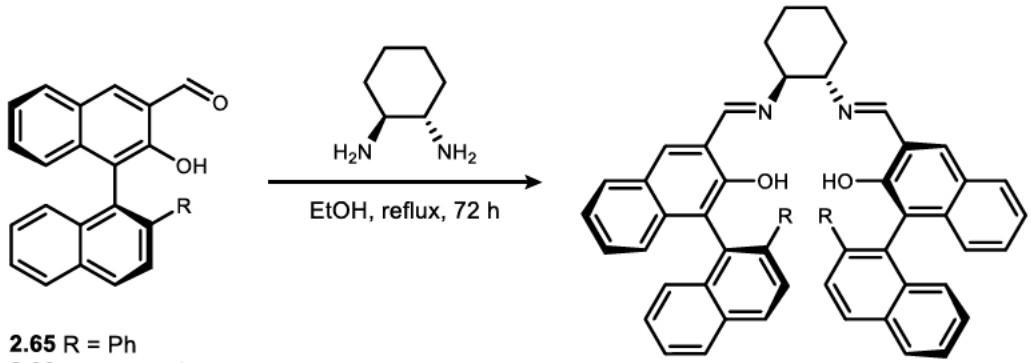

2.65 R = Ph
2.66 R = 4-tBu-C_6H_4

2.63 R = Ph, 62%
2.64 R = 4-tBu-C_6H_4, 85%

Scheme 21: Synthesis of *Katsuki* type salen ligands *via* condensation.

The ligands chiral amine backbone features two stereogenic centres, with the binaphthols axial chirality adding another stereoelement.[71] *Katsuki* type ligands are easily tuneable by variation of the backbone and the C3'-substituents in the biaryl section of the molecule.[72] Synthesis of the ligands was achieved after simple *Schiff* base condensation of aldehydes **2.65** and **2.66** with (*S*,*S*)-1,2-diaminocyclohexane to deliver ligands **2.63** and **2.64** in good yields.
Using the successfully synthesised ligands, Co^{II}·salen complexes **2.67** and **2.68** were prepared following a literature known procedure by *Ebisawa et al.* (Scheme 22).[73]

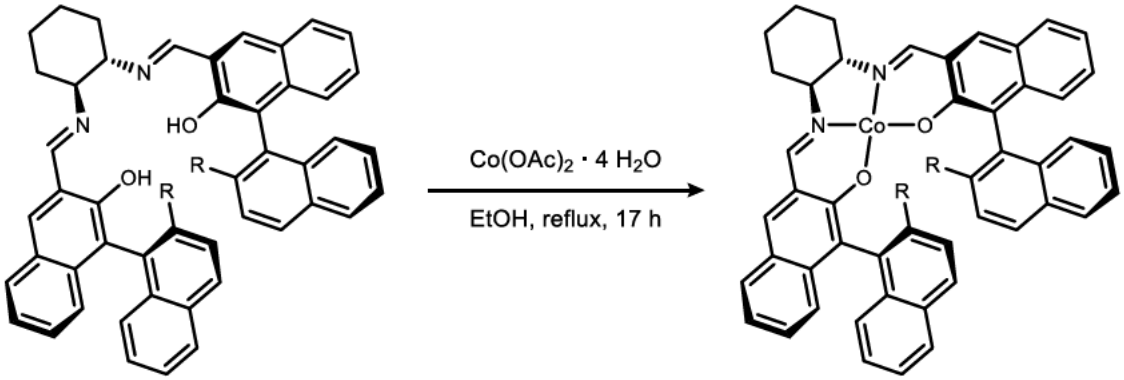

2.63 R = Ph
2.64 R = 4-tBu-C_6H_4

2.67 R = Ph, 71%
2.68 R = 4-tBu-C_6H_4, 88%

Scheme 22: Synthesis of Co^{II}·salen complexes.

Additionally, the complex ***epi*-2.67** was prepared in a similar way by employing **2.63** and (*R*,*R*)-1,2-diaminocyclohexane to synthesise *epi*-**2.67**, followed by complexation to yield the desired product in good yield (Scheme 23).

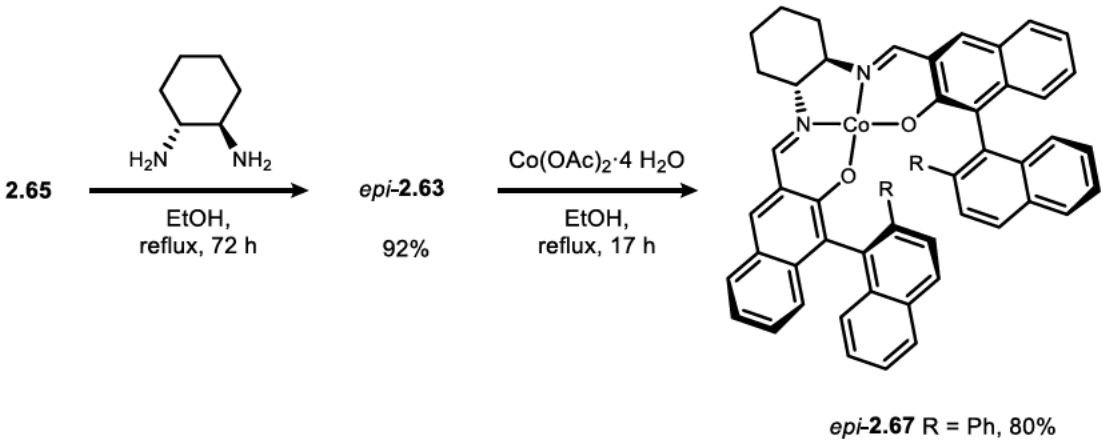

Scheme 23: Synthesis of *epi*-2.67 *via* condensation and complexation.

2.3 Norrish-Yang cyclisation of *alpha*-substituted acetophenones

A reliable and predictable photocyclisation is essential for the development of a build and release strategy and α-aminoacetophenones were chosen as a platform for a systematic investigation of the Norrish-Yang reaction (*cf.* chapters 1.1 and 2.1.1). All reactions were performed in a *Luzchem* Photoreactor (Figure 26) equipped with mercury fluorescence lamps (355 nm) under identical conditions, so that individual reaction rates could be compared. A study on 25 µM scale monitored by nuclear magnetic resonance (NMR) spectroscopy was envisioned. This allows for an easy comparison of potential substrates in the synthesised library by evaluating their respective conversion, cyclisation and fragmentation rates against an internal standard. Deuterated acetonitrile (CD_3CN) was employed as the main solvent, as it is known to support an efficient reaction in the Norrish-Yang cyclisation.[74] Compared to deuterated derivatives of other frequently employed solvents for this reaction, *e.g.* *N*,*N*-dimethylformamid-d_7, it is also more affordable.[75] Additionally, the possibility to directly investigate the reaction mixture *via* ^{1}H NMR eliminates intrinsic errors, as some products and side products were found to be unstable under certain workup conditions, indicated by a substantially lowered yield in the isolation compared to the NMR yield.

The substituents on the alpha amino ketone core were systematically altered and their cyclisation tendency under irradiation was investigated (Table 1).

At first, the influence of the aromatic moiety on the transformation was analysed. The *N*-tosyl protected acetonaphthone **2.45** was tested against acetophenone-based **2.5** to investigate the influence of the extension of a larger conjugated π-

systems. As expected, a red-shift of the n-π* absorption band to the vis region was observed (*cf.* chapter 4.4) for acetonaphthone **2.45** compared to acetophenone **2.5** as a result of the larger conjugated system.[76] However, the extent of the conjugated system might also influence the efficiency of triplet generation and stabilise the biradical species.[77] When probing this theory, tosyl-protected 2-acetonaphtone **2.45** showed low conversion towards azetidinol **2.69** (Table 1, entry 1, synthesis performed by [redacted]) compared to the tosyl protected acetophenone **2.5**, which gave azetidinol **2.6** in 81% yield with 14% formation of acetophenone **2.70** as the side product (Table 1, entry 2). Therefore, acetophenone was chosen to be the core structure and the study was continued by investigating the influence of the alkyl substituent. Introduction of *N*-ethyl and *N*-benzyl substituents led to decreased cyclisation yields and gave azetidinols **2.71** (54% yield) and **2.72** (63% yield) without a pronounced diasteroselectivity (Table 1, entries 3 & 4). Additionally, an increased formation of side products was observed *via* ^{1}H NMR analysis of the reaction mixture, the main one being acetophenone from the Norrish II fragmentation. Clearly, the introduction of substituents does not improve the cyclisation yields, with the seemingly stabilising residues leading to decreased reactivity and increased fragmentation. When changing the protecting group to mesyl, an identical trend was observed (Table 1, entries 5-7). Azetidinol **2.73** was formed in decreased yield compared to substrate **2.6**, and introduction of substituents led to a stark increase in side reactions, with azetidinols **2.74** and **2.75** generated without control over the diasteroselectivity. Next, the protecting group was changed to phenyl (Table 1, entry 8) which led to formation of *N*-phenyl-azetidinol **2.76** in 12% yield, with a drop in conversion and an increased tendency for the formation of unselective side reactions. Ethyl substitution followed this trend, with the conversion stalling to 27% and only 2% yield of azetidinol **2.77** (Table 1, entry 9). The overall lack of diastereocontrol supports the assumption of a diradical triplet intermediate which rapidly undergoes ISC and cyclises, before an equilibration to conformations with decreased steric repulsion can occur.[48] In order to separate the influence of radical stabilisation from the influence of steric size on the cyclisation efficiency, another set of substrates was devised and then synthesised by [redacted] (Table 1, entries 10-12). Formation of products **2.78** and **2.79** was unsuccessful, with only the sterically demanding benzhydryl group allowing access to azetidinol **2.80** in 10% yield.

Table 1: NMR study of the effect of structural variation on the cyclisation. Reactions were performed on 25 µM scale in 0.5 mL CD_3CN (50 mM), NMR yield and diastereomeric ratios (*dr*) based on ^1H NMR using mesitylene as internal standard.

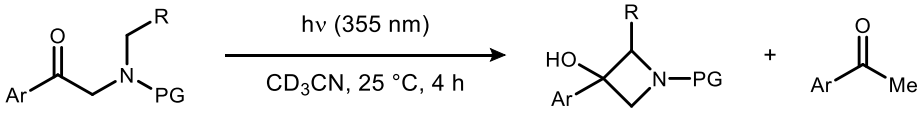

Entry	Products			Conversion	Cyclisation	Fragmentation
1	Ar = Nph	PG = Ts	R = H (**2.69**)[a]	23%	11%	4%
2	Ar = Ph	PG = Ts	R = H (**2.6**)	>99%	81%	14%
3	Ar = Ph	PG = Ts	R = Me (**2.71**)	>99%	54% (*dr* 54:46)	26%
4	Ar = Ph	PG = Ts	R = Ph (**2.72**)	>99%	63% (*dr* 60:40)	20%
5	Ar = Ph	PG = Ms	R = H (**2.73**)	>99%	67%	14%
6	Ar = Ph	PG = Ms	R = Me (**2.74**)	>99%	44% (*dr* 51:49)	42%
7	Ar = Ph	PG = Ms	R = Ph (**2.75**)	>99%	37% (*dr* 52:48)	22%
8	Ar = Ph	PG = Ph	R = H (**2.76**)	90%	12%	3%
9	Ar = Ph	PG = Ph	R = Me (**2.77**)	27%	2% (*dr* 52:48)	6%
10	Ar = Ph	PG = Me	R = H (**2.78**)[b]	87%	<1%	53%
11	Ar = Ph	PG = Ph	R = H (**2.79**)[b]	>99%	<1%	65%
12	Ar = Ph	PG = Bzh	R = H (**2.80**)[b]	94%	10%	74%

[a] Synthesis performed by [redacted]. [b] Starting material synthesised by [redacted]. Nph = naphthyl, Bzh = benzhydryl.

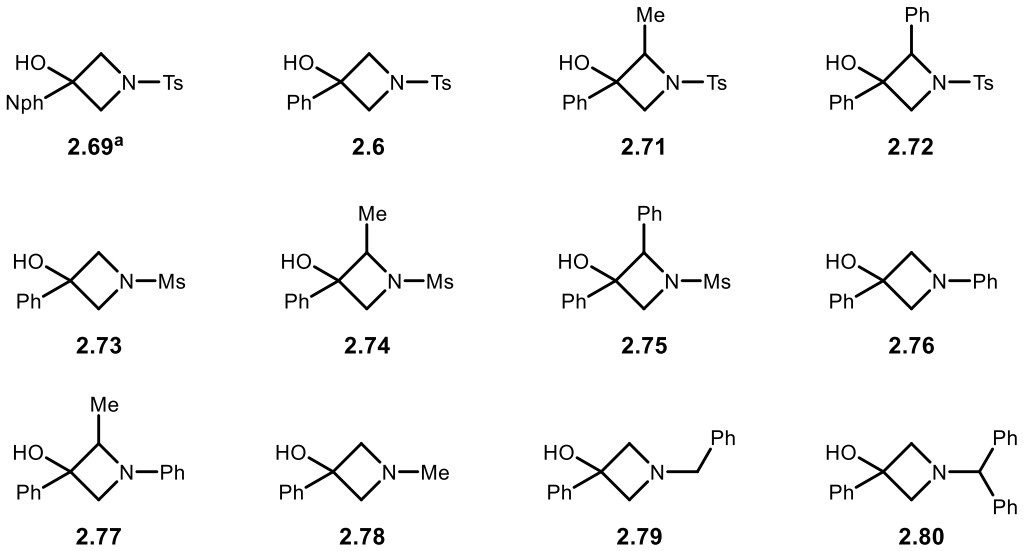

Figure 3: Overview of the obtained 3-azetidinols after irradiation. [a] Synthesis performed by [redacted].

As evident from the obtained data, a delicate balance exists, where sterically demanding substituents can either enable or hinder the successful cyclisation

reaction. The introduction of sterically demanding substituents limits the rotational freedom of a molecule in the ground and excited state (Scheme 24).

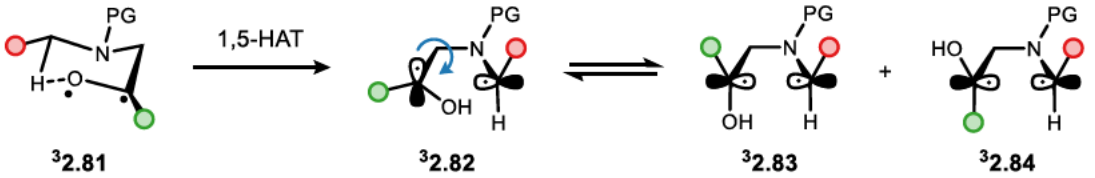

Scheme 24: Graphical depiction of a possible excited state 1,5-HAT and ring-closing sequence.

After 1,5-HAT from the six-membered excited transition state ^{3}**2.81** to biradical ^{3}**2.82**, the molecule must rotate, in order to facilitate positive orbital overlap and hence allow for a *C*–*C* bond formation from biradicals ^{3}**2.83** or ^{3}**2.84** after ISC to the respective singlet states. Throughout all steps of the process, sterically demanding residues or protecting groups can influence the flexibility of the system. Depending on the steric size of the residues, one of the excited state conformations is preferred (Scheme 25).

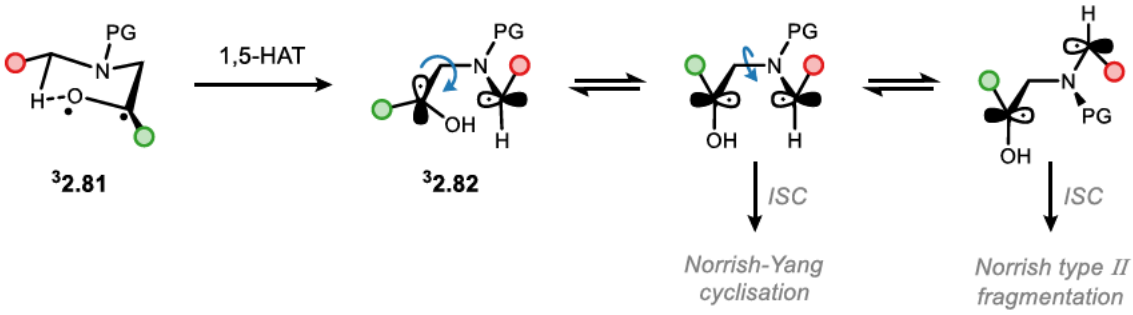

Scheme 25: Graphical depiction of exemplary transition states for radical recombination *via* Norrish-Yang cyclisation and fragmentation *via* Norrish type II after ISC.

Steric clash leads to increased fragmentation in most cases, and can hinder a molecule to adapt the beneficial 6-membered transition state prior to excitation.[43] As seen in the successful formation of benzhydryl protected azetidinol **2.80**, the increase of steric demand on the nitrogen atom can also be beneficial, possibly by providing beneficial molecular conformations for 1,5-HAT or recombination. Additionally, the findings underline the unique reactivity of sulfonyl protected amines in the Norrish-Yang cyclisation with azetidinols **2.6** and **2.73** delivered in good yields. This effect has been attributed to a dipole-dipole interaction between the electron deficient excited state ketone and a sulfonyl group and a newly formed hydrogen bond between the latter and the formed hydroxy group after 1,5-HAT in the transition state (Scheme 26).[39]

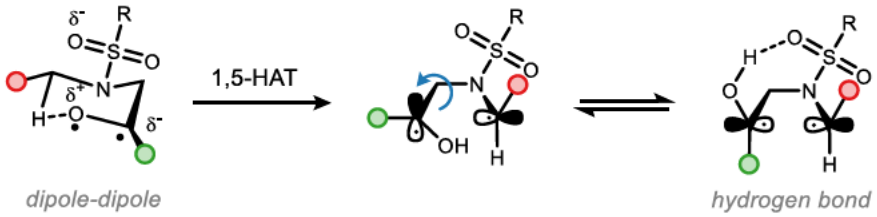

Scheme 26: Stabilising effects for sulfonyl protected α-aminoacetophenones.[39]

In order to provide a proof-of-concept for the use of 3-oxetanols as central intermediates in a build and release strategy using light, the initial photochemical synthesis of the stained ring *via* a Norrish-Yang cyclisation was aimed for. As previously discussed, this is a challenging endeavour (*cf.* chapter 2.1.1). Nonetheless, an initial proof-of-concept could be provided by subjecting α-oxoacetophenone **α-methoxyacetophenone 2.47** to irradiation with UV light (Scheme 27). The 3-oxetanol **2.55** was formed as the main product in 37% yield.

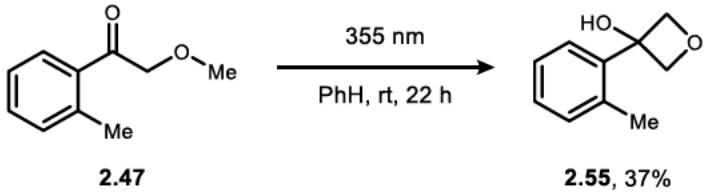

Scheme 27: Photochemical synthesis of 2.55 *via* Norrish-Yang cyclisation. Reaction was performed on a 0.2 mM scale in benzene [0.18 M] at rt for 22 h. PhH = benzene.

The use of benzene as an unpolar solvent was found to be crucial to achieve acceptable yields, whereas the use of acetonitrile led to increased Norrish type II cleavage, as already described by *Lewis* and *Turro*.[78]
For the realisation of the envisioned build and release strategy, the ring-opening reaction of 3-azetidinols was investigated next.

2.4 Ring-opening of 3-azetidinols

After successful evaluation of potential candidates for the photochemical cyclisation, substrate **2.6** was chosen as a model substrate for the envisioned ring-opening reaction using transient hemi-ketals. Electron deficient ketone **2.52** was selected based on its ability to form stable hemi-ketals as shown by [redacted] as part of his own work (*vide infra*, chapter 2.5). Initial attempts to facilitate a ring-opening were met with limited success (Scheme 28). However, existence of the expected hemi-ketal **2.85** was observed *via* NMR spectroscopy. Therefore, the addition of different additives to the reaction mixture was investigated. A series of *Lewis* acid catalysts **2.67**, **2.68** and **2.86** to **2.90**, *Brønsted* acids **2.91**, **2.92**

and **2.93** and *Brønsted* base **2.94** were employed, nonetheless all ultimately failed in enabling the desired transformation towards dioxolane **2.95**.

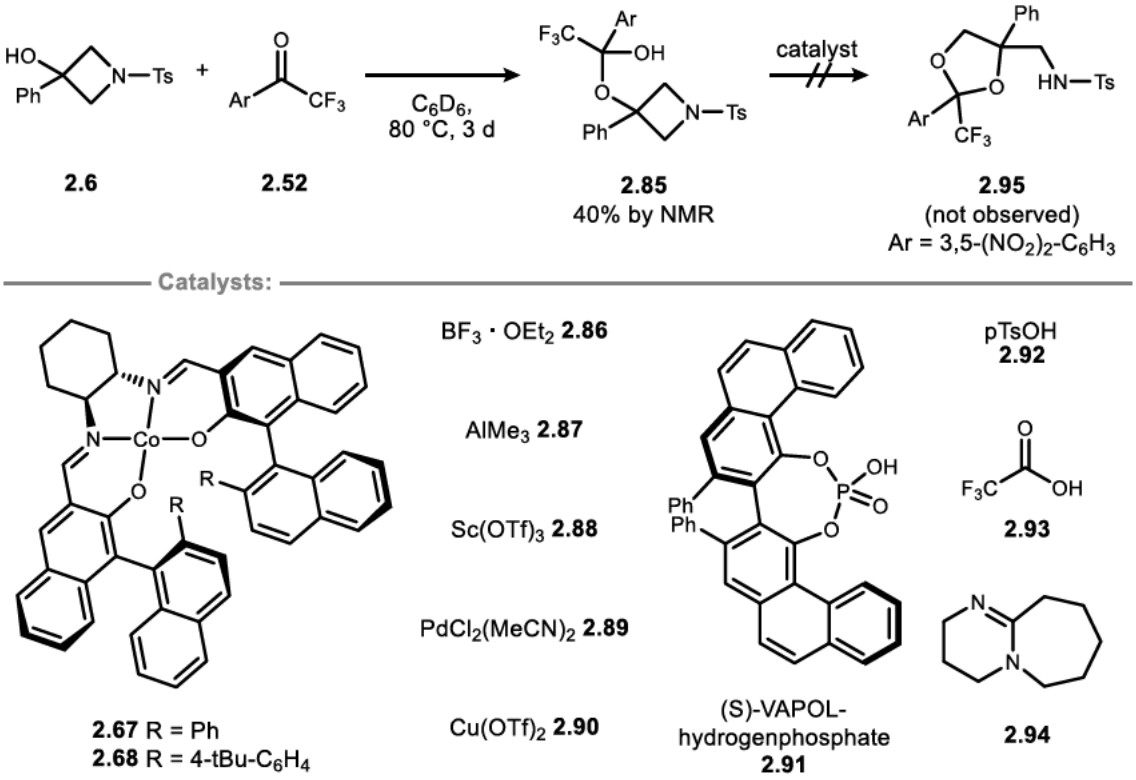

Scheme 28: Attempted ring-opening of 2.6. Reactions were run in C_6D_6 [0.2 M] on a 0.1 mmol scale. Reactions were evaluated *via* ^{19}F NMR with $PhCF_3$ as internal standard.

With this result at hand, the influence of the protecting group on the nitrogen atom was assessed. Benzhydryl protected amine **2.80** was chosen, as this protecting group seems to have a unique role in the ring-opening reaction of azetidines, with several reports showcasing the successful opening of benzhydryl protected azetidines.[79b,79c,65,63b,79a] Indeed, the reaction of azetidinol **2.80** with ketone **2.52** proceeded smoothly towards 1,3-dioxolane **2.96** in 90% yield, with excellent diastereocontrol (>20:1 *dr*) and without the need for additional activation (Scheme 29). Further, the relative configuration of dioxolane **2.96** could be determined by nuclear *Overhauser* effect spectroscopy (NOESY) experiments. Next, other activated ketones and aldehydes known to form stable hemi acetals were tested under the reaction conditions. While aldehydes and ketones **2.97** to **2.101** only showed traces of hemi ketal or acetal formation, ethyl 3,3,3-trifluoropyruvate **2.102** delivered dioxolane **2.103** in 70% yield, although with diminished diasteroselectivity (40:60 *dr*). A pathway of intermolecular protonation of the azetidine by an acidic hemi-ketal is proposed (Scheme 29, bottom). This simultaneously renders the hemi-ketalate more nucleophilic as the azetidinium becomes more electrophilic. Subsequently, a ring-opening reaction proceeds for

matching acidity of a hemi-ketal with a basic azetidine. The basicity is influenced by the protecting group, which in turn explains the lack of reactivity for the essentially non-basic tosyl protected azetidinol **2.6**. [80]

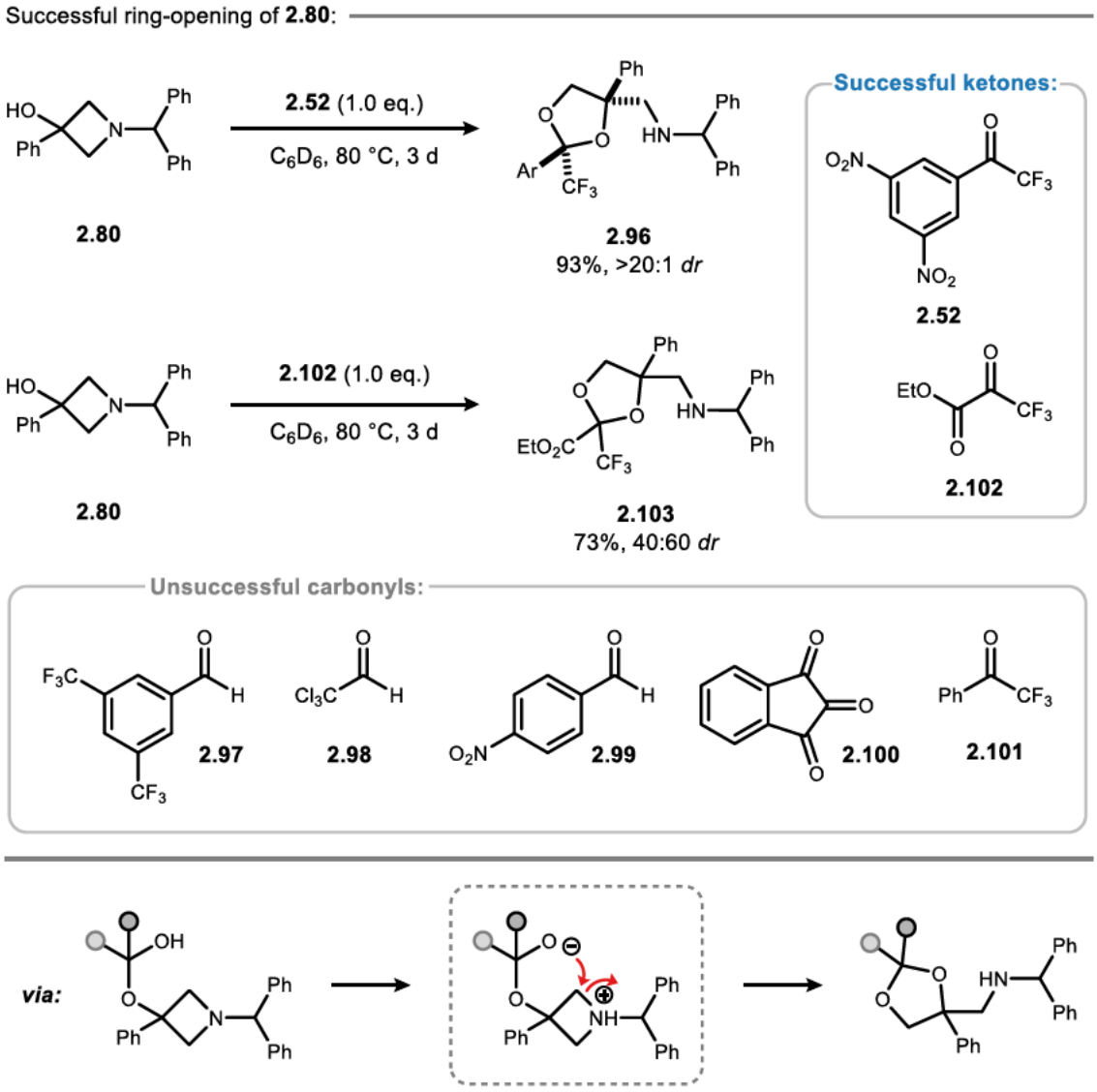

Scheme 29: Ring-opening of azetidinol 2.80 using electron deficient ketones. Reactions were run in C_6D_6 [0.2 M] on a 0.2 mmol scale. Diastereomeric ratios determined *via* ^{19}F NMR after isolation. Bottom: potential reaction pathway *via* protonated azetidine.

2.5 Ring-opening of 3-oxetanols

As part of the envisioned use of 3-oxetanols in a build and release strategy, the ring-opening of 3-oxetanols was investigated in collaboration with [redacted]. The initial catalyst development, optimisation of reaction conditions and mechanistic investigation for the enantioselective ring-opening reaction were performed by [redacted]. Compared to the previously discussed ring-opening of 3-azetidinols, gaining access to enantioenriched products is a clear advantage. Additionally, the tolerance of a broader range of substrates could help to improve

the overall useability of the method. As part of this work, the expansion of the scope of the reaction was tested and a proof-of-concept for the use in the desired build and release approach was to be provided. In the following, excerpts of the optimisation will be briefly discussed and all results by [redacted] stated as such. At first, the electron deficient 3',5'-dinitro trifluoroacetophenone **2.52** was identified as a source for stable hemi ketals by [redacted], and their structure characterised by X-Ray and NMR analysis. Following a catalyst optimisation ([redacted]), *Katsuki* type Co^{II}·salen complexes were identified as suitable catalysts for the transformation of 3-oxetanols to 1,3-dioxolanes (Table 2), and no background reaction was observed between cyclobutanol **2.104** and the ketone(entry 1). Catalyst **2.67** delivered dioxolane **2.105** in 90% yield with good stereocontrol (entry 2, 90:10 *dr*, 75:25 *er*), while the use of the epimer of the catalyst epi-**2.67** resulted in decreased yield and enantiocontrol (entry 3). Therefore, catalyst **2.68** was synthesised as part of my work after additional optimisation by [redacted] resulting in an increased stereocontrol (96:4 *dr*, 86:14 *er*) with high yields (entry 4, 88%). This catalyst was found to be especially effective for the sp^2 substituted cyclobutanols tested by [redacted], a fact that is attributed to the increased steric size of the aryl substituent, which ultimately leads to a better enantiofacial discrimination during the enantiodetermining step.

Table 2: Selected entries of the catalyst optimisation, reactions performed by [redacted] on 0.1 mmol scale in CH_2Cl_2 [0.2 M]. NMR yield and *dr* determined *via* ^{19}F NMR with $PhCF_3$ as internal standard, *er* determined *via* high-performance liquid chromatography (HPLC) using chiral stationary phases.

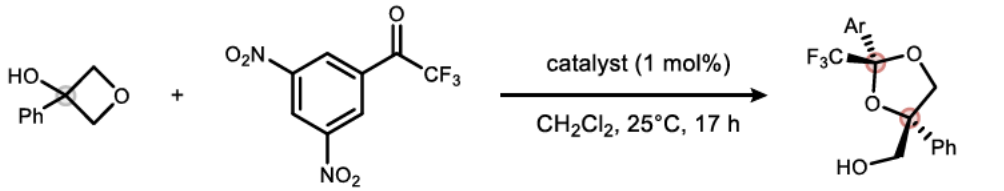

2.104 **2.52** **2.105**
Ar = 3,5-$(NO_2)_2$-C_6H_3

Entry	Catalyst	NMR yield	*dr*	*er*
1	–	–	–	–
2	**2.67**	90%	90:10	75:25
3	*epi*-**2.67**	52%	90:10	58:42
4	**2.68**	88%	96:4	86:14

For the use with alkynyl substituted substrates , catalyst **2.67** was found to be the superior catalyst, with overall improved yields and better stereocontrol in the

formation of dioxolane **2.106** (Table 3). Therefore, the scope of alkynyl substrates was probed using said catalyst.

Table 3: Evaluation of the catalyst for the transformation of arynes. Reactions performed on 0.1 mmol scale in CH_2Cl_2 [0.2 M]. NMR yield and *dr* determined *via* ^{19}F NMR with $PhCF_3$ as internal standard, *er* determined *via* high-performance liquid chromatography (HPLC) using chiral stationary phases.

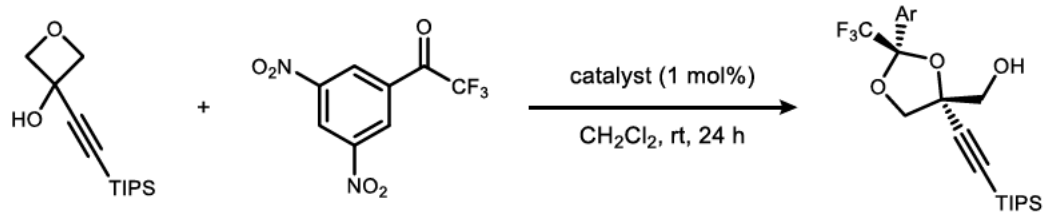

2.58 **2.52** **2.106**
Ar = 3,5-$(NO_2)_2$-C_6H_3

Entry	Catalyst	Isolated yield	*dr*	*er*
1	**2.68**	81%	99:1	88:12
2	**2.67**	87%	99:1	92:08

Following the optimisation of reaction conditions, the scope of alkyl and alkynyl substituted 3-oxetanols was investigated (Scheme 30). Several dioxolanes were prepared using the optimised conditions (*vide supra*). Alkyl substitution was tolerated with formation of dioxolane **2.107** in high yield and diasteroselectivity, but with diminished enantioselectivity. The introduction of alkynyl substituents resulted in a boost in reactivity, with overall excellent diastereo- and enantiocontrol up to 99:1 *dr* and 91:9 *er* and high yields of dioxolanes **2.108** to **2.111**. Furthermore, unsubstituted 3-oxetanol was tolerated and gave dioxolane **2.112** in good yield, though with a lower stereoselectivity. The overall scope featured broad tolerance of aryl and heteroaromatic systems with up to 98% yield, 98:2 *dr* and 96:4 *er*. Exemplary, substrate **2.113** from the scope of [redacted] is depicted. Still, the method remains limited to 3-oxetanols, as formation of dioxolane **2.114** was not observed under the reaction conditions. The reaction of alkyl or unsubstituted oxetanols was found to be sluggish, whereas aryl and alkynyl substituted substrates performed well under the reaction conditions. It can therefore be assumed, that interactions between the π-systems of the catalyst and substrate are a prerequisite for good stereoinduction.

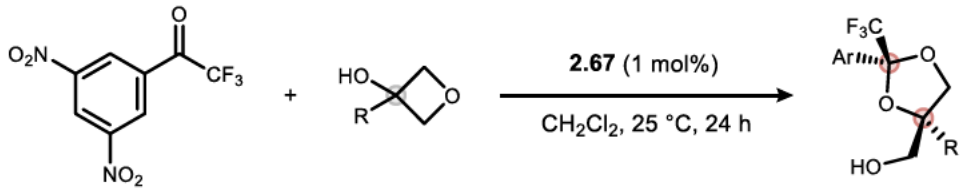

2.52

Ar = 3,5-$(NO_2)_2$-C_6H_3

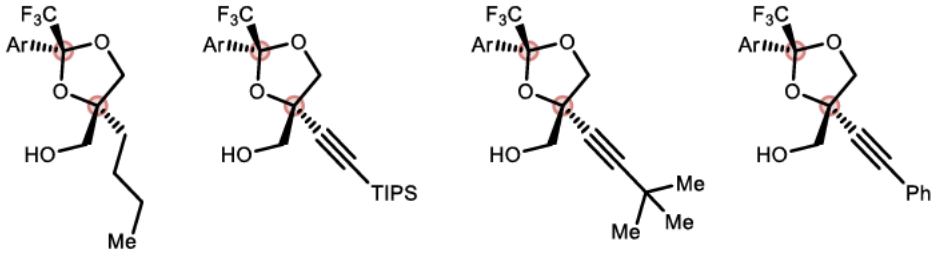

	2.107[c,d,e]	**2.108**	**2.109**	**2.110**
NMR yield[a]:	84%, 95:5 *dr*	97%, 99:1 *dr*	90%, 99:1 *dr*	94%, 98:2 *dr*
Isolated[b]:	78%, 72:28 *er*	85%, 91:9 *er*	87%, 88:12 *er*	92%, 86:14 *er*

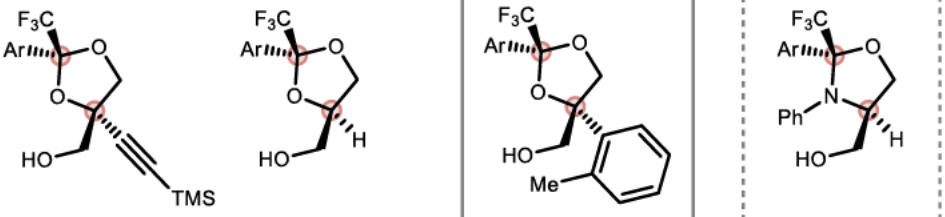

	2.111	**2.112**[d]	**2.113**[d,f]	**2.114**
NMR yield:	92%, 99:1 *dr*	85%, 72:28 *dr*	89%, 97:3 *dr*	Limitation
Isolated:	85%, 92:8 *er*	83%, 75:25 *er*	85%, 82:18 *er*	NMR yield: 0%

Scheme 30: Performed reactions in the scope of the desymmetrisation of oxetanols. Reactions were run on a 0.2 mmol scale in CH_2Cl_2 [0.2 M]. [a]Yield and diasteromeric ratios were determined by ^{19}F NMR using $PhCF_3$ as an internal standard. [b]The isoltated yield and *er* corresponds to the isolated major isomer, *er* was determined *via* HPLC using chiral stationary phases. [c]Oxetanols prepared by [redacted]. [d]Reactions were run with catalyst 2.68 instead of 2.67. [e] Reaction run at 40 °C. [f]Reaction performed by [redacted].

Next, the feasibility of other electron deficient ketones in the reaction was evaluated by a change from a CF_3 to a CF_2Cl group, and chlorodifluoro-acetophenone **2.53** was tested under the reaction conditions. Synthesis of dioxolane **2.115** was achieved in good yield and diasteroselectivity, however, with diminished enantioselectivity. This is probably due to the increased steric bulk of the CF_2Cl group, hindering enantiofacial discrimination during the reaction.

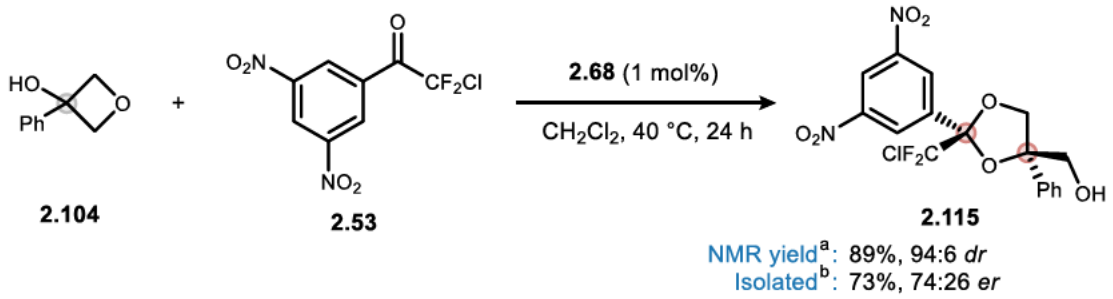

Scheme 31: Additional ketone used in the ring-opening; reaction performed by [redacted]. [a]Yield and diasteromeric ratio were determined by ^{19}F NMR using $PhCF_3$ as an internal standard. [b]The isoltated yield and *er* corresponds to the isolated major isomer, *er* was determined *via* HPLC using chiral stationary phases.

With the scope of the reaction established, further experiments were conducted to elucidate the mechanisms of the underlying transformation. As part of the investigation of the reactivity of different 3-oxetanols, electron deficient alkyne **2.56** was synthesised and its reaction with ketone **2.52** analysed. The formation of hemi ketal **2.116** was not spectroscopically detectable, yet dioxolan **2.117** was isolated after 24 h in 80% yield, most likely after Michael addition of the hemiketal to the activated alkyne. This result did not directly prove the existence of a transient species, but certainly suggests its existence as a necessity for product formation. Additionally, this reaction gave rise to the question, whether chemoselective functionalisation of alkynyl substituted oxetanols would be possible (*vide infra*).

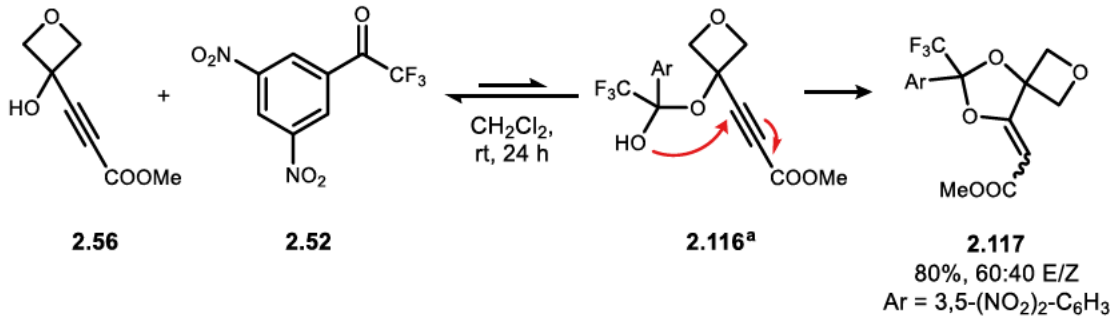

Scheme 32: Cascade reaction of a proposed transient hemi-ketal. [a] Spectroscopically not observed.

Consecutively, the chemoselective synthesis of dioxolanes **2.110** and **2.118** was realised by changing the metal catalyst from Co^{II} to Ag^{I}. The combination of silver nitrate and 1,8-diazabicyclo(5.4.0)undec-7-ene (DBU) efficiently catalyses the transformation from oxetanol **2.60** to dioxolane **2.118,** presumably by double activation of the alkyne and alcohol.

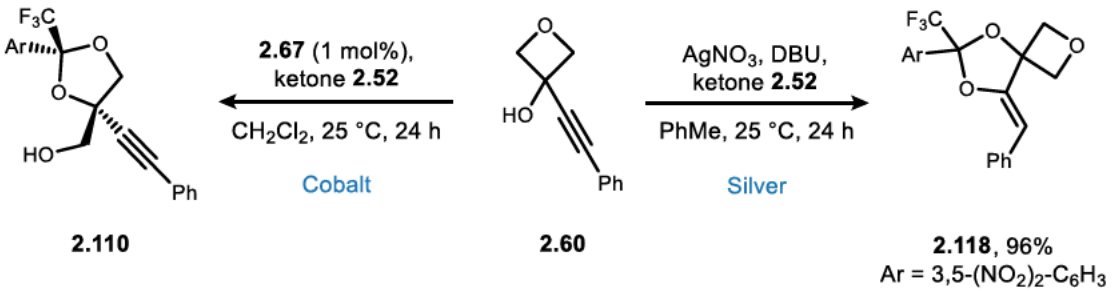

2.110 **2.60** **2.118**, 96%
Ar = 3,5-$(NO_2)_2$-C_6H_3

Scheme 33: Stereodivergent reaction depending on the choice of catalyst. Left: Reaction under standard conditions in CH_2Cl_2 [0.2 M] (see Scheme 30). Right: Reaction using silver and base, performed on 0.2 mM scale in toluene [0.2 M].

Gathering all the above-described information, a mechanism consisting of the integral formation of a transient hemi ketal in a DKR was devised by [redacted] (Scheme 34). Herein, the reaction of oxetanol **2.104** with ketone **2.52** leads to the dynamic formation of the hemi ketals **2.119** and *epi*-**2.119**, which can react with Co^{II}·salen **2.68** in different reaction rates based on an assumed stereogenic match/mismatch scenario. The increased acidity of the transient hemi ketals with an expected pK_a below 10, allows for the required aerobic oxidation of the catalyst to Co^{III},[81] and facilitates generation of intermediate **2.120**. The increased nucleophilicity of hemi ketalate **2.120** leads to ring opening towards cobalt alkoxide **2.121**, which can regenerate intermediate **2.120** under proton exchange with hemi ketal **2.119**, thus closing the catalytic cycle and giving dioxolane **2.122** as the major product of the transformation. Consequently, formation of the minor isomers occurs from hemi ketalates *epi*-**2.120** or **2.120**, where the nucleophile would then attack the sterically less accessible side of the oxetane.

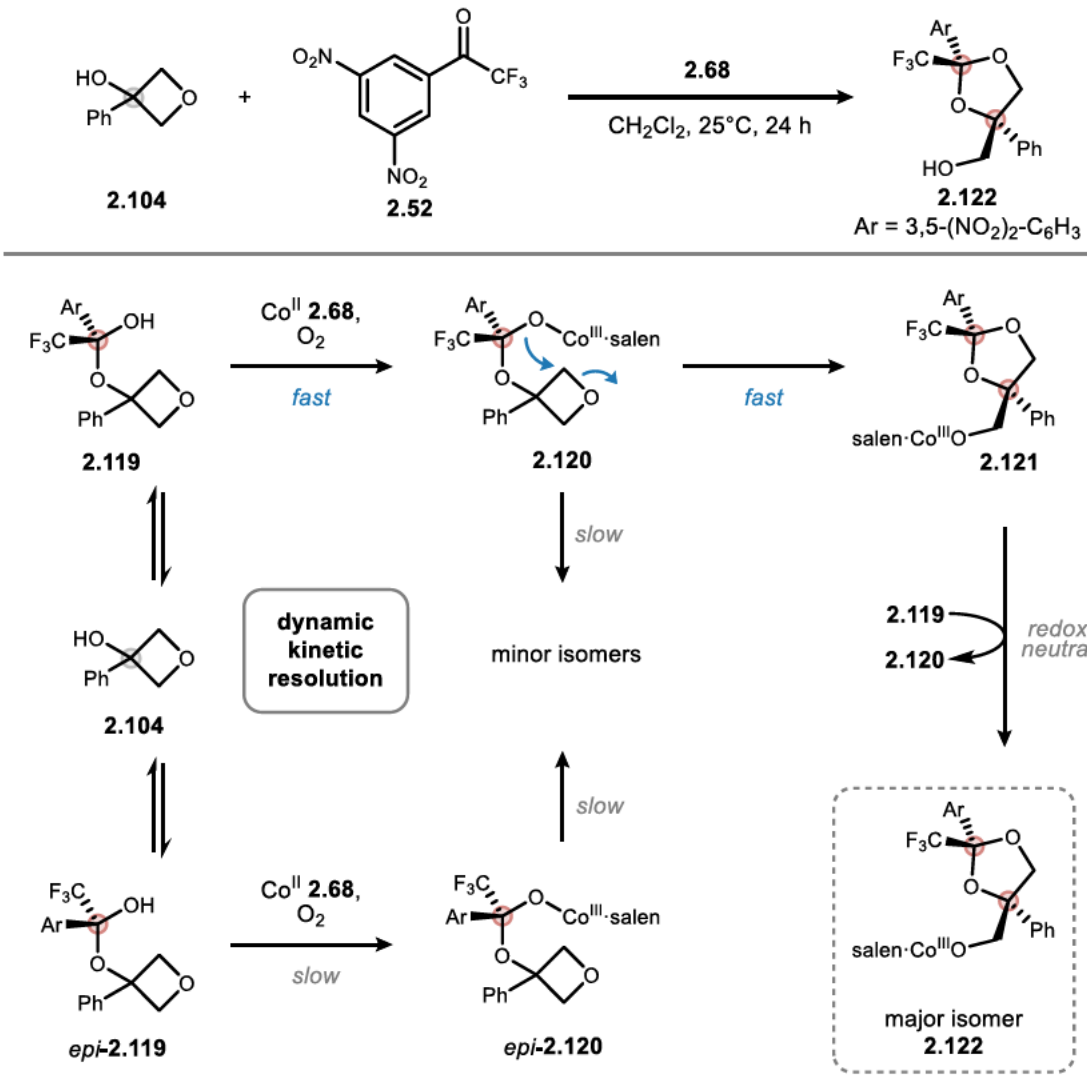

Scheme 34: Mechanistic proposal for the desymmetrisation *via* a dynamic kinetic resolution of a transient hemi ketal by [redacted].

2.6 Summary and outlook

The successful proof-of-concept of a build and release strategy for the synthesis of 1,3-dioxolanes from strained 3-azetidinols and 3-oxetanols was provided over the course of this project. *α*-Aminoacetophenones were identified as a versatile platform for the systematic investigation of the underlying geometric requirements of the Norrish-Yang cyclisation and a substance library was created from easily available building-blocks. Protecting groups at the heteroatom were found to have a strong influence on the cyclisation to fragmentation ratio and *N*-sulfonamides were found to be privileged for the photochemical synthesis of azetidines. Furthermore, the influence of sterically demanding substituents was accessed, and a balance between facilitation and hindrance of the cyclisation was determined. This culminated in the successful synthesis of azetidinol **2.80**, which

stems from an *α*-aminoacetophenone with the nitrogen protected by a sterically very demanding benzhydryl group. Additionally, the photochemical synthesis of 3-oxetanol **2.55** was demonstrated *via* Norrish-Yang cyclisation.

Next, the strain release reaction featuring 3-azetidinols was investigated, and the ring-opening demonstrated using transient hemi ketals. Again, the benzhydryl protection group was found to be crucial, delivering highly functionalised dioxolanes in good yields. Ring-opening reaction occurred without the need for external activation, when acidic hemi ketals from very electron-deficient ketones were employed. By sequential synthesis and ring-opening of benzhydryl-protected azetidinol **2.80** from acetophenone **2.123** (synthesised by [redacted]), the envisioned build and release strategy was conceptionally proven (Scheme 35).[82]

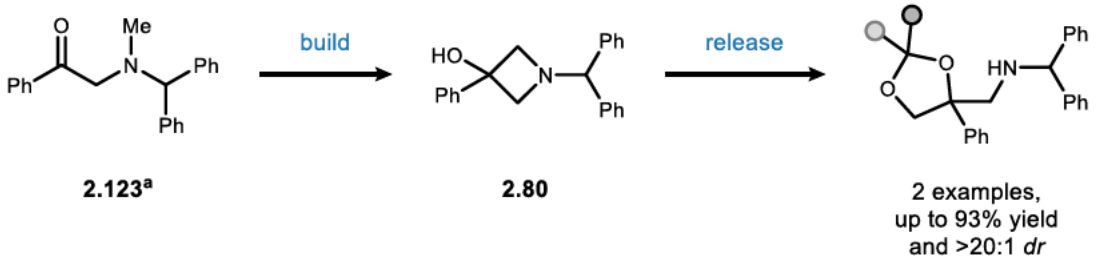

Scheme 35: Example of a successful build and release strategy using 3-azetidinols. [a] Acetophenone synthesised by [redacted].

In the third part of the project, the ring-opening of 3-oxetanols was investigated together with [redacted].[83] Contributions were made in the synthesis of electron-deficient 3'-5'-dinitroacetophenones, which were assigned as ideal reagent to form stable hemi-ketals by [redacted]. As evident above, the immense reactivity of these reagents can be successfully harnessed by more than one scaffold. Several alkynyl-substituted 3-oxetanols were synthesised and the uncatalysed intramolecular addition of the nucleophilic hemi-ketal into an activated alkyne was demonstrated. This provided further evidence for the needed catalytic activation of the oxetane-ring to be successfully ring-opened and inspired the silver-catalysed stereodivergent synthesis of spirocyclic dioxolane **2.118** in excellent yields. Following extensive optimisation by [redacted], *Katsuki*-type Co^{II}·salen complexes were synthesised, which delivered 1,3-dioxolanes in high diastero- and enantioselectivity. The scope of the reaction was expanded in this work to alkyl- and alkynyl-substituted oxetanols, with high yields for both diastereomers from 84 to 97% and stereoselectivities of up to 92:8 *dr* and 98:2 *er* (*cf.* chapter 2.5, Scheme 30; Scheme 36).

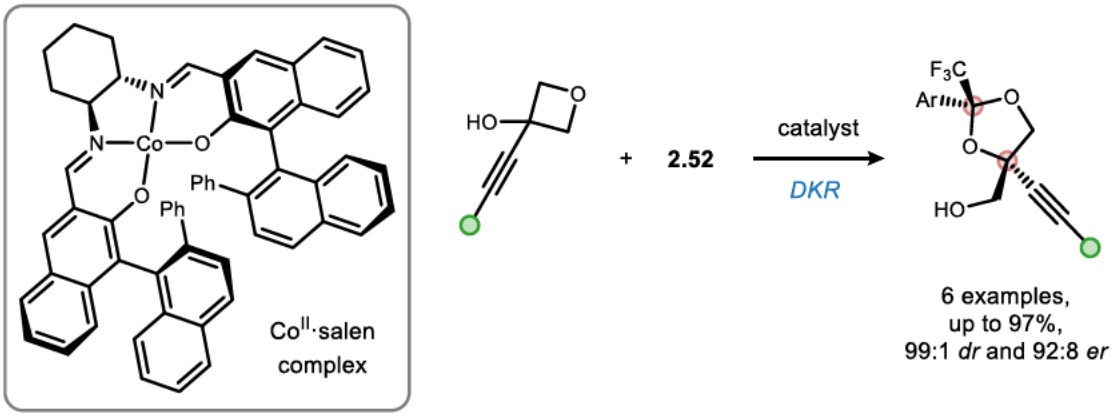

Scheme 36: Synthesis of alkynyl-substituted 1,3-dioxolanes from 3-oxetanols.

Since, the photochemical synthesis of 3-oxetanol **2.55** was demonstrated *via* Norrish-Yang cyclisation. Thereby, the formal proof-of-concept for the use of 3-oxetanols in a photochemical build and release approach was finally established, as well (Scheme 37).

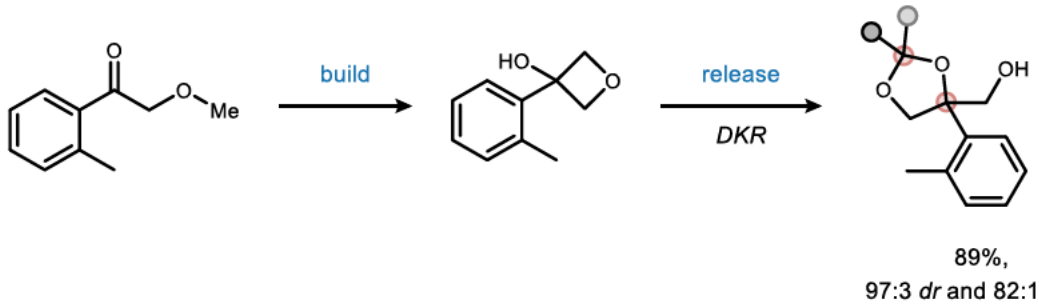

Scheme 37: Photochemical generation of a 3-oxetanol and enantioselective ring-opening. [a] Desymmetrisation reaction performed by [redacted]

For further developing the presented build and release strategies, improvements in the formation of strained heterocycles have to be made. Therefore, other sterically demanding substituents could be tested on the nitrogen atom in the discussed Norrish-Yang cyclisation of α-aminoacetophenones, ideally without abstractable hydrogen atoms. Here, introducing a trityl group seems to be a promising alternative, since it offers increased steric size while having similar electronic effects on the electron-density on the nitrogen atom compared to the best performing benzhydryl group in this work (Scheme 38, top). The photochemical synthesis of 3-oxetanols was proven to be feasible. Still, this reaction is underexplored and a systematic study, analogous to the generation of 3-azetidinols, could help in shedding light on the Norrish-Yang cyclisation of α-oxoacetophenones. (Scheme 38, middle).

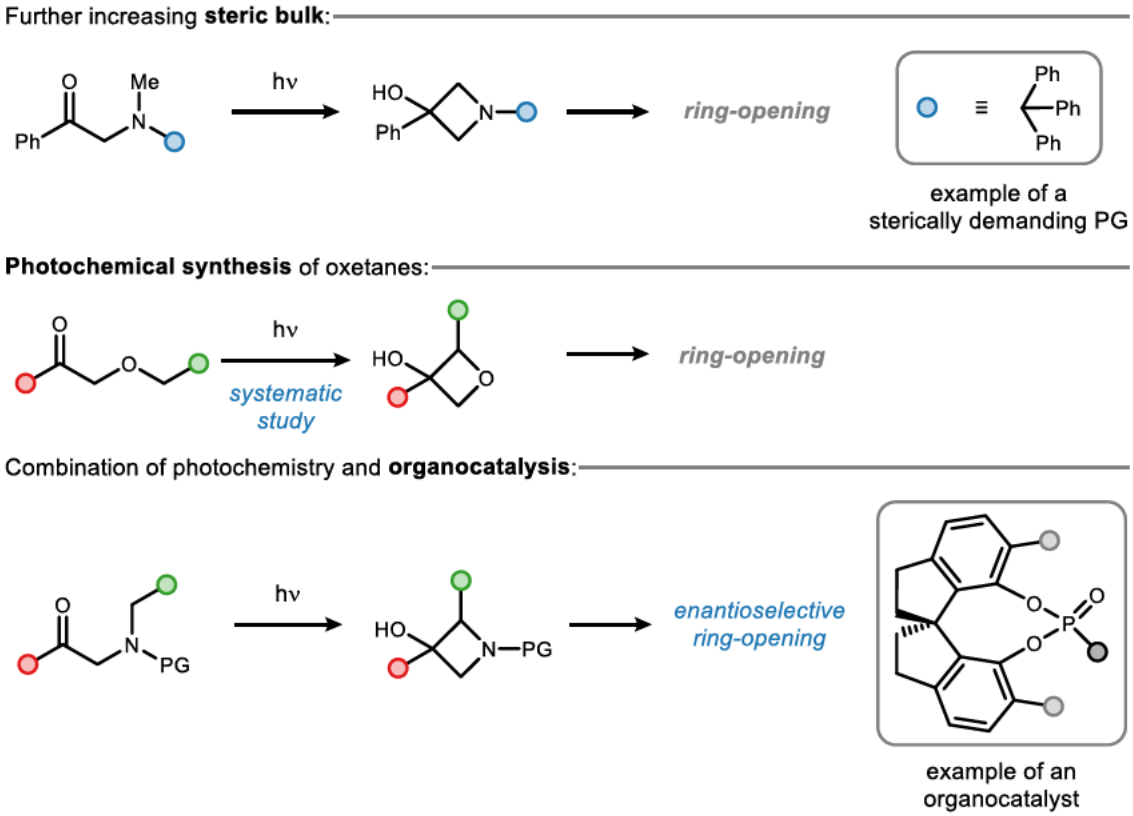

Scheme 38: Top: Improvement of the photocyclisation by introduction of sterically demanding trityl group. Middle: Systematic study of the photogeneration of 3-oxetanols. Bottom: Use of organocatalysts for an enantioselective ring-opening after photochemical formation of an3-azetidinol, generic phosphoric acid catalyst previously employed by *e.g.* *Sun* and coworkers.[55]

For improving the second half reaction[84] in the build and release strategy, compatible catalysts need to be found which allows for higher control over the stereoselectivity. Especially *Lewis* acid or *Brønsted* acid catalysts are promising (*cf.* 2.1.2, Scheme 10), as the activation of the nitrogen atom inside the strained heterocycle is the key for successful ring-opening reactions (Scheme 38, bottom).

3 Development of a molecular solar thermal system

3.1 Introduction

In the previous chapter, the Norrish-Yang cyclisation of *a*-substituted acetophenones towards strained four-membered heterocycles was used as the cornerstone of a build and release strategy using light (*cf.* chapter 2). While a proof-of-concept of both partial reactions was delivered, the selectivity of the initial photoreaction remains a drawback. The use of a structurally more rigid system was envisioned, hence limiting fragmentation reactions *via* the Norrish type II cleavage (*cf.* chapter 2.1.1). Photoreactions with high selectivity towards strained molecules provide rapid access to molecular complexity (*cf.* chapter 1.1). However, when a photochemical cyclisation towards a strained intermediate is combined with a selective back-isomerisation, the concept of the build and release of molecular strain can also be used for the storage of light energy in chemical bonds.

3.1.1 Storage of photon energy in molecular isomers

The concept of storing light energy in chemical bonds was first postulated in 1909 by *Weigert*.[85] He investigated the reaction of anthracene with sun light, which leads to formation of an insoluble product.[86] Upon heating, the starting material could be regenerated and additional thermal energy was released. This process was identified as a dimerisation process and hence the first storage of light energy inside a molecule was described.[87] Today, systems capable of storing energy during the photochemical isomerisation process of a molecule are referred to as molecular solar thermal (MOST) systems. Essentially, MOST systems follow the previously described rules of an endergonic build and release strategy (*cf.* chapter 1.1). However, the chemically stored photon energy is harnessed as heat, and not as fuel for endergonic chemical transformations. Following excitation with light (Scheme 39, A), a ground state isomer **3.1** is converted to its excited state **3.2**. This isomer can relax *via* internal conversion to its ground state, or react to the metastable isomer **3.3** (Scheme 39, B). The energetic difference ($\Delta H_{\text{storage}}$) between **3.1** and **3.3** defines how much energy is stored in the process. Ideally,

this energy is controllably released after external activation, *e.g.* by heating or through the addition of a catalyst (Scheme 39, C). Steps A and B together, are the charging of the system, in analogy to conventional energy storage systems like lithium-ion batteries. The step C can be interpreted as a discharging of the molecular energy and repetition of charging and discharging is referred to as a cycle of the MOST system.

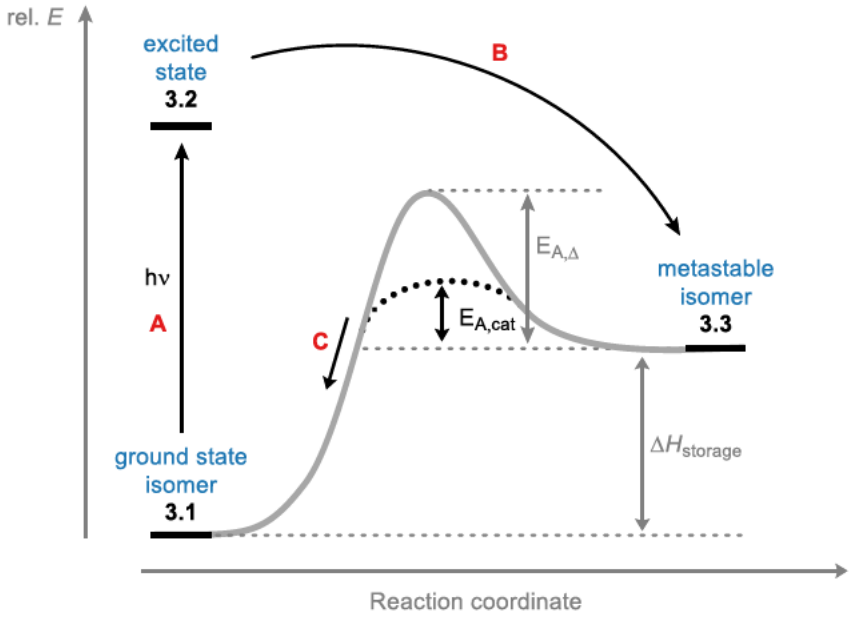

Scheme 39: Graphical representation of the processes of a MOST cycle. A: Excitation under absorption of light; B: Conversion process to form metastable isomer; C: Back-conversion to ground state isomer *via* thermal or catalytic activation.

A set of parameters of an ideal MOST system was devised by *Yoshida* in 1985,[88] and refined by several other authors over the years.[89] As 50% of all photons that reach the earth from the sun have a wavelength between 300 and 800 nm, the absorption spectrum of an ideal system should match this range.[89b] This includes visible light and a part of the UV spectrum. Furthermore, the efficiency of the conversion to a metastable isomer after irradiation should be as high as possible. The efficiency for this conversion is measured as the quantum yield (Φ) and should be close to unity, where each absorbed photon would induce a successful transformation to the desired isomer. An ideal system has a metastable state of very high energy that is indefinitely stable, unless an external trigger like heat, light of a different wavelength or a catalyst is applied. Unfortunately, the instability of a system usually increases with larger values of the energy storage density $\Delta H_{storage}$, as highly strained intermediates tend to spontaneously degrade over time (*cf.* chapter 1.1). Therefore, more realistic timespans, like months to bridge a cold winter or hours to bridge the gap between days and nights are usually

aimed for.[90] Additionally, the energy storage density $\Delta H_{storage}$ should exceed 300 kJ/kg to be practically applicable, which is higher than the value of conventional heat storage systems like salt hydrates.[89b,91] In order to maximise the efficiency of the transformation, the metastable isomer should have a shifted absorption spectrum compared to the ground state isomer. A lack of competition between the isomers for incoming photons reduces the risk of a backreaction or degradation of the metastable isomer during the irradiation. Generally, a high selectivity and lack of degradation are mandatory in during charging and discharging to allow for a high cycle number, that is repetition of storing and releasing of energy. The last criterion for the system is its sustainability. Hence, all compounds should be nontoxic and environmentally benign.[89a] So far, no system which matches all mentioned criteria was developed.

Prominent examples of advanced MOST systems are the pairs norbornadiene (NBD) ⇄ quadricyclane (QC) and *E*-azobenzene (*E*-azo) ⇄ *Z*-azobenzene (*Z*-azo). *Cristol* and *Snell* described the first photoreaction of NBD **3.4** towards QC **3.5** in a photochemical [2+2] cycloaddition (Figure 4, top).[92] Although nearly 1000 J/g are storable in the system NBD ⇄ QC and the possibility of energy release after heating, or by addition of metal catalysts is given,[93] a significant drawback exist. Unsubstituted NBD absorbs light only in the UV region,[94] rendering a direct employment as a solar light driven MOST system impossible. Attempts to overcome this hurdle were undertaken by addition of sensitisers to the process[95] and by molecular engineering. Introduction of substituents allows the absorption of NBD-derivatives to be shifted towards the visible spectrum, still this usually leads to an increased rate of back-isomerisation or degradation for derivatives with a high energy density.[96]

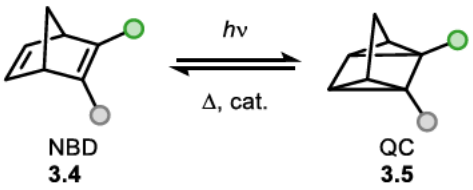

Absorption	UV
$\tau_{1/2}$	hours-days
ΔHstorage	≤ 1000 J/g
Trigger	Δ, catalyst

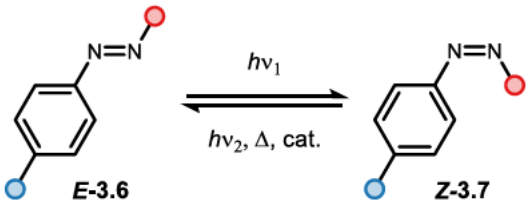

Absorption	300-500 nm, competition E/Z
$\tau_{1/2}$	hours-days
$\Delta H_{storage}$	100-400 J/g
Trigger	Δ, catalyst, *hν*

Figure 4: Top: NBD ⇄ QC system by *Cristol* and *Snell* for unsubstituted NBD,[92] and parameters of typical systems (right)[96]. Bottom: *E*-Azo ⇄ *Z*-Azo system.[97]

Another well-developed system is the *E*-Azo ⇄ *Z*-Azo pair (Figure 4, bottom). *E*-Azo **3.6** undergoes a π→π* transition after absorption of UV light and isomerises to *Z*-azo **3.7**. The stored energy is releasable by irradiation with more energetic light, heating or by addition of a catalyst.[98] The *E*-Azo ⇄ *Z*-Azo pair is precisely tunable by variation of the substituents, which affects the absorption spectrum, energy density and storage time.[99] Typically, the overall absorption spectrum is shifted to more energetic wavelength upon reaction from *E*-Azo **3.6** to *Z*-Azo **3.7**, however the difference is generally very small. As the back-isomerisation is catalysed by excitation of the isomer *Z*-Azo **3.7** with light, the use of precise filters is needed to achieve full conversion of a system by selective excitation of *E*-Azo **3.6**. Otherwise, both isomers will exist in equilibrium in a photo stationary state, limiting the total amount of storable energy.[100]

Many parameters of MOST systems are interdependent. Optimisation of *e.g.* the red-shift of the absorption of a substance will directly influence $\Delta H_{storage}$. Substituents that extend the conjugated system to achieve the desired absorption range are usually introduced at the downside of increasing the molecular weight, which will in turn diminish the energy storage capacity (kJ/kg).[101] Often, EWGs and EDGs are combined in a push-pull configuration for a maximised effect.[102] However, this shift of the absorption spectrum to longer wavelength is usually met with a decreased barrier of activation for the back-isomerisation, which will lower the possible storage time.[103] Additionally, modifications of the substrates

structure will change other inherent molecular properties. The quantum yield, for example, might drastically change with different substituents and so far, no strategies for its optimisation or tuning are known.[89a]

The inherent struggle of detrimental interdependency of system properties was met with several ideas based on molecular engineering. Two or more photoswitches can be combined in one molecule by a linker, which allows for tuning of absorption maximum, energy density and storage time.[104] One example are systems sharing an electron donor-acceptor linker, where the energy density is increased as the systems share both the benefit of the absorption shift and molecular weight penalty.[105] Also, selective switching of the different molecules inside the system becomes possible and simultaneously allows for a broader absorption of the solar spectrum, if the chromophores of the systems differ enough.[106] The overall system must be taken into account, as solvents and additional components will negatively influence the overall possible energy density. Using very high concentrations is needed in this regard, and molecular liquids were designed to use systems neat without any solvent.[107] Still, efforts to introduce solubilising chains increased the molecular weight and led to more side reactions or degradation. [108] Actual heat release was shown for a fully charged push-pull QC system to reach 85 °C of temperature change in one minute,[109] and other examples of the release of more than 50 °C were shown.[110] The solar capture efficiency can also be increased to 85% by combination of MOST devices with traditional solar systems. This was demonstrated with NBD derivatives in a fluid reactor, where solar light was first absorbed by the MOST system and the residual light used to heat water in a layer below the MOST system.[111]

3.1.2 Motivation and aim

As outlined above, several MOST systems, that can satisfy multiple of the ideal parameters devised by *Yoshida,* exist. Yet, no system satisfies all parameters, and sufficient coverage of the solar spectrum and high energy density are often antagonistic. Substrate **3.8** was envisioned as a model substrate for a systematic investigation of the feasibility of *ortho*-alkylacetophenones for the application as MOST systems (Scheme 40). Although their cyclisation under irradiation with light towards benzocyclobutenols and the heat induced opening of the latter substance class are known,[69] the system *ortho*-alkylacetophenone ⇄ benzocyclobutenol was not extensively investigated as a potential MOST system. The combination of a strained four-membered ring and a low expected molecular weight are promising prerequisites to obtain a high energy storage density. Inspired by the successful application of an NMR scale approach in chapter 2, the strategic incorporation of a fluorine group can allow for the monitoring the reaction progress *via* ^{19}F NMR spectroscopy. Thereby, even the slightest notion towards side-reactions or degradation are detectable by changes in the chemical shift.

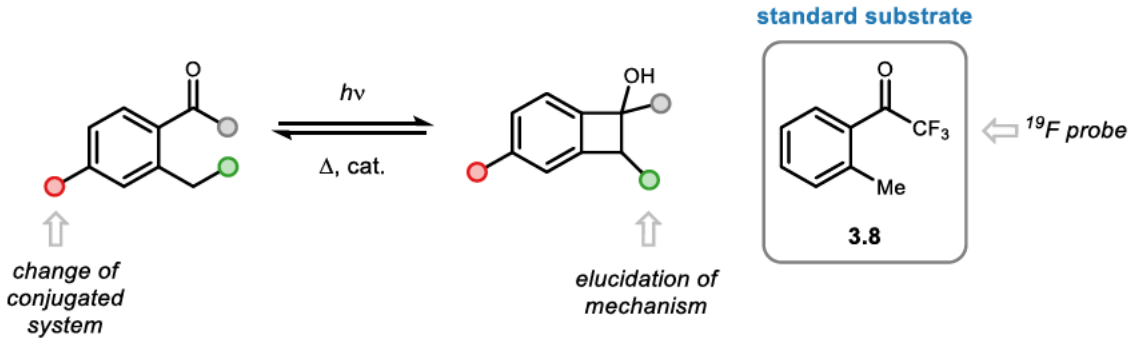

Scheme 40: *Ortho*-alkylacetophenones as platform for MOST system development.

Following a thorough investigation of the properties of *ortho*-alkylacetophenone **3.8**, molecular variations by introduction of substituents were to be tested. *Para*-substitution of acetophenones shifts the absorption maximum and changes the nature of the lowest excited states.[112] Hence, possibilities for tuning the reactivity of the system are presented. Additionally, incorporation of substituents in the *ortho*-position aids in determining the underlying mechanism of the transformation, which will be investigated, as well.

3.2 Synthesis of starting materials

As described above, *ortho*-alkylacetophenones were sought to be used as the core structure of this project. Generally, due to the observed high volatility of the desired *ortho*-alkylacetophenones, the use of low boiling solvents for their preparation and separation is emphasised. Additionally, bulb-to-bulb distillation was deemed crucial to obtain reproducible results in the following photoreactions.
Reactions were run in diethyl ether and column chromatography was performed in pentane or pentane/diethyl ether mixtures, as some products were found to co-evaporate in solvents like ethyl acetate (EtOAc) or THF. Additionally, bulb-to-bulb distillation was deemed crucial to obtain reproducible results in the following photoreactions.
A library of trifluoroacetophenones (**3.8** to **3.16**) was synthesised following a modified literature procedure through nucleophilic addition of carbon nucleophiles to ethyl trifluoroacetate **3.17**.[113]

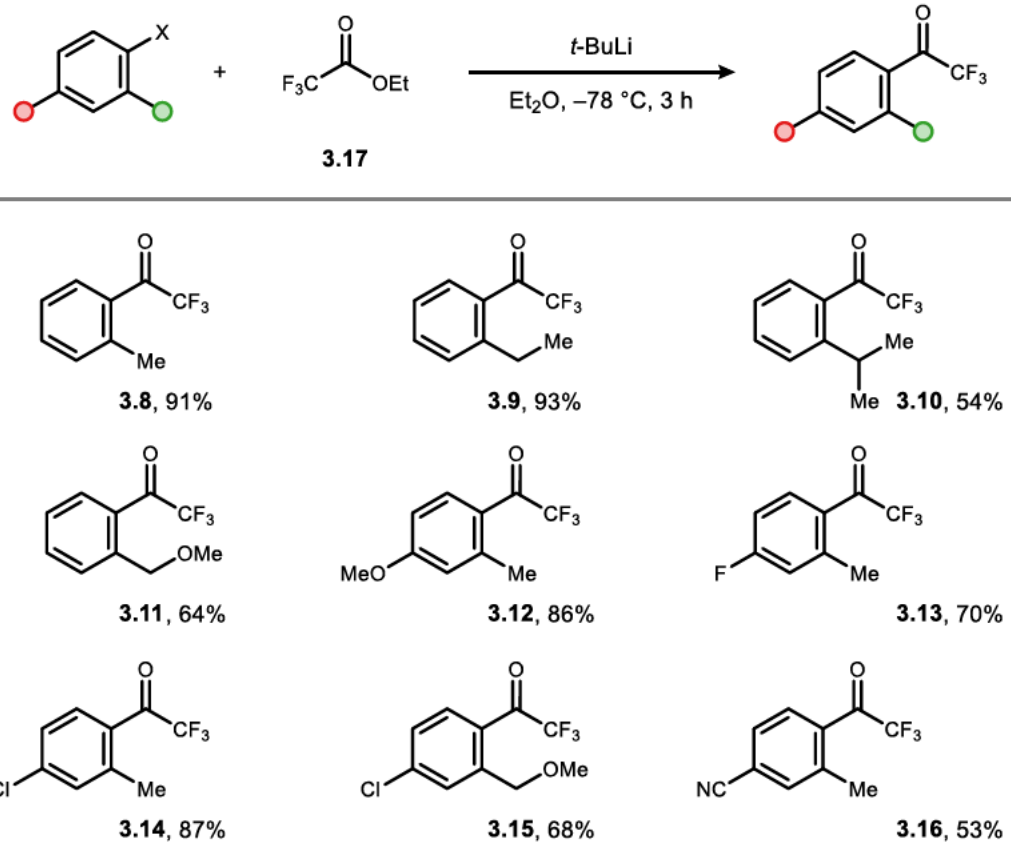

Scheme 41: Synthesis of trifluoroacetophenone derivatives *via* lithium-halogen exchange and subsequent nucleophilic addition of carbon nucleophiles.

Aryl lithium species were generated *via* lithium-halogen exchange from aryl halogenides, preferably bromides and iodides. Both methods delivered the desired products in good to excellent yields, however, use of bromides resulted in a

higher selectivity in the formation of the desired products under the optimised conditions.

Other partially fluorinated 2-substituted acetophenones were synthesised, following an adapted procedure from *Yang et al.*[114] The single fluorinated acetophenone **3.18** was obtained from 2-bromotoluene **3.19** and fluoroacetonitrile **3.20**. Initial lithium-halogen exchange is followed by a nucleophilic addition to acetonitrile, and aqueous work-up generates the acetophenone structure.

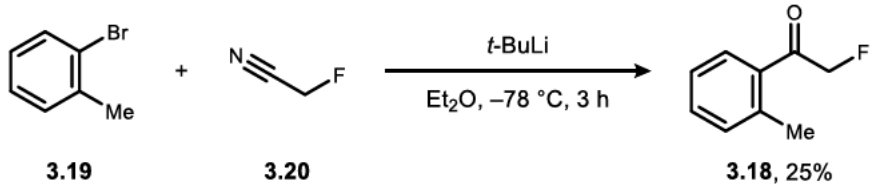

3.19 **3.20** **3.18**, 25%

Scheme 42: Preparation of 2-fluoroacetophenone 3.18 *via* an adapted literature procedure.[114]

Following a procedure from *Olah* and coworkers, selective removal of a fluorine allowed the generation of difluoroacetophenone **3.21** via the difluoroenol silyl ether **3.22** from **3.8**. The exact mechanism of the transformation was not elucidated, but it was postulated to occur *via* a reductive two-electron transfer process from magnesium.[115]

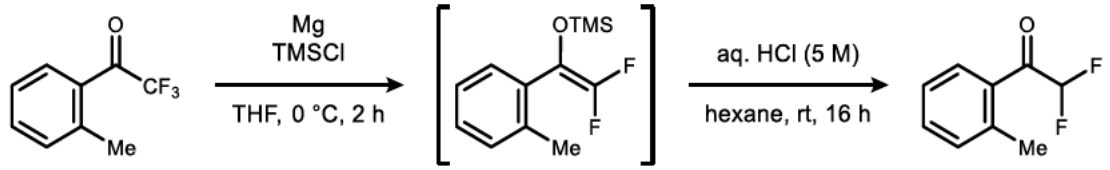

3.8 **3.22** **3.21**, 40%

Scheme 43: Synthesis of 2,2-difluoroacetophenone 3.21 according to *Olah* and coworkers.[115a]

The benzoyl formiate ester **3.23** was prepared following a procedure from *Liang et al.*[116] Chloroform and sodium hydroxide generate dichlorocarbene, which adds into aldehyde **3.24** in a nucleophilic attack. Hydrolysis generates *ortho*-methylmandelic acid, which is converted to intermediate **3.25** in an esterification with methanol and sulfuric acid. Oxidation with *Jones* reagent finally gives the desired product **3.23**.

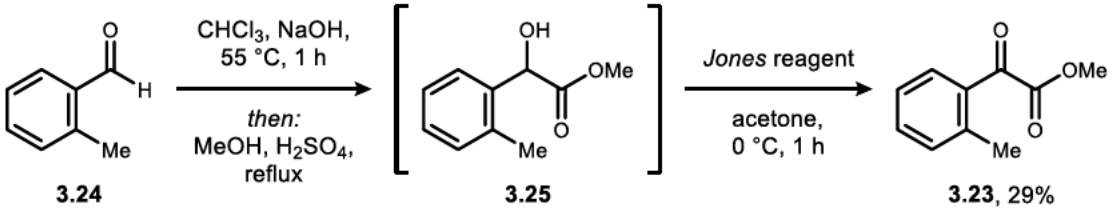

3.24 **3.25** **3.23**, 29%

Scheme 44: Synthesis of benzoyl formiate ester 3.23 according to *Liang et al.*[116]

3.3 Development of reaction conditions

3.3.1 Solvent screening

At first, a solvent screening on NMR scale using the standard substrate **3.8** was performed (Table 4). Generally, solvents were degassed (3 × freeze-pump-thaw) and in this optimisation, the solvent was removed after the reaction. Reactions were performed in the *Luzchem* photoreactor (*cf.* chapter 4.1, Figure 26). The trifluoromethyl group of **3.8** allows for a convenient monitoring *via* ^{19}F NMR, even in non-deuterated solvents. Methanol as a polar protic solvent failed to deliver the product **3.26** in relevant yields (Table 4, entry 1), whereas polar aprotic solvents like acetonitrile facilitated the desired transformation (entry 2). Ethyl acetate showed the highest yield with 70% (entry 3), but formation of side-products was evident from the ^{19}F NMR spectra. Apolar solvents were successfully used (entries 4-6), from which benzene (PhH) stands out based on an outstanding performance with a perfect selectivity for product formation without any detectable side reactions (entry 6).

Table 4: Solvent optimisation, reactions were performed on 0.05 mmol scale in degassed solvents (20 mM) under inert gas atmosphere. Solvent was removed under reduced pressure and residue dissolved in $CDCl_3$. Yields determined using ^{1}H NMR with mesitylene as internal standard.

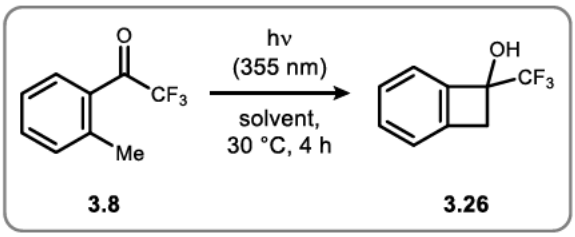

Entry	Solvent	Yield
1	MeOH	5%[a]
2	MeCN	32%[a]
3	EtOAc	70%[a]
4	CyH	41%[a]
5	hexane	34%[a]
6	PhH	45%

[a]Several signals detected in ^{19}F NMR.

Deuterated benzene (C_6D_6) provides additional advantages, as it is readily available and allows for a direct analysis of the crude reaction mixture *via* ^{1}H and ^{19}F NMR spectroscopy. The omitting of a reaction work-up provides an ecological benefit through chemical waste minimisation and prevents substance loss, as the product was found to be volatile. A loss of at least 10% of the employed mass through co-evaporation was detected for all solvents as evident by ^{1}H NMR spectra against mesitylene as an internal standard. Therefore, the following optimisations were performed in deuterated benzene.

3.3.2 Robustness of the reaction

The robustness of the reaction was evaluated next, following a literature known procedure from *Pitzer et al.*[117] Here, an initial reaction is performed to establish a benchmark performance, and sequentially the individual parameters of the reaction are changed to determine their influence on the reaction outcome. Highly reproducible reaction set-ups and the use of stock-solutions are necessary to achieve accurate results und reactions were performed under dry and degassed conditions. This allows for easy and measured changes to *e.g.* the water or oxygen content. Additionally, the light intensity was varied by changing the distance of samples to the lamp, different concentrations and reaction scales were employed and the influence of temperature was evaluated. Reactions were performed on an NMR scale and a 370 nm Kessil lamp was used for irradiation (for setup details see chapter 4.1, Figure 27).

At first, the influence of the parameters on the initial rate of the reaction were assessed (Table 5, Figure 5). All reactions were terminated after 30 minutes, which meant 39% yield in the reference reaction. The reactions were performed sequentially, and control reactions were performed throughout the process to validate the reproducibility of the reaction under unchanged conditions (Table 5, entries 5 & 9). The initial rates of the reaction depend most strongly on the intensity of the illumination source (entries 1 & 2), with a clear deviation of –69% respective to the reference for low irradiation intensity (*I*). A finding, which is in accordance to the presumed activation through photon excitation. Still, the reaction shows a dependency of its initial rates on the amount of oxygen inside the reaction vessel (entries 3 & 4) and the temperature (*T*, entries 6 & 7). A high water content (entry 8) and the scale of the reaction (entry 13) are not detrimental to its initial rates. However, an influence of the concentration was evident (entries 10 to 12).

Table 5: Sensitivity screening after 30 min, reactions run at 10 µmol scale in 0.5 mL C_6D_6 [20 mM] at 30 °C with 1 cm distance to 370 nm Kessil lamp (standard conditions), NMR yield based on ^{19}F NMR using $PhCF_3$ as internal standard.

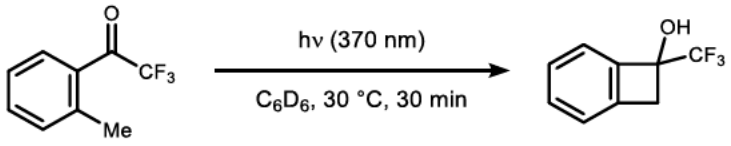

3.8 **3.26**

Entry	Change to conditions	Procedure	Yield	Deviation
1	low *I*	*d* = 10 cm	12%	–69%
2	medium *I*	*d* = 5 cm	30%	–23%
3	medium O_2	no degassing	33%[a]	–15%
4	high O_2	purge with O_2	30%[a]	–23%
5	control 1	-	39%	0%
6	low *T*	15 °C	33%	–15%
7	high *T*	45 °C	57%	46%
8	high H_2O	+5 µL H_2O	45%	15%
9	control 2	-	41%	5%
10	low conc.	10 mM	47%	21%
11	medium conc.	40 mM	40%	1%
12	high conc.	200 mM	32%	–18%
13	big scale	2 mM scale	39%	0%

[a] Formation of another product visible *via* ^{19}F NMR.

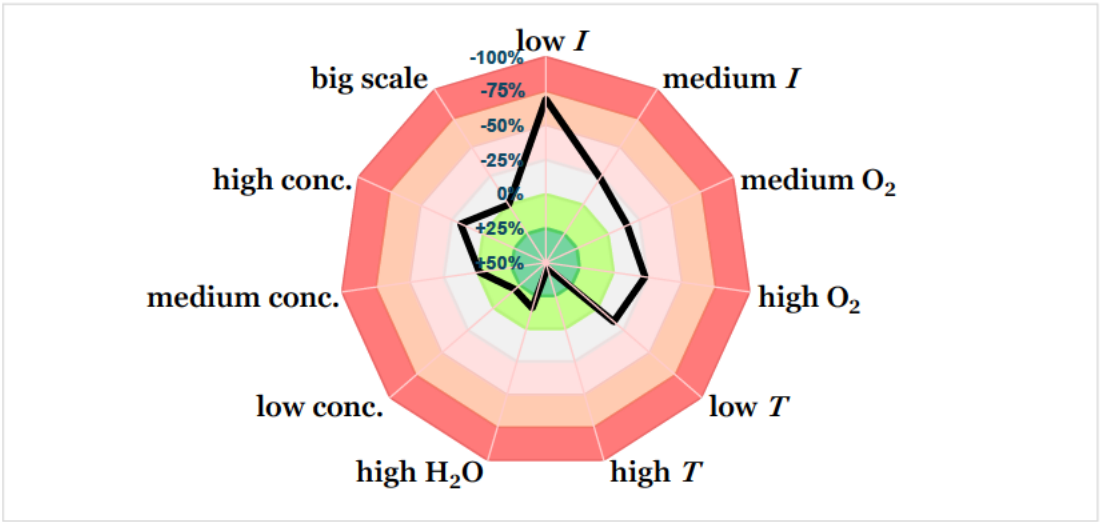

Figure 5: Visualisation of the sensitivity screening after 30 min according to *Pitzer et. al.*[117]

From these initial rates, no clear conclusions regarding the usability and robustness of the overall system can be drawn. Therefore, another set of experiments was envisioned, where the reactions were driven to full conversion, allowing for the assessment of the reactions global performance. The reaction time was envisioned to be 8 h for full conversion and the yields were determined *via* ^{19}F NMR spectroscopy (Table 6, Figure 6). The actual set-up of these reactions was performed by [redacted] following the developed methods in the initial rates experiment.

As evident from the data, the overall reaction is very robust with no dependency on intensity (Table 6, entries 1 & 2), temperature (entries 6 & 7), concentration (entries 9 - 11) or scale (entry 12). Yet, a stark influence of oxygen on the reaction was displayed by ~20% diminished yield in both cases (entries 4 & 5). Additionally, no influence of the water content inside the reaction vessel (entry 8) was found and a reproducibility under unchanged conditions was validated (entry 3).

Table 6: Sensitivity screening after 8 h, reactions run at 10 µmol scale in 0.5 mL C_6D_6 [20 mM] at 30 °C with 1 cm distance to 370 nm Kessil lamp (standard conditions) performed by [redacted], NMR yield based on ^{19}F NMR using $PhCF_3$ as internal standard.

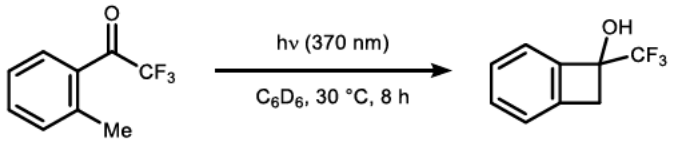

3.8 **3.26**

Entry	Change to conditions	Procedure	Yield	Deviation
1	low *I*	*d* = 10 cm	98%	–1%
2	medium *I*	*d* = 5 cm	99%	0%
3	control 1	-	>99%	1%
4	medium O_2	no degassing	79%[a]	–20%
5	high O_2	purge with O_2	76%[a]	–22%
6	low *T*	20 °C	99%	0%
7	high *T*	45 °C	>99%	1%
8	high H_2O	+5 µL H_2O	>99%	1%
9	low conc.	10 mM	99%	0%
10	medium conc.	40 mM	95%	–4%
11	high conc.	200 mM	96%	–3%
12	big scale	2 mM scale	92%	-7%

[a] Formation of another product visible *via* ^{19}F NMR.

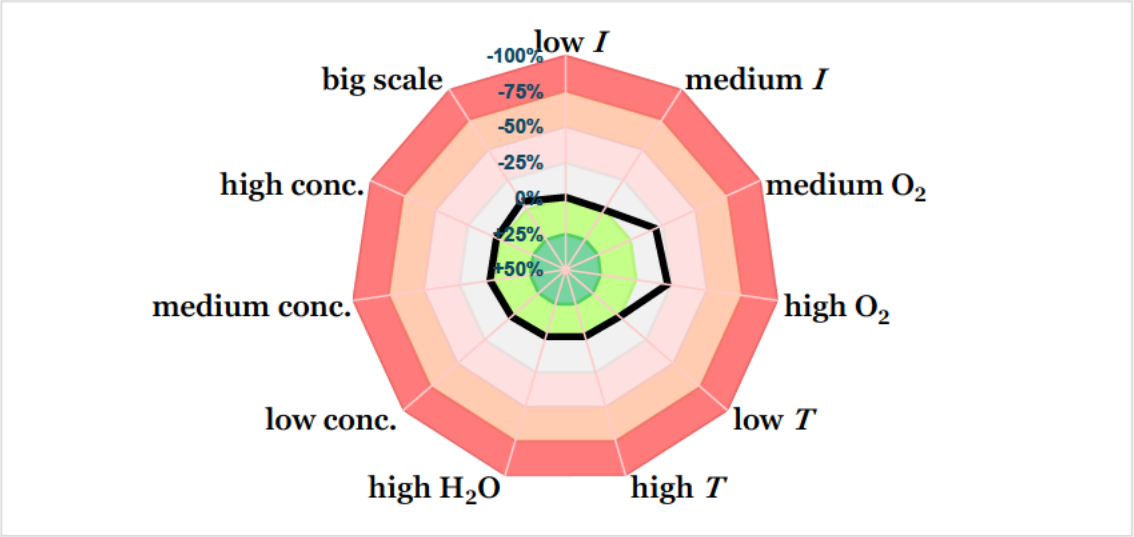

Figure 6: Visualisation of the sensitivity screening after 8 h according to *Pitzer et. al.*[117]

3.3.3 Investigation of key parameters

The oxygen content of the solution was found to be the most determining parameter for the successful transformation of acetophenones **3.8** to benzocyclobutenol **3.26** (*vide supra*). Therefore, a thorough investigation of the influence of oxygen was performed by irradiation of acetophenone **3.8** in oxygen saturated C_6D_6 (Scheme 45). Indeed, formation of a new species was observed *via* NMR spectroscopy and high resolution mass spectrometry (HRMS) and assigned to be the peroxide **3.27.**

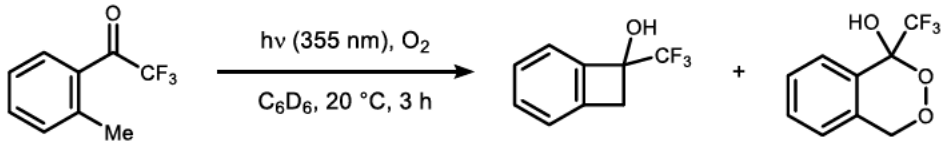

3.8 **3.26**, 37% **3.27**, 32%[a]

Scheme 45: Synthesis of a cyclic peroxide 3.27, reaction performed on 10 µmol scale in oxygen saturated C_6D_6 (20 mM) in the *Luzchem* photoreactor (355 nm), NMR yield based on ^{19}F NMR using $PhCF_3$ as internal standard. [a] Residual percentage unreacted starting material.

The cyclisation product **3.26** was isolated as a colourless solid, which has a melting point of 39-44 °C. Furthermore, its molecular structure was unambiguously identified *via* X-Ray diffraction (CCDC 2371853, Scheme 46). Elongation of the benzocyclobutenol C–C bond is detected (1.58 Å), which reflects the distortion of the strained ring.

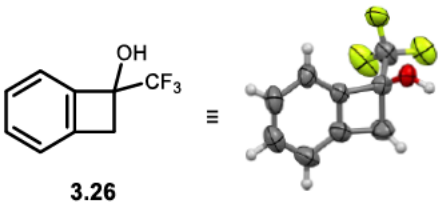

3.26

Scheme 46: Graphical representation of the molecular structure of product 3.26 determined *via* X-ray diffraction, thermal ellipsoids are depicted at 50% probability. CCDC 2371853.

Peroxide **3.27** was stable towards column chromatography and storable at –20 °C for months, however found to slowly decompose in solution towards hemiacetals **3.28** (Scheme 47). The structure of the dihydroisobenzofuran **3.28** was unambiguously identified *via* X-ray diffraction (CCDC 2371855).

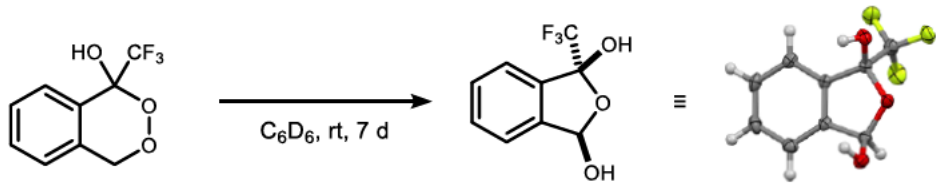

3.27 **3.28,** 2:1 *dr*

Scheme 47: Decomposition of peroxide 3.27 to dihydroisobenzofuran 3.28 in solution. Right: Molecular structure of the decomposition product 3.28 determined *via* X-ray diffraction, thermal ellipsoids are depicted at 50% probability. CCDC 2371855.

The structure of the cyclic peroxide was further supported by synthesis of benzocyclobutenol **3.29** and peroxide **3.30**. The reaction was performed under oxygen atmosphere in hexane, which dissolves higher amounts of oxygen compared to benzene (Scheme 48).[118]

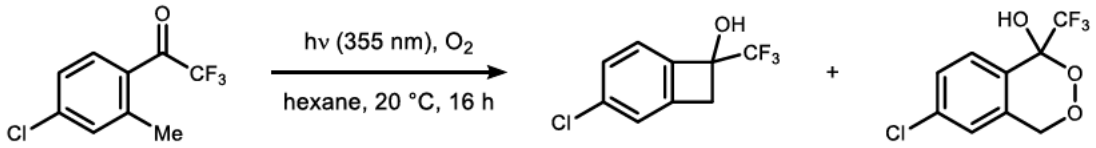

3.14 **3.29**, 16% **3.30**, 84%[a]

Scheme 48: Synthesis of benzocyclobutenol 3.29 and peroxide 3.30, reaction performed on 0.5 mmol scale in hexane (20 mM) under oxygen atmosphere with 355 nm lamp, [a] NMR yield based on ^{19}F NMR using $PhCF_3$ as internal standard.

Indeed, peroxide **3.30** was formed as the major product and its structure was unambiguously determined *via* X-ray diffraction (CCDC 2371857, Scheme 49).

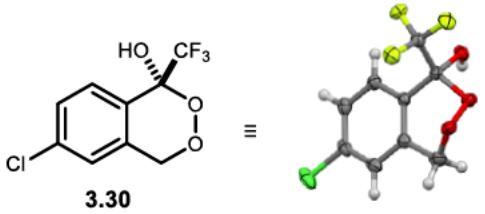

3.30

Scheme 49: Graphical representation of the molecular structure of peroxide 3.30 determined *via* X-ray diffraction, thermal ellipsoids are depicted at 50% probability. CCDC 2371857.

As a high lamp intensity was found to be beneficial for the overall performance, different sources were compared next. (Table 7).

Table 7: Evaluation of different irradiation sources, reactions were performed on 0.01 mmol scale in degassed C_6D_6 (20 mM) under inert gas atmosphere at 28 °C, yield determined *via* ^{19}F NMR with $PhCF_3$ as internal standard. Lamps used: *Luzchem* photoreactor (355 nm, 10 × 8 W mercury fluorescence lamps; 420 nm, 10 × 8 W LED), 45 W Kessil LED lamps (370 nm, 390 nm).

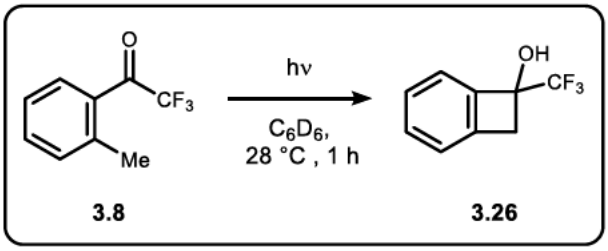

Entry	Wavelength	Yield
1	355 nm	13%
2	370 nm	86%
3	390 nm	11%
4	420 nm	0%

Here, all lamps that emit light in the UV region, namely 355 nm, 370 nm and 390 nm (entries 1-3), facilitate the desired transformation, while visible light does not (entry 4). The 370 nm Kessil LED delivers the highest yield (entry 2) and provides strongly focused light and was therefore selected as illumination source for single sample experiments (cf. chapter 4.1, Figure 27). The 355 nm lamps in the *Luzchem* photoreactor show a significant lower reaction rate but have a clear advantage when several experiments need to be measured at the same time, as the evenly illuminated space inside the *Luzchem* photoreactor is bigger. Additionally, a sample turntable can be employed, which guarantees even illumination of all samples over time (*cf.* chapter 4.1, Figure 26). Therefore, multi-sample experiments were conducted inside the photoreactor under extension of the irradiation duration. Altogether, these results show, that light in the UV range of the solar spectrum can charge the envisioned MOST system. Accordingly, the use of sun light was investigated next.

A reaction set-up consisting of an NMR tube and a light reflector was constructed and samples of acetophenone **3.8** in degassed C_6D_6 were subjected to sunlight on different days with varying weather conditions (Figure 7, Table 8).

Figure 7: Set-up for solar irradiation. An NMR tube is held by a clamp and a reflector made from half-circular plastic tube and a silver-coated foil is used for focussing solar light.

As expected from the successful employment of lamps in the spectral range from 355 to 390 nm, solar irradiation gave benzocyclobutenol **3.26** in excellent yields of up to 95%, even on a cloudy day (Table 8, entry 1). Employing the system outside of the controlled environment of a chemical laboratory emphasised the need for careful preparation and sealing of samples, as oxygen exclusion remains a challenge (entry 3).

Table 8: Reaction of acetophenone 3.8 under solar irradiation, reactions were performed on 0.01 mmol scale in degassed C_6D_6 (20 mM) under inert gas atmosphere at 28 °C for 4 h, yield determined *via* ^{19}F NMR with $PhCF_3$ as internal standard.

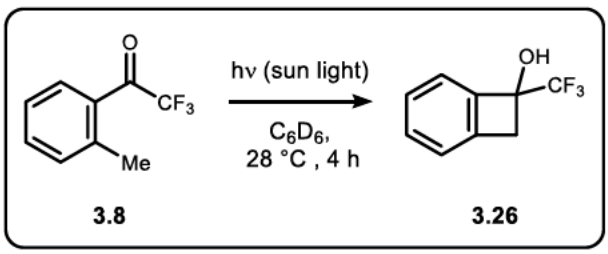

Entry	Date	Yield
1	22.08.2023	81%[a]
2	06.09.2023	95%
3	07.09.2023	84%[b]

[a] Cloudy sky. [b] Formation of 6% peroxide **3.27** detected.

In the sensitivity screening, no influence of the scale of the reaction on its overall performance was determined (*cf.* chapter 3.3.2). For an application of a MOST system and general synthetic purposes, it is advantageous if large scale syntheses of the desired substances are achievable. Therefore, several reactions employing larger scales were demonstrated (Table 9). On 4.7 mmol scale (entry 1), near quantitative isolation was achieved. However, the reaction time was extensive with 90 hours, and the illumination source was changed from mercury fluorescence lamps (355 nm) to an LED (370 nm). Changing to a more efficient LED with a smaller optical focus allowed the irradiation time to be dropped to 10 hours, while still maintaining a high isolated yield (entry 2). At last, the reaction was conducted on a 10.7 mmol scale at almost double the concentration (0.9 M), which showed no signs of side reactions or degradation and was isolated in good yield (79%, entry 3).

Table 9: Large scale reactions, performed in degassed PhH in the *Luzchem* photoreactor (355 nm) or with a Kessil lamp (370 nm) at rt, NMR yields determined *via* ^{19}F NMR using $PhCF_3$ as internal standard.

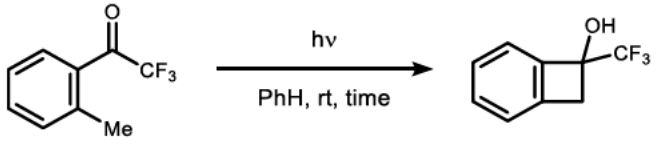

3.8 **3.26**

Entry	Scale	Concentration	Wavelength	Time	NMR yield	Yield
1	4.73 mmol	0.47 mol/l	355 nm	90 h	-	98%
2	7.86 mmol	0.44 mol/l	370 nm	10 h	>99%	90%
3	10.7 mmol	0.90 mol/l	370 nm	10 h	>99%	79%[a]

[a] Isolated yield after column chromatography and distillation.

Next, the strong dependency of the initial rates on temperature (*cf.* chapter 3.3.2) was investigated by performing the reaction at different temperatures (Figure 8).

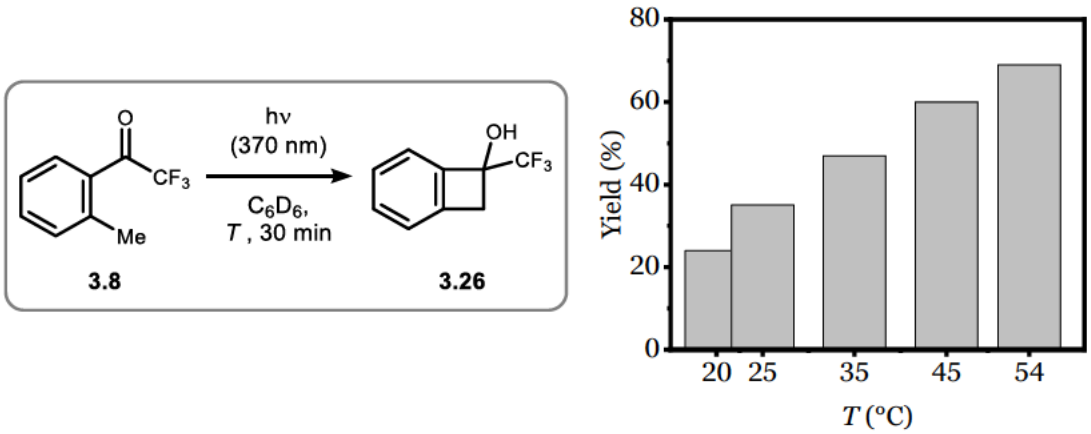

Figure 8: Investigation of the temperature dependency, reactions performed on 0.01 mmol scale in degassed C_6D_6 [20 mM] with 370 nm for 30 min, yield determined *via* ^{19}F NMR with $PhCF_3$ as internal standard.

Elevated temperatures were beneficial for the reaction yields, evident from the increasing yield of the transformation towards the benzocyclobutenol **3.26** whereas low temperatures slowed the reaction progress down (20 °C).

3.4 Mechanistic studies

3.4.1 Kinetic studies

The underlying mechanism of the overall reaction from acetophenones to benzocyclobutenols was further analysed, beginning with a study of the reaction kinetics. Samples of acetophenone **3.8** with different concentrations were irradiated with a 370 nm lamp and the reaction towards benzocyclobutenol **3.26** monitored by ^{19}F NMR techniques (Figure 9).

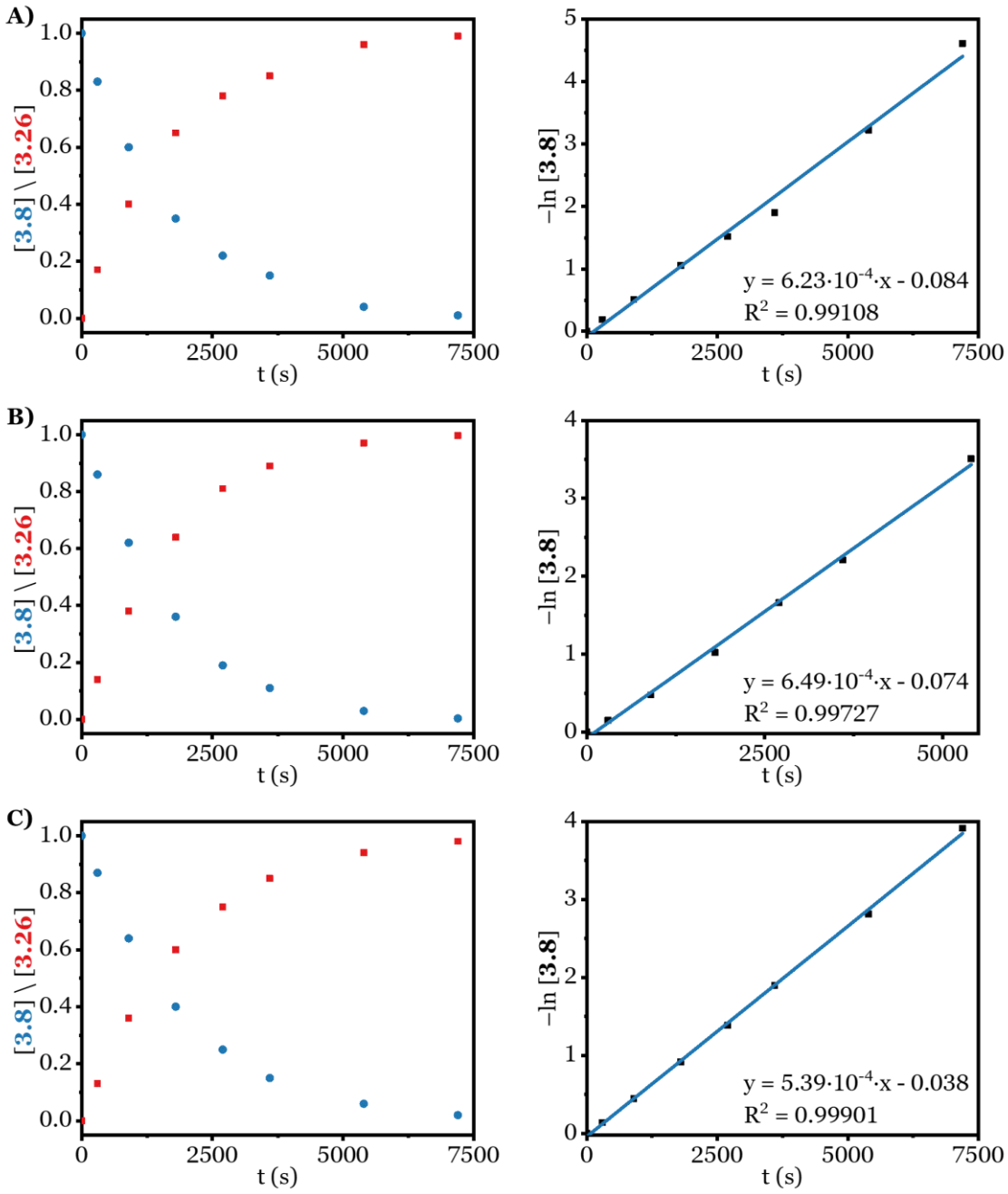

Figure 9: Plots of the concentration dependent transformation of acetophenone 3.8 towards product 3.26 under irradiation with 370 nm. Starting concentration of acetophenone 3.8 A: 2 mM, B: 20 mM, C: 200 mM.

For all three tested concentrations, a first order reactivity was observed by plotting the negative logarithmic concentration versus the time (Figure 9, right). The reaction rates were thus obtained as the slopes of the linear fits of the data points. Here, values in the same order of magnitude were obtained, which resembles the observed near uniform reactivity for this concentration range (Figure 9, right).

3.4.2 Mechanistic picture

An initial mechanistic picture for the transformation of *ortho*-methylacetophenones to benzocyclobutenols can be drawn according to literature known reports (Scheme 50).[119] Following excitation of the *syn*-conformer **3.31** the triplet species ^{3}**3.31** is generated after ISC. Biradical ^{3}**3.32** is formed, which is long lived enough to allow for free bond rotation.[120] Therefore, photoenol species ***E*-3.33** and ***Z*-3.33** are generated simultaneously after ISC. The underlying formation for a photoenol as the central intermediate explains the previously found temperature dependency and sensitivity towards oxygen of the photocyclisation.[119b] After formation of a photoenol, two pathways are possible: a productive 4-π electrocyclisation (EC) from the long-lived photoenol ***E*-3.33** to generate benzocyclobutenol **3.34**, or an unproductive [1,5] hydride shift which regenerates *ortho*-methylacetophenone **3.31**. The unproductive backreaction from photoenol ***Z*-3.33** is known to be very quick, whereas the [1,5] hydride shift of the photoenol ***E*-3.33** is slow compared to the productive 4-π EC.[121]

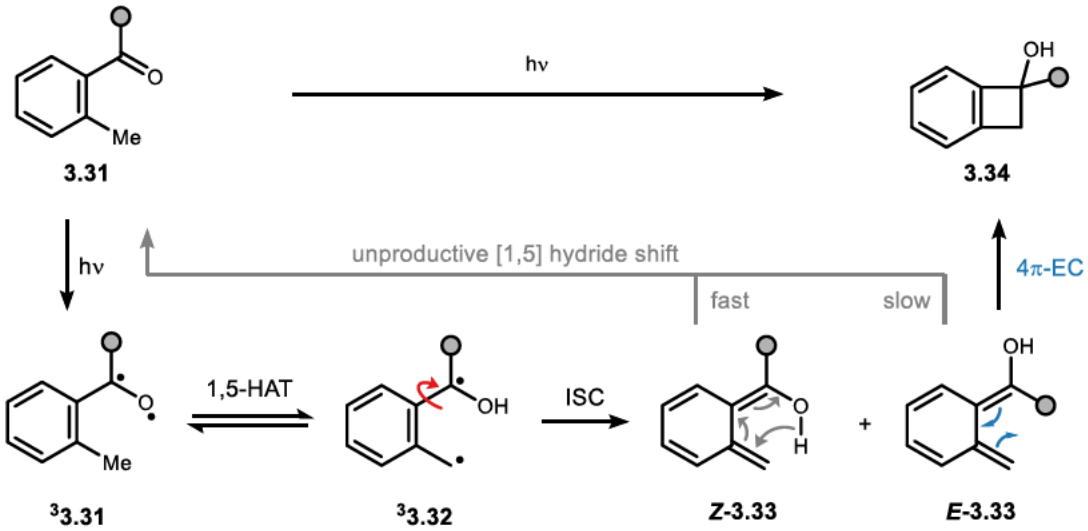

Scheme 50: Mechanistic picture of the photocyclisation of *ortho*-methylacetophenones

3.4.3 Investigation of the reaction pathway

The existence of the photoenols **3.33** as central intermediates of the studied photocyclisation was sought to be investigated further. When abstractable hydrogens

are available in the photoenol ***E*-3.33**, the productive 4-π EC also competes with another [1,5] hydride shift towards enol **3.35** (Scheme 51).

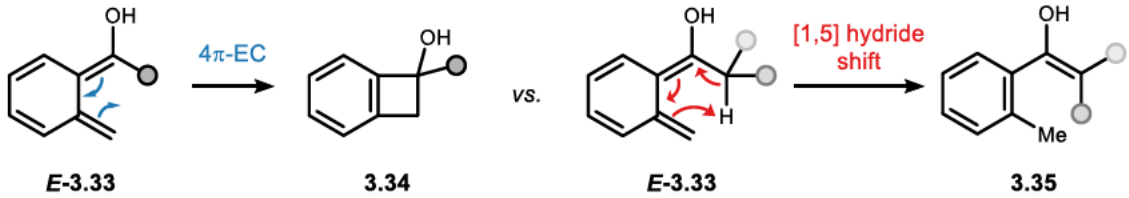

Scheme 51: Influence of abstractable hydrogens on the reactivity of photoenol *E*-3.33.

The trifluoromethyl group of the preciously employed *ortho*-methylacetophenone **3.8** features no abstractable atoms, as the *C–F* bonds can be considered inert. Hence, the influence of the trifluoromethyl group on the overall reaction was evaluated. If the reactions unproductive path proceeds *via* [1,5] hydride shift, the displacement of fluorine with hydrogen in acetophenone **3.8** would lead to an overall decrease in efficiency, as the possibility of [1,5] hydride shifts from the *E*-photoenol increases. A set of compounds with increasing hydrogen content was synthesised and its performance tested under the reaction conditions (Table 10).

Table 10: Effect of the displacement of fluorine with hydrogen, reactions performed on 0.01 mmol scale in degassed C_6D_6 [20 mM] with 355 nm for 3 h at 20 °C, yield determined *via* ^{1}H NMR with mesitylene as internal standard.

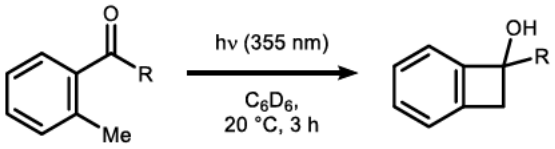

Entry	Product	Conversion	Yield
1	R = CF_3 (**3.26**)	66%	66%
2	R = CHF_2 (**3.36**)	55%	48%
3	R = CH_2F (**3.37**)	8%	1%[a]
4	R = CH_3 (**1.10**)	4%	1%

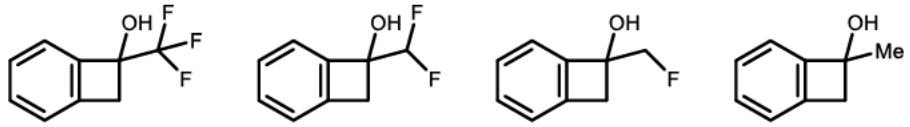

3.26 **3.36** **3.37** **1.10**

[a]Formation of a second species detected *via* NMR.

Indeed, the expected beneficial effect of the trifluoromethyl group was validated. Benzocyclobutenol **3.26** was formed in 66% yield (entry 1), and exchange of a fluorine atom with a hydrogen atom lead to diminished yields, with benzocyclobutenol **3.36** formed in 48% yield (entry 2). As expected, formation of benzocyclobutenol **1.10** was sluggish (1% yield, entry 4),[30] but cyclisation product **3.37**

was also formed with a low yield (entry 3). The formation of a new species was detected by ^{1}H NMR spectroscopy, which slowly converted back to the starting material **3.18** over hours. The detected species presumably is the enol **3.38** (Scheme 52), which is generated from an unproductive [1,5] hydride shift of the photoenol ***E*-3.39**.

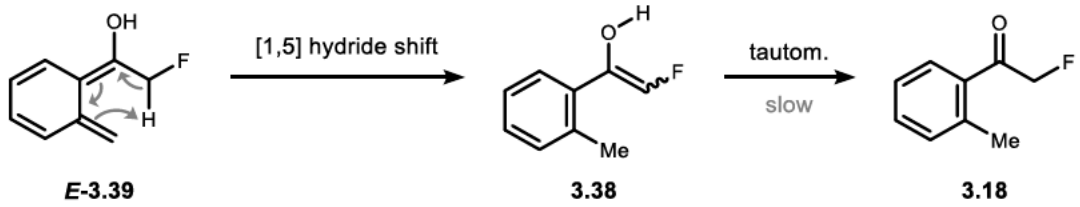

***E*-3.39** **3.38** **3.18**

Scheme 52: Pathway for the postulated enol formation from the *E*-photoenol.

The formation of an inactive long-lived species reduces the effective concentration of **3.18** available for photoreactions in solution. Consequently, less ^{3}**3.18** is formed, which gives a diminished probability for the productive 4-π EC, ultimately resulting in a decreased reaction rate of the overall transformation.

Still, the reactivity of acetophenone **3.8** *via* a photoenol species was to be proven. For the photocyclisation of acetophenone **3.8** no differentiation between a biradical recombination and a 4-π EC can be made, as both pathways deliver the same product **3.26**. This changes for longer alkyl chains, as a biradical recombination delivers diastereomers (*cf.* chapter 2.1.1 and 2.3), whereas a 4-π EC proceeds stereoselectively, yielding only one diastereomer. Indeed, irradiation of *ortho*-ethylacetophenone **3.9** resulted in the formation of a single diastereomer **3.40**, which is well in accordance with a thermally allowed 4-π EC that proceeds in a conrotatory fashion from photoenol **3.41** (Scheme 53, top).[122] The conformation of **3.40** was confirmed *via* ^{1}H ^{1}H NOESY and ^{19}F ^{1}H hetero nuclear NOESY (HOESY) spectroscopy. Additionally, an unambiguous identification of the conformation of the diastereomer was possible through synthesis of its chlorine bearing derivative **3.42** from acetophenone **3.15** (Scheme 53, middle; CCDC 2371856). Furthermore, trapping of the postulated photoenol ***E*-3.43** *via* a Diels-Alder reaction was envisioned, analogous to studies by *Yang* and *Rivas* [123] and Dell'Amico *et al.*[124] (Scheme 53, bottom). *N*-Methylmaleimide **3.44** was chosen as a dienophile based on a literature report.[125] Tricycle **3.45** was formed as a single diastereomer when acetophenone **3.8** was irradiated in the presence of the mentioned dienophile, supporting the existence of the postulated photoenol pathway. Further proof was provided by [redacted] as part of his own work. Irradiation of *ortho*-ethylacetophenone **3.9** and *N*-methylmaleimide yielded a

single diastereomer of tricycle **3.46**, and the structure could be unambiguously identified as the endo product *via* X-Ray diffraction (CCDC 2371854).

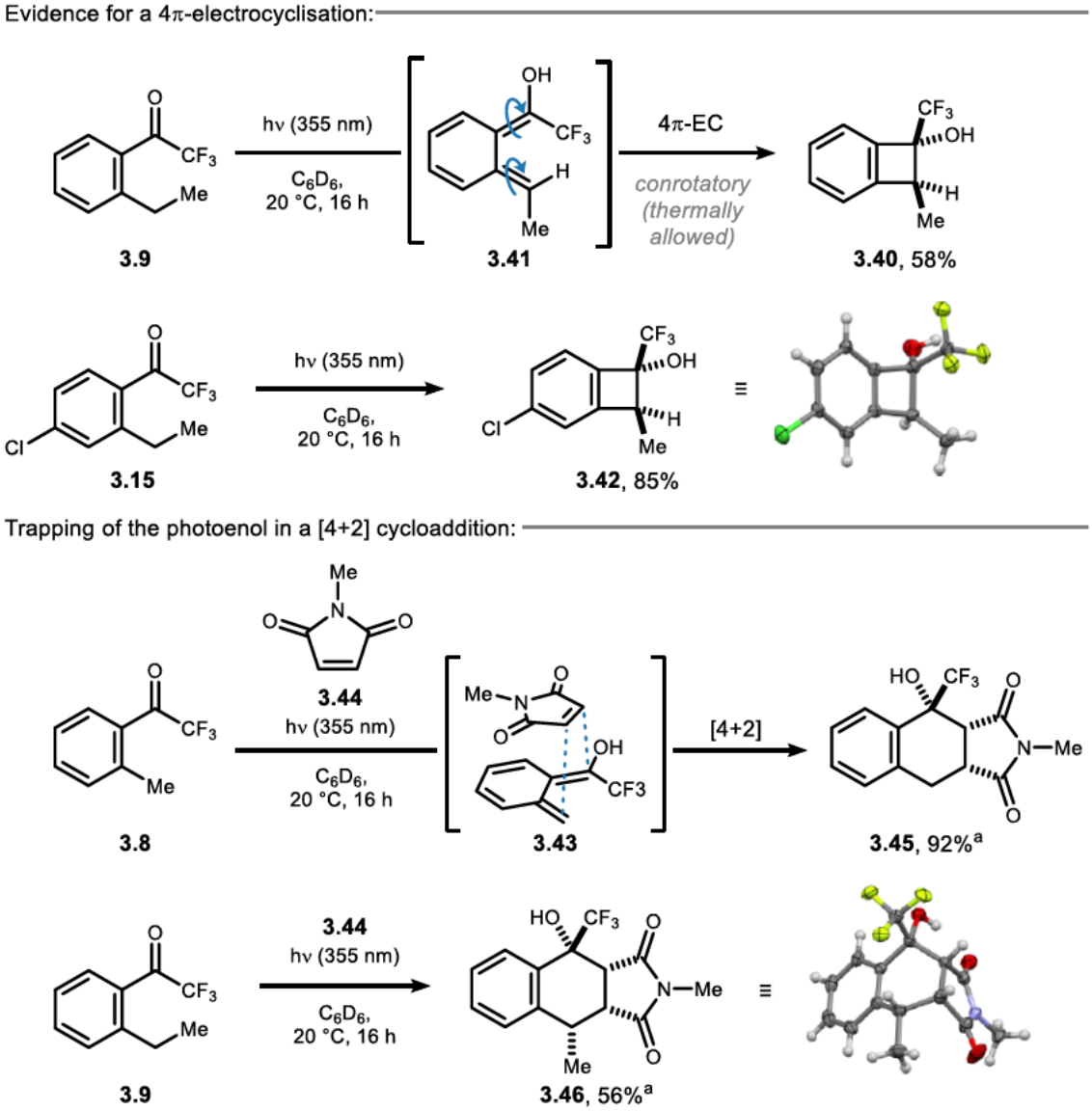

Scheme 53: Top: Stereoselective synthesis of benzocyclobutenols 3.40 and 3.42. and graphical representation of the molecular structure of 3.42 determined *via* X-ray diffraction, thermal ellipsoids are depicted at 50% probability. CCDC 2371856. Bottom: Trapping of photoenols from *ortho*-alkylacetophenones with dienophile 3.44 in a [4+2] cycloaddition. Synthesis of 3.46 was performed by [redacted]. Bottom right: Graphical representation of the molecular structure of 3.46, thermal ellipsoids are depicted at 50% probability. CCDC 2371854. [a] Yield determined *via* ^{1}H NMR with CH_2Br_2 as internal standard.

3.4.4 Mechanism of the peroxide formation

Following the identification of a photoenol as the central intermediate in the transformation from acetophenone **3.8** to benzocyclobutenol **3.26**, the process of the peroxide formation towards **3.27** was to be investigated. In literature, two pathways for the formation of endo-peroxides are described.[119b] Either, the biradical ^{3}**3.32** reacts with ^{3}**O$_2$** (Scheme 54, A),[126] or the photoenols **3.33** react with ^{1}**O$_2$** (Scheme 54, B)[127], whereby both pathways are spin allowed processes.

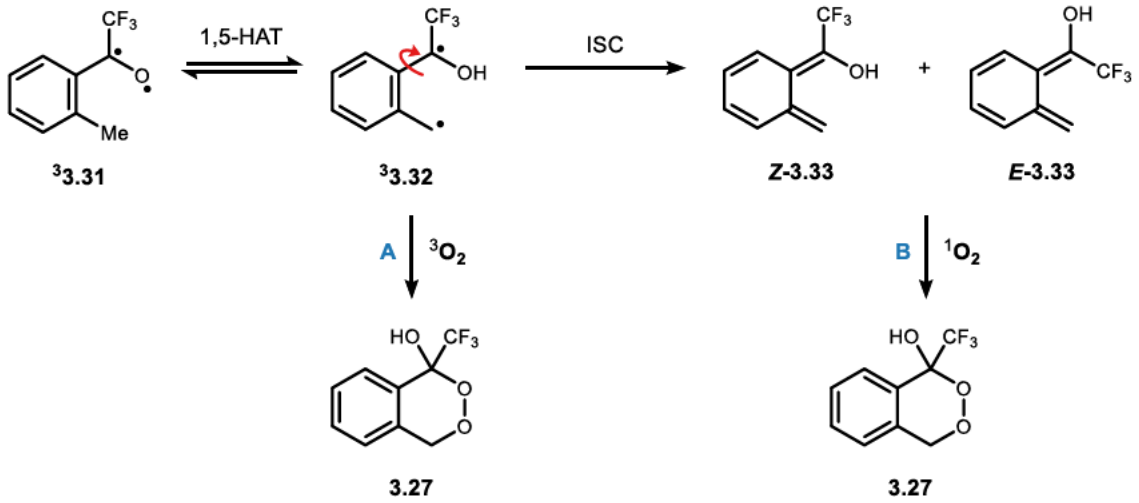

Scheme 54: Possible pathways for the formation of 3.27. [119b]

The ground state of molecular oxygen is ^{3}**O$_2$**, but ^{1}**O$_2$** is generated by quenching of other triplet states. Here, biradicals ^{3}**3.31** and ^{3}**3.32** are the triplets states, able to generate small concentrations of ^{1}**O$_2$**. If the reaction were to proceed between the photoenols **3.33** and ^{1}**O$_2$**, a reaction rate increase would be expected for higher concentrations of singlet oxygen in solution. Therefore, a set of experiments was devised, in which the efficient singlet oxygen generator tetraphenylporphyrin (TPP) **3.47** was added to the reaction mixture (Table 11.).[128]. A cool-white LED (CW-LED) was used for the broad excitation of TPP **3.47** and hence generation of ^{1}**O$_2$**. Formation of biradical ^{3}**3.32** and photoenol **3.33** was achieved by using a 355 nm lamp. By simultaneously activating both lamps, a rate increase would be expected for pathway B (Scheme 54).

Table 11: Control experiments for a potential reaction of singlet oxygen generated from TPP 3.47, reactions performed on 500 µmol scale in C_6D_6 [20 mM] under oxygen atmosphere for 4 h at 22 °C, yield determined *via* ^{19}F NMR with $PhCF_3$ as internal standard.

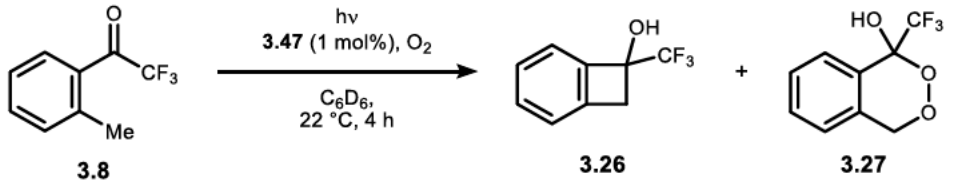

3.8 3.26 3.27

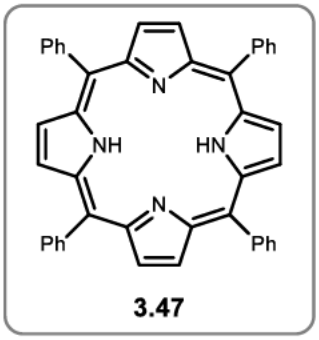

3.47

Entry	Irradiation source	Addition of **3.47**	Yield **3.26**	Yield **3.27**
1	CW-LED	yes	0	0
2	CW-LED + 355 nm	-	5%	7%
3	CW-LED + 355 nm	yes	1%	3%
4	355 nm	-	3%	6%
5	355 nm	yes	1%	2%

No background reaction was found for solely using the CW-LED as a light source (entry 1), whereas activation of the additional 355 nm lamp resulted in product formation (entry 2). Addition of the catalyst **3.47** (entries 3 & 5) resulted in a drop of reactivity compared to solutions without catalyst (entries 2 & 4), most likely due to competitive absorption. However, competitive quenching of biradicals ^{3}**3.31** and ^{3}**3.32** from the triplet state of TPP ^{3}**3.47** could also explain the observed reduced reactivity. Finally, no increase of the reaction rate was found in presence of $^1\mathbf{O_2}$ (compare entries 3 & 5). Therefore, the formation of the endoperoxide from the biradical ^{3}**3.32** and $^3\mathbf{O_2}$ would seem most likely.

3.5 Scope

Over the course of this study, several *ortho*-alkylacetophenone derivatives were synthesised and their performance in the desired photochemical transformation towards benzocyclobutenols was evaluated (Table 12). Standard substrate **3.8** serves as a benchmark with a good yield of benzocyclobutenol **3.26** to investigate the differing effects of varying substrates. At first, the effect of different *ortho*-substituents was investigated. Introduction of an ethyl group led to a diminished yield of product **3.40** of 27% (entry 2), whereas the sterically demanding isopropyl residue led to no formation of benzocyclobutenol **3.48** (entry 3). The electron donating (EDG) methoxy substituent also led to only 30% formation of benzocyclobutenol **3.49**, which was formed as a single diastereomer (entry 4). Next, the influence of *para*-substitution was investigated. The introduction of an EDG in *para*-position of acetophenone **3.12** led to a strong increase in conversion (91%), but also increased the amount mount of unidentified side-products (28%), with still 63% formation of product **3.50** (entry 5). Electron withdrawing groups (EWGs) increased the conversion, but also showed an increase in side reactions, with formation of cyclisation product **3.51** in 60% yield (entry 6) and **3.52** with 42% yield (entry 7). Introduction of a chlorine atom was beneficial, with an increase in yield to 74% of benzocyclobutenol **3.29** (entry 8). The formation of the *ortho*- and *para*-substituted products **3.42** was slower (entry 9), therefore *ortho*-substitution was abandoned altogether. At last, substitution of the CF_3-group was evaluated by employing a benzoyl formiate ester. Indeed, the product **3.53** was formed in excellent selectivity with a yield of 79% (entry 10). The previously used substrates with abstractable hydrogens were included for completeness (entries 11-13, *cf.* chapter 3.4). The formation of benzocyclobutenol **3.36** was achieved in 48% yield, whereas products **3.37** and **1.10** were only formed in trace amounts.

Table 12: Substrate scope and selectivity, reactions performed on 10 µM scale in 0.5 mL C_6D_6 [20 mM] at 20 °C in the *Luzchem* photoreactor with 355 nm lamps, conversion and yield based on ^1H NMR with mesitylene as internal standard or ^{19}F NMR with $PhCF_3$ as internal standard as mean value of three experiments.

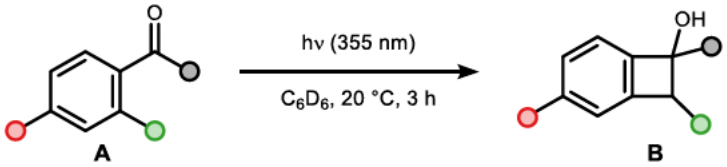

Entry	A	B	NMR standard	Conversion	Yield	Unidentified side products
1	**3.8**	**3.26**	$PhCF_3$	66%	66%	-
2	**3.9**	**3.40**	$PhCF_3$	33%	27%[a]	~6%
3	**3.10**	**3.48**	$PhCF_3$	8%	0%	8%
4	**3.11**	**3.49**	$PhCF_3$	37%	30%[a]	7%
5	**3.12**	**3.50**	$PhCF_3$	91%	63%	28%
6	**3.13**	**3.51**	$PhCF_3$	69%	60%	9%
7	**3.16**	**3.52**	$PhCF_3$	48%	42%	6%
8	**3.14**	**3.29**	$PhCF_3$	79%	74%	5%
9	**3.15**	**3.42**	$PhCF_3$	41%	36%[a]	5%
10	**3.23**	**3.53**	mesitylene	82%	79%	3%
11	**3.21**	**3.36**	mesitylene	55%	48%	7%
12	**3.18**	**3.37**	mesitylene	8%	~1%	7%[c]
13	**1.9**	**1.10**	mesitylene	~4%[b]	~1%	3%

[a] Formation of a single diastereomer. [b] Conversion not precisely determined due to signal overlap. [c] Formation of enol **3.38**.

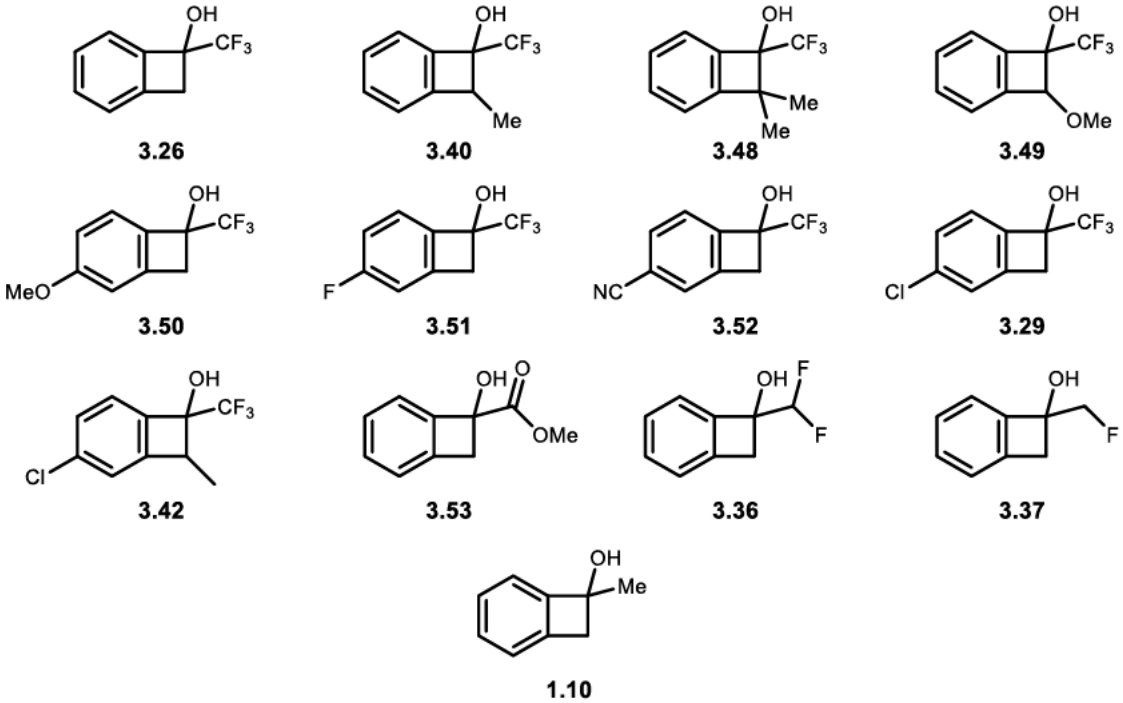

Scheme 55: Formed products after irradiation, corresponding to Table 12.

As evident from the gathered data, the systems acetophenone ⇄ benzocyclobutenol **3.8** ⇄ **3.26**, **3.14** ⇄ **3.29** and **3.23** ⇄ **3.53** performed best. To investigate their synthesis and isolation further, another set of experiments was performed on larger scale with longer reaction times, and the products were isolated (Scheme 56).

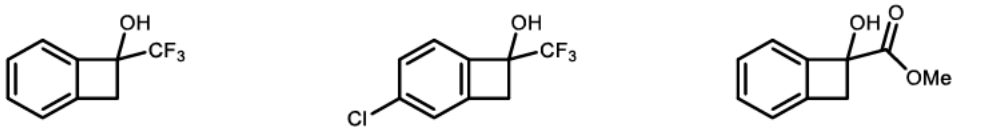

3.26, 70% (75%) **3.29**, 53% (56%) **3.53**, 84% (93%)

Scheme 56: Synthesis and isolation of benzocyclobutenols 3.26, 3.29 and 3.53 on larger reaction scale. Reactions performed on 0.1 mmol scale in degassed benzene [20 mM] at 21 °C in the *Luzchem* photoreactor with 355 nm lamps for 8 h, NMR yield in brackets, based on ^{1}H NMR with mesitylene as internal standard or ^{19}F NMR with $PhCF_3$ as internal standard.

On the bigger scale, the formation of benzocyclobutenol **3.26** was equally selective and high yielding (70% yield). On the other hand, the irradiation of acetophenones **3.14** and **3.23** led to the formation of unidentified side products. Nevertheless, the desired products were obtained in good to high yields, although the formation of *para*-chlorosubstituted benzocyclobutenol **3.29** was diminished with 56% formation evident by the ^{19}F NMR spectrum compared to the NMR scale experiments (Table 12, 79%). Based on the good selectivity for the cyclobutanol formation, standard couple **3.8** ⇄ **3.26** was used for the following mechanistic investigations of the ring-opening to establish a highly productive MOST system.

3.6 Ring-opening reaction

3.6.1 Thermal ring-opening

As described above, the high energy isomer of many MOST systems can be transformed into the ground state isomer at elevated temperatures.[89a] This holds true for benzocyclobutenols, that are known to undergo an electrocyclic ring-opening between 100-150 °C.[129,69] Therefore, the thermal stability of benzocyclobutenol **3.26** in different high-boiling solvents was investigated (Table 13). Heating of closed vials in a metal block for prolonged times up to 150 °C did not induce any reaction towards acetophenone **3.8** (entries 1 & 2), whereas heating above 200 °C facilitate the desired transformation (entries 3-5). However, evaporation of

material was evident from the ^{19}F NMR spectra against internal standard, which can be attributed to an estimated boiling point of benzocyclobutenol **3.26** from 150-180 °C. Above 180 °C, complete evaporation of substance **3.26** from the solution was observed, with condensation above the solvent level. To achieve a better solubility, diphenyl ether was chosen as a solvent and a yield of 25% was observed after 1 h at 220 °C (entry 5). It must be noted, that the complete flask had to be fully submerged into the heating source, in order for evaporating material to react in the gas phase above the reaction mixture.

Table 13: Investigation of the electrocyclic ring-opening in different solvents, reactions were performed on 20 µmol scale in different solvents [40 mM], yield based on ^{19}F NMR with $PhCF_3$ as internal standard.

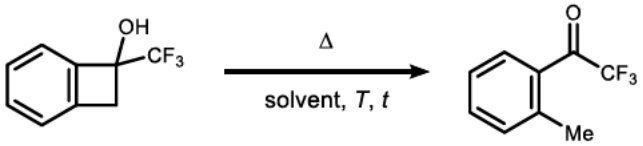

3.26 **3.8**

Entry	Solvent	*T*	*t*	Yield
1	PhMe	120 °C	16 h	0%
2	mesitylene	150 °C	16 h	0%
3	1,3,5-triethylbenzene	210 °C	1 h	~20%[a]
4	dodecane	210 °C	2 h	~9%[a]
5	diphenyl ether	220 °C	1 h	25%

[a] Evaporation of material observed by ^{19}F NMR against internal standard.

Still, achieving reproducible results was found challenging and another method was employed. Herein, samples of benzocyclobutenol **3.26** were flame sealed in NMR tubes without any solvent under nitrogen atmosphere, to eliminate the risk of evaporation and full submerged in a metal heating block to guarantee uniform reactivity (Figure 10). Increasing the temperature to 250 °C cleanly facilitated the reaction towards acetophenone **3.8** with 49% yield in one hour.

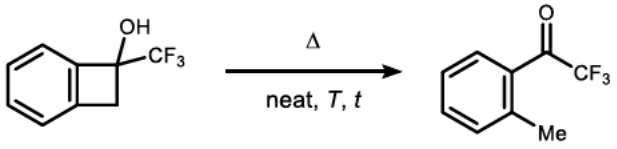

3.26 **3.8**

Entry	*T*	*t*	Yield
1	200 °C	1 h	1%
2	220 °C	1 h	16%
3	250 °C	1 h	49%[a]

[a] Mean value of three experiments.

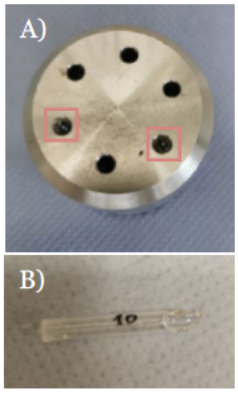

Figure 10: Electrocyclic ring-opening of cyclobutanol 3.26 in flame sealed NMR tubes, reactions performed on 50 µM scale, with the vials fully submerged into a fully equilibrated metal heating block. Yield based on ^{19}F NMR with $PhCF_3$ as internal standard. A) Metal heating block with fully submerged vials. B) Fused NMR tube containing a solid sample 3.26.

A systematic study of the thermal half-life was conducted, and the rate constants of the back-isomerisation were measured for different temperatures to determine the activation energy (E_a). The back-isomerisation is a unimolecular process[90b], so first-order kinetics apply, which is resembled in the conversion-time-plots as an exponential decay (Figure 11, left). By plotting the negative logarithm of the concentration of benzocyclobutenol **3.26** versus time (Figure 11, right), the reaction rates can be determined as the slope of the linear fit.[76] From these experiments, the preparation and measurement of the data for 503.15 K was performed by [redacted] (Figure 11, B). For increasing temperatures, the ring-opening reaction proceeds faster, which is resembled in the reaction rates which are the slope of the linear fits (Figure 11, right)

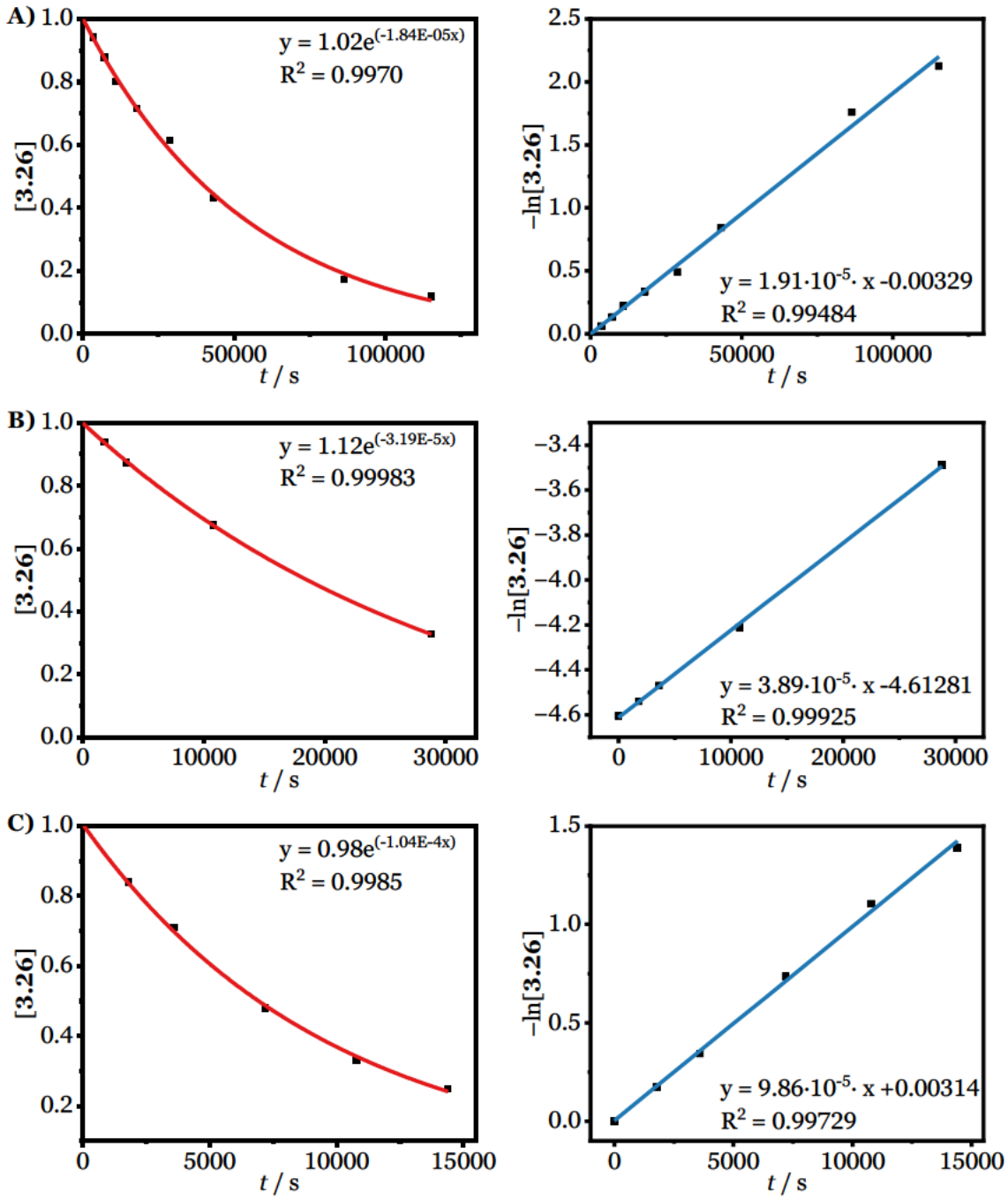

Figure 11: Concentration-time plots of the thermal electrocyclic ring-opening reaction (left) and plot of –ln[3.26] vs. time (right). Temperature = 493.15 K (A), 503.15 K (B), 513.15 K (C).

With the calculated reaction rates at different temperatures, the activation energy E_a can be determined following the Arrhenius rate law (Figure 12).[76]

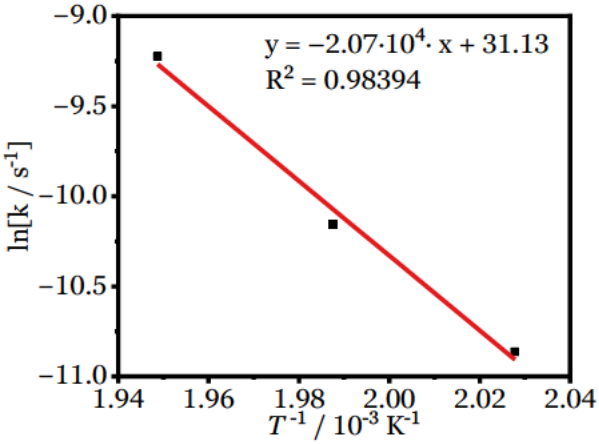

E_a = 172 kJ/mol.

$\tau_{1/2}$ = 5 × 10⁸ years.

Figure 12: Arrhenius plot of the temperature dependent reaction rates (left), calculated activation energy and half-life (right).

Thereby, an activation energy E_a of 172 kJ/mol was determined, which corresponds to an extrapolated half-life $\tau_{1/2}$ of 5 × 10⁸ years (Figure 12, right). This clearly shows that the system is suitable for long time storage.

3.6.2 Base-accelerated ring-opening

The activation barrier of a thermal electrocyclic ring-opening reaction of benzocyclobutenols can be lowered by deprotonation and the formed benzocyclobutenolates were reported to undergo electrocyclic ring-opening *via* an alcoholate **3.54** even at room temperature.[130] Hence, the employment of bases as catalysts for the back-isomerisation of benzocyclobutenol **3.26** to acetophenone **3.8** was tested (Table 14). Subjecting cyclisation product **3.26** to hydroxyl bases resulted in formation of HCF_3 as evident from ^1H and ^{19}F NMR (entries 1&2), which is presumably formed in a haloform reaction with the ring-opened acetophenone **3.8**.[131] However, use of the organic base DBU **2.94** (Figure 13) cleanly delivered standard substrate **3.8** in 93% yield (entry 3). Lowering the temperature to 30 °C led to decreased reactivity (entry 4), which could be reinstated by switching to a stronger base **3.55** (TBD, entry 5). The catalytic loading could be decreased while still maintaining good reactivity (entry 6). Another guanidine base **3.56** (*N*-Me-TBD) was effective after optimising the conditions (entries 7-9). Use of a polystyrene supported base **3.57** (PS-TBD) for envisioned heterogeneous catalysis (*vide infra*) was successful (entry 10). The use of a very strong organic base **3.58** (BTPP) was found to be very effective with 97% yield (entry 11). Since BTPP **3.58** is very sensitive to water, rigorous precautions for the exclusion of moisture

must be taken requiring elaborate reaction set-ups. Therefore, further experiments were conducted using the more practically applicable bases **2.94**, **3.56** and **3.57**, which performed equally successful.

Table 14: Base catalysed ring opening of benzocyclobutenol 3.26, Reactions run on 0.05 mmol scale in C_6D_6 under inert gas atmosphere. Yields determined by ^1H NMR and ^{19}F NMR with $PhCF_3$ as internal standard.

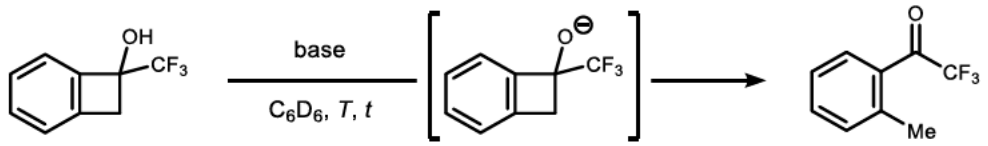

3.26 **3.54** **3.8**

Entry	Base	Equivalents	*T*	*t*	Yield
1	NBu_4OH	0.50	80 °C	96 h	0%[a]
2	KO*t*Bu	0.50	80 °C	96 h	49%[a]
3	DBU	0.50	80 °C	96 h	93%
4	DBU	0.50	30 °C	16 h	7%
5	TBD	0.50	30 °C	16 h	89%
6	TBD	0.20	30 °C	23 h	81%
7	*N*-Me-TBD	0.50	30 °C	16 h	34%
8	*N*-Me-TBD	0.50	30 °C	44 h	75%
9	*N*-Me-TBD	0.50	30 °C	120 h	97%
10	PS-TBD	0.50	30 °C	16 h	72%
11	BTPP	0.43	30 °C	16 h	99%

[a]HCF_3 detected in ^{19}F NMR.

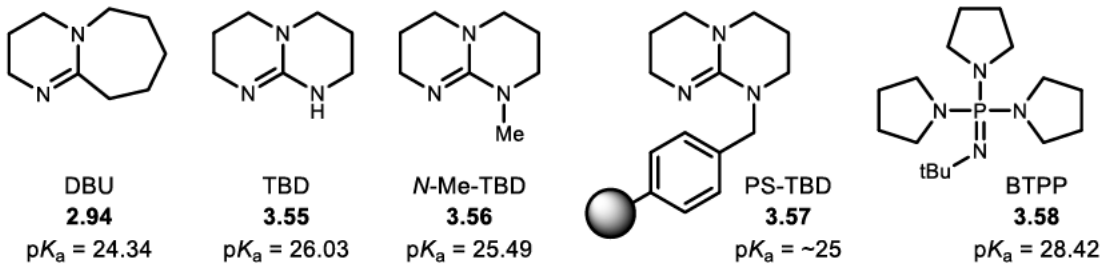

Figure 13: Employed bases in the ring-opening reaction (Table 14), basicity in acetonitrile according to *Kaljurand et. al.*[132] Basicity of base 3.57 estimated compared to 3.56.

With the established bases, the ring-opening reaction under base catalysis of the three previously determined candidates **3.26**, **3.29** and **3.53** was compared (Table 15).

Table 15: Reaction of the three MOST candidates with organic bases, reactions performed on 0.05 mmol scale in C_6D_6 under inert gas atmosphere. Yields determined by ^1H NMR with mesitylene and ^{19}F NMR with $PhCF_3$ as internal standard.

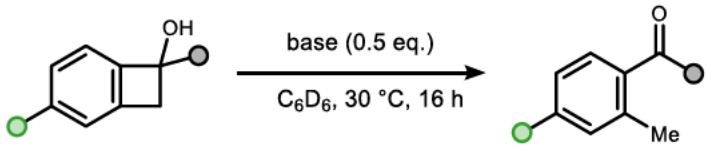

Entry		DBU **2.94**	TBD **3.55**	*N*-Me-TBD **3.56**
1	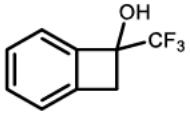 **3.26**	7% yield	89% yield	34% yield
2	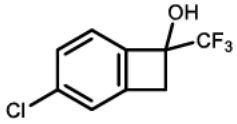 **3.29**	22% yield [a]	78% yield [a]	93% yield [a]
3	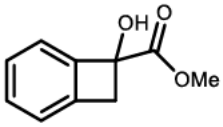 **3.53**	38% yield [a]	38% yield [a]	78% yield [a]

[a] Solution changes colour upon addition of base.

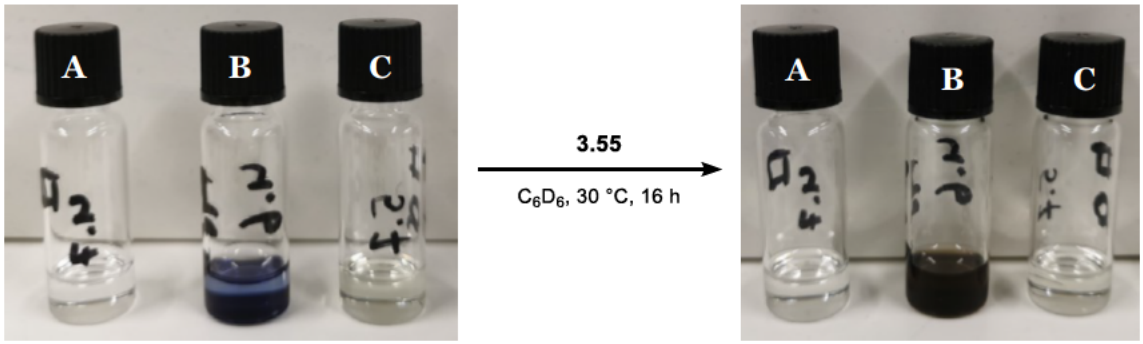

Figure 14: Visual colour change of a colourless solution after addition of 3.55, corresponding to Table 15. Left: Picture taken 30 s after injection of base, right: after 16 h. A) Reaction of 3.26, B) 3.53, C) 3.29.

Whereas the standard substrate **3.26** was successfully transformed into its ground-state isomer under base catalysis (entry 1), ring-opening of substrates **3.29** and **3.53** was overall less efficient (entries 2 & 3). Benzocyclobutenol **3.29** showed a change from colourless to champagne after 16 h for all three bases visible to the bare eye (Figure 14, C). Subjecting cycle **3.53** to base, resulted in the instant change from colourless to blue, which changed to black with formation of a precipitate after 16 h (Figure 14, B). Analysis by ^1H and ^{19}F NMR showed decomposition of candidates **3.29** and **3.53**, probably caused by nucleophilic

attacks of the bases, during or after the transformation.[133] The standard substrate-pair **3.26** ⇄ **3.8** showed no signs of decomposition and was finally established as the MOST pair with the best potential for application.

3.6.3 Determination of the energy storage density

The energy storage density $\Delta H_{storage}$ of the potential MOST pair **3.8**⇄**3.26** was determined by dynamic scanning calorimetry (DSC) measurements. Measurements were conducted in a micro reaction calorimeter, which features a precision syringe and allows for controlled and automated addition of substances. The syringe is enclosed with the sample cell in an insulative body and equilibrated before measurements to guarantee isothermal addition of the substance. *N*-Me-TBD **3.56** was chosen as a catalyst for the desired transformation, to achieve good reactivity. Furthermore base **3.56** is a liquid, which, in combination with the calorimeter used, allows for easier handling. As evident from previous experiments (Table 14, entry 7), the ring-opening reaction between benzocyclobutenol **3.26** and base **3.56** was slow at 30 °C, therefore the reaction temperature was elevated to 90 °C. A mixture of base **3.56** in toluene was placed in the sample cell and the potential MOST substance **3.26** was added neat to this mixture *via* the syringe in four portions, resulting in the measurement of four data points (Table 16, entries 1-4). Indeed, a fast reaction occurred, as evident from the spectrum (Figure 15, A) and the completeness of the reaction was confirmed by ^{19}F NMR after the last addition had reacted according to the DSC device. Accordingly, another experiment was performed with catalytic amounts of base (Table 16, entries 5-8). Here, base **3.56** was dissolved in toluene in a catalytic amount (0.3 equivalents (eq.)) with respect to each individual injection performed during the experiment (Figure 15, B).

Table 16: DSC measurements of the addition of benzocyclobutenol 3.26 into a solution of base 3.56 in toluene at 90 °C, reaction completion confirmed by ^{19}F NMR with $PhCF_3$ as internal standard.

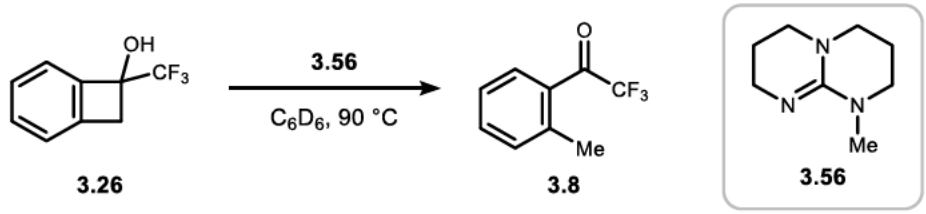

Entry	Added amount of **3.26**	Equivalents base	Energy
1	5 µL (35 µmol)	1.00 eq.	0.090 J
2	30 µL (210 µmol)	1.00 eq.	11.187 J
3	30 µL (210 µmol)	1.00 eq.	11.214 J
4	30 µL (210 µmol)	1.00 eq.	11.343 J
5	5 µL (35 µmol)	0.30 eq.	0.606 J
6	30 µL (209 µmol)	0.30 eq	10.827 J
7	30 µL (209 µmol)	0.30 eq	10.828 J
8	30 µL (209 µmol)	0.30 eq	10.931 J

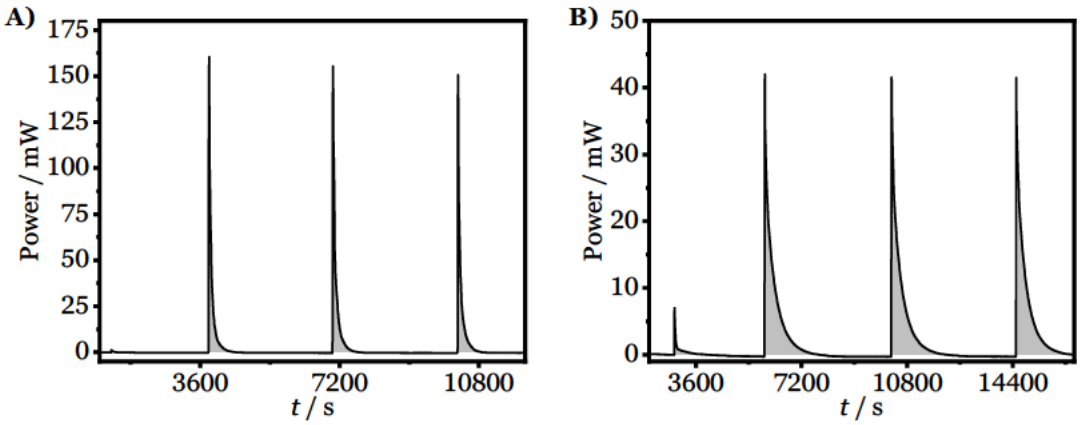

Figure 15: DSC measurements of the ring-opening of cyclobutanol 3.26, reactions performed on 0.7 mmol scale in toluene at 90 °C. Base 3.56 used with A) 1.00 eq, B) 0.10 eq. Reaction completion confirmed by ^{19}F NMR with $PhCF_3$ as internal standard.

The first addition was performed to ensure that no bubbles were developed during the equilibration period. During the equilibration, the syringe is heated to the measurement temperature and the contained sample expands, leading to the formation of small bubbles at the bottom and top of the syringe. These bubbles alter the added amount of substance, which in turn falsifies the measured values. Hence, a small injection is performed at the beginning of a measurement, in order to remove existing bubbles (entry 1). Afterwards, larger volumes were added afterwards (entries 2-4). All values were found to be in the same range, indictive of a uniform reactivity for equimolar and catalytic amount of base. However, a small increase per injection was noticeable, which was identified as the endergonic heat

of mixing between **3.26** and toluene. To correct the initial values for the influence of the heat of mixing, another DSC measurement was performed. The heat of mixing was measured by injection of **3.26** into toluene at 90 °C and was found to be endothermic (Table 17, Figure 16).

Table 17: Determination of the heat of mixing by DSC measurements of the addition of benzocyclobutenol 3.26 into toluene at 90 °C for the determination of the heat of mixing.

Entry	Added amount of **3.26**	Equivalents base	Energy
1	5 µL (35 µmol)	-	–0.022 J
2	30 µL (209 µmol)	-	–1.196 J
3	30 µL (209 µmol)	-	–1.115 J
4	30 µL (209 µmol)	-	–1.026 J

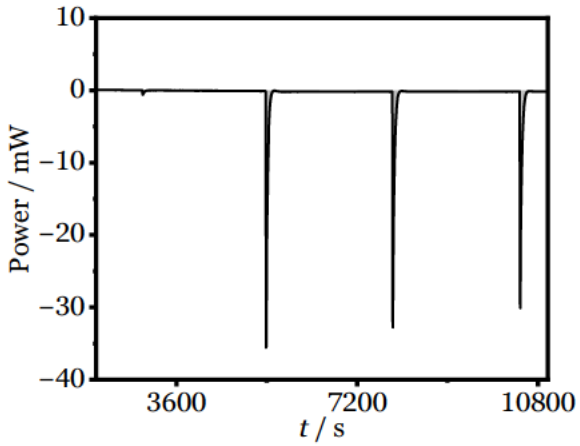

Initial measurement
(11.055 J for 30 µL)
⇩
Correction for heat of mixing
(–1.112 J for 30 µL)
⇩
12.167 J for 30 µL (39.1 mg)
equals 311 J/g

Figure 16: Left: DSC measurement of the heat of mixing of 3.26 and toluene. Right: Energy storage density of 3.26.

With the heat of mixing determined, the value $\Delta H_{storage}$ of MOST candidate **3.26** could be calculated as 311 J/g.

In order to further support these findings, the inverse addition of the base **3.56** to substrate **3.26** was performed (Table 18). Here, a single drop of a solution of base **3.56** in toluene was added to a solution of benzocyclobutenol **3.26** in toluene at 90 °C, which caused a complete transformation towards acetophenone **3.8**. The reactions progress was controlled by ^{19}F NMR experiments and repeated with different concentrations of catalyst and MOST substance to validate the robustness of the reaction (Figure 17). An additional measurement of the heat of mixing between the solution of the base **3.56** and toluene was performed (Table 18, entry 4; Figure 18 left). With the heat of mixing determined, the initial values were corrected and the energy storage density $\Delta H_{storage}$ was calculated as 311 J/g (Figure 18, right). As this value matches the one of the previously

measured additions of **3.26** to base **3.56** in toluene (311 J/g), it can be assumed to be accurate.

Table 18: DSC measurements of the dropwise addition of base 3.56 in toluene into a solution of benzocyclobutenol 3.26 in toluene (0.2 mL), reactions performed at 90 °C.

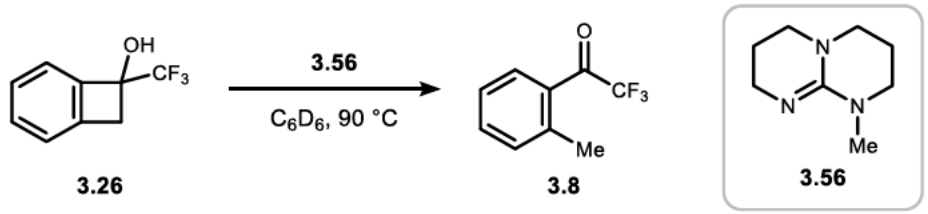

Entry	Amount of **3.26**	Equivalents of added base	Energy
1	550 µmol	0.06 eq. (50 µL)	32.442 J
2	271 µmol	0.05 eq. (25 µL)	15.337 J
3	550 µmol	0.13 eq (75 µL)	32.214 J
4	-	50 µL	–0.092 J

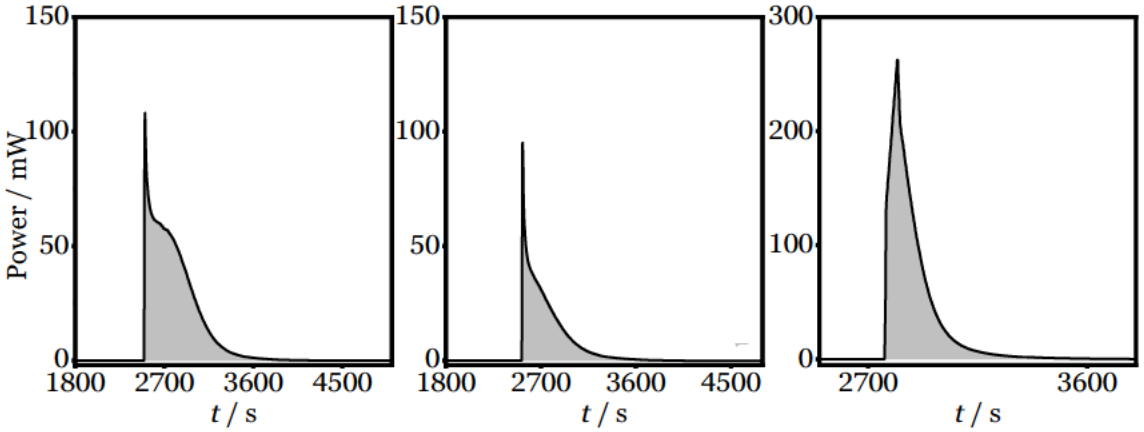

Figure 17: DSC measurements of the dropwise addition of base 3.56 into benzocyclobutenol 3.26, corresponding to Table 18. Left: entry 1, middle: entry 2, right: entry 3.

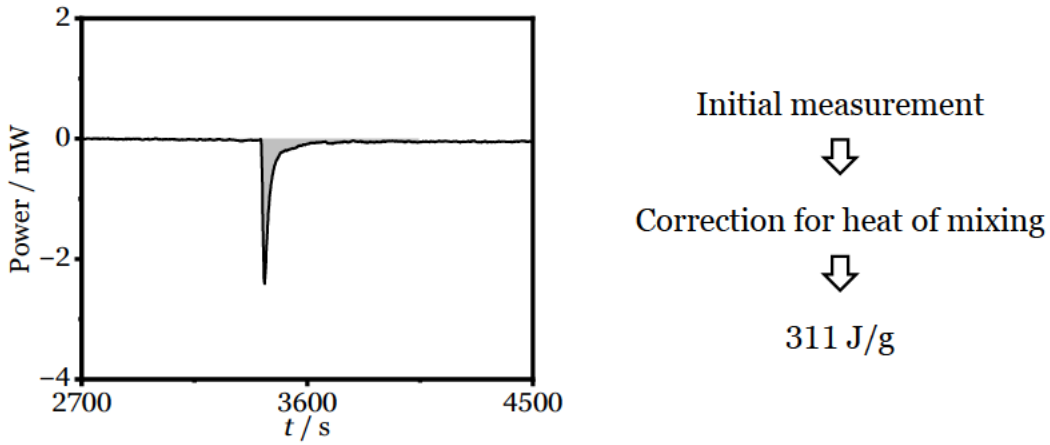

Figure 18: Left: DSC measurement of the heat of mixing of base 3.56 and toluene. Right: Energy storage density of benzocyclobutenol 3.26.

3.7 Cyclability of the system

The cyclability is a central parameter of MOST systems. It was hence investigated whether the photocyclisation and base-accelerated ring-opening of the standard system could be combined into a circular process.

For the initial photoreaction, a scale of 0.5 mmol of acetophenone **3.8** in benzene (100 mM) was envisioned according to the successful employment of large scales in the optimisation if the key parameters (*cf.* chapter 3.3). The solution was degassed, and the reaction run under nitrogen atmosphere to exclude oxygen. A 370 nm Kessil lamp was used to achieve fast reaction rates even at ambient temperature thus enabling simple reaction set-ups. For the ring opening, the polymer supported base **3.57** was used, and the reaction was run for 24 h to achieve a relevant conversion. Indeed, the first irradiation proceeded in near quantitative yield without formation of side products (>99%, Figure 19, reaction 1), and the base opening proceeded in a good yield of 90% (reaction 2). Here, the residual material was determined to be benzocyclobutenol **3.26** and a combined substance recovery of 98% was achieved. At last, the retrieved material was successfully charged with light again (>99% yield, reaction 3), demonstrating the feasibility of multiple cycles.

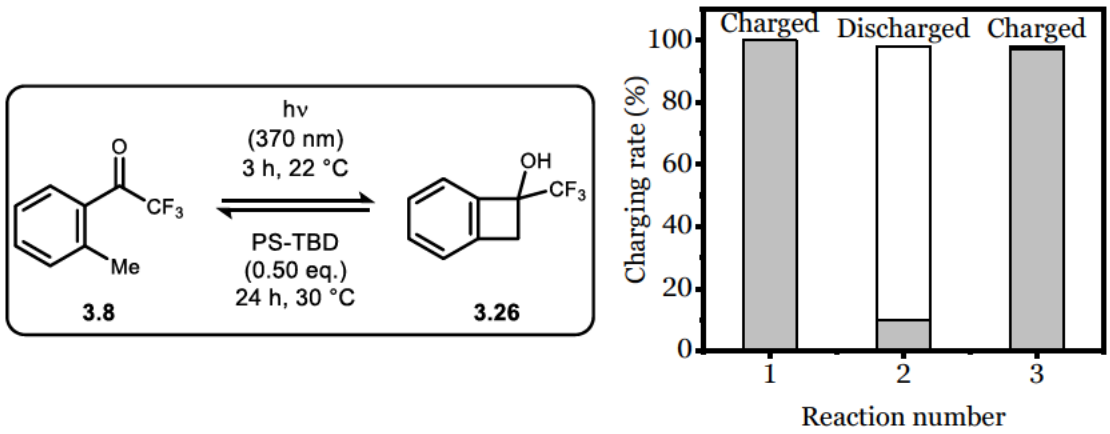

Figure 19: Charge/Discharge experiments for the system 3.8 ⇄ 3.26. Reaction performed on 0.5 mmol scale in degassed benzene (100 mM) at 30 °C, yields determined by ^{19}F NMR with $PhCF_3$ as internal standard as the mean value of two experiments. Discharging performed using PS-TBD 3.57 (0.50 eq.) as catalyst. Right: Graphical representation of the cycles. The grey bar corresponds to the charging status of the system, whereas the combined amount of substance of the system is indicated by the height of the white bar.

3.8 Summary and outlook

The successful development of a MOST system based on the pair **3.8** ⇄ **3.26** was described. Charging of the system proceeds in perfect selectivity without formation of side-products in benzene, and there is no competition in absorption between starting material and product. Isolation of benzocyclobutenol **3.26** was demonstrated in yields up to 99% as a colourless solid. The reaction is very robust, and product formation is not restrained by concentration (up to 0.9 mol/l), scale (>10 mmol), temperature or light intensity. However, a high sensitivity towards the oxygen content of the reaction vessel was identified. Consequently, the mechanism of the reaction was investigated. Formation of benzocyclobutenol **3.26** follows first order kinetics, and a photoenol formed through [1,5] hydride shift was identified as the crucial intermediate of the reaction. The central photoenol was trapped with dienophiles to deliver stereoselective tricycles. A thermally allowed 4-π EC was recognised as the central step of the reaction based on diastereoselective reactivity of *ortho*-ethyl trifluoroacetophenones. This key-step explains the acceleration of reaction rates with increased temperature, which is reflected in the increased cyclisation quantum yields for the transformation (measured by [redacted], Φ = 10% at 20 °C, Φ = 17% at 45 °C). For higher temperatures, the 4-π EC becomes faster than an unproductive [1,5] hydride shift and thereby higher reaction yields are observed. The competition between 4-π EC and another potential [1,5] hydride shift for substrates with abstractable hydrogens was investigated. Starting from 2,2,2-trifluoro-substituted *ortho*-methylacetophenone **3.8** (CF_3-group), substrates were synthesised, where a fluorine atom was iteratively exchanged with a hydrogen atom, giving substituted acetophenones **3.21** (CHF_2-group), **3.18** (CH_2F-group) and **1.9** (CH_3-group). By comparison of the yields of their respective photocyclisation, a unique beneficial effect of a CF_3-group for the formation of benzocyclobutenols was substantiated. The aforementioned influence of oxygen was analysed in detail, with elucidation of the formed side products and their degradation products. Additionally, unambiguous confirmation of all relevant products by X-Ray diffraction was achieved.

Several other benzocyclobutenols were synthesised over the course of this project, from which three substances emerged based on their reactivity. A visualisation of the relative reaction rates of the employed substrates to the standard pair **3.8** ⇄ **3.26** is depicted in a bubble diagram in Figure 20. The energy storage

density of benzocyclobutenol **3.26** (*vide infra*) was used to calculate the energy densities of the different derivatives (*cf.* chapter 4.3.4.1).

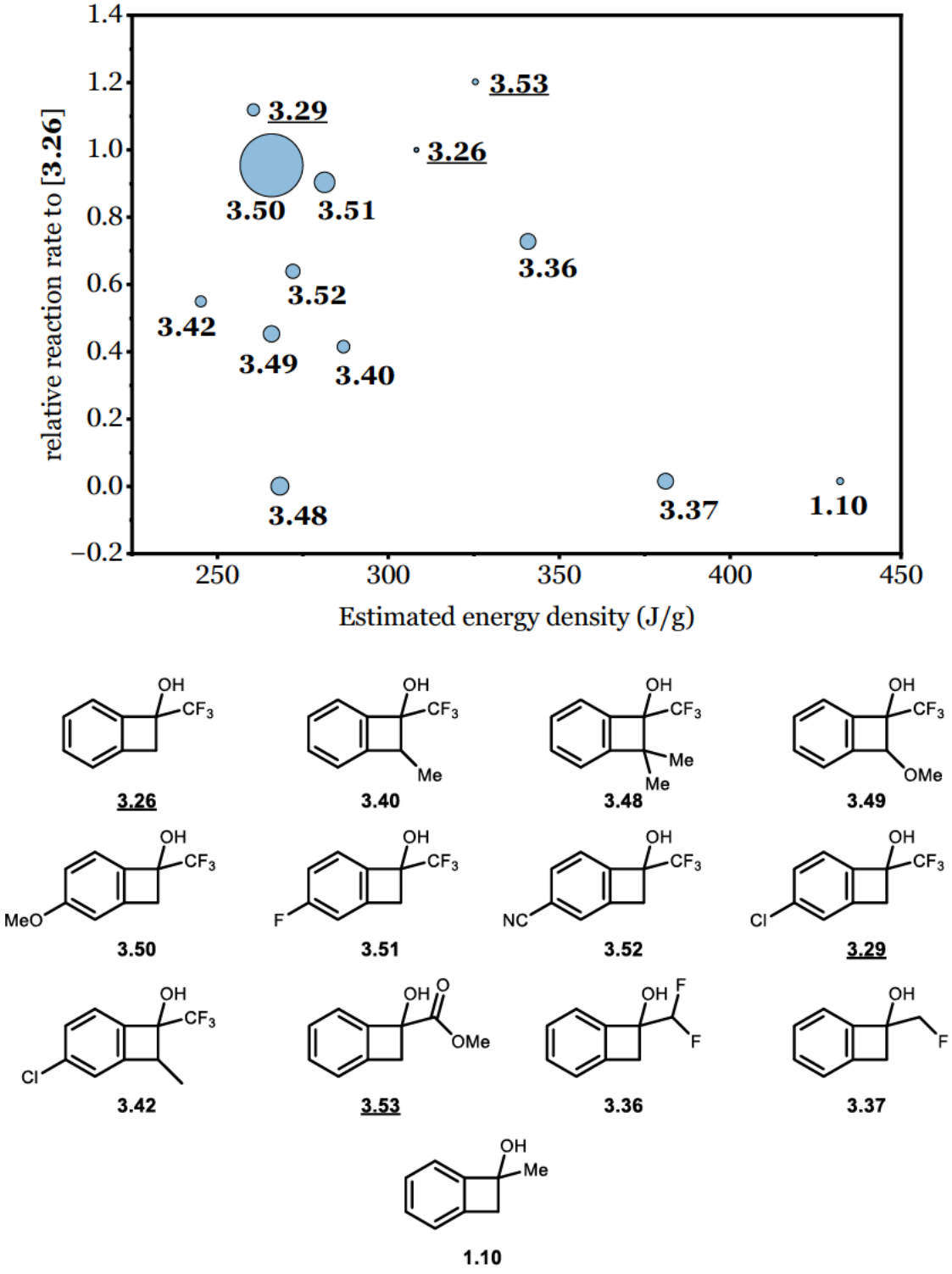

Figure 20: Visualization of the relative rates of the photocyclisation relative to the standard product 3.26. The size of the bubbles indicates the difference between conversion and yield of product, where bigger bubbles correspond to a larger amount of side reactions.

The standard product **3.26** and the benzocyclobutenol **3.29** and **3.53** were formed with the highest reaction (Figure 20, top). Several of the synthesised benzocyclobutenols show higher potential energy densities (*e.g.* **1.10** and **3.37**), but

their low synthetic accessibility excludes them as potential MOST candidates. The selected visualisation neglects the potential influence of molecular substitution on the absolute energetic properties of the molecule, which would in turn alter the achievable values of the potential energy density of the different benzocyclobutenols. Fortunately, this effect is expected to be small for the three molecules **3.26**, **3.29** and **3.53**, underlining their status as auspicious MOST candidates.

The ring-opening of benzocyclobutenols was investigated. The thermal back-isomerisation was analysed for the substrate pair **3.8** ⇄ **3.26** at elevated temperatures (220–250 °C) and the half-life of benzocyclobutenol **3.26** at room temperature was extrapolated to be 5×10^8 years. Its evident stability renders it practically inert under uncatalysed conditions at ambient temperatures and makes it an excellent candidate for long-term storage. The use of high temperatures for the release of the stored energy is impracticable, hence a way to increase the reaction rate through catalysis was sought after. Indeed, an acceleration of the rate of back-isomerisation by addition of catalytic amounts of strong organic bases could be demonstrated. Subsequently, the reaction temperature was lowered to room temperature. Several bases were successful in catalysing the ring-opening of benzocyclobutenols, from which polymer-supported base **3.57** was identified as a heterogeneous catalyst for application purposes. Here, the candidates **3.29** and **3.53** were excluded from the study based on evidence of degradation upon their base-catalysed ring opening. DSC measurements of benzocyclobutenol **3.26** revealed an energy density of 311 J/g. Finally, the use of solar light for the formation of benzocyclobutenol **3.26** from acetophenone **3.8** was shown with up to 95% yield and the successful cyclisation of the system was demonstrated. Thereby, the MOST system **3.8** ⇄ **3.26** is presented, which satisfies *Yoshidas* parameters pretty well (Figure 21).[88]

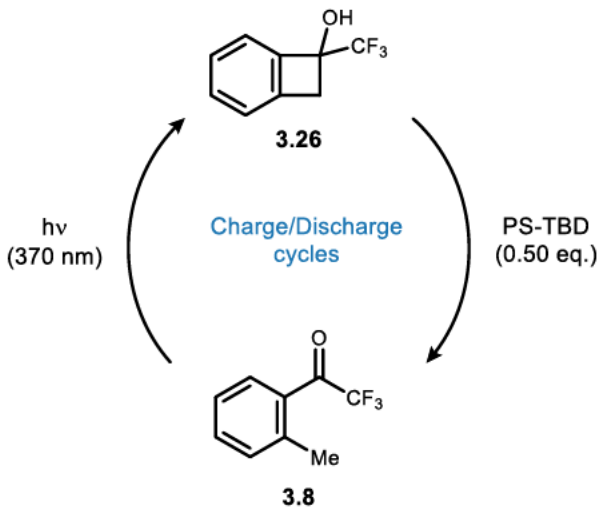

Absorption	sun light, no competition
Quantum yield	10% (20 °C), increase with higher T [a]
$\tau_{1/2}$	5×10^8 years
$\Delta H_{storage}$	311 J/g
Trigger	base initiation
Cyclability	no degradation

Figure 21: Summary of the properties of the developed MOST system 3.8⇄3.26. Left: Schematic representation of charge/discharge cycles. Right: Summary of the relevant parameters. [a] Quantum yield determined by [redacted].

The introduced substance pair **3.8** ⇄ **3.26** provides several benefits compared to established MOST systems (*cf.* chapter 3.1.1). An ideal MOST system can be charged using energy from the sun, whereby the reaction temperature is inevitably elevated due to the accompanying infrared irradiation. Many systems with high energy densities around 300 J/g already degrade at temperatures around 60 °C and hence need additional cooling equipment to stay efficient.[134] In contrast, the efficiency of the developed system towards generation of benzocyclobutenol **3.26** increases for elevated reaction temperatures. Besides, the formed product evaporates before it releases its energy under thermal activation, which could enable concentration by distillation for energy efficient transportation of the neat MOST substance. Compared to traditional storage systems, the outstanding half-life outcompetes most of the commercially available energy storage systems today. Eventually, all heat storing devices radiate off their stored energy, hydrogen gas evaporates from storage tanks[135] and lithium-ion battery arrays self-discharge 46% in a year.[136] Although the estimated overall efficiency of MOST systems (15%)[90b] will be less than the one of solar cells (32%),[137] the direct applicability for heat storage and clever engineering can narrow the gap. Exemplarily, the use of a transparent MOST systems as a window coating was already demonstrated by *Moth-Poulsen* and coworkers.[138] Here, the system is charged over the day and releases heat into the room throughout the night, increasing the energy efficiency compared to normal windows. The optical

transparency of the herein designed system makes it ideal for such applications, as well as combination with traditional solar cell systems. An upper MOST filter layer could be charged with sunlight, whereas the residual photons could be harnessed by a solar cell layer beneath. Therefore, the general cycle setup will need to be improved. The polymer supported base **3.57** could be loaded into a fixed-bed reactor with a heat-exchange chamber and the cycle could be automated using flow chemistry. UV-vis spectroscopy could help to determine the charge status of a secluded system which could then be cycled automatically using pumping systems and reservoirs. Using a closed system allows for the exclusion of oxygen and could hence be a promising strategy for successful employment of the designed MOST system.

Currently, the energy density $\Delta H_{storage}$ of the system **3.8** ⇄ **3.26** is low compared to other established systems (*cf.* chapter 3.1.1). Furthermore, the absorption spectrum of **3.8** does only partially match the solar emission spectrum. These two drawbacks are addressable by structural variation of the parent compound **3.8** to contain several active MOST units or by combination with other known MOST systems (Scheme 57).

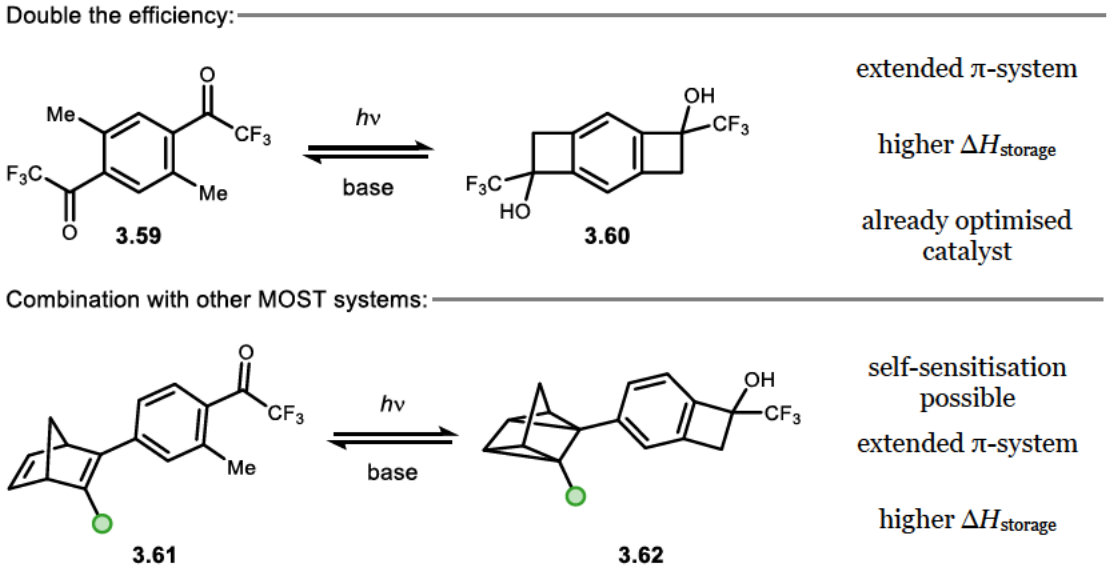

Scheme 57: Outline for potential improved MOST systems through combination of existing systems.

The existing system could be improved by mirroring the existing functional moieties into one acetophenone **3.59**. Extension of the conjugated π-system would be achieved and could red-shift the absorption. By generation of two strained rings in the photocyclisation towards product **3.60**, the energy density is increased, considering the shared molecular weight penalty compared to twice the storable energy. Another promising opportunity lies in the combination with

established MOST systems. The UV active system NBD⇄QC of starting material **3.61** can be sensitised by acetophenones, which could allow both systems to react under sunlight irradiation.[95] Here an estimated interplay might increase the overall quantum yield even further. Incorporating the two systems into one molecule could improve the spectral coverage of the solar spectrum and overall energy density. Existing catalysts could be used to selectively release energy of one of the systems of product **3.62**, or new catalysts would need to be developed if a tandem opening under ambient conditions was desired.

At last, the toxicity of the employed trifluoroacetophenones and trifluoromethyl substituted benzocyclobutenols is untested and needs to be determined for potential applications.

4 Experimental part

4.1 General information

Analytical Methods: ^{1}H NMR, ^{19}F NMR, ^{13}C NMR spectra were recorded by the analytical department of the Department Chemie at Johannes Gutenberg-Universität Mainz. The following spectrometers were used: Avance III HD 300 (*Bruker*), Avance II 400 (*Bruker*), Avance III HD 400 (*Bruker*), and Avance III 600 equipped with a cryo-probe head (Bruker). Spectra were recorded at 22 °C (unless otherwise noted). Chemical shifts are reported in ppm with the solvent resonance as the internal standard (^{1}H NMR $CHCl_3$: δ = 7.26 ppm, C_6HD_5: δ = 7.16 ppm, $(CHD_2)(CD_3)SO$: δ = 2.50 ppm; CHD_2CN: δ = 1.94 ppm; ^{13}C NMR $CDCl_3$: δ = 77.16 ppm, C_6D_6 δ = 128.06 ppm, $(CD_3)_2SO$: δ = 39.50 ppm, CD_3CN: δ = 118.26 ppm). All carbon spectra were recorded proton decoupled, and with additional fluorine decoupling whenever mentioned. Chemical shifts of ^{19}F NMR are referenced to internal or external standards according to *Togni* and coworkers.[139] The data is reported as follows: chemical shift, multiplicity (s = singlet, d = doublet, t = triplet, q = quartet, p = pentet, br = broad, m = multiplet or combinations of these), coupling constants (Hz) and integration.

Melting points (m.p.) were measured on a *Büchi* B-540 melting-point apparatus and are reported uncorrected.

Infrared (**IR**) spectra were obtained on a on a FT/IR-4100 (*Jasco*) or a Tensor 27 spectrometer (*Bruker*) using a diamond ATR unit and are reported in wavenumbers (cm^{-1}). Bands are characterized as broad (br), strong (s), medium (m), and weak (w).

Optical rotations were measured on a *Perkin-Elmer* 241 polarimeter at 589 nm wavelength (sodium D-line) using a standard 10 cm cell (1 mL). Specific rotations, $[\alpha]_D^{20}$, are reported in degree mL/(g·dm) at the specific temperature. Concentrations (*c*) are given in grams per 100 mL of the specific solvent.

Analytical HPLC measurements were performed on the following system: *Knauer* HPLC Pump Smartline 1000 with degassing unit, *Knauer* Autosampler Smartline

3950, *Knauer* UV-detector Smartline 2550, *Knauer* RI-detector Smartline 2300. Separation was performed using Lux® i-Cellulose-5 (4.6 x 250 nm x 5 µm, *Phenomenex* Ltd.), Lux® Cellulose-1 (4.6 x 250 nm x 5 µm, *Phenomenex* Ltd.), Lux® Amylose-1 (4.6 x 250 nm x 5 µm, *Phenomenex* Ltd.), Lux® i-Amylose-3 (4.6 x 250 nm x 5 µm, *Phenomenex* Ltd.), or Reprosil Chiral-AMS (4.6 x 250 nm x 5 µm, *Dr Maisch* GmBH.).

High Resolution Mass Spectrometry (**HRMS**) was performed by the analytical department of the Department Chemie at Johannes Gutenberg-Universität Mainz. Spectra were recorded on a *Thermo-Fisher Scientific* DFS (GC-MS, ionization *via* electron ionization (EI) or chemical ionization (CI)) or on an *Agilent* 6545 Q-ToF (LC-MS, ionization *via* electron spray ionization (ESI), atmospheric-pressure chemical ionization (APCI)). Signals are reported as mass to charge ratio *m/z*.

Differential scanning calorimetry (**DSC**) was performed using a *µRC*® micro Reaction Calorimeter (*Thermal Hazard Technology, THT*) and analysis was conducted using the *µRC Analysis software 2.6.5*.

Purification methods: Purification was performed either with standard column chromatography techniques using *Geduran*® Si 60 silica gel (0.063-0.200 mm, *Merck*), on an automated flash chromatography system *Biotage Isolera One* utilizing *Biotage Sfär Silica D-Duo* 60 µm columns (5 g, 25 g, 100 g) or on an automated flash chromatography system Teledyne Isco with *Biotage Sfär Silica C18-Duo* 100 Å 30 µm columns (12 g).Glass silica gel plates 60 F254 (*Merck*) were used for analytic thin layer chromatography applying either UV light (254/366 nm), $KMnO_4$ (1.5 g $KMnO_4$, 5 g $NaHCO_3$ and 5 mL NaOH 10% in 200 mL H_2O) or CAM (0.5g $Ce(NH_4)_2(NO_3)_6$ and 24.0 g of $(NH_4)_6Mo_7O_{24}{\cdot}4H_2O$, 28 mL H_2SO_4 in 200 mL H_2O) for detection.

Reaction Set-up: Chemicals were purchased from *Alfa Aesar*, *Acros Organics*, *Sigma Aldrich*, *BLDpharm*, *FluoroChem*, *Carbolution* or *ABCR* and (unless otherwise stated) used as received. All reactions involving air or moisture sensitive reagents were carried out in oven- (125 °C) and flame-dried glassware under nitrogen atmosphere using standard *Schlenk* techniques. Dry solvents were

collected from an *MBraun MB SPS-800* (Et_2O: MB-KOL-A and MB-KOL MT2-250, THF: 2 × MB-KOL MT2-150°CCl_2: 2 × MB-KOL-A). A positive argon pressure was used to pass the solvents through the columns. Unless otherwise noted, all work-up and purification procedures were carried out with pre-distilled technical grade solvents. Photochemical reactions were performed in a *Luzchem* LZC-ORG photoreactor equipped with 10 × 8 Watt *Luzchem* LZC-355 mercury lamps, 10 × 8 Watt *Luzchem* LZC-420-LED lamps, 10 × 8 Watt *Luzchem* LZC-LCW-LED lamps or by using a 40 W 370 nm Gen 2 KSPR160L Kessil LED (see Figure 22 to Figure 25 for emission spectra and Figure 26 and Figure 27 for reaction set-up).

Documentation: The experimental work was partly documented using the electronic lab notebook (ELN) *Chemotion*. A respective sample number is indicated in the corresponding entries. Otherwise, the documentation was carried out using conventional lab notebooks in paper form.

X-Ray diffraction: Data sets for compounds **3.26**, **3.28**, **3.30** and **3.42** were collected by [redacted] with a STOE IPDS-2T Diffractometer system. Programs used: data collection: X-Area WinXpose 2.0.22.0 [140] (*X-RED* and *X-AREA*, Stoe & Cie, **2019**), cell refinement: X-Area Recipe 1.36.0 [140] (*X-RED* and *X-AREA*, Stoe & Cie, **2019**), data reduction: X-Area Integrate 1.78.3 [140] (*X-RED* and *X-AREA*, Stoe & Cie, **2019**), structure solution *SHELXT-2014* [141](Sheldrick, G. M. *Acta Cryst.,* **2015**, *A71*, 3-8); structure refinement *SHELXL-2018/3* [142](Sheldrick, G. M. *Acta Cryst.,* **2015**, *C71* (1), 3-8) and graphics Platon [143] (Spek, A. L. *Acta Cryst.,* **2009**, *D65*, 148-155). *R*-values are given for observed reflections, and wR^2 values are given for all reflections.

Emission spectra of the lamps:

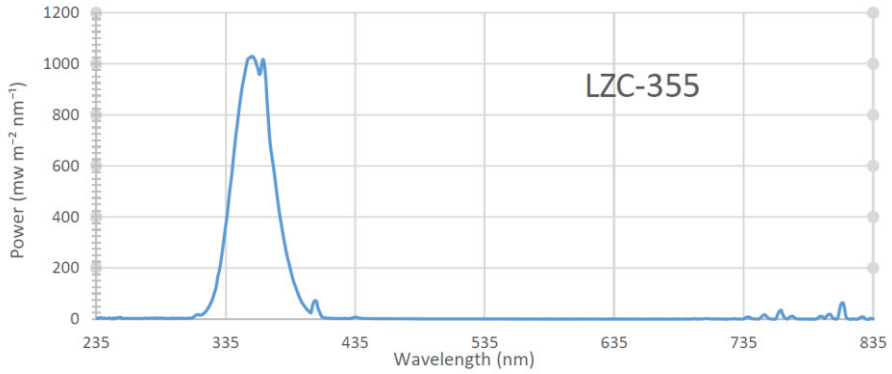

Figure 22: Emission spectrum of the *Luzchem* LZC-355 fluorescence lamp.[144]

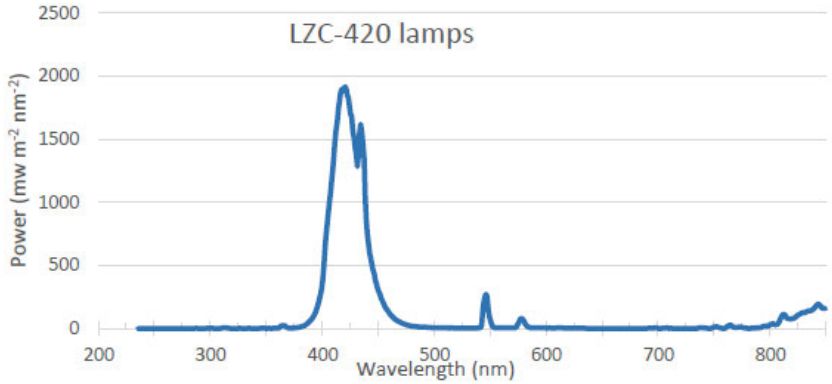

Figure 23: Emission spectrum of the *Luzchem* LZC-420 fluorescence lamp.[144]

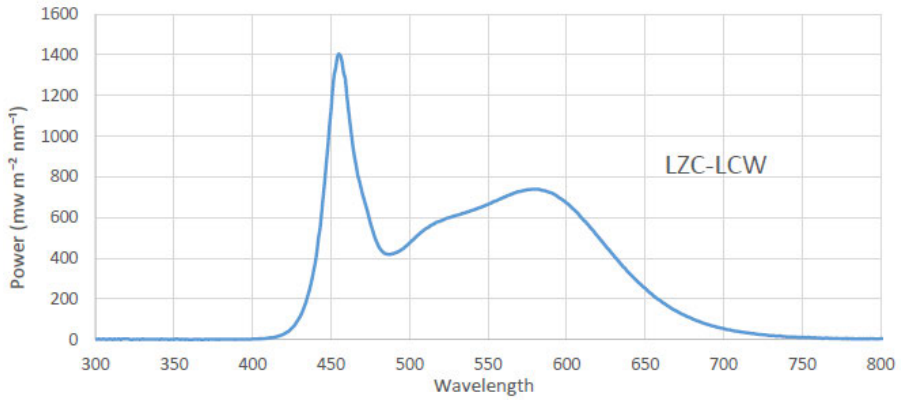

Figure 24: Emission spectrum of the *Luzchem* LZC-LCW LED lamp.[144]

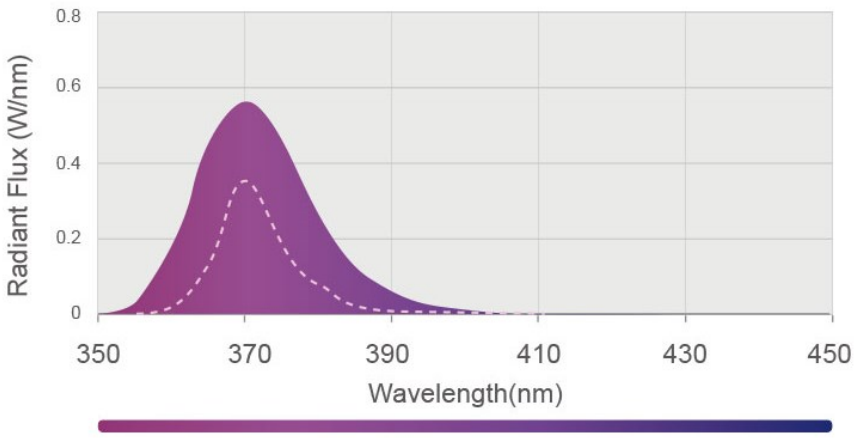

Figure 25: Emission spectrum of the *Kessil* 370 nm Gen 2 KSPR160L LED.[145]

Irradiation set-ups:

Reactions were either performed in a *Luzchem* Photoreactor (Figure 26) or using Kessil lamps (Figure 27). In the photoreactor, samples were placed in a rotatable sample holder for uniform irradiation (Figure 26, A) or stirred using the integrated magnetic stirrer (Figure 26, A). The temperature was monitored using a temperature probe and maintained by the integrated fan unit at 5 °C above room temperature, and the integrated timer was used to ensure that all reactions were terminated simultaneously. When using a Kessil lamp, reactions were performed inside the *Luzchem* Photoreactor to benefit from the cooling and shielding it provides (Figure 27, A) or a water bath was used for maintaining the desired temperature (Figure 27, B).

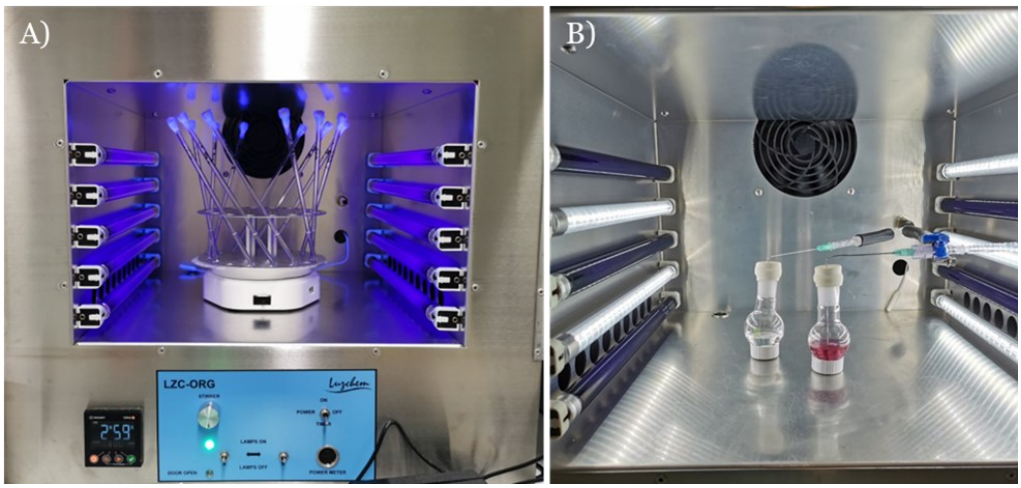

Figure 26: Irradiation in a *Luzchem* photoreactor. A: Simultaneous irradiation of several samples using a rotatable sample carousel for even distribution of light over time. B: Irradiation of samples under oxygen atmosphere, which are agitated using the integrated magnetic stirrer and stir bars and connected to an external ballon of oxygen outside the reactor with black tubing.

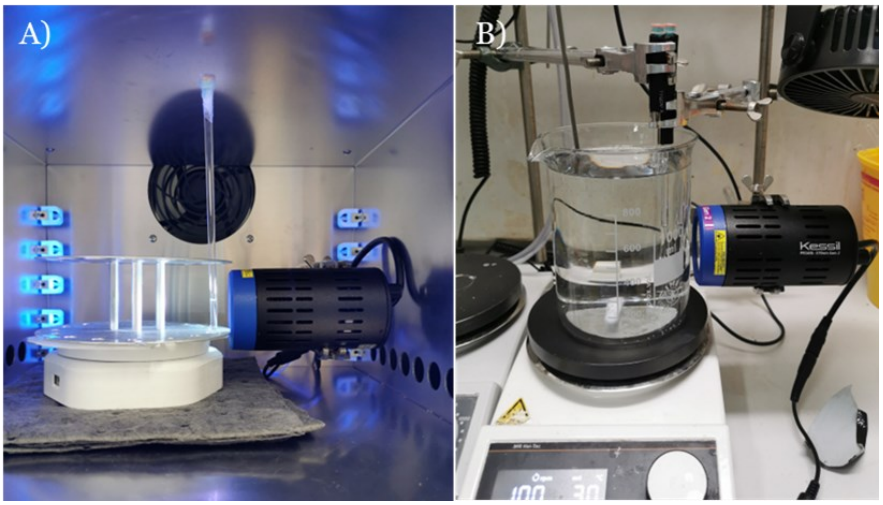

Figure 27: Irradiation set-up using a Kessil lamp (370 nm) from 1 cm distance. b) Irradiation at variable temperatures with 370 nm and 2 cm distance.

4.2 Construction and ring-opening of four-membered heterocycles

General procedures

General procedure A (GP-A) for the preparation of *α*-aminoacetophenones from *α*-bromoacetophenones:

α-Aminoacetophenones were prepared following an adapted literature known protocol.[46] A secondary amine (1.00 eq.) was dissolved in acetonitrile (1 M) and an *α*-bromoacetophenone (1.00 eq.) and K_2CO_3 (2.00 eq.) were added. The mixture was stirred at rt for 16 h, the solids were filtered-off and washed with acetonitrile. The solvent was removed under reduced pressure and the desired product was isolated after flash chromatography (FC), automated FC, reversed phase medium pressure liquid chromatography (RP-MPLC) or recrystallization.

General procedure B (GP-B) for the preparation of 3-oxetanols from oxetan-3-one:

3-Substituted oxetanols were prepared following a lab-own protocol,[83] adapted from literature known reports.[146] A halogenated arene or alkyne (1.20 eq.) was dissolved in dry THF (0.1 M) under inert atmosphere and cooled to −78°C at which temperature *n*-BuLi (2.5 M, 1.20 eq.) was added dropwise. After 1 h, oxetan-3-one (1.00 eq.) was added slowly and the mixture was stirred at −78°C for 3 h, before it was slowly warmed up to rt for 17 h. The solution was diluted with Et_2O and NH_4Cl sat. was added. The organic phase was separated, and the aqueous phase was extracted with Et_2O (3x). The combined organic fractions were dried over $MgSO_4$ and the solvent was removed *in vacuo*. The products were isolated after FC or automated FC.

General procedure C (GP-C) for the preparation of Co^{II}·salen complexes:

Co^{II}·salen complexes were prepared following a literature known protocol with minor alterations.[73] EtOH was deoxygenated by purging with a constant flow of nitrogen for 10 min. $Co(OAc)_2 \cdot 4H_2O$ (1.00 eq.) was dissolved under inert atmosphere in the deaerated EtOH and stirred until the salt was dissolved completely.

Then a salen-type ligand (1.00 eq.) was added and the mixture was heated to reflux for 17 h. The solution was cooled to −18 °C, the resulting precipitate was filtered off and washed with small portions of ice-cold EtOH. The filtrate was concentrated under reduced pressure, and the obtained residue was recrystallised to gain a second crop of the complex.

General procedure D (GP-D) for the synthesis of 3-phenylazetidinols from *α*-aminoacetophenones:

3-Phenylazetidinols were prepared following a literature known protocol[46]. An *α*-aminoacetophenone was dissolved in acetonitrile or THF (50 mM) and was irradiated using a Luzchem Photoreactor equipped with 10 8 Watt LZC-UVA (355 nm) lamps at rt (Figure 26). The solvent was removed under reduced pressure and desired product was isolated after FC, automated FC, or RP-MPLC.

General procedure E (GP-E) for the synthesis of 3-phenylazetidinols from *α*-aminoacetophenones:

An *α*-aminoacetophenone was dissolved in *N*,*N*-dimethylformamide (DMF) (50 mM) and was irradiated using a Luzchem Photoreactor equipped with 10 8 Watt LZC-UVA (355 nm) lamps at rt (Figure 26). EtOAc (10 mL) was added and the mixture was washed with aq. LiCl solution (5%, 3 x 10 mL) to remove DMF and the organic phase was dried over $MgSO_4$. The solvent was removed under reduced pressure and desired product was isolated after FC, automated FC, or RP-MPLC.

General procedure F (GP-F) for the desymmetrisation of 3-substituted oxetanols:

Ketone **2.52** (52.8 mg, 0.20 mmol, 1.00 eq.) and Co^{II}·salen complex **2.67** or **2.68** (1 mol%) were dissolved in dry CH_2Cl_2 (0.4 M) at rt. A 3-substituted oxetanol (0.20 mmol, 1.00 eq.) was added to this solution. The temperature was maintained for 24 h before silica gel was added and the mixture was passed over a filter. The resulting silica gel plug was flushed with Et_2O, and the filtrate was concentrated under reduced pressure. The NMR yield and *dr* of the crude reaction mixture were determined by ^{19}F NMR using $PhCF_3$ (0.10 mmol) as the internal standard. The product diastereomers were separated by automated FC or RP-MPLC.

4.2.1 Synthesis of starting materials

4.2.1.1 Synthesis of *α*-substituted acetophenones

N-Methyl-p-toluenesulfonamide (4.1)

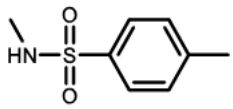

N-Methyl-p-toluenesulfonamide **4.1** was prepared following a literature known protocol.[46] *p*-Toluenesulfonyl chloride (6.08 g, 31.87 mmol, 1.00 eq.) was dissolved in Et_2O (30 mL) and an aqueous solution of methylamine (40 wt%, 6.34 mL, 73.87 mmol, 2.32 eq.) was added at 0 °C. The mixture was stirred at rt for 16 h and water (30 mL) was added. The phases were separated, and the aqueous layer was extracted with EtOAc (3 x 40 mL). The combined organic fractions were washed with brine (40 mL) and were dried over $MgSO_4$. The solvent was removed under reduced pressure and the crude product was purified *via* automated FC (CyH : EtOAc, 100:0 to 60:40) and the product was obtained as a colourless solid (5.68 g, 30.7 mmol, 96%).

^{1}H NMR (400 MHz, $CDCl_3$): δ = 7.77 – 7.72 (m, 2H)), 7.35 – 7.29 (m, 2H), 4.26 (s, 1H), 2.65 (d, J = 4.5 Hz, 3H), 2.43 (s, 3H). **^{13}C NMR (101 MHz, $CDCl_3$)**: δ = 143.7, 135.9, 129.9, 127.4, 29.5, 21.7. Spectroscopic data was in agreement to those previously reported. [147]

Chemotion ELN sample number: HMA-4-47.

N,4-Dimethyl-N-(2-oxo-2-phenylethyl)benzenesulfonamide (2.5)

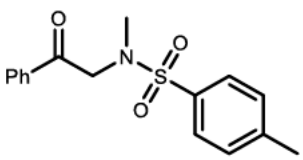

Following **GP-A** with minor alterations, using N-methyl-p-toluenesulfonamide **4.1** (1.85 g, 10.0 mmol, 1.00 eq.), 2-bromoacetophenone (2.00 g, 10 mmol, 1.00 eq.) and K_2CO_3 (1.30 g, 10 mmol, 1.00 eq.) in acetonitrile (20 mL). The

desired product was obtained after automated FC (CyH : EtOAc, 100:0 to 90:10) as a colourless solid (1.90 g, 6.24 mmol, 62%).

^{1}H NMR (400 MHz, $CDCl_3$): δ = 8.01 – 7.94 (m, 2H), 7.76 – 7.69 (m, 2H), 7.65 – 7.57 (m, 1H), 7.52 – 7.44 (m, 2H), 7.36 – 7.31 (m, 2H), 4.57 (s, 2H), 2.83 (s, 3H), 2.45 (s, 3H). **^{13}C NMR (101 MHz, $CDCl_3$)**: δ = 193.9, 143.8, 134.9, 134.0, 129.8, 129.0, 128.4, 127.7, 56.2, 35.7, 21.7.[a] Spectroscopic data was in agreement to those previously reported.[46]

Chemotion ELN sample number: HMA-3-3.

N-Ethyl-4-methylbenzenesulfonamide (4.2)

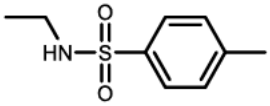

p-Toluenesulfonyl chloride (381 mg, 2.00 mmol, 1.00 eq.) and ethylamine (69% in water, 303 mg, 374 µL, 4.64 mmol, 2.32 eq.) were dissolved in Et_2O (5.00 mL) and the mixture was stirred for 18 h. Water was added (5 mL) and the aqueous phase was extracted with EtOAc (3 x 15 mL). The combined organic fractions were dried over $MgSO_4$, and the solvent was removed under reduced pressure. The crude product was used without further purification.

^{1}H NMR (400 MHz, $CDCl_3$): δ = 7.79 – 7.71 (m, 2H), 7.35 – 7.28 (m, 2H), 4.29 (s, 1H), 3.00 (qd, J = 7.2, 6.0 Hz, 2H), 2.43 (s, 3H), 1.10 (t, J = 7.2 Hz, 3H). **^{13}C NMR (101 MHz, $CDCl_3$)**: δ =143.5, 137.1, 129.8, 127.3, 38.4, 21.7, 15.2. Spectroscopic data was in agreement to those previously reported.[148]

Chemotion ELN sample number: HMA-4-452.

[a] Signals missing due to signal overlapping.

N-Ethyl-4-methyl-N-(2-oxo-2-phenylethyl)benzenesulfonamide (2.38)

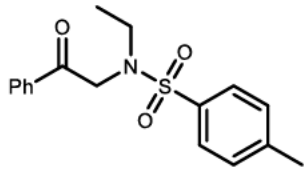

Following general procedure **GP-A**, using the crude product **4.2** without further purification, 2-bromoacetophenone (398 mg, 2.00 mmol, 1.00 eq.) and K_2CO_3 (553 mg, 4.00 mmol, 2.00 eq.) in acetonitrile (2 mL). The desired product was obtained after automated FC (CyH : EtOAc, 100:0 to 90:10) as a colourless solid (437 mg, 1.38 mmol, 69%).

M.P.: 95 – 98 °C. **IR (neat)**: $\tilde{\nu}$ = 3064 (w), 2977 (w), 2930 (w), 2876 (w), 1701 (m), 1597 (w), 1580 (w), 1494 (w), 1449 (w), 1415 (w), 1383 (w), 1332 (m), 1306 (w), 1289 (w), 1225 (m), 1209 (m), 1183 (w), 1155 (s), 1121 (w), 1090 (m), 1041 (w), 1019 (w), 1001 (w), 970 (m), 932 (w), 894 (m), 815 (m), 787 (w), 754 (m), 735 (s), 690 (m), 669 (m), 642 (m), 569 (w), 548 (s), 483 (w). **^{1}H NMR (400 MHz, $CDCl_3$)**: δ = 7.99 – 7.92 (m, 2H), 7.79 – 7.72 (m, 2H), 7.64 – 7.56 (m, 1H), 7.53 – 7.43 (m, 2H), 7.34 – 7.28 (m, 2H), 4.75 (s, 2H), 3.33 (q, J = 7.2 Hz, 2H), 2.43 (s, 3H), 1.09 (t, J = 7.2 Hz, 3H). **^{13}C NMR (101 MHz, $CDCl_3$)**: δ = 194.3, 143.5, 137.0, 135.0, 133.9, 129.7, 129.0, 128.2, 127.6, 52.5, 43.2, 21.7, 13.5. **HRMS (ESI)**: Calculated for $C_{17}H_{20}NO_3S$ $[M+H]^+$: 318.1158 found 318.1155.

Chemotion ELN sample number: HMA-3-39.

N-Benzyl-4-methylbenzenesulfonamide (4.3)

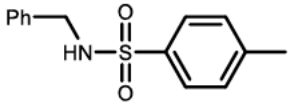

N-Benzyl-4-methylbenzenesulfonamide **4.3** was prepared following a literature known protocol. [149] Benzylamine (107 mg, 109 µL, 1.00 mmol, 1.00 eq.) and triethylamine (152 mg, 209 µL, 1.50 mmol, 1.50 eq.) were dissolved in dichloromethane (1 mL) and *p*-toluenesulfonyl chloride (191 mg, 1.00 mmol, 1.00 eq.)

was added dropwise as a solution in dichloromethane (3 mL). The reaction mixture was stirred for 3 h and water (5 mL) was added. The aqueous phase was extracted with dichloromethane (3 x 10 mL) and the combined organic fractions were dried over $MgSO_4$. The solvent was removed under reduced pressure and the mixture was purified *via* automated FC (CyH : EtOAc, 100:0 to 40:60) and was obtained as a colourless solid (212 mg, 811 µmol, 81%).

M.P.: 115 – 118 °C. **IR (neat)**: $\tilde{\nu}$ = 3269 (s), 3051 (w), 3034 (w), 2916 (w), 1598 (w), 1496 (w), 1455 (m), 1422 (m), 1381 (w), 1364 (w), 1322 (s), 1289 (w), 1177 (m), 1164 (s), 1094 (w), 1083 (m), 1060 (m), 1029 (w), 875 (m), 812 (w), 741 (s), 703 (m), 683 (m), 601 (m), 551 (s), 541 (m), 519 (w), 478 (w), 461 (w). **^{1}H NMR (400 MHz, $CDCl_3$)**: δ = 7.87 – 7.71 (m, 2H), 7.34 – 7.29 (m, 2H), 7.29 – 7.24 (m, 3H), 7.23 – 7.17 (m, 2H), 4.63 (t, J = 6.2 Hz, 1H), 4.12 (d, J = 6.1 Hz, 2H), 2.44 (s, 3H). **^{13}C NMR (101 MHz, $CDCl_3$)**: δ = 143.7, 137.0, 136.4, 129.9, 128.9, 128.1, 128.0, 127.3, 47.4, 21.7. **HRMS (ESI)**: Calculated for $C_{14}H_{16}NO_2S$ $[M+H]^+$: 262.0896, found: 262.0894. Spectroscopic data was in agreement to those previously reported [150].

Chemotion ELN sample number: HMA-4-73.

N-Benzyl-4-methyl-N-(2-oxo-2-phenylethyl)benzenesulfonamide (2.39)

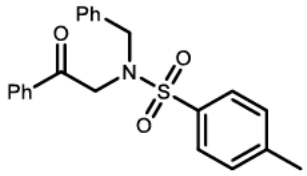

Following **GP-A**, using N-benzyl-p-toluenesulfonamide **4.3** (1.31 g, 5.00 mmol, 1.00 eq.), 2-bromoacetophenone (995 mg, 5.00 mmol, 1.00 eq.) and K_2CO_3 (1.38 g, 10.0 mmol, 2.00 eq.) in acetonitrile (10.0 mL). The desired product was obtained after FC (pentane / EtOAc (100:20) and recrystallisation from CyH / toluene (90:10) as a colourless solid (650 mg, 1.71 mmol, 34%).

M.P.: 116 – 118 °C. **IR (neat)**: $\tilde{\nu}$ = 3064 (w), 3031 (w), 2923 (w), 1699 (m), 1598 (w), 1581 (w), 1495 (w), 1449 (w), 1404 (w), 1337 (m), 1306 (w), 1289 (w), 1226 (m), 1156 (s), 1094 (m), 1058 (w), 1029 (w), 993 (w), 936 (w), 904 (w), 814

(w), 752 (m), 739 (m), 691 (m), 670 (m), 651 (w), 603 (w), 550 (m). **^{1}H NMR (400 MHz, DMSO-d_6)**: δ = 7.87 – 7.82 (m, 2H), 7.78 – 7.73 (m, 2H), 7.67 – 7.58 (m, 1H), 7.52 – 7.44 (m, 2H), 7.44 – 7.36 (m, 2H), 7.29 – 7.22 (m, 3H), 7.21 – 7.15 (m, 2H), 4.71 (s, 2H), 4.41 (s, 2H), 2.42 (s, 3H). **^{13}C NMR (101 MHz, DMSO-d_6)**: δ = 193.9, 143.1, 137.0, 135.8, 134.6, 133.6, 129.6, 128.7, 128.4, 128.3, 127.9, 127.6, 127.2, 53.1, 51.6, 21.0. **HRMS (ESI)**: Calculated for $C_{22}H_{22}NO_3S$ $[M+H]^+$ 380.1315, found: 380.1309. Spectroscopic data (^{1}H NMR) was in agreement to those previously reported.[151]

Chemotion ELN sample number: HMA-3-68.

N-Methylmethanesulfonamide (4.4)

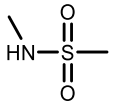

Methanesulfonyl chloride (1.15 g, 774 µL, 10.0 mmol, 1.00 eq.) was dissolved in dry THF under nitrogen atmosphere and methylamine in THF (932 mg, 15.0 mL, 30.0 mmol, 2.00 M, 3.00 eq.) was added dropwise over 15 min at 0 °C. The mixture was stirred at 0 °C for 15 min and then at rt overnight. The solvent was removed under reduced pressure and the crude product was purified *via* bulb-to-bulb distillation (0.87 mbar, 125 °C to 140 °C) to obtain a colourless oil (1.04 g, 9.53 mmol, 95%).

IR (neat): $\tilde{\nu}$ = 3578 (w), 3295 (w), 3020 (w), 2937 (w), 2823 (w), 1633 (w), 1464 (w), 1406 (w), 1305 (s), 1148 (s), 1130 (s), 1070 (m), 971 (m), 836 (m), 754 (m), 643 (w), 521 (s), 456 (m). **^{1}H NMR (600 MHz, $CDCl_3$)**: δ = 4.23 (s, 1H), 2.95 (s, 3H), 2.84 (s, 3H). **^{13}C NMR (151 MHz, $CDCl_3$)**: δ = 39.0, 29.5. **HRMS (ESI)**: Calculated for $C_2H_6NO_2S$ $[M-H]^-$ 108.0125, found: 108.0116. Spectroscopic data was in agreement to those previously reported [152].

Chemotion ELN sample number: HMA-4-26.

N-Methyl-N-(2-oxo-2-phenylethyl)methanesulfonamide (2.40)

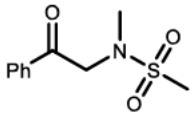

Following **GP-A**, using N-methylmethanesulfonamide **4.4** (518 mg, 4.75 mmol, 1.00 eq.), 2-bromoacetophenone (945 mg, 4.75 mmol, 1.00 eq.) and K_2CO_3 (1.31 g, 9.49 mmol, 2.00 eq.) in acetonitrile (10 mL). The desired product was obtained after automated FC (CyH : EtOAc, 100:0 to 50:50), and subsequent re-crystallisation from hot EtOAc as a colourless solid (970 mg, 4.27 mmol, 90%).

M.P.: 104 – 105 °C. **IR (neat)**: $\tilde{\nu}$ = 3064 (w), 2933 (w), 1698 (m), 1597 (w), 1450 (w), 1410 (w), 1328 (s), 1225 (m), 1155 (s), 1024 (w), 969 (m), 946 (w), 917 (w), 817 (w), 779 (m), 757 (m), 690 (w), 647 (w), 520 (m), 485 (w). **^{1}H NMR (600 MHz, $CDCl_3$)**: δ = 7.95 – 7.90 (m, 2H), 7.63 (m, 1H), 7.53 – 7.47 (m, 2H), 4.83 (s, 2H), 3.06 (s, 3H), 3.04 (s, 3H). **^{13}C NMR (151 MHz, $CDCl_3$)**: δ = 194.8, 134.6, 134.3, 129.1, 128.0, 56.3, 38.9, 35.6. **HRMS (ESI)**: Calculated for $C_{10}H_{13}NO_3SNa$ $[M+Na]^+$: 250.0508, found 250.0508.

Chemotion ELN sample number: HMA-4-28.

N-Ethylmethanesulfonamide (4.5)

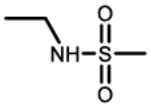

Ethylamine hydrochloride (815 mg, 10.0 mmol, 2.00 eq.) and K_2CO_3 (1.52 g, 11.0 mmol, 2.20 eq.) were added to THF (5.00 mL) and methanol (0.25 mL) and stirred for 5 min, then methanesulfonyl chloride (573 mg, 387 µL, 5.00 mmol, 1.00 eq.) was added dropwise at 0 °C and the mixture was stirred at rt for 16 h. The solution was filtered, and the solvent was removed under reduced pressure. The crude product was purified *via* automated FC (CyH : EtOAc, 100:00 to 20:80) and was obtained as a colourless oil (407 mg, 3.30 mmol, 66%).

IR (neat): $\tilde{\nu}$ = 3576 (w), 3284 (w), 2982 (w), 2937 (w), 2882 (w), 1454 (w), 1433 (w), 1412 (w), 1385 (w), 1310 (s), 1151 (s), 1063 (m), 978 (m), 939 (w), 860 (w),

785 (w), 761 (w), 648 (w), 630 (w), 617 (w), 600 (w), 521 (m), 488 (w), 476 (w), 466 (w), 453 (w). **^{1}H NMR (400 MHz, $CDCl_3$)**: δ = 4.43 (s, 1H), 3.29 – 3.11 (m, 2H), 2.96 (s, 3H), 1.23 (t, J = 7.2 Hz, 3H). **^{13}C NMR (101 MHz, $CDCl_3$)**: δ = 40.5, 38.4, 15.8. **HRMS (ESI)**: Calculated for $C_3H_9NO_2SNa$ $[M+Na]^+$: 146.0246, found 146.0242. Spectroscopic data was in agreement to those previously reported [153].

Chemotion ELN sample number: HMA-4-33.

N-Ethyl-N-(2-oxo-2-phenylethyl)methanesulfonamide (2.41)

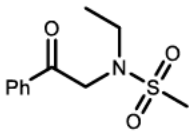

Following **GP-A**, using 2-bromoacetophenone (651 mg, 3.27 mmol, 1.00 eq.), N-ethylmethanesulfonamide **4.5** (403 mg, 3.27 mmol, 1.00 eq.) and K_2CO_3 (904 mg, 6.54 mmol, 2.00 eq.) in acetonitrile (6.50 mL). The desired product was obtained after automated FC (CyH : EtOAc, 100:00 to 60:40) as a colourless solid (562 mg, 2.33 mmol, 71%).

M.P.: 80 – 82 °C. **IR (neat)**: $\tilde{\nu}$ = 2978 (w), 2935 (w), 1699 (m), 1597 (w), 1580 (w), 1450 (w), 1413 (w), 1325 (s), 1226 (m), 1210 (m), 1184 (w), 1148 (s), 1079 (w), 1044 (w), 961 (m), 897 (w), 775 (m), 755 (m), 690 (w), 648 (w), 515 (w), 498 (w). **^{1}H NMR (600 MHz, $CDCl_3$)**: δ = 7.95 – 7.92 (m, 2H), 7.65 – 7.61 (m, 1H), 7.53 – 7.48 (m, 2H), 4.85 (s, 2H), 3.41 (q, J = 7.2 Hz, 2H), 3.07 (s, 3H), 1.21 (t, J = 7.1 Hz, 3H). **^{13}C NMR (151 MHz, $CDCl_3$)**: δ = 195.2, 134.7, 134.3, 129.1, 128.0, 52.4, 42.9, 40.2, 14.1. **HRMS (ESI)**: Calculated for $C_{11}H_{16}NO_3S$ $[M+H]^+$: 242.0845, found 242.0842.

Chemotion ELN sample number: HMA-4-36.

N-Benzylmethanesulfonamide (4.6)

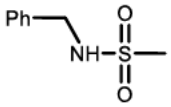

N-Benzylmethanesulfonamide **4.6** was prepared following a literature known protocol. [154] Benzylamine (1.18 g, 1.20 mL, 11.0 mmol, 1.10 eq.) was dissolved in dichloromethane (35.0 mL) and methanesulfonyl chloride (1.15 g, 774 µL, 10.0 mmol, 1.00 eq.) and triethylamine (2.53 g, 3.48 mL, 25.0 mmol, 2.50 eq.) were added. After 30 min, HCl (1 N, 10 mL) was added and the mixture was stirred for 10 min. The phases were separated, and the aqueous phase was extracted with dichloromethane (3 x 30mL) and Et_2O (30 mL). The combined organic phases were washed with brine (30 mL) and water (30 mL) and were dried over $MgSO_4$. The solvent was removed under reduced pressure. The crude mixture was purified *via* automated FC (CyH : EtOAc, 100:00 to 50:50) to obtain N-benzylmethanesulfonamide (1.63 g, 8.78 mmol, 88%) as a colourless solid.

IR (neat): $\tilde{\nu}$ = 3229 (m), 3034 (w), 3021 (w), 2933 (w), 2861 (w), 1494 (w), 1456 (m), 1437 (w), 1413 (w), 1379 (w), 1337 (w), 1204 (w), 1161 (m), 1133 (s), 1083 (w), 1083 (w), 1017 (w), 978 (w), 879 (w), 769 (m), 739 (m), 698 (m), 586 (w), 557 (w), 531 (m), 504 (m), 450 (w). **^{1}H NMR (400 MHz, $CDCl_3$)**: δ = 7.43 – 7.29 (m, 5H), 4.66 (s, 1H), 4.33 (d, J = 6.0 Hz, 2H), 2.87 (s, 3H). **^{13}C NMR (101 MHz, $CDCl_3$)**: δ = 136.7, 129.1, 128.3, 128.0, 47.4, 41.3. **HRMS (ESI)**: Calculated for $C_8H_{15}N_2O_2S$ $[M+NH_4]^+$: 203.0847, found 203.0849. Spectroscopic data was in agreement to those previously reported.[155]

Chemotion ELN sample number: HMA-4-58.

N-Benzyl-N-(2-oxo-2-phenylethyl)methanesulfonamide (2.42)

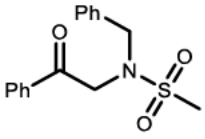

Following **GP-A**, using N-benzylmethanesulfonamide **4.6** (1.50 g, 8.12 mmol, 1.00 eq.), 2-bromoacetophenone (1.62 g, 8.12 mmol, 1.00 eq.) and K_2CO_3 (2.25 g, 16.2 mmol, 2.00 eq.) in acetonitrile (20.0 mL). The desired product was

obtained after automated FC (CyH : EtOAc, 90:10) as an off-white solid (1.48 g, 4.89 mmol, 60% yield).

IR (neat): $\tilde{\nu}$ = 3063 (w), 3031 (w), 1696 (m), 1597 (w), 1581 (w), 1495 (w), 1450 (w), 1409 (w), 1370 (w), 1328 (s), 1226 (m), 1146 (s), 1090 (w), 1062 (w), 1029 (w), 995 (w), 965 (w), 939 (m), 916 (w), 813 (w), 785 (m), 753 (m), 690 (m), 661 (w), 594 (w), 520 (m), 504 (m). **^{1}H NMR (400 MHz, $CDCl_3$)**: δ = 7.85 – 7.80 (m, 2H), 7.60 (ddt, J = 8.7, 7.0, 1.3 Hz, 1H), 7.50 – 7.40 (m, 2H), 7.37 – 7.28 (m, 5H), 4.66 (s, 2H), 4.56 (s, 2H), 3.17 (s, 3H). **^{13}C NMR (101 MHz, $CDCl_3$)**: δ = 195.3, 135.4, 134.7, 134.3, 129.1, 129.0, 128.7, 128.4, 128.0, 51.8, 51.1, 40.6. **HRMS (ESI)**: Calculated for $C_{16}H_{18}NO_3S$ $[M+H]^+$: 304.1002, found 304.1002. Spectroscopic data was in agreement to those previously reported.[41]

Chemotion ELN sample number: HMA-4-60.

2-(Methyl(phenyl)amino)-1-phenylethan-1-one (2.43)

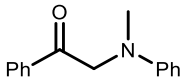

Following **GP-A** with minor alterations, using 2-bromoacetophenone (1.99 g, 10.0 mmol, 1.00 eq.), N-methylaniline (1.07 g, 1.08 mL, 10.0 mmol, 1.00 eq.) and K_2CO_3 (2.07 g, 15.0 mmol, 1.50 eq.) in acetonitrile (10 mL) at 70 °C for 14 h. The crude mixture was filtered, the solvent was removed under reduced pressure. EtOH (20 mL) was added and an off-white precipitate was formed. The solid was filtered, washed with cold EtOH (3 x 5 mL) and pentane (10 mL) and dried under reduced pressure. The product was obtained as a bright yellow solid (1.689 g, 7.50 mmol, 75%).

M.P.: 120 – 122 °C. **IR (neat)**: $\tilde{\nu}$ = 3062 (w), 2900 (w), 2168 (w), 1697 (s), 1599 (s), 1579 (w), 1506 (s), 1448 (w), 1371 (w), 1345 (w), 1254 (w), 1221 (s), 1118 (w), 987 (w), 972 (w), 943 (w), 918 (w), 748 (s), 690 (s), 666 (w), 572 (w), 542 (w), 519 (w), 494 (w), 482 (w), 447 (w), 439 (w). **^{1}H NMR (600 MHz, $CDCl_3$)**: δ = 8.02 – 7.97 (m, 2H), 7.64 – 7.58 (m, 1H), 7.53 – 7.47 (m, 2H), 7.25 – 7.18 (m, 2H), 6.73 (tt, J = 7.4, 1.0 Hz, 1H), 6.71 – 6.67 (m, 2H), 4.79 (s, 2H), 3.11 (s, 3H). **^{13}C NMR (151 MHz, $CDCl_3$)**: δ = 196.5, 149.2, 135.5, 133.7, 129.4,

129.0, 127.9, 117.4, 112.5, 59.1, 39.8. **HRMS (ESI)**: Calculated for $C_{15}H_{16}NO$ $[M+H]^+$: 226.1226, found: 226.1218. Spectroscopic data was in agreement to those previously reported.[156]

Chemotion ELN sample number: HMA-4-44.

2-(Ethyl(phenyl)amino)-1-phenylethan-1-one (2.44)

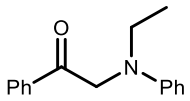

Following **GP-A**, using 2-bromoacetophenone (995 mg, 5.00 mmol, 1.00 eq.), N-ethylaniline (606 mg, 629 µL, 5.00 mmol, 1.00 eq.) and K_2CO_3 (1.38 g, 10.0 mmol, 2.00 eq.) in acetonitrile (10.0 mL). The product was obtained after automated FC (CyH : EtOAc, 100:00 to 70:30) and recrystallised from CyH/Toluene (80:20). The product was obtained as a yellow solid (651 mg, 2.72 mmol, 54%).

M.P.: 89 – 96 °C. **IR (neat)**: $\tilde{\nu}$ = 3062 (w), 2972 (w), 2927 (w), 1698 (s), 1598 (s), 1506 (s), 1449 (m), 1427 (w), 1391 (m), 1376 (w), 1353 (m), 1275 (w), 1247 (m), 1220 (s), 1195 (m), 1160 (w), 1129 (w), 1076 (w), 1041 (w), 1001 (w), 987 (w), 965 (m), 887 (w), 790 (w), 747 (s), 690 (s), 666 (w), 573 (w), 548 (w), 520 (w). **^{1}H NMR (400 MHz, $CDCl_3$)**: δ = 8.08 – 7.94 (m, 2H), 7.67 – 7.57 (m, 1H), 7.50 (ddd, J = 8.1, 6.6, 1.3 Hz, 2H), 7.24 – 7.15 (m, 2H), 6.74 – 6.68 (m, 1H), 6.65 (d, J = 8.2 Hz, 2H), 4.75 (s, 2H), 3.52 (q, J = 7.1 Hz, 2H), 1.23 (t, J = 7.1 Hz, 3H). **^{13}C NMR (101 MHz, $CDCl_3$)**: δ = 196.5, 148.0, 135.6, 133.7, 129.4, 129.0, 128.0, 117.1, 112.5, 57.0, 46.4, 12.6. **HRMS (ESI)**: Calculated for $C_{16}H_{18}NO$ $[M+H]^+$: 240.1383, found: 240.1382. Spectroscopic data was in agreement to those previously reported.[156]

Chemotion ELN sample number: HMA-4-37.

2-Bromo-1-(naphthalen-2-yl)ethan-1-one (4.7)

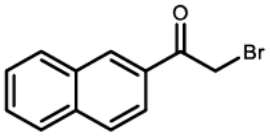

2-Bromo-1-(naphthalen-2-yl)ethan-1-one **4.7** was prepared following a literature known protocol.[157] 1-Naphthalen-2-ylethanone (1.70 g, 10.0 mmol, 1.00 eq.) and silica-gel (170 mg, 2.83 mmol, 0.283 eq., 10%w) were dissolved in methanol (20.0 mL) in a 250 mL three-neck flask under inert atmosphere. The mixture was heated to reflux and N-Bromosuccinimide (2.14 g, 12.0 mmol, 1.20 eq.) was added in 5 portions over 30 min. After additional 30 min the mixture was allowed to cool to rt and was filtered. The solvent was removed under reduced pressure and the crude product was purified *via* FC (pentane : toluene, 50:50 to 25:75). The product was obtained as an off-white solid (1.863 g, 7.48 mmol, 75%).

M.P.: 80 – 83 °C. **IR (neat)**: $\tilde{\nu}$ = 3059 (w), 2944 (w), 1676 (s), 1626 (m), 1595 (w), 1577 (w), 1507 (w), 1469 (m), 1435 (w), 1390 (w), 1355 (w), 1291 (m), 1234 (w), 1181 (m), 1157 (w), 1124 (w), 1105 (w), 1027 (w), 992 (w), 943 (w), 917 (w), 855 (w), 821 (m), 775 (w), 761 (w), 682 (w), 625 (w), 588 (w), 564 (w), 531 (w), 476 (m), 422 (w). **^{1}H NMR (600 MHz, $CDCl_3$)**: δ = 8.53 – 8.51 (m, 1H), 8.03 (dd, J = 8.6, 1.8 Hz, 1H), 7.99 (dd, J = 8.2, 1.3 Hz, 1H), 7.93 (d, J = 8.6 Hz, 1H), 7.90 (dd, J = 8.2, 1.2 Hz, 1H), 7.64 (ddd, J = 8.2, 6.8, 1.3 Hz, 1H), 7.58 (ddd, J = 8.1, 6.8, 1.3 Hz, 1H), 4.59 (s, 2H). **^{13}C NMR (151 MHz, $CDCl_3$)**: δ = 191.5, 136.0, 132.5, 131.4, 131.1, 129.8, 129.2, 129.0, 128.0, 127.2, 124.3, 31.1. **HRMS (ESI)**: Calculated for $C_{12}H_{10}BrO$ $[M+H]^+$: 248.9910, found: 248.9904. Spectroscopic data was in agreement to those previously reported.[158]

Chemotion ELN sample number: HMA-3-20.

N,4-Dimethyl-N-(2-(naphthalen-2-yl)-2-oxoethyl)benzenesulfonamide (2.45)

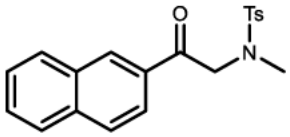

Following **GP-A**, using 2-Bromo-2'-acetonaphthone **4.7** (498 mg, 2.00 mmol, 1.00 eq.), N-methyl-*p*-toluenesulfonamide **4.1** (370 mg, 2.00 mmol, 1.00 eq.) and K_2CO_3 (415 mg, 3.00 mmol, 1.50 eq.). The desired product was obtained after automated FC (CyH : EtOAc, 100:00 to 80:20) as an off-white solid (537 mg, 1.52 mmol, 76%).

M.P.: 135 – 141 °C. **IR (neat)**: $\tilde{\nu}$ = 3060 (w), 2915 (w), 1696 (m), 1627 (w), 1597 (w), 1470 (w), 1336 (m), 1306 (w), 1277 (w), 1258 (w), 1216 (w), 1187 (m), 1162 (s), 1123 (w), 1089 (m), 1019 (w), 997 (w), 980 (w), 932 (m), 862 (w), 817 (m), 749 (w), 728 (m), 654 (m), 549 (m), 476 (w). **^{1}H NMR (400 MHz, $CDCl_3$)**: δ = 8.56 (d, J = 1.8 Hz, 1H), 8.05 – 7.97 (m, 2H), 7.95 – 7.86 (m, 2H), 7.81 – 7.73 (m, 2H), 7.60 (dddd, J = 22.0, 8.2, 6.9, 1.3 Hz, 2H), 7.40 – 7.31 (m, 2H), 4.70 (s, 2H), 2.87 (s, 3H), 2.45 (s, 3H). **^{13}C NMR (101 MHz, $CDCl_3$)**: δ = 193.9, 143.8, 136.0, 134.9, 132.5, 132.2, 130.5, 129.9, 129.9, 129.1, 128.9, 128.0, 127.8, 127.2, 123.8, 56.3, 35.8, 21.7. **HRMS (ESI)**: Calculated for $C_{20}H_{20}NO_3S$ $[M+H]^+$: 354.1158, found: 354.1151.

Chemotion ELN sample number: HMA-3-35.

2-Bromo-1-(o-tolyl)ethan-1-one (2.46)

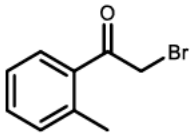

2-Bromo-1-(o-tolyl)ethan-1-one was prepared following a literature known procedure.[159] In a 100 mL round-bottom flask, Montmorillonite K10 (268 mg, 744 µmol, 0.04 eq.) and 2'-Methylacetophenone **1.9** (2.67 g, 2.60 mL, 19.9 mmol, 1.00 eq.) were suspended in methanol (40.0 mL) and the mixture was warmed to 65 °C. NBS (4.27 g, 24.0 mmol, 1.21 eq:) was added in 6 portions over

30 min and the mixture was stirred at 65 °C for 1 h. The mixture was allowed to cool to rt, and a saturated aqueous solution of sodium metabisulfite was added (10 mL). The organic phase was separated, the aqueous phase was extracted with CH_2Cl_2 (3 x 30 mL), the combined organic phases were dried over Na_2SO_4, and the solvent was removed under reduced pressure. The desired product was obtained after automated FC (CyH : EtOAc, 100:0 to 90:10) and bulb-to-bulb distillation (135 °C, 1.0 mbar) as a yellow oil (2.11 g, 9.90 mmol, 50%).

IR (neat): $\tilde{\nu}$ = 3062 (w), 2972 (w), 1682 (s), 1601 (w), 1570 (w), 1487 (w), 1456 (m), 1435 (w), 1383 (w), 1297 (w), 1261 (s), 1208 (w), 1186 (m), 1110 (w), 1034 (w), 1007 (w), 979 (w), 789 (w), 737 (m), 688 (w), 630 (m), 618 (m), 540 (w), 477 (w), 449 (w), 420 (w). **^{1}H NMR (400 MHz, $CDCl_3$):** δ = 7.67 (dd, J = 8.2, 1.5 Hz, 1H), 7.43 (td, J = 7.5, 1.4 Hz, 1H), 7.32 – 7.27 (m, 2H), 4.43 (s, 2H), 2.53 (s, 3H). **^{13}C NMR (101 MHz, $CDCl_3$):** δ = 194.3, 139.9, 134.6, 132.5, 132.5, 129.2, 125.9, 33.9, 21.6. **HRMS (APCI)**: Calculated for $C_9H_{10}BrO$ $[M+H]^+$: 212.9910, found: 212.9906. Spectroscopic data was in agreement to those previously reported.[158]

Chemotion ELN sample number: HMA-4-301 and HMA-4-289.

2-Methoxy-1-(o-tolyl)ethan-1-one (*α*-methoxyacetophenone 2.47)

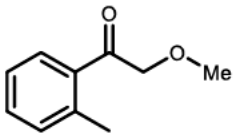

2-Bromo-1-(o-tolyl)ethan-1-one (1.06 g, 4.97 mmol, 1.00 eq.) was dissolved in MeOH (50 mL) and NaOMe (2.70 g, 50.0 mmol, 10.0 eq.) was added. The mixture was stirred at 40 °C for 48 h, and water was added (10 mL). The mixture was neutralised with HCl (3 M) and the phases were separated. The aqueous layer was extracted with CH_2Cl_2 (3 x 30 mL), the combined organic fractions were dried over Na_2SO_4, and the solvent was removed under reduced pressure. The product was obtained after FC (pentane : Et_2O, 70:30) and bulb-to-bulb distillation (150 °C, 1.5 mbar) as a colourless oil (185 mg, 1.13 mmol, 23%).

IR (neat): $\tilde{\nu}$ = 2929 (w), 2824 (w), 1698 (s), 1601 (w), 1572 (w), 1488 (w), 1456 (m), 1382 (w), 1293 (w), 1226 (m), 1196 (s), 1165 (w), 1121 (s), 1077 (w), 1038 (m), 1018 (w), 975 (m), 924 (m), 824 (w), 757 (m), 741 (m), 660 (w), 578 (w), 467 (w), 425 (w). **^{1}H NMR (400 MHz, C_6D_6):** δ = 7.24 (dd, J = 7.7, 1.4 Hz, 1H), 7.05 – 6.99 (m, 1H), 6.94 – 6.85 (m, 2H), 4.08 (s, 2H), 3.11 (s, 3H), 2.46 (s, 3H). **^{13}C NMR (101 MHz, C_6D_6):** δ = 200.3, 138.7, 136.2, 132.1, 131.4, 128.9, 125.6, 76.8, 58.8, 21.2. **HRMS (APCI)**: Calculated for $C_{10}H_{13}O_2$ $[M+H]^+$: 165.0910, found: 165.0914. Spectroscopic data was in agreement to those previously reported.[160]

Chemotion ELN sample number: HMA-4-291.

4.2.1.2 Synthesis of 3,5-dinitroacetophenones

3'5'-Dinitro-2,2,2-trifluoroacetophenone monohydrate (2.50)

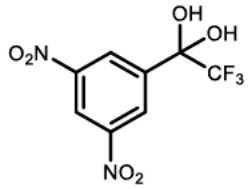

2,2,2, Trifluoroacetophenone (1.98 g, 11.4 mmol, 1.00 eq.) was dissolved in H_2SO_4 conc. (50 mL) and HNO_3 aq. (65%, 15 mL) was added slowly at 0 °C and stirred for 30 min before the reaction mixture was heated to 130 °C. After 4 h the reaction mixture was cooled down to rt before another portion of HNO_3 aq. (65%, 15 mL) was added. The solution was refluxed at 130 °C for 3 d before it was poured on ice. The aqueous phase was extracted with Et_2O (3 x 25 mL) and the organic phase was carefully washed with $NaHCO_3$ sat. until no gas evolution was observed. The organic phase was dried over K_2CO_3 and the solvent was removed *in vacuo*. The crude product was recrystallised from H_2O to yield the hydrate as colourless crystals (1.65 g, 6.24 mmol, 55%).
^{1}H NMR (400 MHz, DMSO-d_6): δ = 8.91 (t, J = 2.1 Hz, 1H), 8.67 (d, J = 2.1 Hz, 2H), 8.45 (s, 2H). **^{13}C NMR (101 MHz, DMSO-d_6):** δ = 148.0, 142.7, 127.4, 122.8 (q, J = 289.0 Hz), 119.7, 91.8 (q, J = 32.0 Hz). **^{19}F NMR (376 MHz, DMSO-d_6):** δ = – 82.6 (*s*, CF_3). Spectroscopic data was in agreement to those previously reported.[83]

3'5'-Dinitro-2,2,2-trifluoroacetophenone (2.52)

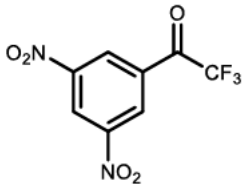

3'5'-Dinitro-2,2,2-trifluoroacetophenone monohydrate **2.50** was refluxed with toluene in a *Dean-Stark* apparatus for 4 h. The water-free product was obtained as a light yellow solid (quantitative conversion of the hydrate).

^{1}H NMR (400 MHz, $CDCl_3$): δ = 9.37 (t, J = 2.1 Hz, 1H), 9.19 (dd, J = 2.0, 0.9 Hz, 2H).**^{13}C NMR (101 MHz, $CDCl_3$):** δ = 177.4 (q, J = 38.0 Hz), 149.3, 132.6, 129.6 (q, J = 2.2 Hz), 124.5, 116.0 (q, J = 290.2 Hz, CF_3). **^{19}F NMR (377 MHz, $CDCl_3$):** δ = – 71.8 (*s*, CF_3). Spectroscopic data was in agreement to those previously reported.[83]

3'5'-Dinitro-2,2-difluoro-2-chloroacetophenone (2.53)

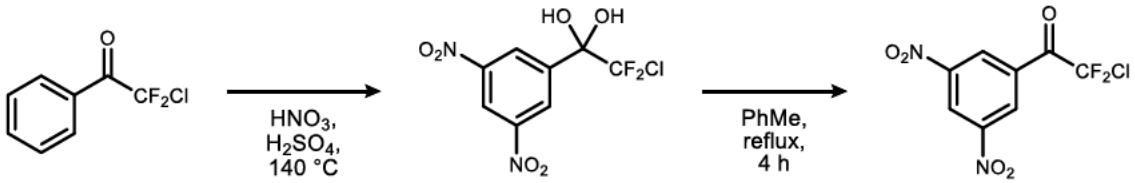

2,2-Difluoro-2-chloroacetophenone (2.00 g, 10.5 mmol, 1.00 eq.) was dissolved in H_2SO_4 conc. (50 mL) and HNO_3 aq. (65%, 10 mL) was added slowly at 0 °C and stirred for 30 min before the reaction mixture was heated to 100 °C. After 3 h the reaction mixture was cooled down to rt before another portion of HNO_3 aq. (65%, 10 mL) was added. The solution was refluxed at 140 °C for 3 d before it was poured on ice. The aqueous phase was extracted with Et_2O (3 x 100 mL) and the organic phase was carefully washed with $NaHCO_3$ sat. until no gas evolution was observed. The organic phase was dried over K_2CO_3 and the solvent was removed *in vacuo*. The crude product was recrystallised from H_2O and the 3'5'-Dinitro-2,2-difluoro-2-chloroacetophenone monohydrate was separated *via* automated FC (CH_2Cl_2 to CyH : EtOAc, 40:60) by [redacted] and afterwards refluxed with toluene in a *Dean-Stark* apparatus for 4 h. The water-free product was obtained as a light yellow solid (685 mg, 2.44 mmol, 23%).

M.P.: 32 – 33 °C. **IR (neat)**: $\tilde{\nu}$ = 3101 (w), 1735 (m), 1629 (m), 1546 (s), 1345 (s), 1281 (w), 1190 (m), 1147 (m), 1121 (m), 1026 (m), 942 (m), 838 (w), 730

(s), 706 (s). **^{1}H NMR (400 MHz, $CDCl_3$):** δ = 9.36 – 9.34 (m, 1H), 9.25 – 9.23 (m, 2H). **^{13}C NMR (101 MHz, $CDCl_3$):** δ = 177.8 (t, $^3J_{C\text{-}F}$ = 31.5 Hz), 149.1, 132.2, 130.0 (t, $^5J_{C\text{-}F}$ = 2.8 Hz), 124.2, 119.4 (t, $^2J_{C\text{-}F}$ = 303.9 Hz, CF_2Cl). **^{19}F NMR (282 MHz, $CDCl_3$):** δ = – 62.1 (*s*, CF_2Cl). **HRMS (APCI)**: Calculated for $C_9H_4ClF_2N_2O_7$ [M+HCOO]$^-$: 324.9675, Found: 324.9676.

4.2.1.3 Synthesis of 3-substituted oxetanes

3-(o-Tolyl)oxetan-3-ol (2.55)

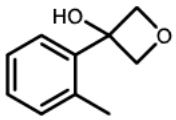

Following **GP-B** using oxetan-3-one (320 µL, 5.00 mmol, 1.00 eq.), *n*-BuLi (2.50 M, 2.40 mL, 6.00 mmol, 1.20 eq.) and 2-mehtyl-iodobenzene (765 µL, 6.00 mmol, 1.20 eq.). The desired product was obtained after automated FC (CyH : EtOAc 80:20 to 60:40) as a yellow oil (683 mg, 4.15 mmol, 83%).

IR (neat): $\tilde{\nu}$ = 3396 (m), 2951 (m), 2876 (w), 2352 (w), 1491 (w), 1456 (m), 1397 (w), 1176 (w), 1131 (m), 1064 (w), 1033 (m), 975 (s), 950 (w), 881 (m), 831 (m), 760 (s), 729 (s). **^{1}H NMR (400 MHz, $CDCl_3$):** δ = 7.28 – 7.15 (m, 3H), 7.18 – 7.09 (m, 1H), 5.25 – 5.16 (m, 2H), 4.91 – 4.82 (m, 2H), 2.57 (br, 1H), 2.25 (s, 3H). **^{13}C NMR (101 MHz, $CDCl_3$):** δ = 139.4, 136.5, 131.8, 128.9, 126.1, 125.8, 83.6, 78.0, 19.3.

Methyl 3-(3-hydroxyoxetan-3-yl)propiolate (2.56)

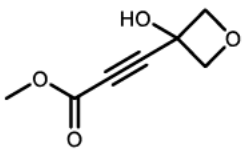

Following **GP-B** using oxetan-3-one (320 µL, 5.00 mmol, 1.00 eq.), *n*-BuLi (2.50 M, 2.40 mL, 6.00 mmol, 1.20 eq.) and methyl propiolate (540 µL, 6.00 mmol, 1.20 eq.), the desired product was obtained after automated FC (CyH : EtOAc, 90:10 to 70:30) as a yellow oil (167 mg, 1.07 mmol, 21%).

IR (neat): $\tilde{\nu}$ = 3395 (w), 2953 (w), 2880 (w), 2240 (w), 1718 (s), 1437 (m), 1275 (s), 1153 (m), 984 (m), 918 (w), 866 (m), 750 (s). **^{1}H NMR (400 MHz, $CDCl_3$):** δ = 4.87 (dd, J = 6.8, 1.0 Hz, 2H), 4.72 (dd, J = 6.8, 1.0 Hz, 2H), 3.81 (s, 3H), 3.72 (s, 1H). **^{13}C NMR (101 MHz, $CDCl_3$):** δ = 153.8, 85.5, 83.5, 77.4, 66.6, 53.3. **HRMS (APCI):** Calculated for $C_7H_9O_4$ $[M+H]^+$: 157.0501, Found: 157.0492.

3-(3,3-Dimethylbut-1-yn-1-yl)oxetan-3-ol (2.57)

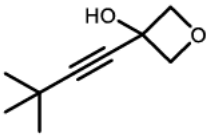

Following **GP-B** using oxetan-3-one (320 µL, 5.00 mmol, 1.00 eq.), *n*-BuLi (2.50 M, 2.40 mL, 6.00 mmol, 1.20 eq.) and 3,3-dimethyl-1-butyne (750 µL, 6.00 mmol, 1.20 eq.), the desired product was obtained *via* automated FC (CyH : EtOAc, 90:10 to 80:20) as a colourless solid (699 mg, 4.53 mmol, 91%).

M.P.: 58 – 59 °C. **IR (neat)**: $\tilde{\nu}$ = 3345 (m), 2972 (s), 2876 (w), 1278 (m), 1136 (s), 973 (s), 849 (m), 747 (s). **^{1}H NMR (400 MHz, $CDCl_3$):** δ = 4.78 (dd, J = 6.4, 0.9 Hz, 2H), 4.68 (dd, J = 6.4, 0.9 Hz, 2H), 2.83 (s, 1H), 1.22 (s, 9H).**^{13}C NMR (101 MHz, $CDCl_3$):** δ = 95.5, 85.2, 78.2, 67.3, 30.9, 27.5. **HRMS (APCI):** Calculated for $C_9H_{15}O_2$ $[M+H]^+$: 155.1072, Found: 155.1065.

3-((Triisopropylsilyl)ethynyl)oxetan-3-ol (2.58)

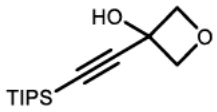

Following **GP-B** using oxetan-3-one (193 µL, 3.00 mmol, 1.00 eq.), *n*-BuLi (1.60 M, 2.25 mL, 3.60 mmol, 1.20 eq.) and 1-(triisopropylsilyl)-1-propyne (811 µL, 3.60 mmol, 1.20 eq.), the desired product was obtained *via* automated FC (pentane : Et_2O, 60:40) as a colourless oil (635 mg, 2.50 mmol, 83%).

IR (neat): $\tilde{\nu}$ = 3394 (m), 2948 (s), 2866 (s), 2172 (w), 1464 (m), 1235 (m), 1135 (m), 988 (s), 920 (s), 883 (s), 838 (s), 772 (m). **^{1}H NMR (400 MHz, $CDCl_3$):** δ = 4.84 (dd, J = 6.4, 1.0 Hz, 2H), 4.72 (dd, J = 6.5, 0.9 Hz, 2H), 2.65

(s, 1H), 1.08 (s, 21H). **^{13}C NMR (101 MHz, $CDCl_3$):** δ : = 106.5, 88.1, 84.9, 67.5, 18.7, 11.2. **HRMS (APCI):** Calculated for $C_{14}H_{27}O_2Si$ $[M+H]^+$: 255.1780, Found: 255.1771.

3-((Trimethylsilyl)ethynyl)oxetan-3-ol (2.59)

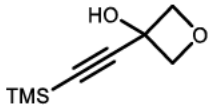

Following **GP-B** using oxetan-3-one (320 µL, 5.00 mmol, 1.00 eq.), *n*-BuLi (1.60 M, 3.75 mL, 6.00 mmol, 1.20 eq.) and trimethylsilylacetylene (854 µL, 6.00 mmol, 1.20 eq.), the desired product was obtained *via* FC (pentane : Et_2O, 85:15) as a colourless oil (800 mg, 4.70 mmol, 94%).

IR (neat): $\tilde{\nu}$ = 3396 (w), 2953 (w), 2880 (w), 2180 (w), 1251 (m), 1134 (m), 978 (m), 921 (m), 839 (s). **^{1}H NMR (400 MHz, $CDCl_3$):** δ = 4.83 (dd, J = 6.5, 1.0 Hz, 2H), 4.69 (dd, J = 6.6, 0.9 Hz, 2H), 2.61 (s, 1H), 0.19 (s, 9H). **^{13}C NMR (101 MHz, $CDCl_3$):** δ = 104.2, 91.7, 84.6, 67.5, -0.1. **HRMS (APCI):** Calculated for $C_8H_{15}O_2Si$ $[M+H]^+$: 171.0841, Found: 171.0836.

3-(Phenylethynyl)oxetan-3-ol (2.60)

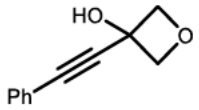

Following **GP-B** using oxetan-3-one (320 µL, 5.00 mmol, 1.00 eq.), *n*-BuLi (2.50 M, 2.40 mL, 6.00 mmol, 1.20 eq.) and phenylacetylene (659 µL, 6.00 mmol, 1.20 eq.), the desired product was obtained *via* FC (pentane:Et_2O, 70:30) as a colourless solid (791 mg, 4.54 mmol, 91%).

^{1}H NMR (400 MHz, $CDCl_3$): δ = 7.48 – 7.42 (m, 2H), 7.39 – 7.29 (m, 3H), 4.94 (d, J = 6.5 Hz, 2H), 4.80 (dd, J = 6.5, 1.0 Hz, 2H), 2.86 (s, 1H). **^{13}C NMR (101 MHz, $CDCl_3$):** δ = 131.8, 129.1, 128.6, 121.9, 88.0, 86.5, 84.8, 67.7. Spectroscopic data was in agreement to those previously reported.[22]

N-phenyloxetan-3-amine (2.62)

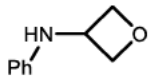

N-phenyloxetan-3-amine **2.62** was prepared following an adapted literature known procedure for reductive aminations.[70] Sodium borohydride (106 mg, 2.80 mmol, 1.40 eq.) was added to an oven-dried flask under inert-gas atmosphere and benzene (3 mL) was added. Glacial acetic acid (520 µL, 9.10 mmol, 4.55 eq.) was added dropwise and after evaporation of H_2-gas, the mixture was heated to reflux for 30 min. A clear solution was formed and the flask allowed to cool to rt. In a second, oven-dried flask, oxetan-3-one (320 µL, 5.00 mmol, 1.00 eq.), glacial acetic acid (114 µL, 2.00 mmol, 1.00 eq.) and aniline (190 µL, 2.00 mmol, 1.00 eq.) were dissolved in 1,2-dichloroethane (3.5 mL) under inert-gas atmosphere. This mixture was added dropwise to the first flask at rt *via* a transfer cannula. The combined solution was stirred at rt for 22 h until a control by TLC showed full conversion. Aqueous NaOH (1 M, 30 mL) was added and the phases were separated. The aqueous phase was extracted with Et_2O (3 × 25 mL), the combined organic fractions were washed with brine (3 × 25 mL) and dried over $MgSO_4$. The solvent was removed under reduced pressure and the product was obtained as a colourless solid after recrystallisation from hot MeOH (4 mL).

^{1}H NMR (400 MHz, $CDCl_3$): δ = 7.23 – 7.15 (m, 2H), 6.77 (tt, J = 7.3, 1.1 Hz, 1H), 6.54 – 6.47 (m, 2H), 5.00 (t, J = 6.7 Hz, 2H), 4.69 – 4.59 (m, 1H), 4.53 (t, J = 6.1 Hz, 2H), 4.09 (s, 1H). **^{13}C NMR (101 MHz, $CDCl_3$):** δ = 146.2, 129.6, 118.7, 113.2, 79.4, 48.7. Spectroscopic data was in agreement to those previously reported.[161]

4.2.1.4 Synthesis of ligands

(*S*)-2'-Phenyl-[1,1'-binaphthalen]-2-ol (4.8)

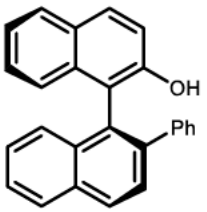

According to a literature known procedure,[162] (*S*)-BINOL (2.00 g, 6.98 mmol, 1.00 eq.) was dissolved in CH_2Cl_2 (40 mL) and *N*,*N*-diisopropylethylamine

(1.33 mL, 7.68 mmol, 1.10 eq.) was added slowly. The solution was cooled to 0 °C and trifluoromethanesulfonic anhydride (1.29 mL, 7.68 mmol, 1.10 eq.) was added dropwise. The reaction mixture was allowed to warm up to rt and was stirred for 17 h. NH_4Cl sat. aq. (40 mL) was added, and the aqueous phase was extracted with CH_2Cl_2 (3x40 mL). The combined organic phases were washed with NaCl sat. aq. (3x50 mL) and were dried over Na_2SO_4. The solvent was removed *in vacuo* and the crude product was used without further purification.

Mg-turnings (1.684 g, 69.8 mmol, 10.0 eq.) were activated with I_2 in a flame-dried Schlenk-flask under nitrogen atmosphere and dry THF (35 ml) was added. Bromobenzene (3.72 mL, 34.9 mmol, 5.00 eq.) was added dropwise at a rate to sustain constant reflux and the mixture was stirred 2 h at rt.

The crude product from the first step was dissolved in THF (30 mL) under nitrogen atmosphere and the freshly prepared Grignard-reagent was added as a solution at 0 °C *via* a transfer cannula and the mixture was stirred at 70 °C for 17 h. After cooling to rt, NH_4Cl sat. aq. (40 mL) was added, and the aqueous phase was extracted with Et_2O (3x50 mL). The combined organic fractions were washed with $NaHCO_3$ sat. aq. (50 mL), NaCl sat. aq. (50 mL), were dried over Na_2SO_4 and the solvent was removed under reduced pressure. The product was obtained after automated FC (CyH : EtOAc, 95:5 to 80:20) as a colourless foam (1.890 g, 5.46 mmol, 78%).

^{1}H NMR (400 MHz, $CDCl_3$): δ = 8.09 (d, J = 8.5 Hz, 1H), 7.99 (dt, J = 8.3, 1.1 Hz, 1H), 7.78 (d, J = 8.5 Hz, 1H), 7.72 (d, J = 8.5 Hz, 1H), 7.52 (ddd, J = 8.1, 6.0, 2.0 Hz, 1H), 7.36 – 7.27 (m, 3H), 7.23 (ddd, J = 15.0, 6.6, 1.5 Hz, 2H), 7.18 – 7.11 (m, 3H), 7.12 – 7.02 (m, 4H), 4.84 (s, 1H). **^{13}C NMR (101 MHz, $CDCl_3$):** δ = 151.1, 141.7, 140.9, 134.3, 133.4, 133.3, 130.0, 129.6, 128.8, 128.7, 128.7, 128.6, 128.3, 128.2, 127.8, 127.3, 127.1, 126.7, 126.6, 126.5, 125.2, 123.3, 117.8, 117.3.[b] **HRMS (APCI)**: Calculated for $C_{26}H_{17}O$ $[M-H]^-$: 345.1279, Found: 345.1281. Spectroscopic data was in agreement to those previously reported.[163]

[b] Missing signals under solvent peak.

(*S*)-2-(Ethoxymethoxy)-2'-phenyl-1,1'-binaphthalene (4.9)

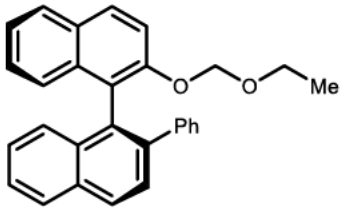

According to a literature known procedure,[164] (*S*)-2'-phenyl-[1,1'-binaphthalen]-2-ol **4.8** (1.870 mg, 5.40 mmol, 1.00 eq.) was dissolved in dry THF (20 mL) in a flame-dried Schlenk-flask under nitrogen atmosphere and a dispersion of sodium hydride in mineral oil (60% NaH, 198 mg, 5.9 mmol, 1.10 eq.) was added portion wise at 0 °C and the mixture was stirred for 50 min at 0 °C. 2-Methoxyethoxymethylchlorid (602 µL, 6.5 mmol, 1.20 eq.) was added dropwise at 0 °C and the mixture was stirred for 20 min at 0°C and 1 h at rt. H_2O (50 mL) and Et_2O (50 mL) were added and the organic phase was extracted with Et_2O (3x50 mL). The combined organic fractions were washed with NaCl sat. aq. (50 mL) and were dried over $MgSO_4$. The solvent was removed under reduced pressure. The product was used without further purification in the next step.

^{1}H NMR (400 MHz, C_6D_6) δ = 7.81 (d, J = 8.6 Hz, 1H), 7.76 (d, J = 8.3 Hz, 1H), 7.68 (d, J = 8.5 Hz, 1H), 7.62 (d, J = 9.1 Hz, 1H), 7.58 (d, J = 8.8 Hz, 1H), 7.53 (d, J = 9.1 Hz, 1H), 7.49 (dq, J = 8.5, 0.9 Hz, 1H), 7.41 – 7.31 (m, 3H), 7.24 (ddd, J = 8.2, 6.8, 1.2 Hz, 1H), 7.11 – 6.94 (m, 3H), 6.92 – 6.84 (m, 2H), 6.84 – 6.77 (m, 1H), 4.74 (d, J = 7.2 Hz, 1H), 4.61 (d, J = 7.2 Hz, 1H), 3.24 – 2.96 (m, 2H), 0.83 (t, J = 7.1 Hz, 3H). **^{13}C NMR (101 MHz, C_6D_6):** δ = 153.7, 142.7, 140.6, 135.1, 133.9, 133.5, 132.7, 129.9, 129.8, 129.3, 128.7, 128.5, 127.7, 127.4, 127.0, 126.8, 126.6, 126.2, 126.0, 124.1, 123.3, 116.6, 93.6, 63.9, 15.1.

(*S*)-2-(Ethoxymethoxy)-2'-phenyl-[1,1'-binaphthalene]-3-carbaldehyde (4.10)

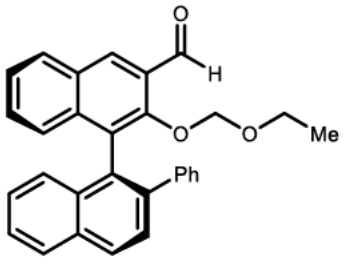

According to a literature known procedure,[162] (*S*)-2-(ethoxymethoxy)-2'-phenyl-1,1'-binaphthalene **4.9** (1.536 g, 3.80 mmol, 1.00 eq.) was dissolved in dry THF (15 mL) under nitrogen atmosphere. The reaction flask was cooled to −78 °C, *n*-BuLi (1.6 M, 1.9 mL, 4.6 mmol, 1.20 eq.) was added dropwise and the mixture was stirred at −78 °C for 30 min and for 90 min at rt. The flask was cooled to −78 °C and *N*,*N*-dimethylformamide (1.50 mL, 19.0 mmol, 5.00 eq.) was added dropwise. The reaction mixture was stirred at −78 °C for 15 min and at rt for 14 h. NH_4Cl sat. aq. (25 mL) was added and the organic phase was extracted with EtOAc (3x25 mL). The combined organic fractions were washed with NaCl sat. aq. (25 mL) and were dried over $MgSO_4$. The solvent was removed under reduced pressure. The product was obtained after automated FC (CyH : Et_2O, 90:10) as a colourless solid (780 mg, 1.80 mmol, 47%).

^{1}H NMR (400 MHz, $CDCl_3$): δ = 10.34 (s, 1H), 8.42 (d, J = 0.8 Hz, 1H), 8.06 (dd, J = 8.6, 0.8 Hz, 1H), 7.98 (dt, J = 8.2, 0.6 Hz, 2H), 7.68 (d, J = 8.5 Hz, 1H), 7.50 (ddd, J = 8.1, 6.7, 1.3 Hz, 1H), 7.45 (ddd, J = 8.1, 6.8, 1.3 Hz, 1H), 7.38 (ddd, J = 8.3, 6.8, 1.4 Hz, 1H), 7.35 – 7.30 (m, 1H), 7.29 – 7.27 (m, 1H), 7.26 – 7.22 (m, 1H), 7.11 – 7.06 (m, 2H), 7.06 – 6.98 (m, 3H), 4.63 (d, J = 6.0 Hz, 1H), 4.47 (d, J = 6.0 Hz, 1H), 3.27 (dq, J = 9.4, 7.0 Hz, 1H), 2.98 (dq, J = 9.4, 7.0 Hz, 1H), 0.83 (t, J = 7.1 Hz, 3H). **^{13}C NMR (101 MHz, $CDCl_3$)** δ = 191.3, 153.5, 141.6, 140.9, 137.8, 133.3, 132.8, 131.2, 130.5, 130.4, 129.7, 129.4, 129.3, 129.0, 128.8, 128.6, 128.3, 127.7, 126.9, 126.8, 126.8, 126.6, 126.0, 125.9, 98.4, 65.4, 14.7.

S)-2-Hydroxy-2'-phenyl-[1,1'-binaphthalene]-3-carbaldehyde (2.65)

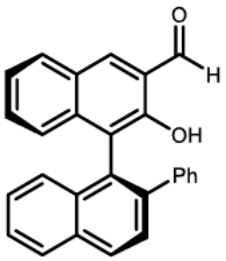

According to a literature known procedure,[162] (*S*)-2-(ethoxymethoxy)-2'-phenyl-[1,1'-binaphthalene]-3-carbaldehyde **4.10** (770 mg, 1.78 mmol, 1.00 eq.) was dissolved in 1,4-dioxane (12 mL) and conc. HCl (4 mL) was added dropwise at rt. The mixture was stirred for 2 h and water was added (20 mL). A yellow

precipitate was formed, that was filtered off, was washed with water (3x20 mL) and was dried over P_4O_{10} for 17 h. The product was obtained as a bright yellow solid (293 mg, 0.78 mmol, 44%).

^{1}H NMR (400 MHz, $CDCl_3$) δ = 10.43 (s, 1H), 10.09 (s, 1H), 8.16 (d, J = 0.8 Hz, 1H), 8.05 (dd, J = 8.5, 0.8 Hz, 1H), 7.98 (dt, J = 8.4, 1.0 Hz, 1H), 7.87 – 7.83 (m, 1H), 7.66 (d, J = 8.5 Hz, 1H), 7.48 (ddd, J = 8.2, 6.5, 1.4 Hz, 1H), 7.35 – 7.28 (m, 3H), 7.27 – 7.24 (m, 1H), 7.23 – 7.19 (m, 2H), 7.13 (ddd, J = 7.7, 1.9, 0.8 Hz, 1H), 7.05 – 6.99 (m, 3H). **^{13}C NMR (101 MHz, $CDCl_3$)** δ = 196.9, 153.7, 142.0, 140.8, 138.0, 137.9, 133.1, 132.7, 130.5, 130.0, 129.8, 128.7, 128.7, 128.4, 128.4, 127.5, 127.2, 126.7, 126.6, 126.2, 126.0, 125.5, 124.3, 121.6, 121.4. Spectroscopic data was in agreement to those previously reported.[163]

3-((*E*)-(((1*S*,2*S*)-2-(((*E*)-((*S*)-2-Hydroxy-2'-phenyl-[1,1'-binaphthalen]-3-yl)methylene)amino)cyclohexyl)imino)methyl)-2'-phenyl- [1,1'-binaphthalen]-2-ol (2.63)

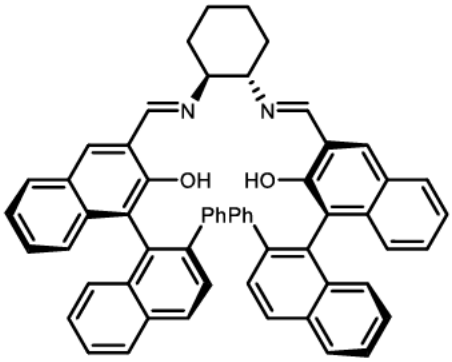

According to a literature known procedure,[72] (1*S*,2*S*)-(−)-1,2-cyclohexanediamine D-tartrate (54 mg, 0.21 mmol, 1.00 eq.) was stirred with K_2CO_3 (57 mg, 0.41 mmol, 2.00 eq.) in EtOH (5 mL) and H_2O (1 mL) for 15 min, before (*S*)-2-hydroxy-2'-phenyl-[1,1'-binaphthalene]-3-carbaldehyde **2.65** (177 mg, 0.41 mmol, 2.00 eq.) was added. The mixture was heated to reflux for 4 h. Water (10 mL) was added and the flask was cooled to −20 °C. A yellow precipitate was formed, that was filtered off, was washed with water (3x20 mL) and ice-cold EtOH (3x5 mL). The product was dried in-vacuo and was obtained as a pale yellow solid (163 mg, 0.17 mmol, 81%).

^{1}H NMR (400 MHz, $CDCl_3$) δ = 13.04 (s, 2H), 8.37 (s, 2H), 8.01 (d, J = 8.5 Hz, 2H), 7.92 (d, J = 8.2 Hz, 2H), 7.65 (d, J = 8.5 Hz, 2H), 7.63 – 7.59 (m, 1H), 7.58 (s, 2H), 7.34 (ddd, J = 8.1, 6.7, 1.2 Hz, 2H), 7.27 – 7.22 (m, 5H), 7.21 – 7.13 (m, 4H), 7.08 (d, J = 8.5 Hz, 2H), 6.99 (td, J = 6.2, 2.7 Hz, 8H), 6.78 (ddd, J = 8.3, 6.8, 1.3 Hz, 2H), 3.32 – 3.21 (m, 2H), 1.94 (d, J = 13.4 Hz, 2H), 1.86 (d, J = 9.9 Hz, 2H), 1.76 – 1.61 (m, 2H), 1.44 (d, J = 10.1 Hz, 2H). **^{13}C NMR (101 MHz, $CDCl_3$)** δ = 165.1, 154.8, 142.3, 140.4, 135.3, 133.3, 133.1, 133.0, 131.4, 128.9, 128.8, 128.4, 128.3, 128.2, 128.2, 127.4, 127.1, 126.5, 126.4, 126.2, 125.8, 125.0, 123.1, 120.0, 119.9, 73.3, 32.9, 24.2.

(*S*)-3-((*E*)-(((1*R*,2*R*)-2-(((*E*)-((*R*)-2-hydroxy-2'-phenyl-[1,1'-binaphthalen]-3-yl)methylene)amino)cyclohexyl)imino)methyl)-2'-phenyl-[1,1'-binaphthalen]-2-ol [*epi*-2.63]

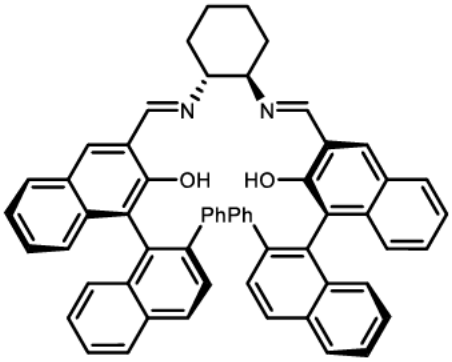

According to a literature known procedure with minor alterations,[165] (1*R*,2*R*)-cyclohexane-1,2-diamine L-tartrate (62 mg, 0.24 mmol, 1.00 eq.) was stirred with K_2CO_3 (65 mg, 0.47 mmol, 2.00 eq.) in EtOH (8 mL) and H_2O (1 mL) for 15 min, before (S)-2-hydroxy-2'-phenyl-[1,1'-binaphthalene]-3-carbaldehyde **2.65** (176 mg, 0.47 mmol, 2.00 eq.) was added. The mixture was heated to reflux for 60 h. Water (10 mL) was added and the flask was cooled to –20 °C. The precipitate was filtered off, and washed with small portions of water and cold EtOH. The product was obtained as a pale yellow solid (183 mg, 0.22 mmol, 82%).

^{1}H NMR (400 MHz, C_6D_6): δ = 13.25 (s, 2H), 7.95 (s, 2H), 7.85 (d, J = 8.5 Hz, 2H), 7.78 (d, J = 8.5 Hz, 2H), 7.74 – 7.67 (m, 4H), 7.43 – 7.37 (m, 4H), 7.36 – 7.31 (m, 4H), 7.24 (ddd, J = 8.1, 6.7, 1.2 Hz, 2H), 7.15 – 7.13 (m, 2H), 7.07 (ddd, J = 8.3, 6.8, 1.3 Hz, 2H), 6.90 (dqd, J = 8.0, 6.7, 1.5 Hz, 4H), 6.33 (t, J = 7.7 Hz,

4H), 6.23 – 6.16 (m, 2H), 2.92 – 2.79 (m, 2H), 1.56 – 1.46 (m, 2H), 1.47 – 1.39 (m, 2H), 1.34 (d, *J* = 12.3 Hz, 2H), 1.11 – 0.95 (m, 2H). **^{13}C NMR (101 MHz, C_6D_6):** δ = 165.5, 156.1, 142.5, 140.8, 135.4, 133.9, 133.8, 133.6, 132.3, 129.0, 128.7, 128.7, 128.5, 128.5, 128.4, 128.0, 127.7, 127.2, 126.8, 126.0, 125.2, 123.4, 120.9, 120.4, 73.2, 32.6, 24.2.[c]

(S)-2'-(4-(tert-Butyl)phenyl)-[1,1'-binaphthalen]-2-ol (4.11)

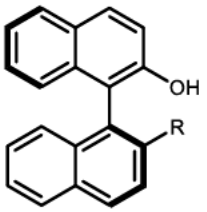

R = 4-tBu-C_6H_4

According to a literature known procedure,[163] (*S*)-BINOL (5.12 g, 17.88 mmol, 1.00 eq.) was dissolved in CH_2Cl_2 (80 mL) and *N*,*N*-diisopropylethylamine (3.30 mL, 19.30 mmol, 1.08 eq.) was added slowly. The solution was cooled to 0 °C and trifluoromethanesulfonic anhydride (3.20 mL, 19.30 mmol, 1.08 eq.) was added dropwise and the reaction mixture was allowed to warm up to rt and was stirred for 17 h. NH_4Cl aq. (80 mL) was added and the aqueous phase was extracted with CH_2Cl_2 (3 x 80 mL). The combined organic phases were washed with Brine (3 x 80 mL) and were dried over $MgSO_4$. The solvent was removed *in vacuo* and the crude product was used without further purification.

Mg-turnings (4.32 g, 179.00 mmol, 10.00 eq.) were activated with I_2 in a flame-flame-dried Schlenk-flask under nitrogen atmosphere and dry THF (70 ml) was added. 1-Bromo-4-(tert-butyl)benzene (11.43 mL, 65.94 mmol, 3.68 eq.) was added dropwise and the mixture was stirred at 70 °C for 3 h.

The crude product was dissolved in THF (50 mL) under nitrogen atmosphere and the Grignard-solution was added at 0 °C *via* a transfer cannula and the mixture was stirred at 70 °C for 17 h. After cooling to rt, NH_4Cl aq. (50 mL) was added and the aqueous phase was extracted with Et_2O (3 x 100 mL). The combined organic fractions were washed with $NaHCO_3$ (50 mL), Brine (3 x 100 mL), were dried over $MgSO_4$ and the solvent was removed under reduced pressure. The

[c] Missing signals under solvent peak.

crude mixture was purified *via* automated FC (CyH:Et_2O, 95:5 to 80:20) and the product was obtained as a colourless solid (4.12 g, 10.24 mmol, 57%).

M.P.: 178.2 – 182.8 °C. **IR (neat)**: $\tilde{\nu}$ = 3495 (m), 2963 (m), 2340 (w), 1620 (w), 1469 (w), 1381 (w), 1204 (m), 1024 (w), 817 (s), 733 (m). **^{1}H NMR (400 MHz, C_6D_6)** δ = 7.78 (d, J = 8.5 Hz, 1H), 7.73 (d, J = 8.2 Hz, 1H), 7.62 (d, J = 8.5 Hz, 1H), 7.56 – 7.49 (m, 1H), 7.45 (d, J = 8.9 Hz, 1H), 7.43 (dd, J = 8.5, 1.0 Hz, 1H), 7.27 – 7.19 (m, 4H), 7.09 (d, J = 8.9 Hz, 1H), 7.08 – 7.01 (m, 2H), 7.01 – 6.98 (m, 1H), 6.98 – 6.93 (m, 2H), 4.72 (s, 1H), 0.99 (s, 10H). **^{13}C NMR (101 MHz, C_6D_6)** δ = 151.8, 149.9, 142.0, 138.6, 135.1, 134.0, 133.7, 130.3, 129.6, 129.3, 128.8, 128.6, 127.5, 127.1, 126.9, 126.5, 125.5, 125.1, 123.5, 118.3, 117.9, 34.3, 31.2.[d] **HRMS (APCI)**: Calculated for $C_{30}H_{25}O$ [M-H]$^-$: 401.1905, Found: 401.1909.

(S)-2-(4-(tert-Butyl)phenyl)-2'-(ethoxymethoxy)-1,1'-binaphthalene (4.12)

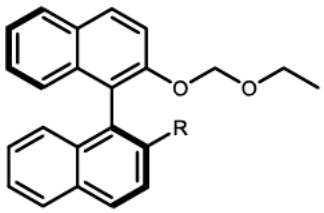

R = 4-tBu-C_6H_4

(S)-2'-(4-(tert-Butyl)phenyl)-[1,1'-binaphthalen]-2-ol (4.00 g, 9.95 mmol, 1.00 eq.) was dissolved in dry THF (35 mL) in a flame-flame-dried Schlenk-flask under nitrogen atmosphere and a dispersion of sodium hydride in mineral oil (60% NaH, 368 mg, 10.95 mmol, 1.10 eq.) was added portion wise at 0 °C and the mixture was stirred for 50 min at 0 °C. 2-Methoxy-ethoxymethylchlorid (1.11 mL, 11.94 mmol, 1.20 eq.) was added dropwise at 0 °C and the mixture was stirred for 20 min at 0°C and 3 h at rt. H_2O (50 mL) and Et_2O (50 mL) were added and the organic phase was extracted with Et_2O (3 x 50 mL). The combined organic fractions were washed with brine (3 x 50 mL) and were dried over $MgSO_4$. The solvent was removed under reduced pressure and the crude mixture was purified *via* automated FC (CyH : Et_2O, 100:0 to 95:5). The product was obtained as an off-white solid (3.36 g, 7.29 mmol, 73%).

[d] Missing signals under solvent peak.

M.P.: 87 – 88 °C. **IR (neat)**: $\tilde{\nu}$ = 3578 (w), 2952 (s), 2916 (s), 2899 (m), 2366 (w), 2359 (w), 2347 (w), 1505 (m), 1269 (m), 1234 (m), 1055 (m), 1034 (s), 1015 (s), 816 (s). **^{1}H NMR (400 MHz, C_6D_6):** δ = 7.83 (d, J = 8.5 Hz, 1H), 7.77 (d, J = 8.5 Hz, 1H), 7.76 (d, J = 8.1 Hz, 1H), 7.63 – 7.59 (m, 1H), 7.61 – 7.57 (m, 1H), 7.53 (d, J = 9.1 Hz, 1H), 7.47 (dq, J = 8.5, 0.9 Hz, 1H), 7.45 – 7.41 (m, 1H), 7.38 – 7.32 (m, 2H), 7.23 (ddd, J = 8.1, 6.8, 1.2 Hz, 1H), 7.10 (ddd, J = 8.2, 6.8, 1.3 Hz, 1H), 7.03 (dt, J = 8.6, 1.7 Hz, 2H), 7.02 – 6.97 (m, 2H), 4.77 (d, J = 7.2 Hz, 1H), 4.60 (d, J = 7.2 Hz, 1H), 3.26 – 2.98 (m, 2H), 1.02 (s, 9H, *t*Bu-C*H*$_3$), 0.84 (t, J = 7.1 Hz, 3H). **^{13}C NMR (101 MHz, C_6D_6):** δ = 153.5, 149.3, 140.5, 139.9, 135.4, 134.0, 133.5, 132.5, 129.9, 129.8, 129.1, 129.0, 128.6, 128.5, 128.5, 127.4, 127.0, 126.6, 126.3, 125.8, 124.8, 124.1, 123.5, 116.7, 93.5, 63.8, 34.3, 31.2, 15.2.[e] **HRMS (ESI)**: Calculated for $C_{33}H_{36}O_2N$ $[M+NH_4]^+$: 478.2746, Found: 478.2736.

(S)-2'-(4-(tert-Butyl)phenyl)-2-(ethoxymethoxy)-[1,1'-binaphthalene]-3-carbaldehyde (4.13)

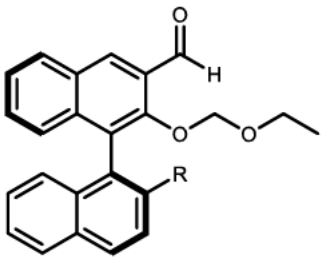

R = 4-tBu-C_6H_4

(S)-2-(4-(tert-Butyl)phenyl)-2'-(ethoxymethoxy)-1,1'-binaphthalene (3.04 g, 6.60 mmol, 1.00 eq.) was dissolved in dry THF (50 mL) under nitrogen atmosphere. The reaction flask was cooled to –78 °C, *n*-BuLi (2.5 M, 3.17 mL, 7.92 mmol, 1.20 eq.) was added dropwise and the mixture was stirred at –78 °C for 30 min and for 90 min at rt. The flask was cooled to –78 °C and *N*,*N*-Dimethylformamide (2.55 mL, 33.00 mmol, 5.00 eq.) was added dropwise. The reaction mixture was stirred at –78 °C for 15 min and at rt for 21 h. NH_4Cl aq. (30 mL) was added and the organic phase was extracted with Et_2O (3 x 30 mL). The combined organic fractions were washed with brine (3 x 30 mL) and were

[e] Missing signals under solvent peak.

dried over $MgSO_4$. The solvent was removed under reduced pressure and the crude mixture was purified *via* automated FC (CyH : Et_2O, 100:0 to 95:5). The product was obtained as an off-white foam (1.69 g, 3.45 mmol, 52%).

IR (neat): $\tilde{\nu}$ = 2928 (m), 1691 (s), 1620 (w), 1589 (w), 1500 (w), 1364 (w), 1205 (w), 1186 (w), 1137 (s), 1102 (m), 965 (s), 821 (m), 736 (w), 715 (w). **^{1}H NMR (400 MHz, C_6D_6):** δ = 10.43 (s, 1H, C*H*O), 8.43 (s, 1H), 7.82 (d, J = 8.5 Hz, 1H), 7.75 (d, J = 8.1 Hz, 1H), 7.70 (d, J = 8.5 Hz, 1H), 7.55 – 7.50 (m, 1H), 7.33 (ddt, J = 8.2, 1.5, 0.8 Hz, 1H), 7.31 – 7.27 (m, 3H), 7.23 (ddd, J = 8.1, 6.8, 1.2 Hz, 1H), 7.05 – 6.93 (m, 5H), 4.60 (d, J = 6.1 Hz, 1H), 4.39 (d, J = 6.1 Hz, 1H), 3.04 (dq, J = 9.4, 7.1 Hz, 1H), 2.76 (dq, J = 9.4, 7.0 Hz, 1H), 0.99 (s, 9H), 0.65 (t, J = 7.0 Hz, 3H). **^{13}C NMR (101 MHz, C_6D_6):** δ = 189.9 (*C*HO), 154.0, 149.8, 141.3, 139.4, 138.0, 133.9, 133.2, 131.6, 131.2, 130.6, 130.2, 130.0, 129.9, 129.3, 129.2, 129.0, 128.9, 128.6, 128.4, 127.3, 127.1, 126.8, 126.1, 125.8, 125.0, 98.6, 65.3, 34.3, 31.2, 14.7.[f] **HRMS (ESI)**: Calculated for $C_{34}H_{32}O_3Na$ $[M+Na]^+$: 511.2249, Found: 511.2237.

(S)-2'-(4-(tert-Butyl)phenyl)-2-hydroxy-[1,1'-binaphthalene]-3-carbaldehyde (2.66)

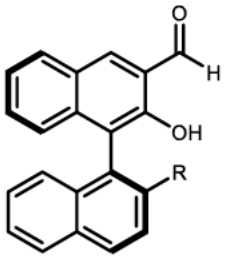

R = 4-tBu-C_6H_4

(S)-2'-(4-(tert-Butyl)phenyl)-2-(ethoxymethoxy)-[1,1'-binaphthalene]-3-carbaldehyde **4.13** (1.68 g, 3.44 mmol, 1.00 eq.) was dissolved in 1,4-dioxane (24 mL) and conc. HCl (8 mL) was added dropwise at rt. The mixture was stirred for 3 h and water was added (20 mL). A yellow precipitate was formed, that was filtered off, was washed with water (3 x 50 mL) and was dried at 60 °C for 48 h. The product was obtained as a bright yellow solid (1.38 g, 3.21 mmol, 93%).

M.P.: decomp. >250 °C. **IR (neat)**: 2960 (w), 2952 (w), 2927 (w), 2916 (m), 1656 (s). **^{1}H NMR** (400 MHz, C_6D_6): δ = 10.89 (s, 1H, C*H*O), 9.25 (s, 1H), 7.81

[f] Missing signals under solvent peak.

(d, *J* = 8.4 Hz, 1H), 7.77 (d, *J* = 8.1 Hz, 1H), 7.68 (d, *J* = 8.4 Hz, 1H), 7.47 – 7.41 (m, 3H), 7.40 – 7.37 (m, 1H), 7.30 – 7.26 (m, 1H), 7.26 – 7.22 (m, 1H), 7.18 (s, 1H, O*H*), 7.09 (ddd, *J* = 8.3, 6.8, 1.3 Hz, 1H), 7.03 – 6.99 (m, 2H), 6.99 – 6.91 (m, 2H), 0.98 (s, 9H, *t*Bu-C*H*$_3$). **^{13}C NMR** (101 MHz, C_6D_6): δ = 196.7 (*C*HO), 154.4, 149.4, 141.4, 140.0, 138.5, 137.9, 133.6, 130.6, 130.4, 129.9, 129.2, 128.9, 128.8, 128.6, 127.3, 126.8, 126.7, 126.0, 125.9, 124.9, 124.0, 122.0, 121.8, 34.3, 31.2.[g] **HRMS (ESI)**: Calculated for $C_{31}H_{27}O_2$ $[M+H]^+$: 431.2011, Found: 431.2004.

2'-(4-(tert-Butyl)phenyl)-3-((E)-(((1R,2R)-2-(((E)-((S)-2'-(4-(tert-butyl)phenyl)-2-hydroxy-[1,1'-binaphthalen]-3-yl)methylene)amino)cyclohexyl)imino)methyl)-[1,1'-binaphthalen]-2-ol (2.64)

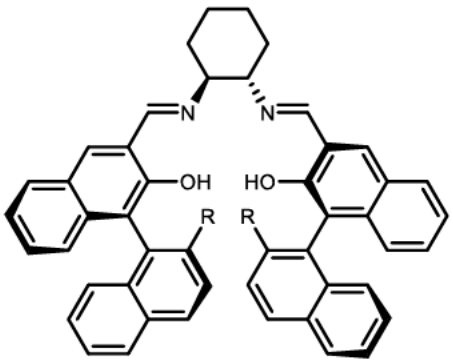

R = 4-tBu-C_6H_4

According to a literature known procedure with minor alterations,[15] (1*S*,2*S*)-(–)-1,2-cyclohexanediamine D-tartrate (186 mg, 0.71 mmol, 1.00 eq.) was stirred with K_2CO_3 (195 mg, 1.41 mmol, 2.0 eq.) in EtOH (25 mL) and H_2O (4 mL) for 15 min, before (S)-2'-(4-(tert-butyl)phenyl)-2-hydroxy-[1,1'-binaphthalene]-3-carbaldehyde **2.66** (606 mg, 1.41 mmol, 2.00 eq.) was added. The mixture was heated to reflux for 72 h. Water (70 mL) was added and the flask was cooled to –18 °C. A yellow precipitate was formed, that was filtered off, was washed with water (3 x 20 mL) and ice-cold EtOH (3 x 10 mL). The product was dried *in vacuo* at 60 °C for 4 d and was obtained as a yellow solid (0.60 g, 0.64 mmol, 91%).)

[g] Missing signals under solvent peak.

M.P.: decomp. >250 °C. **IR (neat)**: $\tilde{\nu}$ = 3031 (w), 2959 (w), 2928 (w), 2868 (w), 1631 (s), 1507 (w), 1339 (w), 817 (m), 753 (m). **^{1}H NMR** (400 MHz, C_6D_6): δ = 13.04 (s, 2H, C*H*N), 7.81 (d, J = 8.5 Hz, 2H), 7.78 – 7.74 (m, 4H), 7.72 (d, J = 8.4 Hz, 2H), 7.56 – 7.52 (m, 4H), 7.52 – 7.48 (m, 2H), 7.33 – 7.24 (m, 4H), 7.20 (s, 2H, O*H*), 7.23 – 7.17 (m, 2H), 7.04 – 6.91 (m, 8H), 6.64 (ddd, J = 8.4, 6.8, 1.3 Hz, 2H), 2.85 – 2.72 (m, 2H), 1.51 – 1.35 (m, 4H), 1.34 – 1.16 (m, 2H), 1.08 – 0.96 (m, 2H), 0.96 (s, 18H). **^{13}C NMR** (101 MHz, C_6D_6) δ (ppm) = 165.5 (*C*HN), 155.6, 149.1, 140.9, 140.2, 136.3, 133.9, 133.8, 133.5, 132.1, 129.2, 129.1, 129.0, 128.6, 128.6, 128.4, 127.5, 126.8, 126.5, 125.8, 125.5, 124.9, 123.2, 120.7, 120.6, 72.9, 34.2, 32.5, 31.2, 24.1.[h] **HRMS (ESI)**: Calculated for $C_{68}H_{63}N_2O_2$ [M+H]$^+$: 939.4890, Found: 939.4871.

4.2.1.5 Synthesis of catalysts

Co^{II}·salen (2.67)

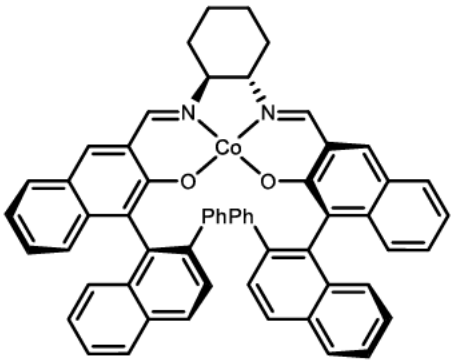

Following **GP-C**, $Co(OAc)_2 \cdot 4H_2O$ (37 mg, 0.15 mmol, 1.00 eq.) was reacted with chiral salen ligand **2.63** (122 mg, 0.15 mmol, 1.00 eq.) to yield the dark red complex (94 mg, 0.10 µmol, 71%).

IR (neat): $\tilde{\nu}$ = 3058 (w), 2931 (w), 2331 (w), 1586 (s), 1548 (m), 1446 (m), 1413 (m), 1333 (s), 1148 (m), 820 (m), 759 (w), 735 (s). **HRMS (ESI):** Calculated for $C_{60}H_{44}CoN_2O_2$ [M]$^+$: 883.2735, Found: 883.2720.

[h] Missing signals under solvent peak.

Co^{II}·salen (*epi*-2.67)

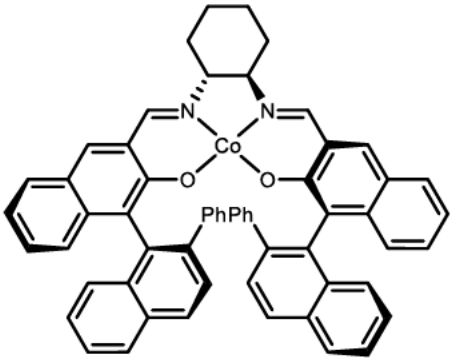

Following **GP-C**, $Co(OAc)_2 \cdot 4H_2O$ (37 mg, 0.15 mmol, 1.00 eq.) was reacted with the chiral salen ligand **2.63** (126 mg, 0.15 mmol, 1.00 eq.) to yield the orange-brown complex (103 mg, 0.12 mmol, 80%).

M.P.: decomp. >250 °C. **IR (neat)**: $\tilde{\nu}$ = 3058 (w), 2929 (w), 2855 (w), 2357 (w), 1631 (m), 1595 (m), 1495 (w), 1446 (w), 1331 (m), 1147 (m), 866 (w), 819 (m), 743 (s), 700 (s). **HRMS (ESI):** Calculated for $C_{60}H_{45}CoN_2O_2$ $[M+H]^+$: 884.2813, Found: 884.2801.

Co^{II}·salen (2.68)

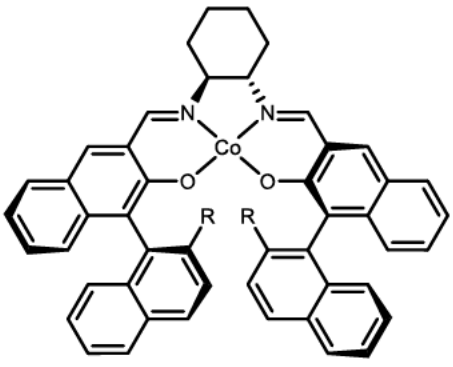

R = 4-tBu-C_6H_4

Following **GP-C**, $Co(OAc)_2 \cdot 4H_2O$ (130 mg, 0.52 mmol, 1.00 eq.) was reacted with the chiral salen ligand **2.64** (487 mg, 0.52 mmol, 1.00 eq.) to yield the orange-brown complex (454 mg, 0.46 mmol, 88%).

M.P.: decomp. >250 °C. **IR (neat)**: $\tilde{\nu}$ = 2961 (w), 2947 (w), 2861 (w), 1589 (m), 1445 (w), 1422 (w), 1333 (w), 1146 (w), 816 (w), 749 (s). **HRMS (ESI):** Calculated for $C_{68}H_{61}CoN_2O_2$ $[M+H]^+$: 996.4065, Found: 995.4060.

4.2.2 Norrish-Yang cyclisation of alpha-substituted acetophenones

4.2.2.1 NMR scale experiments

The investigation of the effect of structural variations on the photoreaction was conducted in CD_3CN to achieve comparative results after 4 h of irradiation. Samples of acetophenones (25 µM) were dissolved in CD_3CN (0.5 mL, 50 mM) and irradiated with 355 nm for 4 h at 25 °C. Mesitylene was added as an internal standard and the reaction was analysed by ^1H NMR.

Table 19: NMR study of the effect of structural variation on the cyclisation. Reactions were performed on 25 µM scale in 0.5 mL CD_3CN (50 mM), NMR yield and *dr* based on ^1H NMR using mesitylene as internal standard.

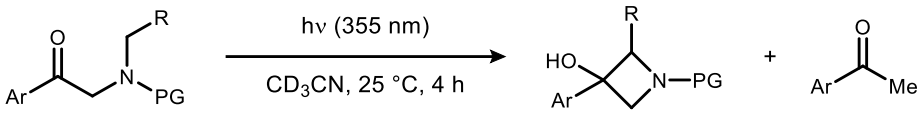

Entry	Products			Conversion	Cyclisation	Fragmentation
1	Ar = Nph	PG = Ts	R = H (**2.69**)[a]	23%	11%	4%
2	Ar = Ph	PG = Ts	R = H (**2.6**)	>99%	81%	14%
3	Ar = Ph	PG = Ts	R = Me (**2.71**)	>99%	54% (*dr* 54:46)	26%
4	Ar = Ph	PG = Ts	R = Ph (**2.72**)	>99%	63% (*dr* 60:40)	20%
5	Ar = Ph	PG = Ms	R = H (**2.73**)	>99%	67%	14%
6	Ar = Ph	PG = Ms	R = Me (**2.74**)	>99%	44% (*dr* 51:49)	42%
7	Ar = Ph	PG = Ms	R = Ph (**2.75**)	>99%	37% (*dr* 52:48)	22%
8	Ar = Ph	PG = Ph	R = H (**2.76**)	90%	12%	3%
9	Ar = Ph	PG = Ph	R = Me (**2.77**)	27%	2% (*dr* 52:48)	6%
10	Ar = Ph	PG = Me	R = H (**2.78**)[b]	87%	<1%	53%
11	Ar = Ph	PG = Ph	R = H (**2.79**)[b]	>99%	<1%	65%
12	Ar = Ph	PG = Bzh	R = H (**2.80**)[b]	94%	10%	74%

[a] Synthesis performed by [redacted]. [b] Starting material synthesised by [redacted]. Nph = naphthyl, Bzh = benzhydryl.

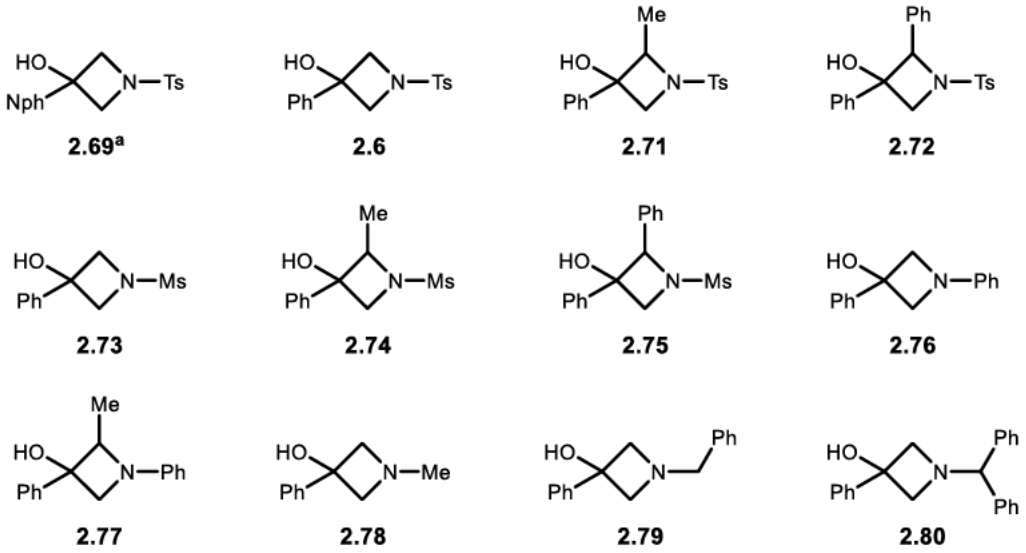

Figure 28: Overview of the obtained 3-azetidinols after irradiation. [a] Synthesis performed by [redacted]. Nph = naphthyl.

4.2.2.2 Isolation of compounds

For the isolation of the respective substances longer irradiation times were needed, and some products precipitated from MeCN in the scale-up after 6 h. Therefore, some reactions were performed in DMF or THF, as it showed a better solubility for some products and is also known to efficiently facilitate the Norrish-Yang reaction.[46]**3-Phenyl-1-tosylazetidin-3-ol (2.6)**

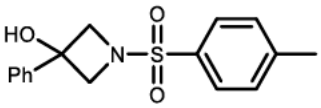

Following **GP-D**, using N,4-dimethyl-N-(2-oxo-2-phenylethyl)benzenesulfonamide **2.5** (346 mg, 1.14 mmol, 1.00 eq.) in acetonitrile (22.0 mL) for 12 h. The solvent was removed under reduced pressure. The product was obtained after automated FC (CyH : EtOAc, 100:0 to 60:40) as a colourless solid (286 mg, 0.94 mmol, 83%).

^{1}H NMR (600 MHz, DMSO-d_6): δ = 7.78 – 7.73 (m, 2H), 7.57 – 7.51 (m, 2H), 7.32 – 7.22 (m, 3H), 7.19 – 7.15 (m, 2H), 6.35 (s, 1H), 3.93 – 3.89 (m, 2H), 3.83 – 3.80 (m, 2H), 2.47 (s, 3H).**^{13}C NMR (151 MHz, DMSO-d_6)**: δ = 144.2, 143.7, 130.4, 130.1, 128.5, 128.2, 127.4, 124.7, 68.6, 65.4, 21.1. Spectroscopic data was in agreement to those previously reported.[46]

Chemotion ELN sample number: HMA-4-48.

3-(Naphthalen-2-yl)-1-tosylazetidin-3-ol (2.69)

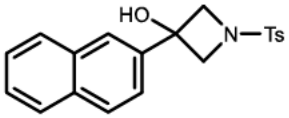

Following **GP-D**, using 3-(naphthalen-2-yl)-1-tosylazetidin-3-ol **2.45** (303 mg, 0.86 mmol) in DMF (40 mL) for 8 h. The desired product was obtained after RP-MPLC (MeCN : H_2O, 50:50) as a colourless solid (51 mg, 0.14 mmol, 16%). The synthesis was performed by [redacted], whereas the purification and characterisation of the sample was performed as part of this work.

M.P.: decomposition above 165 °C. **IR (neat)**: $\tilde{\nu}$ = 3401 (w), 2924 (w), 1598 (w), 1448 (w), 1337 (m), 1160 (s), 1092 (m), 899 (w), 816 (m), 679 (m), 622 (w), 595 (w), 549 (m), 474 (w). **^{1}H NMR (600 MHz, DMSO-d_6)**: δ = 7.88 (dd, J = 7.4, 1.8 Hz, 1H), 7.83 (d, J = 8.6 Hz, 1H), 7.81 – 7.76 (m, 3H), 7.66 (d, J = 2.2 Hz, 1H), 7.56 – 7.43 (m, 4H), 7.30 (dd, J = 8.6, 1.9 Hz, 1H), 6.52 (s, 1H), 4.05 (d, J = 9.0 Hz, 2H), 3.90 (d, J = 9.0 Hz, 2H), 2.43 (s, 3H). **^{13}C NMR (151 MHz, DMSO-d_6)**: δ = 144.3, 140.9, 132.4, 132.1, 130.4, 130.1, 128.5, 128.0, 128.0, 127.4, 126.4, 126.2, 123.3, 123.2, 68.9, 65.2, 21.1. **HRMS (ESI)**: Calculated for $C_{20}H_{20}NO_3S$ $[M+H]^+$: 354.1158 found 354.1151.

2-Methyl-3-phenyl-1-tosylazetidin-3-ol (2.71)

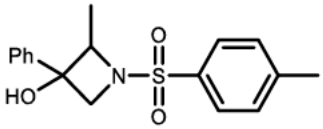

Following **GP-D**, using N-ethyl-4-methyl-N-phenacylbenzenesulfonamide **2.38** (95.2 mg, 300 µmol, 1.00 eq.) in acetonitrile (6.00 mL) for 8 h. The desired product was obtained after automated FC (CyH : Et_2O, 80:20) as a mixture of both diastereomers (dr = 70:30 for isolated material, 41.0 mg, 129 µmol, 43% yield) as a colourless solid.

Diastereomers are assigned from the isolated mixture according to literature[166]:

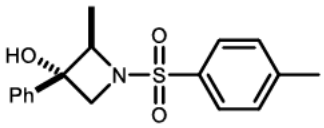

Major-2.71, (2*R*,3*S*)-2-methyl-3-phenyl-1-tosylazetidin-3-ol:

^{1}H NMR (600 MHz, $CDCl_3$): δ = 7.80 – 7.75 (m, 2H), 7.56 – 7.51 (m, 2H), 7.46 – 7.33 (m, 5H), 4.27 (dd, J = 8.5, 1.0 Hz, 1H), 4.00 – 3.93 (m, 1H), 3.65 (d, J = 8.4 Hz, 1H), 2.48 (s, 3H), 2.14 (s, 1H), 0.90 (d, J = 6.5 Hz, 3H). **^{13}C NMR (151 MHz, $CDCl_3$)**: δ = 144.5, 139.1, 131.0, 130.0, 128.7, 128.7, 128.5, 125.8, 74.1, 71.9, 62.9, 21.8, 16.7. Spectroscopic data was in agreement to those previously reported.[166]

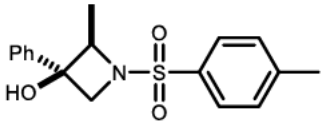

Minor-2.71 (2*R*,3*R*)-2-methyl-3-phenyl-1-tosylazetidin-3-ol:

^{1}H NMR (600 MHz, $CDCl_3$): δ = 7.40 – 7.34 (m, 4H), 7.22 (dd, J = 5.1, 2.0 Hz, 3H), 6.98 – 6.93 (m, 2H), 4.19 (q, J = 6.4 Hz, 1H), 4.00 – 3.93 (m, 1H), 3.88 (dd, J = 9.1, 1.0 Hz, 1H), 2.48 (s, 3H), 2.39 (s, 1H), 1.42 (d, J = 6.4 Hz, 3H). **^{13}C NMR (151 MHz, $CDCl_3$)**: δ = 144.4, 141.6, 131.9, 130.0, 128.7, 128.6, 128.1, 124.8, 73.3, 70.3, 63.0, 21.8, 14.5. Spectroscopic data was in agreement to those previously reported. [166a]

Chemotion ELN sample number: HMA-3-83 and HMA-3-89.

2,3-Diphenyl-1-tosylazetidin-3-ol (2.72)

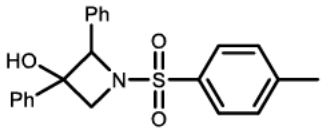

Following **GP-E**, using N-benzyl-4-methyl-N-phenacylbenzenesulfonamide **2.39** (114 mg, 300 µmol, 1.00 eq.) in DMF (6.00 mL) for 12 h. The desired product was obtained after automated FC (CyH : EtOAc, 100:0 to 70:30) as two diastereomers (dr = 49:51 for isolated material) **minor-2.39** (20.0 mg, 53 µmol, 18%) and **major-2.39** (21.0 mg, 55 µmol, 18%), both colourless solids.

Diastereomers are assigned from the mixture according to literature:

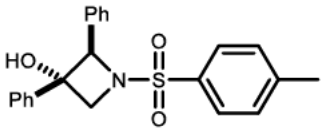

Major-2.39 (2*R*,3*S*)-2,3-diphenyl-1-tosylazetidin-3-ol:

M.P.: 211 – 215 °C. **IR (neat)**: $\tilde{\nu}$ = 3445 (w), 2954 (w), 2918 (m), 2866 (w), 2850 (w), 1450 (w), 1333 (m), 1151 (s), 1087 (w), 823 (w), 778 (w), 697 (m), 677 (m), 600 (m), 550 (w), 536 (w), 525 (w), 513 (w), 513 (w), 457 (m). **^{1}H NMR (400 MHz, DMSO-*d*$_6$)**: δ = 7.76 – 7.66 (m, 2H), 7.54 (d, J = 7.9 Hz, 2H), 7.24 (dt, J = 6.6, 1.4 Hz, 2H), 7.14 – 7.08 (m, 2H), 7.08 – 6.98 (m, 6H), 6.51 (s, 1H), 4.89 (s, 1H), 4.41 – 4.24 (m, 1H), 3.73 (d, J = 8.2 Hz, 1H), 2.47 (s, 3H). **^{13}C NMR (101 MHz, DMSO-*d*$_6$)**: δ = 144.3, 139.9, 135.9, 130.3, 130.1, 128.5, 127.4, 127.2, 127.1, 126.5, 126.1, 78.3, 74.7, 62.0, 21.2.[i] **HRMS (ESI)**: Calculated for $C_{22}H_{22}NO_3S$ [M+H]$^+$: 380.1315, found: 380.1312. Spectroscopic data (^{1}H NMR) was in agreement to those previously reported [41].

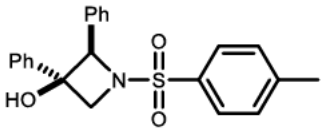

Minor-2.39 (2*R*,3*R*)-2,3-diphenyl-1-tosylazetidin-3-ol**:**

M.P.: 156 – 160 °C. **IR (neat)**: $\tilde{\nu}$ = 3464 (w), 2925 (w), 1698 (w), 1598 (w), 1496 (w), 1450 (w), 1330 (m), 1224 (m), 1158 (s), 1092 (m), 1028 (w), 967 (w), 914 (w), 818 (w), 778 (m), 753 (m), 698 (s), 671 (s), 651 (w), 599 (s), 550 (s), 485 (w). **^{1}H NMR (400 MHz, DMSO-*d*$_6$)**: δ = 7.78 – 7.71 (m, 2H), 7.58 – 7.50 (m, 2H), 7.34 (d, J = 3.4 Hz, 5H), 7.26 – 7.13 (m, 3H), 6.91 – 6.69 (m, 2H), 6.07 (s, 1H), 4.83 (s, 1H), 4.02 (d, J = 9.2 Hz, 1H), 3.94 (dd, J = 9.2, 1.0 Hz, 1H), 2.48 (s, 3H). **^{13}C NMR (101 MHz, DMSO-*d*$_6$)**: δ = 144.5, 143.3, 135.3, 130.4, 130.1, 128.5, 128.1, 127.9, 127.7, 127.7, 127.4, 124.8, 76.9, 72.6, 62.5, 21.1. **HRMS (ESI)**: Calculated for $C_{22}H_{22}NO_3S$ [M+H]$^+$: 380.1315, found: 380.1310. Spectroscopic data (^{1}H NMR) was in agreement to those previously reported [41].

Chemotion ELN sample number: HMA-4-55.

[i] Signals missing due to signal overlapping.

1-(Methylsulfonyl)-3-phenylazetidin-3-ol (2.73)

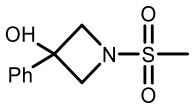

Following **GP-D**, using N-methyl-N-phenacylmethanesulfonamide **2.40** (455 mg, 2.00 mmol, 1.00 eq.) in acetonitrile (40 mL) for 8 h. The desired product was obtained after automated FC (CyH : EtOAc, 50:50 to 15:85) as obtained as a colourless solid (269 mg, 1.18 mmol, 59%).

M.P.: 138 – 142 °C. **IR (neat)**: $\tilde{\nu}$ = 3461 (w), 2935 (w), 1449 (w), 1325 (s), 1146 (s), 1078 (m), 1029 (w), 963 (w), 761 (m), 701 (m), 602 (w), 555 (w), 523 (m). **^{1}H NMR (400 MHz, $CDCl_3$)**: δ = 7.57 – 7.52 (m, 2H), 7.47 – 7.40 (m, 2H), 7.39 – 7.33 (m, 1H), 4.35 – 4.26 (m, 2H), 4.23 – 4.16 (m, 2H), 2.96 (s, 3H), 2.83 – 2.72 (m, 1H). **^{13}C NMR (101 MHz, $CDCl_3$)**: δ = 142.1, 129.0, 128.6, 124.7, 70.6, 64.7, 36.9. **HRMS (ESI)**: Calculated for $C_{10}H_{14}NO_3S$ $[M+H]^+$: 228,0689, found 228,0689.

Chemotion ELN sample number: HMA-4-72.

2-Methyl-1-(methylsulfonyl)-3-phenylazetidin-3-ol (2.74)

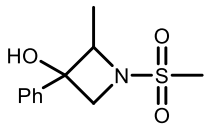

Following **GP-C**, using N-ethyl-N-phenacylmethanesulfonamide **2.41** (90.0 mg, 373 µmol, 1.00 eq.) in DMF (10 mL) for 8 h. The desired product was obtained after automated FC (CyH : EtOAc, 100:00 to 60:40) as two diastereomers (dr = 40:60 for isolated material) **minor-2.74** (8.00 mg, 33.2 µmol, 9%) and **major-2.74** (12.0 mg, 49.7 µmol, 13%), both a colourless wax. The diastereomers were assigned according to **2.71**.

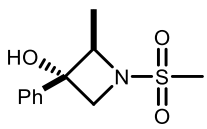

Major-2.74 (2*S*,3*R*)-2-methyl-1-(methylsulfonyl)-3-phenylazetidin-3-ol:

IR (neat): $\tilde{\nu}$ = 3466 (w), 3027 (w), 3012 (w), 2985 (w), 2932 (w), 2890 (w), 1621 (w), 1497 (w), 1470 (w), 1451 (w), 1412 (w), 1377 (w), 1322 (s), 1243 (w), 1144 (s), 1079 (m), 1031 (w), 989 (m), 989 (m), 971 (w), 916 (w), 866 (w), 794 (m), 765 (m), 743 (w), 701 (m), 701 (m), 598 (w), 548 (w), 526 (m), 506 (w). **^{1}H NMR (400 MHz, $CDCl_3$)**: δ = 7.58 – 7.51 (m, 2H), 7.48 – 7.41 (m, 2H), 7.40 – 7.32 (m, 1H), 4.46 (qd, *J* = 6.5, 0.9 Hz, 1H), 4.29 (dd, *J* = 8.6, 0.9 Hz, 1H), 4.09 (d, *J* = 8.6 Hz, 1H), 2.98 (s, 3H), 2.77 (br s, 1H), 0.92 (d, *J* = 6.5 Hz, 3H). **^{13}C NMR (101 MHz, $CDCl_3$)**: δ = 139.1, 128.7, 128.5, 125.9, 73.7, 71.6, 62.5, 36.9, 17.1. **HRMS (ESI)**: Calculated for $C_{11}H_{16}NO_3S$ $[M+H]^+$: 242.0845, found 242.0842.

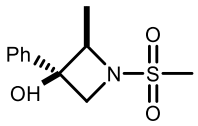

Minor-2.74 (2*S*,3*S*)-2-methyl-1-(methylsulfonyl)-3-phenylazetidin-3-ol**:**

IR (neat): $\tilde{\nu}$ = 3468 (w), 3029 (w), 2979 (w), 2932 (w), 1604 (w), 1497 (w), 1449 (w), 1378 (w), 1315 (s), 1180 (m), 1144 (s), 1076 (m), 1032 (w), 991 (m), 960 (m), 913 (w), 897 (w), 799 (m), 753 (m), 700 (s), 624 (m), 583 (m), 518 (m), 484 (m). **^{1}H NMR (400 MHz, $CDCl_3$)**: δ = 7.46 – 7.38 (m, 4H), 7.37 – 7.29 (m, 1H), 4.67 (qd, *J* = 6.4, 1.0 Hz, 1H), 4.38 (d, *J* = 8.7 Hz, 1H), 3.87 (dd, *J* = 8.7, 1.0 Hz, 1H), 2.92 (s, 3H), 2.44 (br s, 1H), 1.48 (d, *J* = 6.4 Hz, 3H). **^{13}C NMR (101 MHz, $CDCl_3$)**: δ =141.9, 129.0, 128.5, 125.1, 73.0, 68.7, 61.8, 38.9, 14.7. **HRMS (ESI)**: Calculated for $C_{11}H_{16}NO_3S$ $[M+H]^+$: 242.0845, found 242.0841.

Chemotion ELN sample number: HMA-4-77.

1-(Methylsulfonyl)-2,3-diphenylazetidin-3-ol 2.75

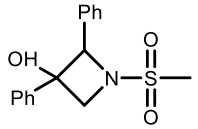

Following **GP-E**, using N-benzyl-N-(2-oxo-2-phenylethyl)methanesulfonamide **2.42** (96.0 mg, 317 µmol, 1.00 eq.) in DMF (12.7 mL) for 8 h. The desired product was obtained after automated FC (CyH : EtOAc, 50:50) as two diastereomers (dr = 44:56) **minor-2.75** (20.0 mg, 65.9 µmol, 21%) and **major-2.75**

(26.0 mg, 85.7 µmol, 27%) as colourless resigns. The diastereomers were not assigned.

Major-2.75:

IR (neat): $\tilde{\nu}$ = 3468 (w), 3063 (w), 3030 (w), 2931 (w), 1496 (w), 1450 (w), 1409 (w), 1320 (s), 1227 (w), 1193 (w), 1146 (s), 1079 (w), 1059 (w), 1027 (w), 965 (m), 913 (w), 870 (w), 826 (w), 784 (m), 756 (w), 732 (w), 698 (s), 644 (w), 625 (w), 579 (w), 529 (m), 512 (w), 472 (w), 462 (w), 446 (w), 421 (w), 410 (w). **^{1}H NMR (400 MHz, $CDCl_3$)**: δ =7.26 – 7.21 (m, 2H), 7.20 – 7.13 (m, 3H), 7.09 (q, J = 3.5 Hz, 3H), 7.07 – 7.02 (m, 2H), 5.43 (s, 1H), 4.45 (d, J = 8.7 Hz, 1H), 4.32 (d, J = 8.7 Hz, 1H), 3.01 (s, 1H), 2.84 (s, 3H). **^{13}C NMR (101 MHz, $CDCl_3$)**: δ = 138.3, 135.2, 128.2, 128.1, 127.1, 126.3, 78.2, 76.0, 59.8, 38.8.[j] **HRMS (ESI)**: Calculated for **$C_{16}H_{18}NO_3S$** [M+H]+: 304.1002, found: 304.0999. Spectroscopic data (^{1}H NMR) was in agreement to those previously reported. [41]

Minor-2.75:

IR (neat): $\tilde{\nu}$ = 3712 (w), 3652 (w), 3465 (w), 3032 (w), 2933 (w), 2349 (w), 2262 (w), 2222 (w), 2184 (w), 2168 (w), 2069 (w), 2038 (w), 1991 (w), 1969 (w), 1727 (w), 1496 (w), 1450 (w), 1313 (s), 1144 (s), 1062 (m), 1027 (m), 963 (m), 908 (w), 828 (w), 790 (m), 751 (m), 732 (m), 698 (s), 651 (w), 635 (w), 582 (m), 519 (m), 466 (w), 456 (w), 442 (w), 418 (w). **^{1}H NMR (400 MHz, $CDCl_3$)**: δ = 7.52 (d, J = 7.7 Hz, 2H), 7.48 – 7.31 (m, 8H), 5.65 (s, 1H), 4.63 (d, J = 8.7 Hz, 1H), 3.96 (d, J = 8.8 Hz, 1H), 2.86 (d, J = 1.9 Hz, 3H), 2.09 (s, 1H). **^{13}C NMR (101 MHz, $CDCl_3$)**: δ = 142.1, 133.6, 129.4, 129.1, 129.0, 128.5, 127.9, 125.3, 75.1, 73.3, 60.9, 40.1. **HRMS (ESI)**: Calculated for $C_{16}H_{18}NO_3S$ [M+H]+: 304.1002, found: 304.0999. Spectroscopic data (^{1}H NMR) was in agreement to those previously reported.[41]

Chemotion ELN sample number: HMA-4-63.

[j] Signals missing due to signal overlapping.

1,3-Diphenylazetidin-3-ol 2.76

Following **GP-D**, using 2-(methyl(phenyl)amino)-1-phenylethan-1-one **2.43** (135.2, 600 µmol, 1.00 eq.) in THF for 8 h. The desired product was obtained after automated FC (CyH : EtOAc, 90:10 to 80:20.) as an off-white solid (75.0 mg, 333 µmol, 55%).

M.P.: 80 – 84 °C. **IR (neat)**: $\tilde{\nu}$ = 3370 (w), 3060 (w), 3031 (w), 2929 (w), 2851 (w), 1599 (s), 1502 (s), 1472 (m), 1449 (w), 1343 (m), 1261 (w), 1228 (w), 1176 (w), 1155 (w), 1126 (w), 1061 (w), 1028 (w), 912 (w), 874 (w), 828 (w), 752 (s), 693 (s), 668 (w), 562 (w), 516 (w). **^{1}H NMR (400 MHz, $CDCl_3$)**: δ = 7.63 – 7.57 (m, 2H), 7.41 (dd, J = 8.4, 6.8 Hz, 2H), 7.36 – 7.30 (m, 1H), 7.29 – 7.22 (m, 2H), 6.81 (tt, J = 7.3, 1.1 Hz, 1H), 6.58 – 6.50 (m, 2H), 4.26 (d, J = 7.8 Hz, 2H), 4.09 (d, J = 7.8 Hz, 2H), 2.62 (s, 1H). **^{13}C NMR (101 MHz, $CDCl_3$)**: δ = 151.3, 143.6, 129.1, 128.7, 127.9, 124.8, 118.3, 112.2, 72.5, 67.2. **HRMS (ESI)**: Calculated for $C_{15}H_{16}NO$ $[M+H]^+$: 226.1226, found: 226.1218. Spectroscopic data was in agreement to those previously reported. [156]

Chemotion ELN sample number: HMA-4-82.

2-Methyl-1,3-diphenylazetidin-3-ol 2.77

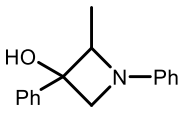

Following **GP-E**, using 2-(N-ethylanilino)-1-phenylethanone **2.44** (145 mg, 606 µmol, 1.00 eq.) in DMF (12.1 mL) for 24h. The desired product was obtained after automated FC (CyH : EtOAc, 100:00 to 70:30) as two diastereomers (dr = 44:56) **minor-2.77** (14.0 mg, 58.5 µmol, 10%) and **major-2.77** (18.0 mg, 75.2 µmol, 12%) as colourless waxes. The diastereomers were not assigned.

Major-2.77:

IR (neat): $\tilde{\nu}$ = 3416 (w), 3088 (w), 3058 (w), 3027 (w), 2977 (w), 2930 (w), 2865 (w), 1682 (w), 1599 (s), 1498 (s), 1447 (m), 1374 (m), 1323 (m), 1260 (w), 1178

(m), 1142 (m), 1064 (m), 1028 (m), 909 (w), 752 (s), 699 (s), 648 (w), 617 (w), 585 (w), 507 (w). **^{1}H NMR (400 MHz, $CDCl_3$)**: δ = 7.48 – 7.41 (m, 2H), 7.40 – 7.34 (m, 2H), 7.32 – 7.21 (m, 3H), 6.81 (tt, J = 7.4, 1.1 Hz, 1H), 6.61 (dtd, J = 8.8, 2.1, 1.2 Hz, 2H), 4.38 – 4.30 (m, 1H), 4.19 – 4.14 (m, 1H), 4.08 (d, J = 8.3 Hz, 1H), 3.65 (br s, 1H), 1.80 – 1.47 (m, 3H). **^{13}C NMR (101 MHz, $CDCl_3$)**: δ = 151.5, 143.3, 129.2, 128.7, 127.9, 125.2, 118.5, 112.8, 74.6, 70.5, 65.6, 15.5. **HRMS (ESI)**: Calculated for $C_{16}H_{18}NO$ $[M+H]^+$: 240.1482, found 240.1382.

Minor-2.77:

IR (neat): $\tilde{\nu}$ = 3401 (w), 3060 (w), 3031 (w), 2925 (m), 2855 (w), 1599 (s), 1499 (s), 1470 (w), 1451 (m), 1377 (w), 1329 (s), 1179 (w), 1147 (m), 1100 (w), 1073 (m), 1032 (w), 1007 (w), 876 (w), 781 (w), 754 (s), 694 (s), 596 (w), 523 (w), 463 (w), 427 (w), 411 (w). **^{1}H NMR (400 MHz, $CDCl_3$)**: δ = 7.68 – 7.61 (m, 2H), 7.48 – 7.40 (m, 2H), 7.39 – 7.31 (m, 1H), 7.29 – 7.20 (m, 4H), 6.82 (tt, J = 7.3, 1.1 Hz, 1H), 6.71 – 6.60 (m, 2H), 4.52 (dd, J = 7.9, 1.0 Hz, 1H), 4.21 (q, J = 6.4 Hz, 1H), 3.83 (d, J = 7.9 Hz, 1H), 2.26 (br s, 1H), 1.02 (d, J = 6.4 Hz, 3H). **^{13}C NMR (101 MHz, $CDCl_3$)**: δ = 152.3, 140.8, 129.2, 128.4, 127.8, 126.1, 118.8, 113.1, 75.5, 72.6, 65.6, 18.2. **HRMS (ESI)**: Calculated for $C_{16}H_{18}NO$ $[M+H]^+$: 240.1482, found 240.1382. Spectroscopic data was in agreement to those previously reported. [156]

Chemotion ELN sample number: HMA-4-67.

1-Benzhydryl-3-phenylazetidin-3-ol (2.80)

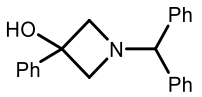

Following **GP-D**, using 2-(benzhydryl(methyl)amino)-1-phenylethan-1-one prepared by [redacted] (284 mg, 900 µmol, 1.00 eq.) in acetonitrile (45 mL) for 12h at 22 °C. The solvent was removed under reduced pressure and the crude product was purified *via* automated FC (CyH : EtOAc, 100:00 to 50:50). The product was obtained as a colourless solid (37.0 mg, 117 µmol, 13%).

M.P.: 99 – 102 °C. **IR (neat)**: $\tilde{\nu}$ = 3363 (w), 3084 (w), 3060 (w), 3027 (w), 2944 (w), 2836 (w), 1600 (w), 1493 (w), 1450 (m), 1390 (w), 1344 (w), 1308 (w), 1267 (w), 1212 (m), 1179 (w), 1157 (w), 1076 (w), 1064 (w), 1028 (w), 913 (w), 890 (w), 858 (w), 754 (m), 741 (m), 698 (s), 638 (w), 623 (w), 614 (w), 550 (w), 472

(w). **^{1}H NMR (400 MHz, $CDCl_3$)**: δ = 7.71 – 7.57 (m, 2H), 7.51 – 7.38 (m, 6H), 7.36 – 7.25 (m, 5H), 7.24 – 7.15 (m, 2H), 4.49 (s, 1H), 3.67 – 3.56 (m, 2H), 3.48 – 3.34 (m, 2H), 2.57 (s, 1H). **^{13}C NMR (101 MHz, $CDCl_3$)**: δ = 144.3, 142.3, 128.6, 128.6, 127.7, 127.6, 127.3, 125.0, 78.2, 71.6, 67.7. **HRMS (ESI)**: Calculated for $C_{22}H_{22}NO$ $[M+H]^+$ 316.1696, found: 316.1691. Spectroscopic data was in agreement to those previously reported.[167]

Chemotion ELN sample number: HMA-4-523 and spectra also HMA-3-36.

3-(o-Tolyl)oxetan-3-ol (2.55)

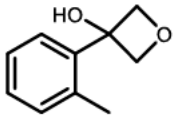

Following **GP-D** with minor alterations using 2-methoxy-1-(o-tolyl)ethan-1-one α-methoxyacetophenone **2.47** (30.0 mg, 0.183 mmol) in benzene (10 mL, 18 mM) for 22 h. The product was obtained after automated FC (CyH : EtOAc, 90:10 to 50:50) as a yellow oil (11.0 mg, 0.067 mmol, 37%).
IR (neat): $\tilde{\nu}$ = 3364 (m), 2948 (m), 2876 (w), 1492 (w), 1456 (m), 1381 (m), 1323 (w), 1264 (m), 1203 (m), 1174 (m), 1132 (s), 1064 (m), 1034 (m), 975 (s), 881 (m), 830 (m), 761 (s), 728 (s), 668 (m), 554 (w), 501 (w), 473 (w), 456 (m). **^{1}H NMR (400 MHz, C_6D_6):** δ = 7.02 (td, J = 7.4, 1.5 Hz, 1H), 6.98 – 6.87 (m, 2H), 6.76 (dd, J = 7.5, 1.5 Hz, 1H), 4.91 (dd, J = 6.7, 1.0 Hz, 2H), 4.65 (dd, J = 6.7, 1.0 Hz, 2H), 1.93 (s, 3H), 1.90 (s, 1H). **^{13}C NMR (101 MHz, C_6D_6):** δ = 139.9, 136.4, 131.3, 128.1, 125.7, 125.5, 82.8, 77.2, 18.8. **HRMS (ESI)**: Calculated for $C_{10}H_{13}O_2$ $[M+H]^+$: 165.0910, found 165.0912.

Chemotion ELN sample number: HMA-4-338.

4.2.3 Ring-opening of 3-azetidinols

4.2.3.1 Unsuccessful attempts for Ts protected azetidinol 2.6

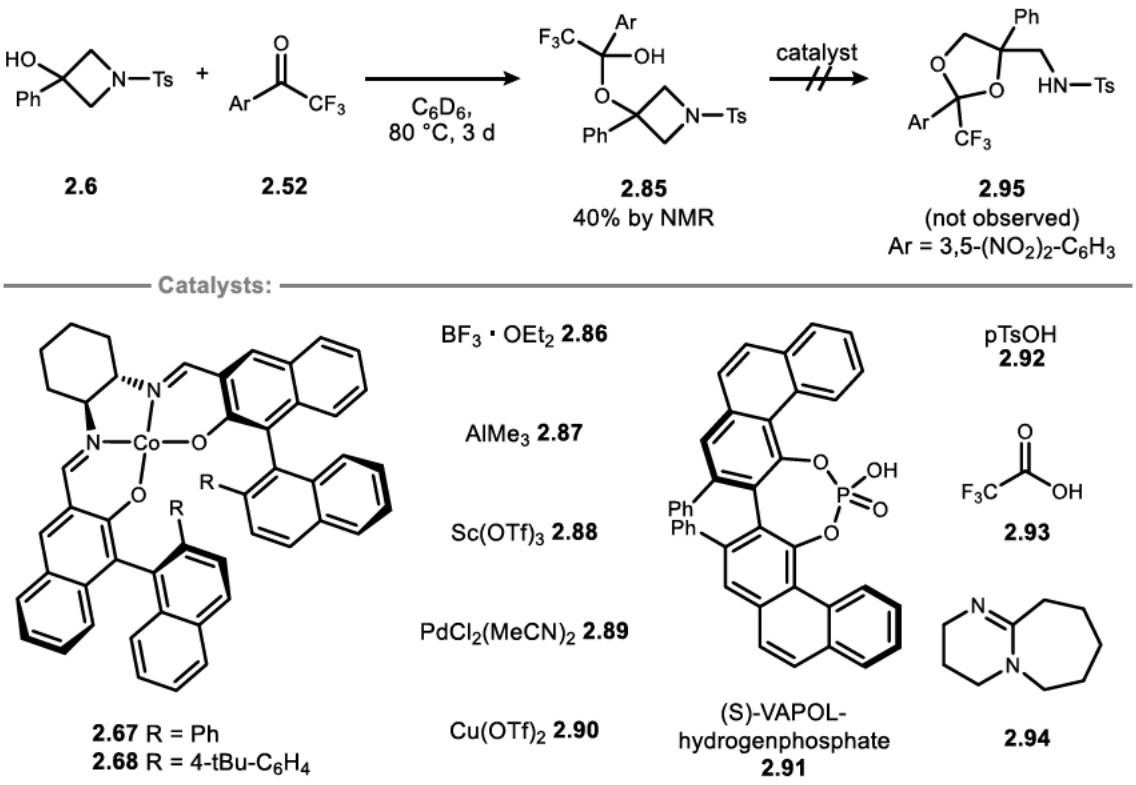

Scheme 58: Attempted ring-opening of 2.6. Reactions were run in C_6D_6 [0.2 M] on a 0.1 mmol scale. Reactions were evaluated *via* ^{19}F NMR with $PhCF_3$ as internal standard.

3-Phenyl-1-tosylazetidin-3-ol **2.6** (30.3 mg ,0.1 mmol, 1.00 eq.) and 3'5'-Dinitro-2,2,2-trifluoroacetophenone **2.52** (26.4 mg, 0.1 mmol, 1.00 eq.) were dissolved in dry C_6D_6 (1.00 mL, 20 mM) under inert-gas atmosphere and an additive (0.1 mmol, 1.00 eq.) was added. The mixture was heated to 80 °C for 72 h. The reaction progress was monitored by ^1H and ^{19}F NMR against $PhCF_3$ as internal standard.

4.2.3.2 Successful dioxolane formation

N-((2-(3,5-Dinitrophenyl)-4-phenyl-2-(trifluoromethyl)-1,3-dioxolan-4-yl)methyl)-1,1-Diphenylmethanamine (2.96)

1-Benzhydryl-3-phenyl-azetidin-3-ol **2.80** (63.1 mg, 200 µmol, 1.00 eq.) and 1-(3,5-dinitrophenyl)-2,2,2-trifluoro-ethanone **2.52** (52.8 mg, 200 µmol, 1.00 eq.) were dissolved in dry C_6D_6 (1.00 mL, 20 mM) under inert-gas atmosphere and heated to 80 °C for 72 h. The flask was allowed to cool to rt, and the crude mixture

was directly purified *via* automated FC (CyH : EtOAc, 100:0 to 50:50) to obtain the product as a single diastereomer (108.0 mg, 186 µmol, 93%) and a colourless oil.

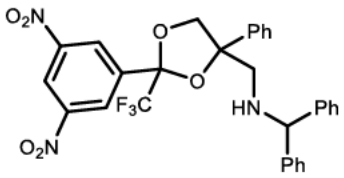

IR (neat): $\tilde{\nu}$ = 3102 (w), 3028 (w), 2281 (w), 1630 (w), 1599 (w), 1543 (s), 1493 (w), 1453 (w), 1344 (s), 1182 (s), 1135 (s), 1103 (m), 1071 (m), 998 (m), 914 (m), 850 (w), 812 (w), 764 (w), 746 (m), 729 (s), 702 (s), 663 (w), 621 (w), 597 (w), 559 (w), 501 (m), 470 (w). **^{1}H NMR (600 MHz, C_6D_6)**: δ = 8.54 (d, J = 2.1 Hz, 2H), 8.08 (t, J = 2.1 Hz, 1H), 7.24 (td, J = 8.4, 1.4 Hz, 4H), 7.15 – 6.95 (m, 7H), 6.91 – 6.75 (m, 4H), 4.54 (s, 1H), 4.44 (d, J = 8.5 Hz, 1H), 3.95 (d, J = 8.5 Hz, 1H), 2.95 – 2.66 (m, 2H), 1.77 (s, 1H). **^{13}C NMR (151 MHz, C_6D_6)**: δ = 148.0, 144.1, 144.1, 140.4, 138.6, 128.9, 128.5, 128.5, 127.6, 127.6, 127.5, 127.4, 127.0, 125.7, 122.4 (d, J = 288.1 Hz), 120.1, 104.5 (q, J = 33.3 Hz), 89.8, 77.7, 73.7, 67.5, 55.5, 27.2. **^{19}F NMR** (282 MHz, C_6D_6): δ = -81.35. **HRMS (ESI)**: Calculated for **$C_{30}H_{25}F_3N_3O_6$** $[M+H]^+$: 580.1690, found: 580.1682.

Chemotion ELN sample number: HMA-4-490.

Determination of the relative configuration of aminodioxolanes

The both diastereotopic CH_2-groups of the substrate **2.96** are unambiguously identified *via* gHMBC or COSY experiments. The relative configuration of the formed major diastereoisomer could be determined *via* 2D-^{1}H,^{1}H NOESY experiments. NOE interactions between the phenyl ring and the H_a protons of the 3,5-dinitrobenzene ring could be observed, as well as NOE interactions from both aromatic rings to an identical proton of the dioxolane ring. It can therefore be concluded, that the two aromatic substituents are positioned *syn* to each other. Another set of NOE interactions was observed for the other diastereotopic proton, with respective interactions to the amine and benzhydryl proton.

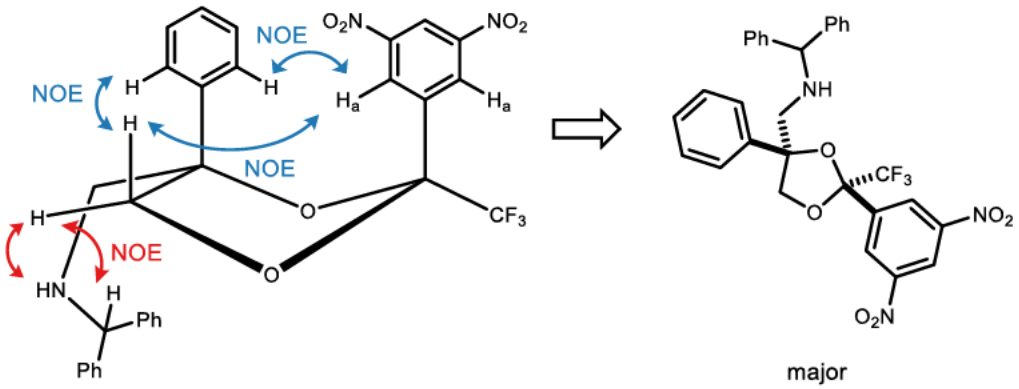

Ethyl 4-((benzhydrylamino)methyl)-4-phenyl-2-(trifluoromethyl)-1,3-dioxolane-2-carboxylate (2.103)

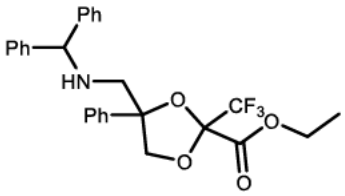

1-Benzhydryl-3-phenyl-azetidin-3-ol **2.80** (63.1 mg, 200 µmol, 1.00 eq.) and ethyl 3,3,3-trifluoro-2-oxopropanoate **2.102** (34.0 mg, 26.5 µL, 200 µmol, 1.00 eq.) were dissolved in dry C_6D_6 (1.00 mL) under inert-gas atmosphere and heated to 80 °C for 72 h. The flask was allowed to cool to rt, and the crude mixture was directly purified *via* automated FC (CyH : EtOAc, 100:0 to 90:10) to obtain the product as a mixture of two diastereomers (dr = 60:40 for isolated substance, 71.0 mg, 146 µmol, 73%) as a colourless oil. The diastereomers were not assigned.

IR (neat): $\tilde{\nu}$ = 1757 (s), 1493 (w), 1451 (w), 1275 (m), 1195 (s), 1138 (s), 1029 (m), 747 (m), 702 (s). **HRMS (ESI)**: Calculated for $C_{27}H_{27}F_3NO_4$ $[M+H]^+$: 486.1887, found: 486.1880.

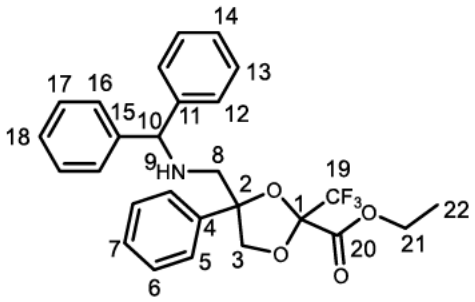

Major-2.103:

^{1}H NMR (600 MHz, C_6D_6): δ = 7.35 – 7.29 (m, 1H, H-7), 7.26 – 6.97 (m, 14H), 4.51 (s, 1H, H-10), 4.43 (d, J = 7.7 Hz, 1H, H-3), 4.30 (d, J = 7.8 Hz, 1H, H-3), 3.75 – 3.63 (m, 2H, H-21), 2.82 – 2.77 (m, 2H, H-8), 1.90 (br s, 1H, H-9), 0.62 (t, J = 7.1 Hz, 3H, H-22). **^{13}C NMR (151 MHz, C_6D_6)**: δ = 164.3 (C-20), 144.3 (2C, C-11, C-15), 141.5 (C-4), 128.8 – 127.3 (14C, $C_{arom.}$), 125.7 ($C_{arom.}$), 122.2 (q, J = 287.9 Hz, CF_3-C19), 102.5 (q, J = 33.2 Hz, C-1), 89.7 (C-2), 75.4 (C-3), 67.3 (C-10), 62.4 (C-21), 55.6 (C-8), 13.5 (C-22). **^{19}F NMR (282 MHz, C_6D_6)**: δ = – 79.85.

Minor-2.103:

^{1}H NMR (600 MHz, C_6D_6): δ = 7.31 – 7.28 (m, 1H, H-7), 7.26 – 6.97 (m, 14H), 4.58 (s, 1H, H-10), 4.43 (d, J = 7.8 Hz, 1H, H-3), 4.10 (d, J = 7.7 Hz, 1H, H-3), 3.90 – 3.76 (m, 2H, H-21), 2.92 – 2.83 (m, 2H, H-8), 2.31 (br s, 1H, H-9), 0.77 (t, J = 7.1 Hz, 3H, H-22). **^{13}C NMR (151 MHz, C_6D_6)**: δ = 164.7 (C-20), 144.4 (2C, C-11, C-15), 141.1 (C-4), 128.8 – 127.3 (14C, $C_{arom.}$), 125.3 ($C_{arom.}$), 122.3 (q, J = 289.6 Hz, CF_3-C19), 102.8 (q, J = 33.8 Hz, C-1), 90.3 (C-2), 75.5 (C-3), 67.6 (C-10), 63.0 (C-21), 56.0 (C-8), 13.6 (C-22). **^{19}F NMR (282 MHz, C_6D_6)**: δ = -79.34.

Chemotion ELN sample number: HMA-4-498.

4.2.4 Ring-opening of 3-oxetanols

((2R,4S)-4-Butyl-2-(3,5-dinitrophenyl)-2-(trifluoromethyl)-1,3-dioxolan-4-yl)methanol (2.106)

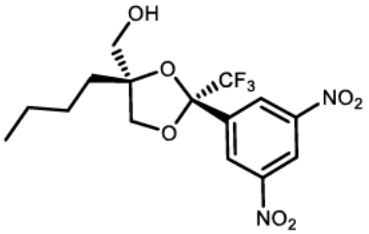

Following **GP-F** using 3-butyloxetan-3-ol **2.61**, synthesised by [redacted] (26.0 mg, 0.20 mmol, 1.00 eq.) and Co^{II}·salen **2.68** (1.9 mg, 2.0 µmol, 1.0 mol%), the major diastereomer (61.0 mg, 0.155 mmol, 78%) was obtained *via* automated FC (CyH : Et_2O, 100:0 to 80:20) as a colourless oil.

IR (neat): 3484 (w),3110 (w), 2960 (w), 2360 (w), 2335 (w), 1547 (s), 1347 (s), 1184 (s), 1140 (s), 1106 (m), 1070 (m), 1000 (m), 918 (m), 729 (s), 710(s). **^{1}H NMR (400 MHz, C_6D_6):** δ = 8.64 (d, J = 2.1 Hz, 2H,), 8.36 (t, J = 2.1 Hz, 1H,), 3.95 (d, J = 8.3 Hz, 1H; CH_2), 3.45 – 3.26 (m, 3H), 1.43 (s, 1H, O*H*), 1.20 – 1.10 (m, 2H), 1.07 – 0.76 (m, 4H), 0.68 (t, J = 7.1 Hz, 3H). **^{13}C NMR (101 MHz, C_6D_6):** δ = 148.4, 139.9, 126.9, 122.5 (q, $^1J_{C\text{-}F}$ = 288.6 Hz, *C*F_3), 120.2, 104.0 (q, $^2J_{C\text{-}F}$ = 33.0 Hz), 88.9, 73.0, 63.4, 34.4, 26.1, 23.1, 13.9. **^{19}F NMR (377 MHz, C_6D_6):** δ = – 81.66 (s, 3F, C*F*$_3$). **Optical Rotation**: $[\alpha]_D^{25}$ = – 3.4 (c = 1.00, $CHCl_3$) for an enantiomerically enriched sample of 72:28 *er*. The enantiomeric purity was established by HPLC analysis using a chiral column (Lux® i-Cellulose-5 column, 22 °C, 0.25 mL/min, 90:10 hexane:isopropanol, 210 nm, t_{major} = 23.741 min, t_{minor} = 25.151 min). See section 15 for HPLC chromatograms. Absolute stereochemistry determined through analogy with CCDC:2141905.[83]

((2R,4S)-2-(3,5-Dinitrophenyl)-2-(trifluoromethyl)-4-((triisopropylsilyl)ethynyl)-1,3-dioxolan-4-yl)methanol (2.108)

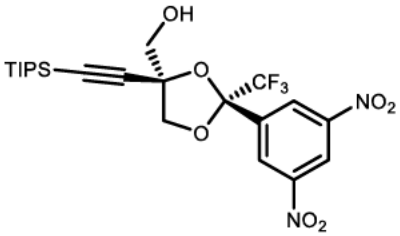

Following **GP-F** using 3-((triisopropylsilyl)ethynyl)oxetan-3-ol **2.58** (50.9 mg, 0.20 mmol, 1.00 eq.) and Co^{II}·salen **2.67** (1.9 mg, 2.0 µmol, 1.0 mol%), the major diastereomer (90.0 mg, 0.174 mmol, 87%) was obtained *via* automated FC (CyH : Et_2O, 100:0 to 80:20) as a yellow oil.

IR (neat): 3968 (w), 3891 (w), 3842 (w), 3780 (w), 3492 (w), 3108 2949 (m), 2868 (w), 1631 (w), 1547 (s), 1463 (w), 1345 (s), 1315 (w), 1202 (m), 1134 (m), 1105 (m), 1067 (m), 1006 (m), 915 (w), 882 (w), 831 (w), 730 (s). **^{1}H NMR (400 MHz, C_6D_6):** δ = 8.78 (d, J = 2.1 Hz, 2H,), 8.64 (t, J = 2.1 Hz, 1H,), 4.12 (d, J = 7.9 Hz, 1H), 3.75 (dd, J = 7.9, 1.0 Hz, 1H), 3.57 (dd, J = 12.4, 4.6 Hz, 1H), 3.32 (dd, J = 12.4, 8.6 Hz, 1H), 1.66 (dd, J = 8.9, 5.2 Hz, 1H, O*H*), 0.74 (dd, J = 7.2, 1.9 Hz, 18H), 0.68 – 0.58 (m, 3H). **^{13}C NMR (101 MHz, C_6D_6):** δ = 148.7, 139.3, 127.3, 122.4 (q, $^1J_{C\text{-}F}$ = 287.9 Hz, *C*F_3), 120.2, 104.6 (q, $^2J_{C\text{-}F}$ = 33.5 Hz) 103.6, 90.5, 81.3, 74.1, 64.0, 18.3, 10.9. **^{19}F NMR (377 MHz, C_6D_6):** δ = – 81.76 (s, 3F, C*F*$_3$). **HRMS (APCI):** Calculated for $C_{23}H_{30}F_3N_2O_9Si$ $[M+HCOO]^-$: 563.1673, Found: 563.1671. **Optical Rotation**: $[\alpha]_D^{25}$ = + 37.1 (*c* = 1.00, $CHCl_3$) for an enantiomerically enriched sample of 91:09 *er*. The enantiomeric purity was established by HPLC analysis using a chiral column (Lux® i-Cellulose-5 column, 22 °C, 1 mL/min, 98:02 hexane:isopropanol, 254 nm, t_{minor} = 6.350 min, t_{major} = 6.891 min). See section 15 for HPLC chromatograms. Absolute stereochemistry determined through analogy with CCDC:2141905.[83]

((2R,4S)-4-(3,3-Dimethylbut-1-yn-1-yl)-2-(3,5-dinitrophenyl)-2-(trifluoromethyl)-1,3-dioxolan-4-yl)methanol (2.109)

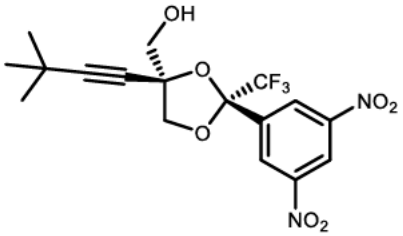

Following **GP-F** using 3-(3,3-dimethylbut-1-yn-1-yl)oxetan-3-ol **2.57** (30.8 mg, 0.20 mmol, 1.00 eq.) and Co^{II}·salen **2.67** (1.9 mg, 2.0 µmol, 1.0 mol%), the major diastereomer (73.0 mg, 0.175 mmol, 87%) was obtained *via* automated FC (CyH : Et_2O, 100:0 to 80:20) as an off-white solid.

M.P.: 72 – 75 °C. **IR (neat)**: 3101 (w), 2972 (w),1547 (s), 1346 (s), 1319 (w), 1202 (m), 1185 (m), 1134 (m), 1105 (w), 1065 (w), 1008 (w), 915 (w), 774 (m), 756 (m), 731 (s). **^{1}H NMR (400 MHz, C_6D_6):** δ = 8.77 (d, J = 2.1 Hz, 2H,), 8.52 (t, J = 2.1 Hz, 1H,), 4.11 (d, J = 7.9 Hz, 1H), 3.65 (dd, J = 7.9, 0.9 Hz, 1H), 3.59 (dd, J = 12.3, 5.1 Hz, 1H), 3.34 (dd, J = 12.3, 8.5 Hz, 1H), 1.69 (dd, J = 8.7, 5.4 Hz, 1H, O*H*), 0.73 (s, 9H). **^{13}C NMR (101 MHz, C_6D_6):** δ = 148.4, 139.3, 127.5, 122.3 (q, $^1J_{C\text{-}F}$ = 287.4 Hz, *C*F_3), 120.1, 104.5 (q, $^2J_{C\text{-}F}$ = 33.4 Hz),.98.0, 81.5, 75.5, 73.9, 64.5, 30.2, 27.2. **^{19}F NMR (377 MHz, C_6D_6):** δ = – 81.66 (s, 3F, C*F*$_3$). **HRMS (APCI):** Calculated for $C_{18}H_{18}F_3N_2O_9$ $[M+CHOO]^-$: 463.0964, Found: 463.0967. **Optical Rotation**: $[\alpha]_D^{25}$ = + 35.4 (c = 1.00, $CHCl_3$) for an enantiomerically enriched sample of 88:12 *er*. The enantiomeric purity was established by HPLC analysis using a chiral column (Reprosil Chiral-AMS column, 22 °C, 1 mL/min, 95:05 hexane:isopropanol, 210 nm, t_{major} = 13.311 min, t_{minor} = 15.586 min). See section 15 for HPLC chromatograms. Absolute stereochemistry determined through analogy with CCDC:2141905.[83]

((2R,4S)-2-(3,5-Dinitrophenyl)-4-(phenylethynyl)-2-(trifluoromethyl)-1,3-dioxolan-4-yl)methanol (2.110)

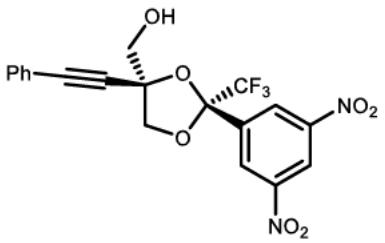

Following **GP-F** using 3-(phenylethynyl)oxetan-3-ol **2.60** (34.8 mg, 0.20 mmol, 1.00 eq.) and Co^{II}·salen **2.67** (1.9 mg, 2.0 µmol, 1.0 mol%), the major diastereomer (81.0 mg, 0.184 mmol, 92%) was obtained *via* automated FC (CyH : Et_2O, 100:0 to 80:20) as a yellow oil.

IR (neat): 3631 (w), 3495 (w), 3440 (w), 3101 (w), 2926 (w), 2237 (w), 1631 (w), 1600 (w), 1544 (s), 1491 (w), 1346 (s), 1321 (w), 1201 (s), 1186 (s), 1137 (s), 1105 (s), 1069 (m), 1062 (m), 1008 (m), 915 (m). **^{1}H NMR** (400 MHz, C_6D_6) δ (ppm) = 8.78 (d, J = 2.1 Hz, 2H,), 8.27 (t, J = 2.1 Hz, 1H,), 7.10 – 7.02 (m, 2H,), 6.89 – 6.74 (m, 3H,), 4.20 (d, J = 8.1 Hz, 1H), 3.83 (dd, J = 8.0, 1.0 Hz, 1H), 3.69 (d, J = 12.2 Hz, 1H), 3.48 (d, J = 12.3 Hz, 1H), 1.80 (s, 1H, O*H*). **^{13}C NMR** (101 MHz, C_6D_6) δ (ppm) = 148.3, 138.6, 131.6, 129.7, 128.7, 127.2, 122.2 (q, $^1J_{C\text{-}F}$ = 287.8 Hz, *C*F_3), 120.9, 120.3, 104.9 (q, $^2J_{C\text{-}F}$ = 33.5 Hz), 89.0, 85.5, 81.8, 73.9, 64.5. **^{19}F NMR** (377 MHz, C_6D_6) δ (ppm) = – 81.48 (s, 3F, C*F*$_3$). **HRMS (APCI):** Calculated for $C_{20}H_{14}F_3N_2O_9$ $[M+CHOO]^-$: 483.0651, Found: 483.0629. **Optical Rotation**: $[\alpha]_D^{25}$ = – 1.9 (c = 1.00, $CHCl_3$) for an enantiomerically enriched sample of 86:14 *er*. The enantiomeric purity was established by HPLC analysis using a chiral column (Lux® i-Cellulose-5 column, 22 °C, 1 mL/min, 98:02 hexane:isopropanol, 254 nm, t_{major} = 23.972 min, t_{minor} = 26.535 min). See section 15 for HPLC chromatograms. Absolute stereochemistry determined through analogy with CCDC:2141905.[83]

((2R,4S)-2-(3,5-Dinitrophenyl)-2-(trifluoromethyl)-4-((trimethylsilyl)ethynyl)-1,3-dioxolan-4-yl)methanol (2.111)

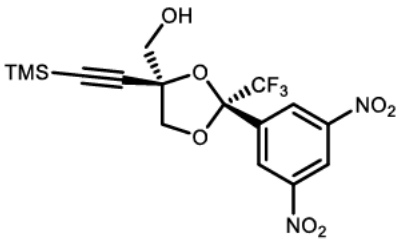

Following **GP-F** using 3-((trimethylsilyl)ethynyl)oxetan-3-ol **2.59** (34.1 mg, 0.20 mmol, 1.00 eq.) and Co^{II}·salen **2.67** (1.9 mg, 2.0 µmol, 1.0 mol%), the major diastereomer (72.0 mg, 0.17 mmol, 85%) was obtained *via* automated FC (CyH : Et_2O, 100:0 to 80:20) as a colourless oil.

IR (neat): 3681 (w), 3672 (w), 3616 (w), 3474 (w), 3110 (w), 2960 (w), 2897 (w), 1631 (w), 1547 (s), 1346 (m), 1320(w), 1275 (m), 1260 (m), 1203 (m), 1188 (m), 1134 (m), 1106 (m), 1065 (w), 1008 (w), 915 (w), 860 (m), 846 (m), 764 (s),

730 (s), 707 (m). **^{1}H NMR (400 MHz, C_6D_6):** δ = 8.76 (d, J = 2.1 Hz, 2H,), 8.52 (t, J = 2.1 Hz, 1H,), 4.08 (d, J = 8.1 Hz, 1H), 3.71 (d, J = 9.0 Hz, 1H), 3.58 (d, J = 12.3 Hz, 1H), 3.35 (d, J = 12.3 Hz, 1H), 1.66 (s, 1H, O*H*), -0.17 (s, 9H). **^{13}C NMR (101 MHz, C_6D_6):** δ = 148.4, 138.9, 127.4, 122.2 (q, $^{1}J_{C\text{-}F}$ = 287.5 Hz, *C*F$_3$); 120.2, 104.7 (q, $^{2}J_{C\text{-}F}$ = 33.5 Hz); 101.4, 94.4, 81.3, 73.7, 64.3, -0.8. **^{19}F NMR (377 MHz, C_6D_6):** δ = – 81.59 (s, 3F, C*F*$_3$). **HRMS (APCI):** Calculated for $C_{17}H_{18}F_3N_2O_9Si$ [M+CHOO]$^-$: 479.0734, Found: 479.0730. **Optical Rotation**: $[\alpha]_D^{25}$ = + 45.8 (c = 1.00, $CHCl_3$) for an enantiomerically enriched sample of 92:08 *er*. The enantiomeric purity was established by HPLC analysis using a chiral column (Reprosil Chiral-AMS column, 22 °C, 1 mL/min, 99:01 hexane:isopropanol, 254 nm, t_{major} = 21.051 min, t_{minor} = 27.267 min). See section 15 for HPLC chromatograms. Absolute stereochemistry determined through analogy with CCDC:2141905.[83]

Methyl 2-(6-(3,5-dinitrophenyl)-6-(trifluoromethyl)-2,5,7-trioxaspiro[3.4]octan-8-ylidene)acetate (*rac*-2.117)

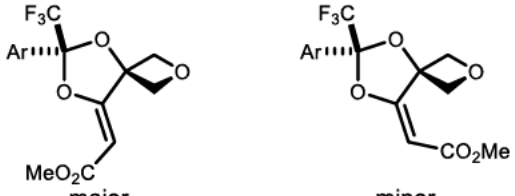

Ketone **2.52** (26.4 mg, 0.10 mmol, 1.00 eq.) and **2.56** (15.6 mg, 0.10 mmol, 1.00 eq.) were dissolved in dry CH_2Cl_2 (0.50 mL) at rt. The temperature was maintained for 24 h before silica gel was added and filtered off. The resulting silica gel plug was flushed with Et_2O, and the filtrate was concentrated. NMR yield and *rr* of the crude reaction mixture was determined by ^{19}F NMR using $PhCF_3$ (12.2 µL, 0.10 mmol) as the internal standard. A mixture of both configurational isomers was obtained *via* automated FC (CyH : Et_2O, 100:0 to 70:30) as an off-white solid (32.0 mg, 0.080 mmol, 80%, E/Z (40/60)).

Mixture:

M.P.: 117 – 120 °C. **IR (neat)**: 2961 (w), 2947 (w), 2861 (w), 1589 (m), 1445 (w), 1422 (w), 1333 (w), 1146 (w), 816 (w), 749 (s). **HRMS (APCI):** Calculated for $C_{15}H_{10}F_3N_2O_9$ [M-H]$^-$: 419.0338, Found: 419.0354 **Optical Rotation**: $[\alpha]_D^{25}$ = – 1.5 (c = 1.00, $CHCl_3$) for a racemic mixture of both configurational isomers

(*E*/*Z* 60/40). The enantiomeric purity was established by HPLC analysis using a chiral column (Lux® i-Amylose-3, 22 °C, 0.5 mL/min, 80:20 hexane:isopropanol, 210 nm, t_{major} = 17.330 min, 18.217 min, t_{minor} = 21.939 min, 31.255 min). See section 15 for HPLC chromatograms. Relative configuration determined *via* NOE-experiments.

Major *Z*-isomer:

^{1}H NMR (400 MHz, C_6D_6): δ = 8.55 (d, *J* = 2.1 Hz, 2H), 8.32 (t, *J* = 2.1 Hz, 1H), 5.48 (s, 1H), 4.66 (d, *J* = 7.7 Hz, 1H), 4.41 (dd, *J* = 7.9, 1.1 Hz, 1H), 4.23 (d, *J* = 7.9 Hz, 1H), 4.01 (dt, *J* = 7.8, 1.0 Hz, 1H), 3.45 (s, 3H). **^{13}C NMR (101 MHz, C_6D_6):** δ = 163.6, 162.4, 148.4, 134.5, 126.4, 121.2 (q, $^1J_{C\text{-}F}$ = 289.2 Hz, *C*F$_3$), 121.1, 106.2 (t, $^2J_{C\text{-}F}$ = 34.3 Hz), 92.1, 86.2, 82.5, 80.4, 51.4. [k] **^{19}F NMR (377 MHz, C_6D_6):** δ = −83.36 (s, 3F, C*F*$_3$).

Minor *E*-isomer:

^{1}H NMR (400 MHz, C_6D_6): δ = 8.41 (d, *J* = 2.1 Hz, 2H,), 8.36 (t, *J* = 2.1 Hz, 1H,), 5.61 (s, 1H), 5.26 (dd, *J* = 7.6, 1.1 Hz, 1H), 5.22 (dd, *J* = 7.5, 1.0 Hz, 1H), 4.73 (dt, *J* = 7.6, 1.1 Hz, 1H), 4.47 (dd, *J* = 7.4, 1.2 Hz, 1H), 3.38 (s, 3H). **^{13}C NMR (101 MHz, C_6D_6):** δ = 165.2, 162.9, 148.4, 134.7, 126.2, 121.5 (q, $^1J_{C\text{-}F}$ = 290.3 Hz, *C*F$_3$), 121.0, 103.7 (t, $^2J_{C\text{-}F}$ = 34.2 Hz), 96.7, 89.1, 80.4, 79.4, 51.4.[l] **^{19}F NMR (377 MHz, C_6D_6):** δ = −83.10 (s, 3F, C*F*$_3$).

Relative configuration determined *via* NOE-experiments:

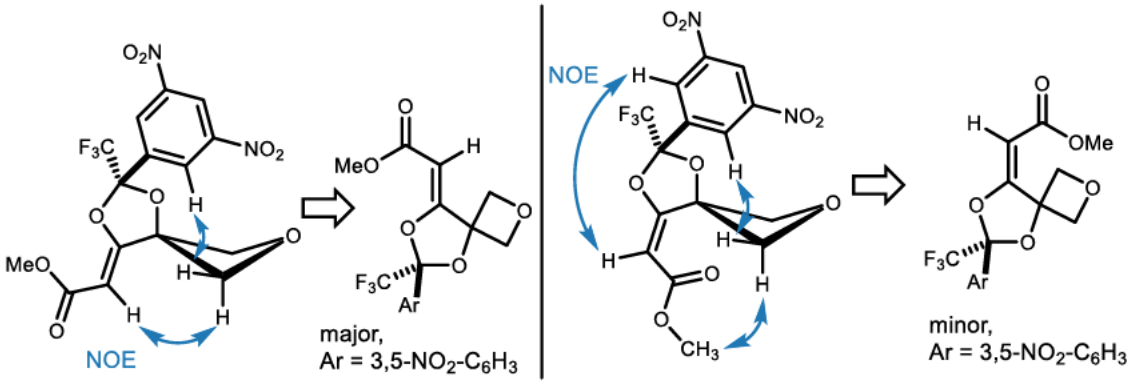

[k] One signal missing due to signal overlap
[l] Missing signals under solvent peak

(R,Z)-8-Benzylidene-6-(3,5-dinitrophenyl)-6-(trifluoromethyl)-2,5,7- trioxaspiro[3.4]octane (2.118)

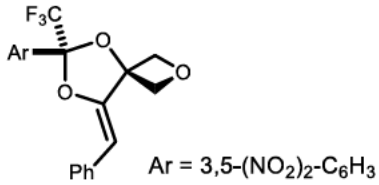

Following a literature known protocol with minor alterations,[168] ketone **2.52** (63.4 mg, 0.24 mmol, 1.20 eq.), 3-(phenylethynyl)oxetan-3-ol **2.60** (32.0 mg, 0.20 mmol, 1.00 eq.), $AgNO_3$ (3.4 mg, 20.0 µmol, 10.0 mol%) and 1,8-diazabicyclo[5.4.0]-7-undecene **2.94** (3.0 µL, 20.0 µmol, 10.0 mol%) were dissolved in dry toluene (1.3 mL) at room temperature. The temperature was maintained for 24 h before silica gel was added and filtered off. The resulting silica gel plug was flushed with Et_2O, and the filtrate was concentrated. NMR yield and *rr* of the crude reaction mixture was determined by ^{19}F NMR using $PhCF_3$ (12.2 µL, 0.10 mmol) as the internal standard. A racemic mixture of the desired product was obtained *via* automated FC (CyH : Et_2O, 100:0 to 70:30) as a pale yellow solid (85.0 mg, 0.19 mmol, 95%).

M.P.: 158.5 – 160.5 °C. **IR (neat)**: 1727 (w), 1701 (w), 1548 (s), 1347 (s), 1319 (w), 1299 (m), 1200 (s), 1147 (s), 1036 (w), 1004 (m), 913 (w), 846 (w), 777 (m), 759 (w), 731 (m), 711 (m). **^{1}H NMR (400 MHz, C_6D_6)** δ = 8.56 (d, J = 2.1 Hz, 2H,), 8.36 (t, J = 2.1 Hz, 1H,), 7.60 – 7.54 (m, 2H,), 7.21 (t, J = 7.8 Hz, 2H,), 7.08 – 7.02 (m, 1H,), 5.85 (s, 1H), 4.89 (d, J = 7.7 Hz, 1H), 4.67 (d, J = 8.9 Hz, 1H), 4.53 (d, J = 7.7 Hz, 1H), 4.41 – 4.33 (m, 1H). **^{13}C NMR (101 MHz, C_6D_6):** δ = 150.3, 148.4, 135.6, 133.4, 129.2, 128.6, 126.4, 121.6 (q, $^1J_{C\text{-}F}$ = 289.6 Hz, CF_3), 120.9, 104.9 (q, $^2J_{C\text{-}F}$ = 34.0 Hz), 101.3, 85.9, 83.6, 83.6, 81.6. **^{19}F NMR (377 MHz, C_6D_6):** δ = – 83.33 (s, 3F, CF_3). **HRMS (APCI):** Calculated for $C_{19}H_{12}F_3N_2O_7$ [M-H]$^-$: 437.0597, Found: 437.0604 **Optical Rotation**: $[\alpha]_D^{25}$ = +0.0 (c = 1.00, $CHCl_3$) for a racemic sample. The enantiomeric purity was established by HPLC analysis using a chiral column (Lux® i-Amylose-3, 22 °C, 1 mL/min, 80:20 hexane:isopropanol, 254 nm, t = 6.298 min and 6.882 min). See section 15 for HPLC chromatograms.

4.3 Development of a molecular solar thermal system

General procedures

General procedure G (GP-G) for the preparation of 2,2,2-trifluoroacetophenones from halogenated arenes with lithium organyls:

2,2,2-Trifluoroacetophenones were prepared following an adapted literature procedure.[113] A halogenated arene (1.00 eq.) was dissolved in dry Et_2O or THF (0.2 M) under nitrogen atmosphere and was cooled to −78 °C at which temperature *t*-BuLi (2.05 eq.) was added dropwise. After 30 min, ethyl trifluoroacetate (1.10 eq.) was added dropwise and the mixture was stirred at −78 °C for 3 h. The reaction was quenched with aqueous saturated NH_4Cl solution, diluted with Et_2O, and allowed to warm up to rt. The organic phase was separated, and the aqueous phase was extracted with Et_2O (3x). The combined organic fractions were dried over $MgSO_4$ and the solvent was removed under reduced pressure. The products were purified *via* flash chromatography (FC) and bulb-to-bulb distillation. Bulb-to-bulb distillation was found to be crucial to achieve reproducible reactivity in the irradiation.

General procedure H (GP-H) for NMR scale irradiation experiments in deuterated benzene:

For NMR scale irradiation experiments, oven dried NMR Tubes with a septum cap were charged with degassed C_6D_6 (0.5 mL, 3 × freeze-pump-thaw) in a Glove Box. An acetophenone was added under inert gas atmosphere *via* a microsyringe through the septum cap and $PhCF_3$ was added as an internal standard. The tubes were irradiated using a *Luzchem* LZC-ORG photoreactor equipped with 10 × 8 Watt LZC-UVA mercury lamps (355 nm) lamps (*cf.* chapter 4.1,Figure 26) or a Kessil 45W PR160L 370nm Gen2 LED at 1 cm distance (*cf.* chapter 4.1,Figure 27).

General procedure I (GP-I) for large scale irradiation experiments:

Oven-dried Schlenk-flasks were charged with an acetophenone was added under inert gas atmosphere and a respective solvent. The mixture was degassed (3 × freeze-pump-thaw) and irradiated. The solvent was removed under reduced pressure and the sample purified using FC, automated FC or RP-MPLC.

4.3.1 Synthesis of starting materials

2,2,2-Trifluoro-1-(o-tolyl)ethan-1-one (3.8)

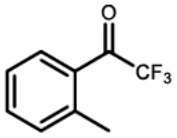

Following **GP-G** using 2-bromotoluene (5.13 g, 3.61 mL, 30.0 mmol, 1.00 eq.), *t*-BuLi (3.92 g, 36.0 mL, 61.2 mmol, 1.70 M, 2.04 eq.) and ethyl trifluoroacetate (4.78 g, 4.00 mL, 33.7 mmol, 1.12 eq.) in Et_2O (150 mL). The desired product was obtained after FC (pentane) and bulb-to-bulb distillation (110 °C, 0.54 mbar) as a colourless oil (5.12 g, 27.2 mmol, 91%).

IR (neat): $\tilde{\nu}$ = 1715 (m), 1604 (w), 1573 (w), 1459 (w), 1385 (w), 1323 (w), 1288 (w), 1184 (s), 1142 (s), 1037 (w), 933 (s), 737 (s), 665 (m), 608 (w), 529 (w), 491 (w), 462 (w), 446 (w), 436 (w). **^{1}H NMR (400 MHz, C_6D_6):** δ = 7.62 (dq, J = 7.9, 1.9 Hz, 1H), 6.91 (td, J = 7.6, 1.4 Hz, 1H), 6.75 (t, J = 7.2 Hz, 2H), 2.28 (s, 3H). **^{13}C NMR (101 MHz, C_6D_6):** δ = 182.2 (q, J = 33.7 Hz), 142.4, 133.8, 132.7, 130.5 (q, J = 3.7 Hz), 129.5, 126.0, 117.1 (q, J = 293.1 Hz), 21.7. **^{19}F NMR (282 MHz, C_6D_6):** δ = -71.54 (d, J = 2.0 Hz, 3F). **HRMS (ESI)**: Calculated for $C_9H_6F_3O$ $[M-H]^-$: 187.0376, found: 187.0381. Spectroscopic data was in agreement to those previously reported.[113]

Chemotion ELN sample number: HMA-4-353.

1-(2-Ethylphenyl)-2,2,2-trifluoroethan-1-one (3.9)

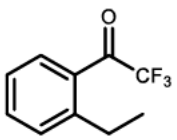

Following **GP-G** using 1-ethyl-2-iodobenzene (1.16 g, 0.71 mL, 5.00 mmol, 1.00 eq.), *t*-BuLi (641 mg, 5.26 mL, 10.0 mmol, 1.90 M, 2.00 eq.) and ethyl

trifluoroacetate (781 mg, 0.65 mL, 5.50 mmol, 1.10 eq.) in THF (20 mL). The desired product was obtained after FC (pentane) and bulb-to-bulb distillation (100 °C, 0.70 mbar) as a colourless oil (937 mg, 4.63 mmol, 93%).

IR (neat): $\tilde{\nu}$ = 2963 (w), 2932 (w), 2155 (w), 2034 (w), 2016 (w), 1720 (m), 1602 (w), 1573 (w), 1450 (w), 1323 (w), 1182 (s), 1144 (s), 934 (s), 790 (w), 754 (m), 734 (m), 662 (m), 635 (w), 607 (w), 586 (w), 564 (w), 556 (w), 540 (w), 528 (w), 518 (w), 507 (w), 498 (w), 482 (w), 468 (w), 459 (w), 449 (w), 429 (w), 418 (m). **^{1}H NMR (400 MHz, C_6D_6):** δ = 7.57 (dp, J = 7.7, 1.9 Hz, 1H), 6.97 (td, J = 7.6, 1.3 Hz, 1H), 6.84 (ddd, J = 7.8, 1.3, 0.6 Hz, 1H), 6.76 (td, J = 7.7, 1.3 Hz, 1H), 2.66 (q, J = 7.5 Hz, 2H), 1.04 (t, J = 7.5 Hz, 3H). **^{13}C NMR (101 MHz, C_6D_6):** δ = 182.8 (q, J = 33.9 Hz), 148.0, 133.9, 131.1, 130.1, 129.6 (q, J = 3.6 Hz), 126.0, 117.2 (q, J = 293.2 Hz), 27.5, 15.6. **^{19}F NMR (282 MHz, C_6D_6):** δ =-71.85 (d, J = 2.0 Hz). **HRMS (APCI)**: Calculated for $C_{10}H_9F_3O$ $[M]^{\cdot-}$: 202.0610, found: 202.0613.

Chemotion ELN sample number: HMA-4-199.

2,2,2-Trifluoro-1-(2-isopropylphenyl)ethan-1-one (3.10)

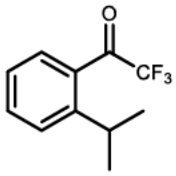

Following **GP-G** using 1-iodo-2-isopropylbenzene (1.23 g, 0.79 mL, 5.00 mmol, 1.00 eq.), *t*-BuLi (641 mg, 5.88 mL, 10.0 mmol, 1.70 M, 2.00 eq.) and ethyl trifluoroacetate (781 mg, 0.65 mL, 5.50 mmol, 1.10 eq.) in THF (20 mL). The desired product was obtained after FC (pentane) as a colourless oil (589 mg, 2.72 mmol, 54%).

IR (neat): $\tilde{\nu}$ = 2960 (m), 2925 (m), 2871 (w), 2854 (w), 1721 (m), 1601 (w), 1463 (w), 1378 (w), 1365 (w), 1202 (s), 1182 (s), 1147 (s), 1035 (w), 936 (s), 758 (m), 728 (w), 660 (m), 624 (w), 610 (w), 600 (w), 573 (w), 565 (w), 540 (w), 530 (w), 515 (w), 506 (w), 490 (m), 462 (m), 444 (w), 433 (w), 417 (w). **^{1}H NMR (600 MHz, $CDCl_3$):** δ = 7.70 (dt, J = 8.0, 1.7 Hz, 1H), 7.61 – 7.56 (m, 1H), 7.55 – 7.51 (m, 1H), 7.34 – 7.30 (m, 1H), 3.40 (p, J = 6.8 Hz, 1H), 1.26 (d, J = 6.9 Hz,

6H). **^{13}C NMR (151 MHz, $CDCl_3$):** δ = 184.3 (q, J = 34.5 Hz), 151.6, 133.8, 130.0, 128.9 (q, J = 292.9 Hz), 127.3, 125.7, 116.4 (q, J = 292.9 Hz), 29.7, 24.1. **^{19}F NMR (282 MHz, C_6D_6):** δ = -72.77 (d, J = 1.8 Hz). **HRMS (APCI)**: Calculated for $C_{11}H_{11}F_3O$ $[M]^{\cdot-}$: 216.0767, found: 216.0768.

Chemotion ELN sample number: HMA-4-186.

1-Bromo-2-(methoxymethyl)benzene (4.14)

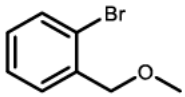

1-Bromo-2-(methoxymethyl)benzene was prepared following a literature known protocol.[169] Sodium hydride (720 mg, 18.0 mmol, 1.20 eq.) was suspended in dry THF (100 mL) under inert gas atmosphere and a prepared solution of (2-bromophenyl)methanol (2.81 g, 15.0 mmol, 1.00 eq.) in dry THF (50 mL) was added dropwise at 0 °C. The mixture was stirred for 15 min and iodomethane (6.39 g, 2.80 mL, 45.0 mmol, 3.00 eq.) was added dropwise at 0 °C. The solution was stirred at 0 °C for 15 minutes and 16°h at rt.NH_4Cl sat. was added and the solution was diluted with CH_2Cl_2 (30 mL). The organic layer was separated, and the aqueous layer was extracted with CH_2Cl_2 (3 x 30 mL). The combined organic fractions were dried over Na_2SO_4 and the solvent was removed under reduced pressure. The product was obtained after FC (pentane : Et_2O, 100:0 to 80:20) as a slightly yellow oil (2.79 g, 13.9 mmol, 92%).
^{1}H NMR (400 MHz, $CDCl_3$): δ = 7.54 (dd, J = 8.0, 1.3 Hz, 1H), 7.46 (ddd, J = 7.6, 1.8, 0.9 Hz, 1H), 7.32 (td, J = 7.5, 1.3 Hz, 1H), 7.20 – 7.10 (m, 1H), 4.53 (s, 2H), 3.47 (s, 3H). **^{13}C NMR (101 MHz, $CDCl_3$):** δ = 137.7, 132.7, 129.1, 129.0, 127.5, 122.8, 74.0, 58.8. Spectroscopic data was in agreement to those previously reported.[169]

Chemotion ELN sample number: HMA-4-315.

2,2,2-Trifluoro-1-(2-(methoxymethyl)phenyl)ethan-1-one (3.11)

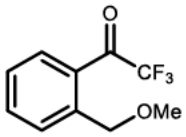

Following **GP-G** using 1-bromo-2-(methoxymethyl)benzene (1.50 g, 7.46 mmol,1.00 eq.), *t*-BuLi (1.00 g, 9.22 mL, 15.7 mmol, 1.70 M, 2.10 eq.) and ethyl trifluoroacetate (1.27 g, 1.06 mL, 8.95 mmol, 1.20 eq.) in Et_2O (100 mL). The desired product was obtained after FC (pentane) as a colourless oil (1.04 g, 4.76 mmol, 64%).

IR (neat): $\tilde{\nu}$ = 2934 (w), 2830 (w), 1737 (w), 1713 (m), 1603 (w), 1574 (w), 1452 (w), 1383 (w), 1324 (w), 1292 (w), 1186 (s), 1143 (s), 1103 (m), 937 (s), 737 (m), 671 (w), 658 (w), 607 (w). **^{1}H NMR (400 MHz, C_6D_6):** δ = 7.50 (dt, J = 7.8, 1.6 Hz, 1H), 7.37 (dd, J = 7.8, 1.3 Hz, 1H), 7.03 (td, J = 7.7, 1.3 Hz, 1H), 6.80 (td, J = 7.7, 1.2 Hz, 1H), 4.42 (s, 2H), 3.03 (s, 3H). **^{13}C NMR (101 MHz, C_6D_6):** δ = 183.5 (q, J = 34.8 Hz), 142.6, 133.4, 129.6 (q, J = 3.2 Hz), 129.3, 127.7, 127.2, 117.1 (q, J = 292.3 Hz), 72.4, 58.3. **^{19}F NMR (377 MHz, C_6D_6):** δ = -72.83 (d, J = 1.7 Hz). **HRMS (APCI)**: Calculated for $C_{10}H_8F_3O_2$ $[M-H]^-$: 217.0482, found 217.0464.

Chemotion ELN sample number: HMA-4-328.

2,2,2-Trifluoro-1-(4-methoxy-2-methylphenyl)ethan-1-one (3.12)

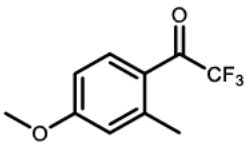

Following **GP-G** using 4-bromo-3-methylanisole (3.12 g, 2.00 mL, 15.5 mmol,1.00 eq.), *t*-BuLi (1.99 g, 16.3 mL, 31.1 mmol, 1.90 M, 2.00 eq.) and ethyl trifluoroacetate (2.43 g, 2.03 mL, 17.1 mmol, 1.10 eq.) in Et_2O (100 mL). The desired product was obtained after FC (pentane) and bulb-to-bulb distillation (140 °C, 1.10 mbar) as a colourless oil (2.93 g, 13.4 mmol, 86%).

^{1}H NMR (600 MHz, $CDCl_3$): δ =7.91 (dq, J = 9.7, 1.7 Hz, 1H), 6.84 – 6.82 (m, 2H), 3.89 (s, 3H), 2.61 (s, 3H). **^{13}C NMR (151 MHz, $CDCl_3$)**: δ = 180.2 (q, J = 33.2 Hz), 164.0, 146.7, 134.0 (q, J = 4.2 Hz), 121.7, 118.4, 117.0 (q, J = 292.9 Hz), 111.2, 55.7, 23.1. **^{19}F NMR (377 MHz, C_6D_6):** δ = -70.47 (d, J = 2.2 Hz, 3F). Spectroscopic data was in agreement to those previously reported.[170]

Chemotion ELN sample number: HMA-4-302 and HMA-4-184.

2,2,2-Trifluoro-1-(4-fluoro-2-methylphenyl)ethan-1-one (3.13)

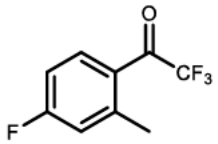

Following **GP-G** using 4-fluoro-1-iodo-2-methylbenzene (3.54 g, 1.98 mL, 15.0 mmol, 1.00 eq.), *t*-BuLi (1.92 g, 15.8 mL, 30.0 mmol, 1.90 M, 2.00 eq.) and ethyl trifluoroacetate (2.34 g, 1.96 mL, 16.5 mmol, 1.10 eq.) in Et_2O (60 mL). The desired product was obtained after FC (pentane) and bulb-to-bulb distillation (60 °C, 0.80 mbar) as a colourless oil (2.18 g, 10.6 mmol, 70%).

IR (neat): $\tilde{\nu}$ = 2926 (w), 1716 (m), 1608 (m), 1581 (s), 1500 (w), 1453 (w), 1329 (w), 1300 (w), 1244 (m), 1204 (s), 1181 (s), 1142 (s), 1108 (s), 973 (s), 910 (m), 871 (w), 825 (w), 773 (m), 742 (w), 699 (w), 632 (m), 591 (w), 536 (w), 455 (w), 430 (w), 412 (w). **^{1}H NMR (400 MHz, $CDCl_3$):** δ = 7.94 (ddq, J = 9.7, 5.7, 1.9 Hz, 1H), 7.15 – 6.94 (m, 2H), 2.61 (s, 3H). **^{13}C NMR (101 MHz, $CDCl_3$):** δ = 180.9 (q, J = 34.2 Hz), 165.7 (d, J = 258.5 Hz), 147.1 (d, J = 9.6 Hz), 134.2 – 133.2 (m), 125.6 (d, J = 3.0 Hz), 112.0 (d, J = 21.5 Hz), 116.6 (q, J = 292.7 Hz), 113.5 (d, J = 21.8 Hz), 22.44 (d, J = 1.5 Hz). **^{19}F NMR (282 MHz, C_6D_6):** δ = -71.37 (d, J = 1.9 Hz, 3F), -103.20 (td, J = 8.7, 5.7 Hz, 1F). **HRMS (ESI)**: Calculated for **$C_9H_5F_4O$** $[M-H]^-$: 205.0282, found: 205.0288.

Chemotion ELN sample number: HMA-4-262.

1-(4-Chloro-2-methylphenyl)-2,2,2-trifluoroethan-1-one (3.14)

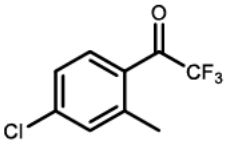

Following **GP-G** using 2-bromo-5-chlorotoluene (3.08 g, 2.00 mL, 15.0 mmol, 1.00 eq.), *t*-BuLi (1.92 g, 15.8 mL, 30.0 mmol, 1.90 M, 2.00 eq.) and ethyl trifluoroacetate (2.34 g, 1.96 mL, 16.5 mmol, 1.10 eq.) in Et_2O (100 mL). The desired product was obtained after FC (pentane) and bulb-to-bulb distillation (90 °C, 1.1 mbar) as a colourless oil (2.90 g, 13.0 mmol, 87%).

IR (neat): $\tilde{\nu}$ = 2983 (w), 2236 (w), 1725 (m), 1608 (w), 1558 (w), 1451 (w), 1386 (w), 1326 (w), 1281 (w), 1206 (m), 1186 (s), 1146 (s), 1038 (w), 958 (s), 894 (m), 838 (w), 775 (w), 742 (w), 713 (w), 631 (w), 587 (w), 558 (w), 525 (w), 450 (w). **^{1}H NMR (400 MHz, C_6D_6):** δ = 7.10 (dq, J = 8.2, 1.9 Hz, 1H), 6.63 (dd, J = 8.2, 1.7 Hz, 1H), 6.55 (d, J = 1.7 Hz, 1H), 1.89 (s, 3H). **^{13}C NMR (101 MHz, C_6D_6):** δ = 181.9 (q, J = 35.0 Hz), 142.2, 135.4, 132.3, 129.8 (q, J = 3.6 Hz), 129.2, 117.4, 117.2, 116.5 (q, J = 292.6 Hz), 20.7. **^{19}F NMR (377 MHz, C_6D_6):** δ = -71.64 (d, J = 2.0 Hz, 3F). **HRMS (ESI)**: Calculated for $C_9H_5ClF_3O$ $[M-H]^-$: 220.9986, found: 220.9986.

Chemotion ELN sample number: HMA-4-277.

1-(4-Chloro-2-ethylphenyl)-2,2,2-trifluoroethan-1-one (3.15)

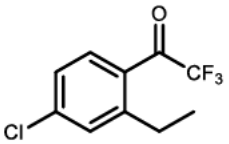

Following **GP-G** using 1-bromo-4-chloro-2-ethylbenzene (409 mg, 0.27 mL, 1.86 mmol, 1.00 eq.), *t*-BuLi (239 mg, 2.19 mL, 3.73 mmol, 1.70 M, 2.00 eq.) and ethyl trifluoroacetate (318 mg, 0.27 mL, 2.24 mmol, 1.20 eq.) in Et_2O (25 mL). The desired product was obtained after FC (pentane) and bulb-to-bulb distillation (110 °C, 1.1 mbar) as a colourless oil (299 mg, 1.26 mmol, 68%).

IR (neat): $\tilde{\nu}$ = 2977 (w), 2880 (w), 1718 (m), 1593 (m), 1559 (w), 1458 (w), 1396 (w), 1323 (w), 1289 (w), 1237 (w), 1195 (s), 1182 (s), 1145 (s), 1106 (m), 1061

(w), 975 (w), 935 (s), 885 (w), 843 (w), 828 (w), 776 (w), 740 (w), 688 (w), 619 (w), 531 (w), 499 (w), 469 (w). **^{1}H NMR (400 MHz, C_6D_6):** δ = 7.27 (dq, J = 8.5, 1.9 Hz, 1H), 6.87 (d, J = 2.1 Hz, 1H), 6.70 (dd, J = 8.5, 2.2 Hz, 1H), 2.47 (q, J = 7.5 Hz, 2H), 0.88 (t, J = 7.5 Hz, 3H). **^{13}C NMR (101 MHz, C_6D_6):** δ = 181.7 (q, J = 34.3 Hz), 150.2, 140.5, 131.5 (q, J = 3.8 Hz), 131.3, 127.6, 126.3, 116.9 (q, J = 293.1 Hz), 27.3, 15.1. **^{19}F NMR (377 MHz, C_6D_6):** δ = -71.92 (d, J = 2.0 Hz, 3F). **HRMS (ESI)**: Calculated for $C_{10}H_7ClF_3O$ [M-H]$^-$: 235.0143, found: 235.0149.

Chemotion ELN sample number: HMA-4-345.

3-Methyl-4-(2,2,2-trifluoroacetyl)benzonitrile (3.16)

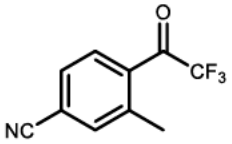

Following **GP-G** using 4-bromo-3-methylbenzonitrile (1.01 g, 5.14 mmol,1.00 eq.), *t*-BuLi (658 mg, 5.41 mL, 10.3 mmol, 1.90 M, 2.00 eq.) and ethyl trifluoroacetate (803 mg, 0.67 mL, 5.65 mmol, 1.20 eq.) in a mixture of Et_2O (20 mL) and THF (5 mL). The desired product was obtained after FC (pentane) and bulb-to-bulb distillation (140 °C, 1.1 mbar) as a colourless solid (576 mg, 2.70 mmol, 53%).

M.P.: 40 – 45 °C. **IR (neat)**: $\tilde{\nu}$ = 2236 (w), 1725 (s), 1607 (w), 1558 (w), 1450 (w), 1386 (w), 1326 (w), 1281 (w), 1206 (m), 1185 (s), 1144 (s), 1038 (w), 958 (s), 894 (s), 838 (w), 775 (m), 742 (m), 713 (w), 630 (w), 588 (w), 559 (w), 524 (w), 450 (w). **^{1}H NMR (400 MHz, C_6D_6):** δ = 7.08 (dq, J = 8.3, 1.8 Hz, 1H), 6.61 (dd, J = 8.2, 1.6 Hz, 1H), 6.54 (t, J = 1.1 Hz, 1H), 1.88 (s, 3H). **^{13}C NMR (101 MHz, C_6D_6):** δ = 181.9 (q, J = 35.1 Hz), 142.2, 135.4, 132.3, 129.7 (q, J = 3.6 Hz), 129.2, 117.4, 117.2, 116.5 (q, J = 292.7 Hz), 20.7. **^{19}F NMR (282 MHz, C_6D_6):** δ =-72.57 (d, J = 1.8 Hz, 3F). **HRMS (ESI)**: Calculated for $C_{10}H_5F_3NO$ [M-H]$^-$: 212.0329, found 212.0336.

Chemotion ELN sample number: HMA-4-309.

2-Fluoro-1-(o-tolyl)ethan-1-one (3.18)

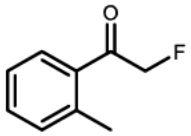

Following **GP-G** with minor alterations using 2-bromotoluene (2.05 g, 1.44 mL, 12.0 mmol,1.00 eq.), *t*-BuLi (1.54 g, 14.1 mL, 24.0 mmol, 1.70 M, 2.00 eq.) and 2-fluoroacetonitrile (1.06 g, 1.00 mL, 18.0 mmol, 1.50 eq., used instead of ethyl trifluoroacetate) in Et_2O (50 mL). The desired product was obtained after FC (pentane : Et_2O, 60:40) and bulb-to-bulb distillation (130 °C, 1.1 mbar) as a colourless oil (456 mg, 3.00 mmol, 25%).

IR (neat): $\tilde{\nu}$ = 2931 (w), 1702 (s), 1601 (w), 1572 (w), 1489 (w), 1456 (w), 1439 (w), 1382 (w), 1296 (w), 1269 (w), 1229 (m), 1167 (w), 1081 (s), 1050 (w), 1036 (w), 963 (s), 819 (w), 757 (s), 719 (m), 658 (m), 576 (w), 459 (w). **^{1}H NMR (400 MHz, C_6D_6):** δ = 7.01 – 6.91 (m, 2H), 6.88 – 6.78 (m, 2H), 4.65 (dd, J = 47.4, 1.1 Hz, 2H), 2.39 (s, 3H). **^{13}C {^{1}H, ^{19}F} NMR (101 MHz, C_6D_6):** δ = 196.4, 139.3, 134.3, 132.3, 132.0, 128.7, 125.6, 83.9, 21.1. **^{19}F NMR (377 MHz, C_6D_6):** δ = -225.74 (t, J = 47.4 Hz, 1F). **HRMS (ESI)**: Calculated for $C_9H_{10}FO$ $[M+H]^+$: 153.0710, found: 153.0706. Spectroscopic data was in agreement to those previously reported.[114]

Chemotion ELN sample number: HMA-4-411.

2,2-Difluoro-1-(o-tolyl)ethan-1-one (3.21)

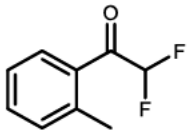

2,2-Difluoro-1-(o-tolyl)ethan-1-one was synthesized following a literature known procedure.[115a]

Mg-turnings (101 mg, 4.15 mmol, 2.15 eq.) were added to an oven-dried 25 mL Schlenk flask and dry THF (10.0 mL) was added. The mixture was cooled to 0 °C and TMS-Cl (902 mg, 650 µL, 8.30 mmol, 4.29 eq.) was added, followed by 2,2,2-trifluoro-1-(o-tolyl)ethan-1-one (364 mg, 1.93 mmol, 1.00 eq.). The mixture was stirred at 0 °C for 2 h and excess TMS-Cl and THF were removed *in vacuo via* a cooling trap. To the residue, hexane was added (20 mL) and the solids were removed *via* filtration. The solvent was removed under reduced pressure,

HCl (5 M, 10 mL) was added and the mixture was stirred over-night. The mixture was extracted with Et_2O (3 x 20 mL) and the combined organic phases were washed with brine (3 x 20 mL), water (3 x 20 mL) and were dried over Na_2SO_4. The solvent was removed under reduced pressure and the crude product was purified *via* FC (pentane : Et_2O, 90:10) and bulb-to-bulb distillation (100 °C, 1.1 mbar) as a colourless oil (401 mg, 2.36 mmol, 40%).

IR (neat): $\tilde{\nu}$ = 2973 (w), 2360 (w), 2172 (w), 2148 (w), 2108 (w), 2060 (w), 2020 (w), 1982 (w), 1707 (s), 1602 (w), 1572 (w), 1491 (w), 1458 (w), 1384 (w), 1346 (w), 1296 (w), 1268 (w), 1236 (w), 1148 (m), 1123 (s), 1065 (s), 967 (w), 873 (w), 860 (w), 789 (w), 760 (w), 725 (m), 651 (w), 584 (w), 554 (w), 543 (w), 486 (w), 458 (w), 451 (w), 441 (w), 431 (w), 410 (w). **^{1}H NMR (400 MHz, C_6D_6):** δ = 7.50 (d, J = 7.7 Hz, 1H), 7.00 – 6.91 (m, 1H), 6.80 (d, J = 7.6 Hz, 2H), 5.65 (t, J = 53.7 Hz, 1H), 2.36 (s, 3H). **^{13}C {^{1}H, ^{19}F} NMR (101 MHz, C_6D_6):** δ = 189.5, 141.4, 133.1, 132.6, 131.5, 130.3, 125.8, 111.0, 21.6. **^{19}F NMR (282 MHz, C_6D_6):** δ = -122.31 (dd, J = 53.7, 1.9 Hz, 2F). **HRMS (APCI)**: Calculated for $C_9H_7F_2O$ $[M-H]^-$: 169.0470, found: 169.0496. Spectroscopic data was in agreement to those previously reported.[171]

Chemotion ELN sample number: HMA-4-292 and HMA-4-458.

4.3.2 Development of reaction conditions

4.3.2.1 Solvent screening

Samples of **3.8** (9.41 mg, 50.0 µmol) were dissolved in a respective solvent (20 mM) and degassed (3 × freeze-pump-thaw). The tubes were irradiated using a *Luzchem* LZC-ORG photoreactor equipped with 10 × 8 Watt LZC-UVA mercury lamps (355 nm) lamps (*cf.* chapter 4.1,Figure 26) for 4 h at 30 °C. The solvent was removed under reduced pressure, $PhCF_3$ was added as an internal standard and the samples subjected to NMR analysis.

Table 20: Solvent optimisation, reactions were performed on 0.05 mmol scale in degassed solvents (20 mM) under inert gas atmosphere. Solvent was removed under reduced pressure and residue dissolved in $CDCl_3$. Yields determined using ^1H NMR with mesitylene as internal standard.

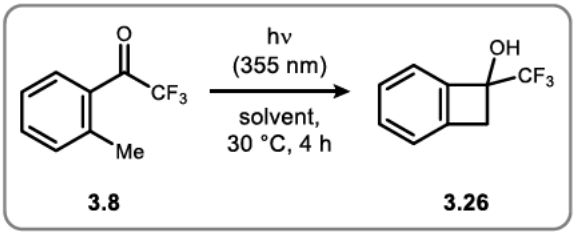

3.8 **3.26**

Entry	Solvent	Yield
1	MeOH	5%[a]
2	MeCN	32%[a]
3	EtOAc	70%[a]
4	CyH	41%[a]
5	hexane	34%[a]
6	PhH	45%

[a]Several signals detected in ^{19}F NMR.

4.3.2.2 Robustness of the reaction

Initial rate

A sensitivity screening was conducted to access the relative rate of the reaction after 30 minutes according to a literature known protocol [117]. Samples of **3.8** were irradiated with a 40 W 370 nm Gen 2 KSPR160L Kessil LED from 2 cm distance in a water bath at 30 °C for 30 min (*cf.* chapter 4.1, Figure 27).

A stock solution was prepared by dissolving **3.8** (26.34 mg, 140 µmol, 1.00 eq.) in C_6D_6 (7 mL, 20 mM) and the solution was degassed (3 × freeze-pump-thaw). $PhCF_3$ (17.5 µL, 144 µM, 1.03 eq.) was added as an internal reference and the concentration verified *via* ^{19}F NMR. Samples were prepared in a Glove Box unless noted otherwise. A second solution was prepared in a similar way for the big scale reaction (entry 13, Table 21) with **3.8** (37.63 mg, 0.2 mmol, 1.00 eq.) in benzene (10 mL, 20 mM) and the mixture was degassed (3 × freeze-pump-thaw). $PhCF_3$

(25 µL, 0.205 mmol, 1.03 eq.) was added together with a stir bar. Samples with lower intensity (entries 1 & 2, Table 21) were irradiated using the same setup but were placed distant to the lamp. A control sample was irradiated at the same time (entry 10, Table 21). For high and medium concentration (entries 11 & 12, Table 21), oven dried NMR Tubes with a septum cap were charged with degassed C_6D_6 (0.5 mL, 3 × freeze-pump-thaw) in a Glove Box. **3.8** (high conc: 18.8 mg, 100 µmol, low conc.: 3.7 mg, 20.0 µmol) was added under inertgas atmosphere *via* a microsyringe through the septum cap and $PhCF_3$ was added as an internal standard. The samples were subjected to ^{19}F NMR to verify the concentration before the irradiation.

Table 21: Sensitivity screening after 30 min, reactions run at 10 µmol scale in 0.5 mL C_6D_6 [20 mM] at 30 °C with 1 cm distance to 370 nm Kessil lamp (standard conditions), NMR yield based on ^{19}F NMR using $PhCF_3$ as internal standard.

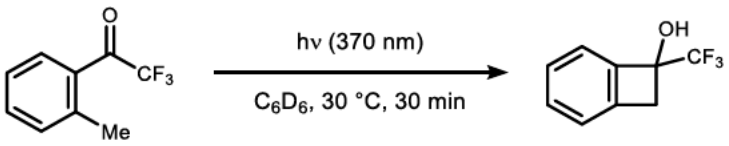

3.8 **3.26**

Entry	Change to conditions	Procedure	Yield	Deviation
1	low *I*	*d* = 10 cm	12%	–69%
2	medium *I*	*d* = 5 cm	30%	–23%
3	medium O_2	no degassing	33%[a]	–15%
4	high O_2	purge with O_2	30%[a]	–23%
5	control 1	-	39%	0%
6	low *T*	15 °C	33%	–15%
7	high *T*	45 °C	57%	46%
8	high H_2O	+5 µL H_2O	45%	15%
9	control 2	-	41%	5%
10	low conc.	10 mM	47%	21%
11	medium conc.	40 mM	40%	1%
12	high conc.	200 mM	32%	–18%
13	big scale	2 mM scale	39%	0%

[a] Formation of another product visible *via* ^{19}F NMR.

Absolute yields

The sensitivity screening was repeated to access the overall performance of the reaction after 8 h using the identical reaction setup (*vide supra*). Only the execution of this experiment was conducted by [redacted].

A stock solution was prepared by dissolving **3.8** (27.14 mg, 144 µmol, 1.00 eq.) in C_6D_6 (7 mL, 20 mM) and the solution was degassed (3 × freeze-pump-thaw). $PhCF_3$ (17.0 µL, 139 µM, 0.96 eq.) was added as an internal reference and the concentration verified *via* ^{19}F NMR. Samples were again prepared in a Glove Box. The solution for the big scale was prepared with **3.8** (37.51 mg, 0.2 mmol, 1.00 eq.) in benzene (10 mL, 20 mM) and the mixture was degassed (3 × freeze-pump-thaw). $PhCF_3$ (5 µL, 41 µmol, 0.21 eq.) was added with a stir bar. For high and medium concentration (entries 10 & 11, Table 22), oven dried NMR Tubes with a septum cap were charged with degassed C_6D_6 (0.5 mL, 3 × freeze-pump-thaw) in a Glove Box. **3.8** was added under inertgas atmosphere *via* a microsyringe through the septum cap and $PhCF_3$ was added as an internal standard. The samples were subjected to ^{19}F NMR to verify the concentration before the irradiation. The results are summarized in Table 22 and deviations from the standard reaction conditions are listed.

Table 22: Sensitivity screening after 8 h, reactions run at 10 µmol scale in 0.5 mL C_6D_6 [20 mM] at 30 °C with 1 cm distance to 370 nm Kessil lamp (standard conditions) performed by [redacted], NMR yield based on ^{19}F NMR using $PhCF_3$ as internal standard.

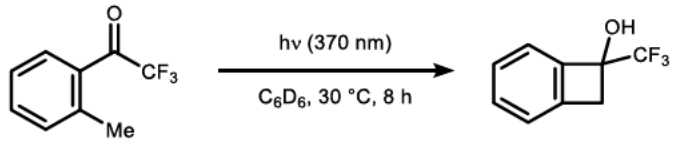

3.8 **3.26**

Entry	Change to conditions	Procedure	Yield	Deviation
1	low *I*	*d* = 10 cm	98%	–1%
2	medium *I*	*d* = 5 cm	99%	0%
3	control 1	-	>99%	1%
4	medium O_2	no degassing	79%[a]	–20%
5	high O_2	purge with O_2	76%[a]	–22%
6	low *T*	20 °C	99%	0%
7	high *T*	45 °C	>99%	1%
8	high H_2O	+5 µL H_2O	>99%	1%
9	low conc.	10 mM	99%	0%
10	medium conc.	40 mM	95%	–4%
11	high conc.	200 mM	96%	–3%
12	big scale	2 mM scale	92%	-7%

[a] Formation of another product visible *via* ^{19}F NMR.

4.3.2.3 Investigation of key parameters

4.3.2.3.1 Oxygen content

The oxygen sensitivity was investigated in detail. Samples of **3.8** were dissolved in several solvents and either degassed or oxygen saturated. The solution was irradiated using 355 nm lamps and analysed *via* ^{19}F NMR using $PhCF_3$ as internal standard. An exemplary spectrum is shown in Figure 29.

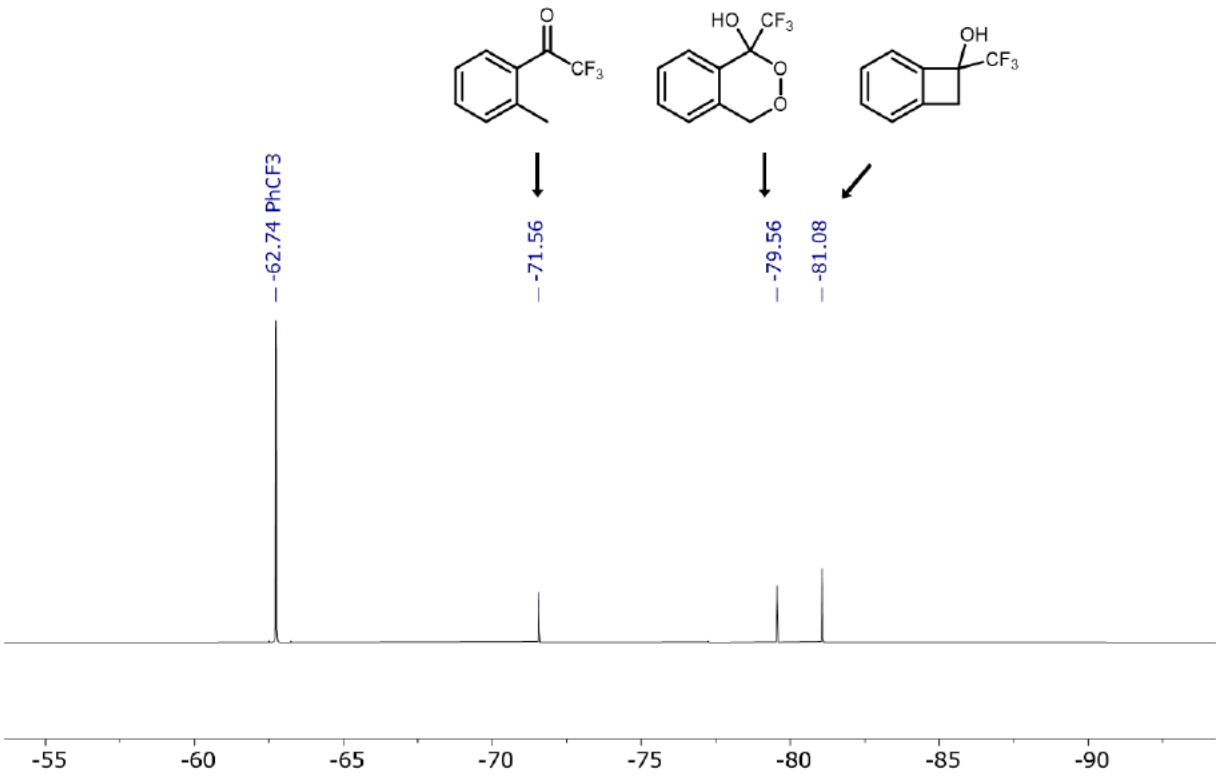

Figure 29: ^{19}F NMR after irradiation of 3.8 (20 mM) in aerated C_6D_6 after 3 h with 355 nm.

1-(Trifluoromethyl)-1,4-dihydrobenzo[d][1,2]dioxin-1-ol (3.27)

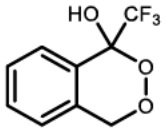

1-(Trifluoromethyl)-1,4-dihydrobenzo[d][1,2]dioxin-1-ol was prepared in hexane to achieve a better solubility of oxygen. [118] **3.8** (980 mg, 5.16 mmol, 1.00 eq.) was dissolved in hexane (250 mL) and a stream of O_2 was purged through the solution for 30 min. The mixture was irradiated at 355 nm for 36 h. The solvent was removed under reduced pressure and the desired product was purified *via* FC (pentane : Et2O, 80:20 to 60:40) to obtain **3.27** as a colourless solid (494 mg, 2.24 mmol, 44%) and **3.8** (306 mg, 1.63 mmol, 32%).

M.P.: 45 – 56 °C**. IR (neat)**: $\tilde{\nu}$ = 3462 (w), 2922 (w), 1458 (w), 1356 (w), 1288 (w), 1254 (w), 1184 (s), 1134 (w), 1089 (m), 1053 (w), 1012 (w), 974 (w), 928 (w), 845 (w), 765 (w), 741 (w), 687 (w), 649 (w), 456 (w). **^{1}H NMR (400 MHz, $CDCl_3$):** δ = 7.71 (dt, J = 7.7, 1.5 Hz, 1H), 7.50 – 7.37 (m, 2H), 7.19 (dq, J = 6.9, 0.8 Hz, 1H), 5.36 (d, J = 15.4 Hz, 1H), 5.08 (d, J = 15.4 Hz, 1H), 3.92 (s, 1H).

^{13}C NMR (101 MHz, $CDCl_3$): δ = 134.1, 130.2, 128.3, 127.7, 127.1 (q, J = 2.3 Hz), 124.7, 122.0 (q, J = 288.1 Hz), 97.2 (q, J = 31.6 Hz), 72.2. **^{19}F NMR (282 MHz, $CDCl_3$):** δ = -79.42. (s, 3F). **^{19}F NMR (282 MHz, C_6D_6):** δ = -79.56 (d, J = 1.4 Hz, 3F). **HRMS (ESI)**: Calculated for **$C_9H_6F_3O_3$** $[M-H]^-$: 219.0275, found: 219.0270.

Attempts to crystallize **3.27** were unsuccessful, instead **3.28** was formed as a sample suitable for X-ray analysis.

Chemotion ELN sample number: HMA-4-170.

1-(Trifluoromethyl)-1,3-dihydroisobenzofuran-1,3-diol (3.28)

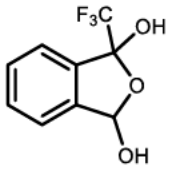

3.28 was prepared by dissolving **3.27** (10 mg) in benzene (1 mL) and letting the solution concentrate for 7 days at room temperature. Colourless crystals were formed, that were washed with C_6D_6 and $CDCl_3$ and dissolved in DMSO-d_6. It was obtained as a mixture of 2 diastereomers (diasteromeric ratio, dr = 2:1) and a sample for X-Ray analysis was obtained. The configuration was unambiguously proven by X-Ray analyses.

M.P.: <35 °C**. IR (neat)**: $\tilde{\nu}$ = 3462 (w), 2178 (w), 1993 (w), 1771 (w), 1457 (w), 1255 (w), 1180 (s), 1144 (m), 1090 (m), 1052 (w), 1029 (w), 975 (m), 929 (w), 845 (w), 765 (m), 741 (m), 701 (w), 687 (w), 648 (w), 590 (w), 548 (w), 525 (w), 493 (w), 453 (w), 418 (w). **HRMS (ESI)**: Calculated for **$C_9H_6F_3O_3$** $[M-H]^-$: 219.0275, found: 219.0273.

Major-[9d]:

^{1}H NMR (600 MHz, DMSO-d_6): δ = 8.29 (s, 1H), 7.60 – 7.43 (m, 5H), 6.33 (d, J = 6.9 Hz, 1H). **^{13}C NMR (151 MHz, DMSO-d_6):** δ = 141.5, 135.7, 130.8, 129.7, 123.2, 123.2, 123.2 (q, J = 286.3 Hz), 101.9 (q, J = 32.9 Hz), 99.8. **^{19}F NMR (282 MHz, DMSO-d_6):** δ = -82.40

Minor-[9d]:

^{1}H NMR (600 MHz, DMSO-d$_6$): δ = 7.96 (s, 1H,), 7.60 – 7.43 (m, 4H), 7.40 – 7.35 (m, 1H), 6.51 (d, J = 6.9 Hz, 1H). **^{13}C NMR (151 MHz, DMSO-d$_6$):** δ = 141.3, 136.3, 130.7, 129.7, 124.7 (q, J = 286.6 Hz), 123.3, 123.1, 102.1 (q, J = 33.3 Hz), 100.4. **^{19}F NMR (282 MHz, DMSO-d$_6$):** δ = -81.57

Chemotion ELN sample number: HMA-4-216.

6-Chloro-1-(trifluoromethyl)-1,4-dihydrobenzo[d][1,2]dioxin-1-ol (3.30)

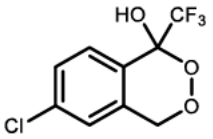

3.30 was prepared by dissolving **3.14** (120 mg, 539 µmol) in hexane (25 mL) analogous to 8d. The solution was oxygenated for 30 min and was irradiated at 355 nm for 16 h. The solvent was removed under reduced pressure and the desired product was purified *via* FC (pentane : Et_2O, 80:20 to 25:75) and was obtained as an oily mixture of **3.30** and **3.29** (82 mg, ratio 85:15), out of which **3.30** crystallised at −20 °C as a colourless solid. A sample suitable for X-Ray Analysis was obtained and verified by NMR spectroscopy.

IR (neat): $\tilde{\nu}$ = 3447 (w), 1604 (w), 1489 (w), 1416 (w), 1340 (w), 1281 (w), 1257 (w), 1186 (s), 1147 (m), 1090 (m), 1031 (w), 972 (w), 933 (w), 868 (w), 825 (w), 751 (w), 740 (w), 671 (w), 612 (w), 512 (w). **^{1}H NMR (600 MHz, C$_6$D$_6$):** δ = 7.22 – 7.18 (m, 2H), 6.81 (dd, J = 8.4, 2.2 Hz, 1H), 6.27 (d, J = 2.1 Hz, 1H), 4.46 (d, J = 15.5 Hz, 1H), 4.16 (d, J = 15.5 Hz, 1H), 3.05 (s, 1H). **^{13}C NMR (151 MHz, C$_6$D$_6$):** δ = 136.3, 135.8, 128.7, 128.4, 126.7, 124.8, 122.6 (q, J = 288.7 Hz), 97.0 (q, J = 31.5 Hz), 71.1. **^{19}F NMR (282 MHz, C$_6$D$_6$):** δ = -79.63 (d, J = 1.3 Hz). **HRMS (ESI)**: Calculated for $C_9H_5ClF_3O_3$ [M-H]$^-$: 252.9885, found 252.9894.

Chemotion ELN sample number: HMA-4-316.

4.3.2.3.2 Lamp choice

As a high lamp intensity was found to be beneficial for the overall performance, different sources were compared (Table 7). Reactions performed following **GP-H**, using **3.8** (1.88 mg, 10.0 µmol) for 1 h with different lamps at 28 °C.

Table 23: Evaluation of different irradiation sources, reactions were performed on 0.01 mmol scale in degassed C_6D_6 (20 mM) under inert gas atmosphere at 28 °C, yield determined *via* ^{19}F NMR with $PhCF_3$ as internal standard. Lamps used: *Luzchem* photoreactor (355 nm, 10 × 8 W mercury fluorescence lamps; 420 nm, 10 × 8 W LED), 45 W Kessil LED lamps (370 nm, 390 nm).

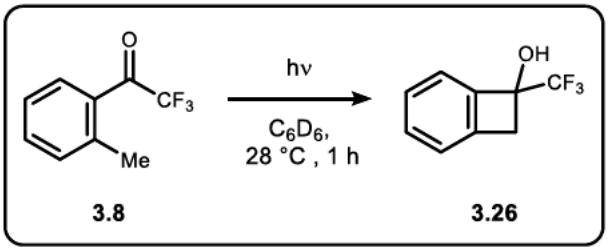

Entry	Wavelength	Yield
1	355 nm	13%
2	370 nm	86%
3	390 nm	11%
4	420 nm	0%

4.3.2.3.3 Sunlight

A reaction set-up consisting of an NMR tube and a light reflector was constructed and samples of **3.8** (1.88 mg, 10.0 µmol) in degassed C_6D_6 were subjected to sunlight on different days with varying weather conditions (Figure 7) following **GP-H** for 4 h at 28 °C.

Figure 30: Set-up for solar irradiation. An NMR tube is held by a clamp and a reflector made from half-circular plastic tube and a silver-coated foil is used for focussing solar light.

Table 24: Reaction of 3.8 under solar irradiation, reactions were performed on 0.01 mmol scale in degassed C_6D_6 (20 mM) under inert gas atmosphere at 28 °C for 4 h, yield determined *via* ^{19}F NMR with $PhCF_3$ as internal standard.

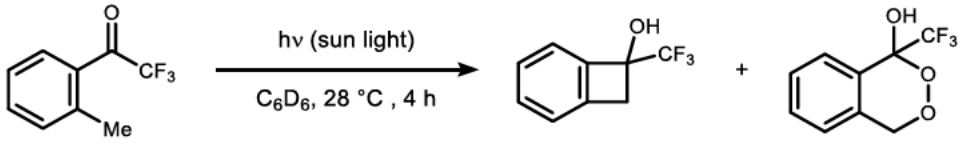

3.8 **3.26** **3.27**

Entry	Date	Weather	Yield **3.26**	Yield **3.27**
1	22.08.2023	cloudy	81%	0%
2	06.09.2023	clear sky	95%	0%
3	07.09.2023	clear sky	84%	6%

4.3.2.3.4 Reaction scale

Following **GP-I**, using **3.8** in benzene. The results are depicted in Table 9. Samples were purified using FC (pentane : Et_2O, 100:0 to 70:30) and bulb-to-bulb distillation (1.1 mbar, rt to 110 °C) when stated (entry 3).

Table 25: Large scale reactions, performed in degassed PhH in the *Luzchem* photoreactor (355 nm) or with a Kessil lamp (370 nm) at rt, NMR yields determined *via* ^{19}F NMR using $PhCF_3$ as internal standard.

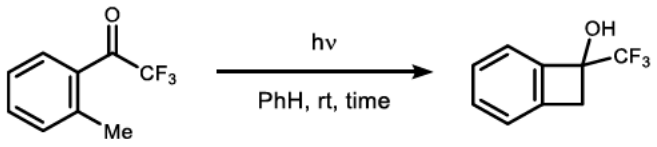

3.8 **3.26**

Entry	Scale	Concentration	Wavelength	Time	NMR yield	Yield
1	4.73 mmol	0.47 mol/l	355 nm	90 h	-	98%
2	7.86 mmol	0.44 mol/l	370 nm	10 h	>99%	90%
3	10.7 mmol	0.90 mol/l	370 nm	10 h	>99%	79%[a]

[a] Isolated yield after column chromatography and distillation.

7-(Trifluoromethyl)bicyclo[4.2.0]octa-1,3,5-trien-7-ol (3.26)

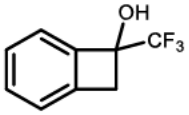

Following **GP-I**, using **3.8** (889 mg, 4.73 mmol) in benzene (10 mL, 473 mM) for 90 h. The product was obtained after automated FC (pentane : Et_2O, 70:30) as a colourless solid (872 mg, 4.63 mmol, 98%).

Following **GP-I**, using **3.8** (1.59 g, 7.86 mmol) in benzene (18 mL, 436 mM) for 10 h at 22 °C. The product was obtained after FC (pentane : Et_2O, 75:25) and bulb-to-bulb distillation (110 °C, 0.8 mbar) as a colourless solid (1.33 g, 7.10 mmol, 90%).

Following **GP-I**, using **3.8** (2.16 g, 10.7 mmol) in benzene (12 mL, 889 mM) for 10 h at 22 °C. The product was obtained after FC pentane : Et_2O, 75:25) and bulb-to-bulb distillation (110 °C, 0.8 mbar) as a colourless solid (1.59 g, 8.43 mmol, 79%).

M.P.: 39 – 44 °C. **IR (neat)**: $\tilde{\nu}$ = 3349 (w), 2942 (w), 1595 (w), 1461 (w), 1428 (w), 1311 (w), 1232 (w), 1153 (s), 1128 (s), 1095 (m), 1069 (m), 1018 (m), 955 (w), 863 (w), 757 (m), 743 (w), 715 (m), 662 (m), 629 (w), 597 (w), 556 (w), 509

(w), 460 (w). **^{1}H NMR (400 MHz, C_6D_6):** δ = 7.02 (td, J = 7.4, 1.3 Hz, 1H), 6.99 – 6.90 (m, 2H), 6.82 – 6.73 (m, 1H), 3.40 (d, J = 14.4, 1H), 2.75 (d, J = 14.4, 1H), 2.23 (s, 1H). **^{13}C NMR (101 MHz, C_6D_6):** δ = 142.2, 142.0 (q, J = 1.9 Hz), 131.1, 128.2, 125.5(q, J = 281.7 Hz), 123.7, 122.2, 78.3 (q, J = 32.8 Hz), 41.8 (q, J = 2.0 Hz). **^{19}F NMR (282 MHz, C_6D_6):** δ = –81.1 (s, 3F). **HRMS (ESI)**: Calculated for $C_9H_6F_3O$ [M-H]$^-$: 187.0376, found: 187.0373.

4.3.2.3.5 Temperature

Following **GP-H**, using **3.8** (1.88 mg, 10.0 µmol) in degassed C_6D_6 (0.5 mL) with 370 nm for 30 min. The setup is depicted in Figure 27 B (*cf.* chapter 4.1).

Table 26: Investigation of the temperature dependency, reactions performed on 0.01 mmol scale in degassed C_6D_6 [20 mM] with 370 nm for 30 min, yield determined *via* ^{19}F NMR with $PhCF_3$ as internal standard.

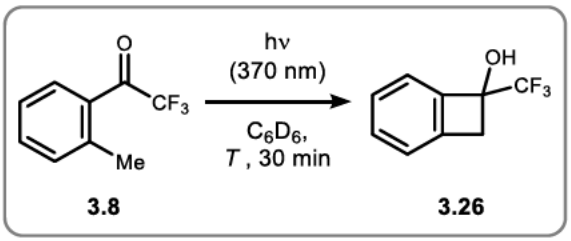

Entry	Temperature	Yield
1	20 °C	24%
2	25 °C	35%
3	35 °C	47%
4	45 °C	60%
5	54 °C	69%

4.3.3 Mechanistic studies

4.3.3.1 Kinetic studies

Following **GP-H,** using **3.8** (18.8 mg, 100 µmol) in degassed C_6D_6 (0.5 mL; 200 mM) at 370 nm for selected time intervals at 22 °C. Two additional samples were prepared by dilution of the initial stock solution to 20 mM and 2 mM concentration, which was verified against an internal standard ($PhCF_3$). The irradiation time was limited with a timer, that cut the power of the lamp after the selected interval. The progress of the reaction was monitored by ^{19}F NMR (Figure 31). The data is summarized in Table 27 and the concentration [**3.26**] versus

time in seconds is visualized in Figure 32. The obtained reaction rates are listed in Table 28.

Table 27: Concentration dependent irradiation of 3.8 on 0.01 mmol scale in degassed C_6D_6 (0.5 mL, 20 mM) with 370 nm at 22 °C, yield determined *via* ^{19}F NMR with $PhCF_3$ as internal standard.

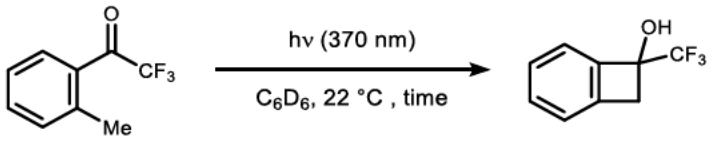

3.8 **3.26**

Entry	time	Yield (2 mM)	Yield (20 mM)	Yield (200 mM)
1	0s	0%	0%	0%
2	300s	17%	14%	13%
3	900s	40%	38%	36%
4	1800s	65%	64%	60%
5	2700s	78%	81%	75%
6	3600s	85%	89%	85%
7	5400s	96%	97%	94%
8	7200s	>99%	>99%	98%

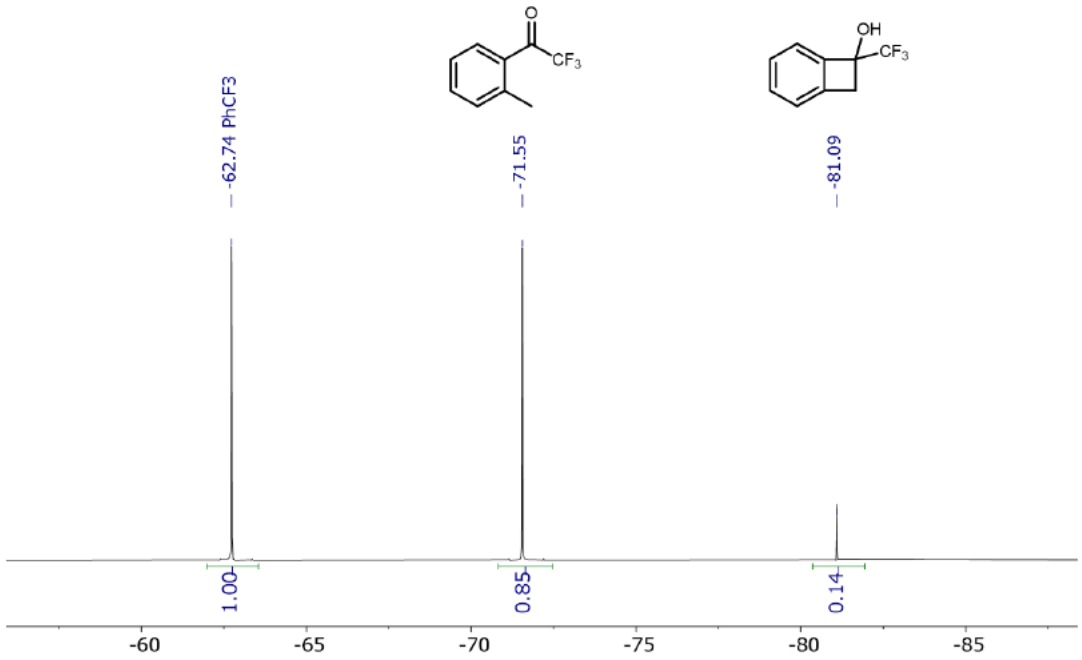

Figure 31: Exemplary ^{19}F NMR of the conversion of 3.8 to 3.26 in degassed C_6D_6 (20 mM) after 5 min with 370 nm.

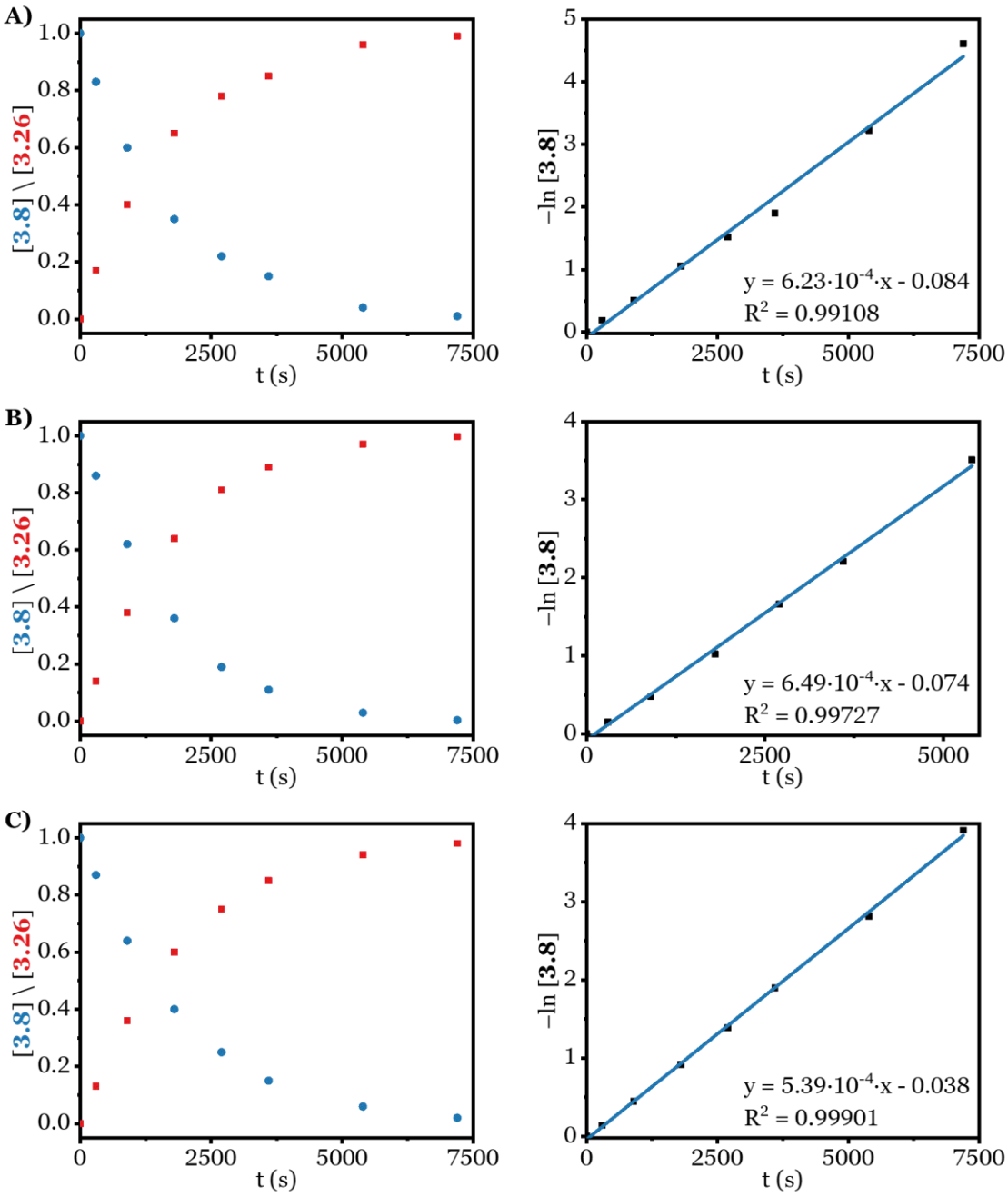

Figure 32: Plots of the concentration dependent transformation of acetophenone 3.8 towards product 3.26 under irradiation with 370 nm. Starting concentration of acetophenone 3.8 A: 2 mM, B: 20 mM, C: 200 mM.

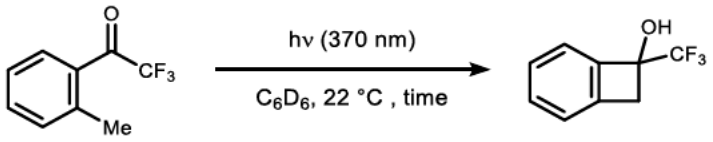

3.8 **3.26**

Table 28: Rate constants for different concentrations, corresponding to Figure 32: Plots of the concentration dependent transformation of acetophenone 3.8 towards product 3.26 under irradiation with 370 nm. Starting concentration of acetophenone 3.8 A: 2 mM, B: 20 mM, C: 200 mM..

Concentrations	2 mM	20 mM	200 mM
Rate constants	$k = 6.24 \times 10^{-4}\ s^{-1}$	$k = 6.49 \times 10^{-4}\ s^{-1}$	$k = 5.39 \times 10^{-4}\ s^{-1}$

4.3.3.2 Mechanistic picture

The effect of CF_3 group was assessed. Following **GP-H** using acetophenones (0.01 mmol) in degassed C_6D_6 (0.5 mL, 20 mM) with 355 nm for 3 h at 20 °C. The reactions were monitored *via* ^1H NMR against mesitylene as internal standard.

Table 29: Effect of the displacement of fluorine with hydrogen, reactions performed on 0.01 mmol scale in degassed C_6D_6 [20 mM] with 355 nm for 3 h at 20 °C, yield determined *via* ^1H NMR with mesitylene as internal standard.

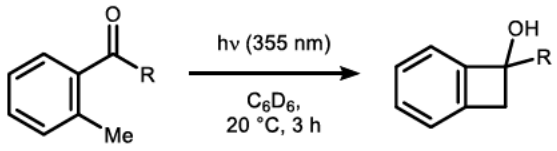

Entry	Product	Conversion	Yield
1	R = CF_3 (**3.26**)	66%	66%
2	R = CHF_2 (**3.36**)	55%	48%
3	R = CH_2F (**3.37**)	8%	1%[a]
4	R = CH_3 (**1.10**)	4%	1%

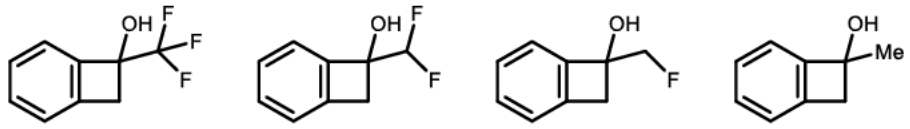

3.26 **3.36** **3.37** **1.10**

[a]Formation of a second species detected *via* NMR.

During the irradiation of **3.18**, the formation of enol **3.38** was visible, which decayed back to **3.18** over time as evident by ^1H and ^{19}F NMR (Figure 34and Figure 35). Assignment of **3.38** is based on a comparison of the NMR shifts to literature data.[115a,172] Furthermore, **3.38** is selectively formed and only present

under/directly after irradiation, which can be explained by a 1,5-H-shift of photoenol ***E*-3.39** (see Figure 33).

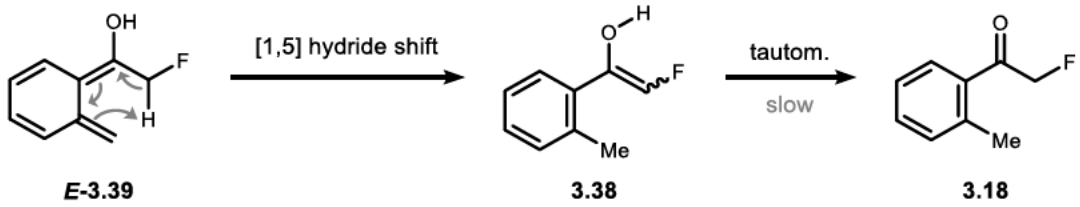

Figure 33: Pathway for the postulated enol formation from the *E*-photoenol.

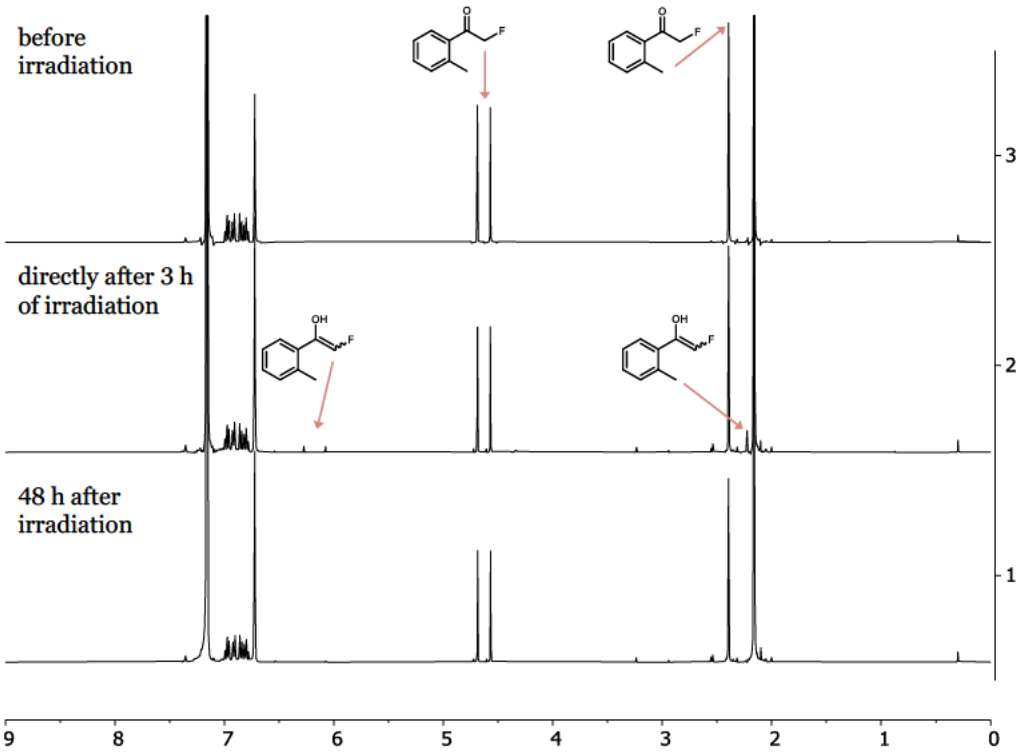

Figure 34: Overlay of ^{1}H NMR Spectra recorded in C_6D_6 [0.2 M] for the reaction of 1b, before (top), after irradiating for 3 h (middle) and 48 h later (bottom).

.

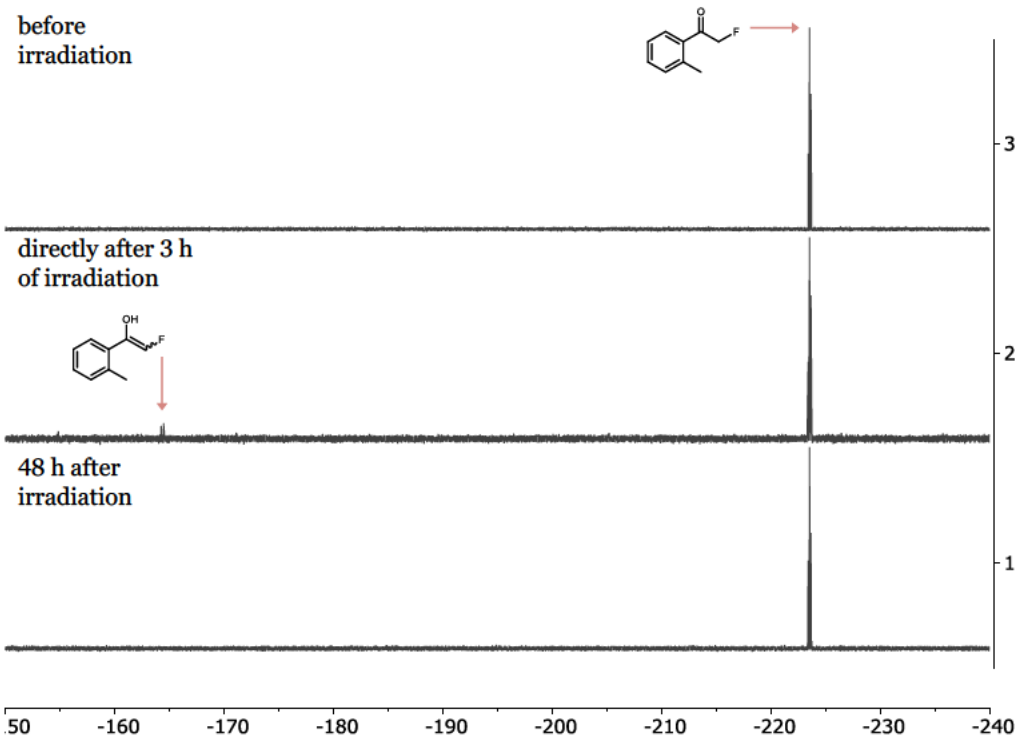

Figure 35: Overlay of ^{19}F NMR Spectra recorded in C_6D_6 [0.2 M] for the reaction of 1b, before (top), after irradiating for 3 h (middle) and 48 h later (bottom).

As **Enol-1b** was only formed in small amounts, an irradiation using a Kessil lamp (370 nm) was performed for 1 h in degassed C_6D_6 (*cf.* chapter 4.1, Figure 27). Here, the formation of **Enol-1b** and the cyclisation product **3b** are observed at the same time. This result supports the competing character of the [1,5] H shift *vs*. electrocyclization as postulated in left side of Fig. 2B. In addition, it highlights a slow enol-keto tautomerization for **1b**, which slows down the formation of ***E*-2b** by lowering the concentration of **1b** in solution.

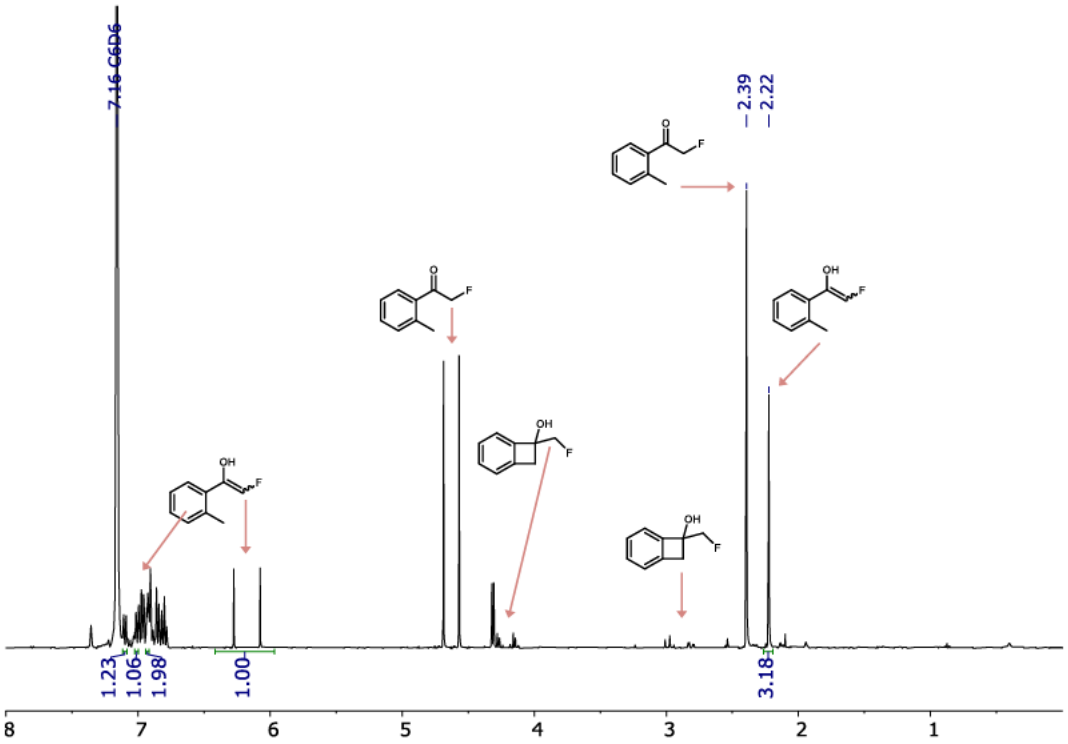

Figure 36: ^{1}H NMR Spectra recorded in degassed C_6D_6 [0.2 M] for the reaction of 1b with 370 nm, reaction performed on 0.01 mmol scale. Integration corresponds to enol species.

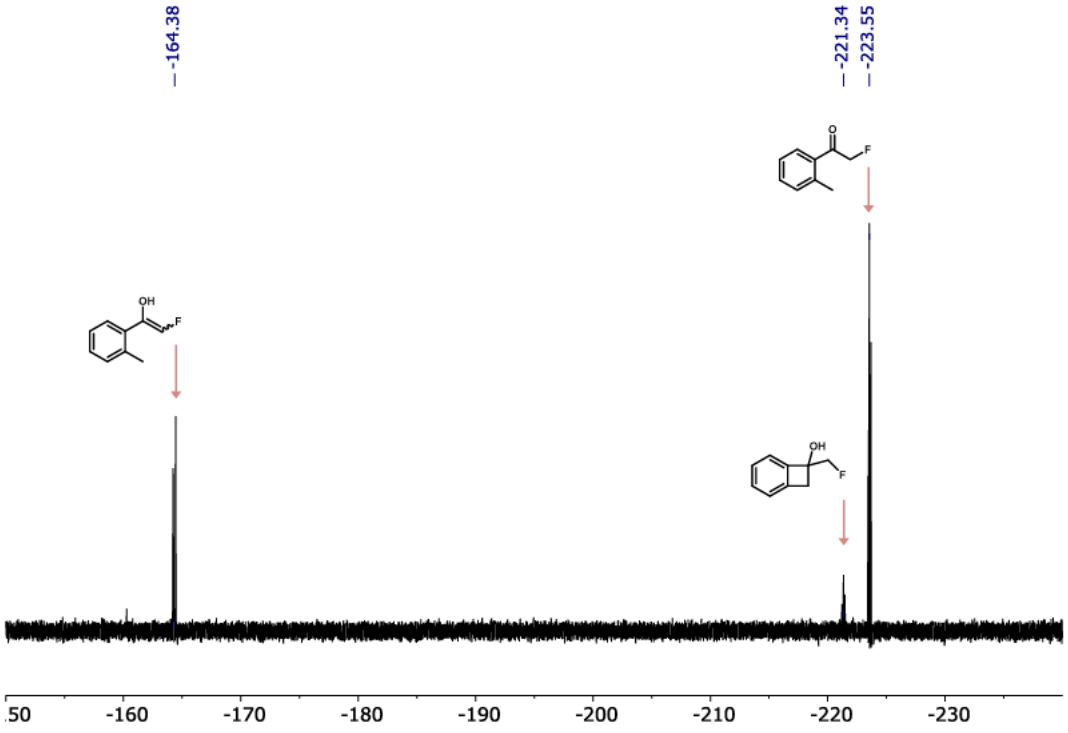

Figure 37: ^{19}F NMR spectrum corresponding to Figure 36.

4.3.3.3 Photoenol reactivity

8-Methyl-7-(trifluoromethyl)bicyclo[4.2.0]octa-1,3,5-trien-7-ol (3.40)

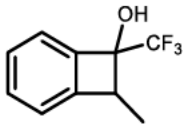

Following **GP-I**, using **3.9** (24 mg, 0.12 mmol) in benzene (6, mL, 20 mM), with 10 8 Watt LZC-UVA (355 nm) lamps for 16 h at rt. The product was isolated after automated FC (pentane : Et_2O, 100:0 to 50:50; exact gradient: 4 column volumes (CV) 100:0, 4 CV 100:0 to 90:10, 4 CV 90:10, 4 CV 80:20, 4 CV 70:30, 4 CV 50:50) as a colourless solid (14 mg, 0.07 mmol, 58%).

M.P.: 30.0 – 38.5 °C. **IR (neat)**: $\tilde{\nu}$ = 3345 (w), 1458 (w), 1343 (w), 1284 (w), 1228 (w), 1148 (s), 1107 (s), 1083 (m), 1051 (m), 951 (m), 935 (m), 894 (w), 757 (m), 744 (m), 662 (m), 640 (w), 593 (w), 532 (w), 471 (w), 453 (w), 434 (w). **^{1}H NMR (400 MHz, C_6D_6):** δ = 7.05 (td, J = 7.4, 1.3 Hz, 1H), 7.02 – 6.99 (m, 1H), 6.98 – 6.93 (m, 1H), 6.81 (dq, J = 7.4, 1.0 Hz, 1H), 3.32 (dddd, J = 8.5, 7.4, 6.3, 1.1 Hz, 1H), 2.17 (s, 1H), 1.30 (dq, J = 7.4, 1.7 Hz, 3H). **^{13}C NMR (101 MHz, C_6D_6):** δ = 147.2, 140.4 (q, J = 2.4 Hz), 131.2, 128.4, 125.6 (q, J = 282.7 Hz), 122.2, 122.2, 80.6 (q, J = 30.8 Hz), 52.2, 13.5 (q, J = 2.3 Hz). **^{19}F NMR (377 MHz, C_6D_6):** δ = –75.8 (s, 3F). **HRMS (ESI)**: Calculated for $C_{10}H_8F_3O$ $[M-H]^-$: 201.0533, found: 201.0535.

Chemotion ELN sample number: HMA-4-210 and HMA-4-477.

The CH_3-group, the CH and the OH were unambiguously identified *via* COSY and HSQC experiments. The relative configuration was determined *via* ^{1}H-^{1}H NOESY and ^{19}F-^{1}H HOESY experiments. A strong HOE correlation between CF_3 and CH_3 and an NOE contact between OH and H were observed. Therefore, it can be concluded that CF_3 and CH_3 are positioned *syn* to each other.

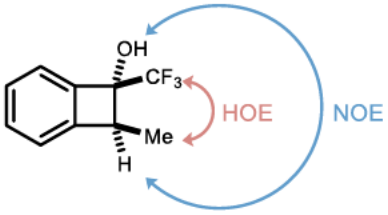

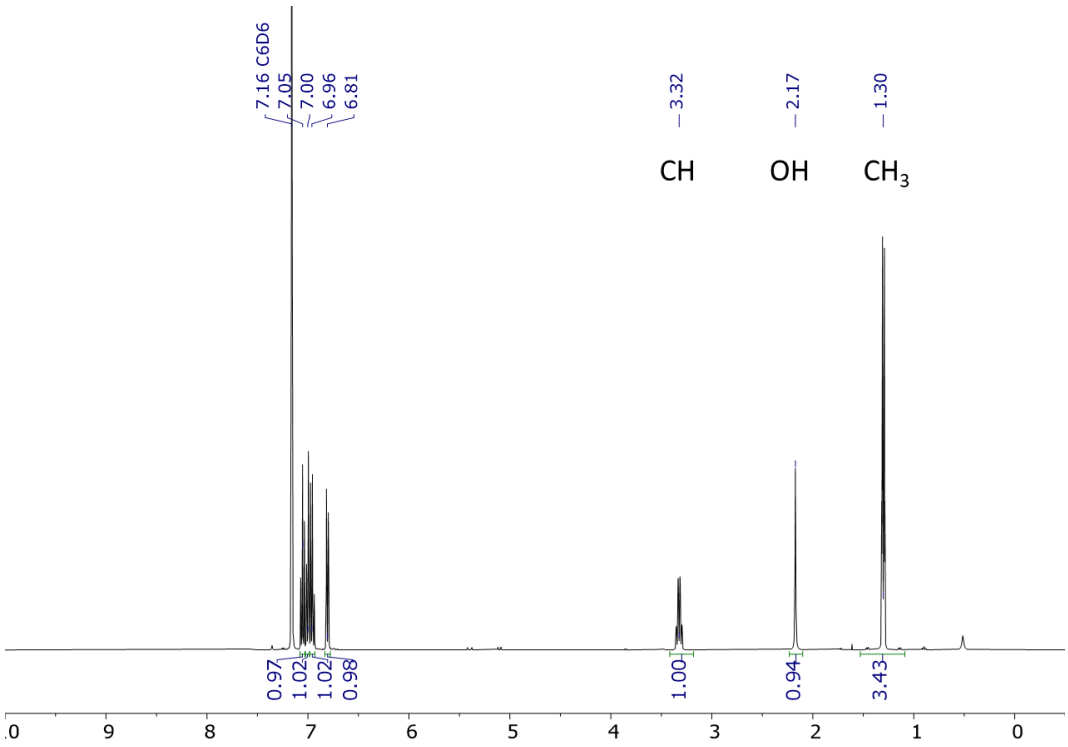

Figure 38: ^{1}H spectrum of 3.40 in C_6D_6. The relevant protons were assigned by COSY and HSQC.

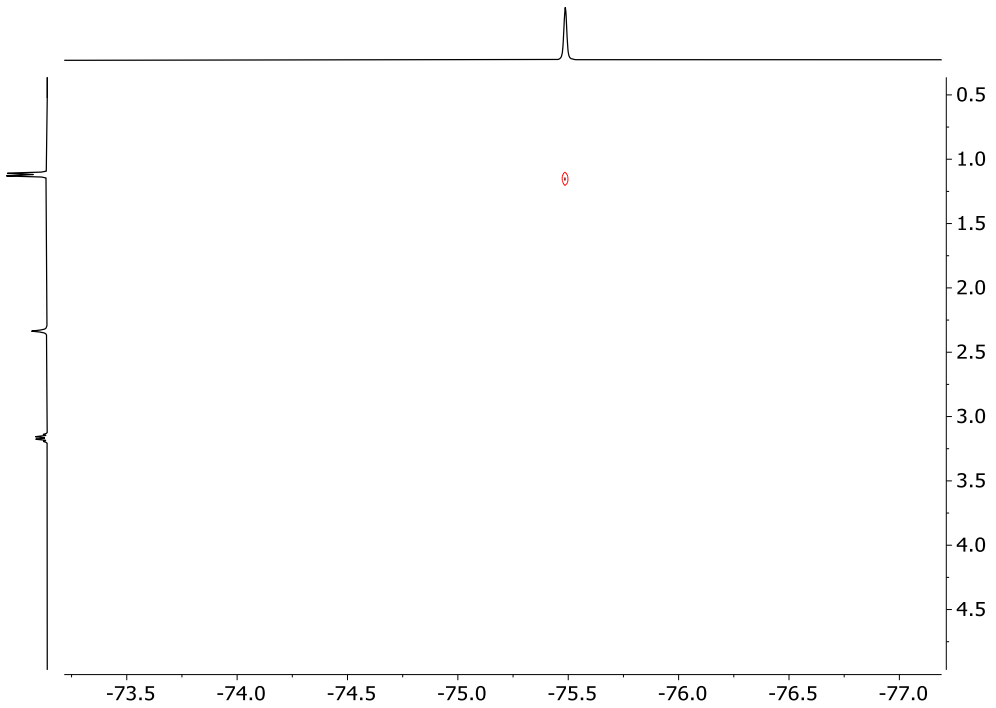

Figure 39: ^{19}F ^{1}H HOESY spectrum of 3.40 in C_6D_6.

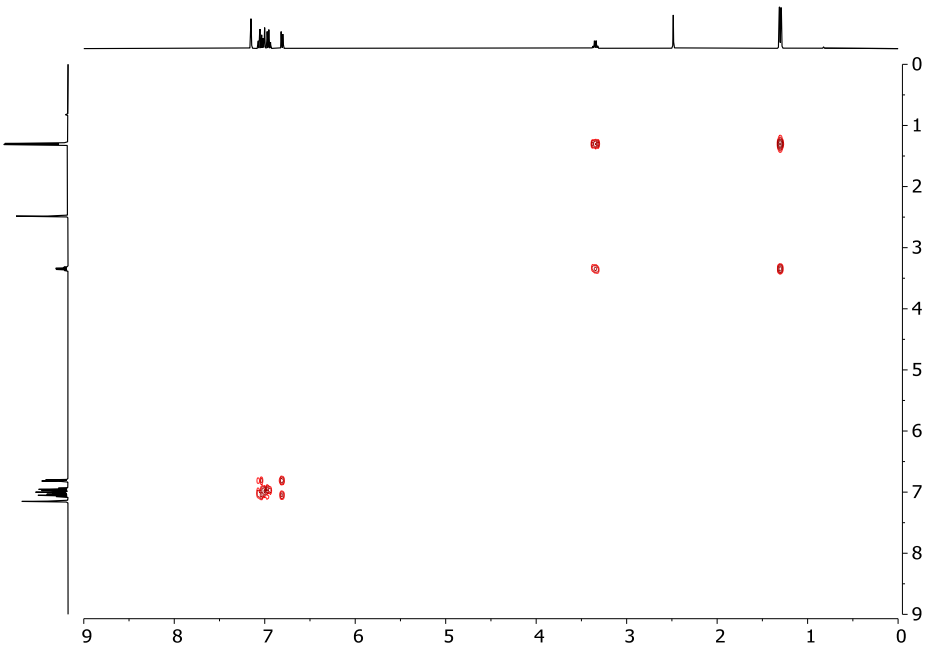

Figure 40: ^{1}H ^{1}H COSY spectrum of 3.40 in C_6D_6.

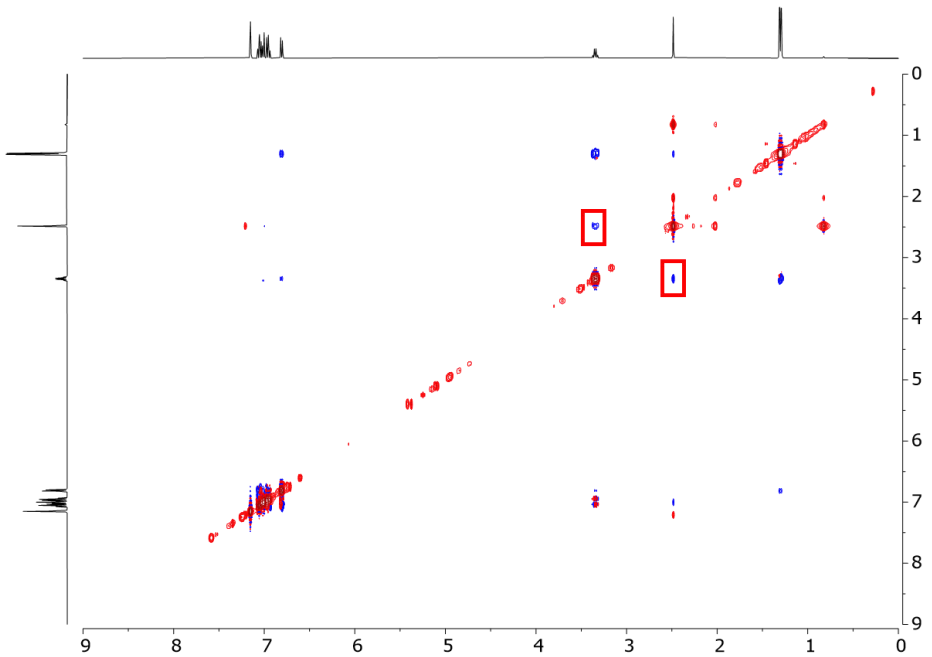

Figure 41: NOESY spectrum of 3.40 in C_6D_6. Relevant contacts highlighted in red.

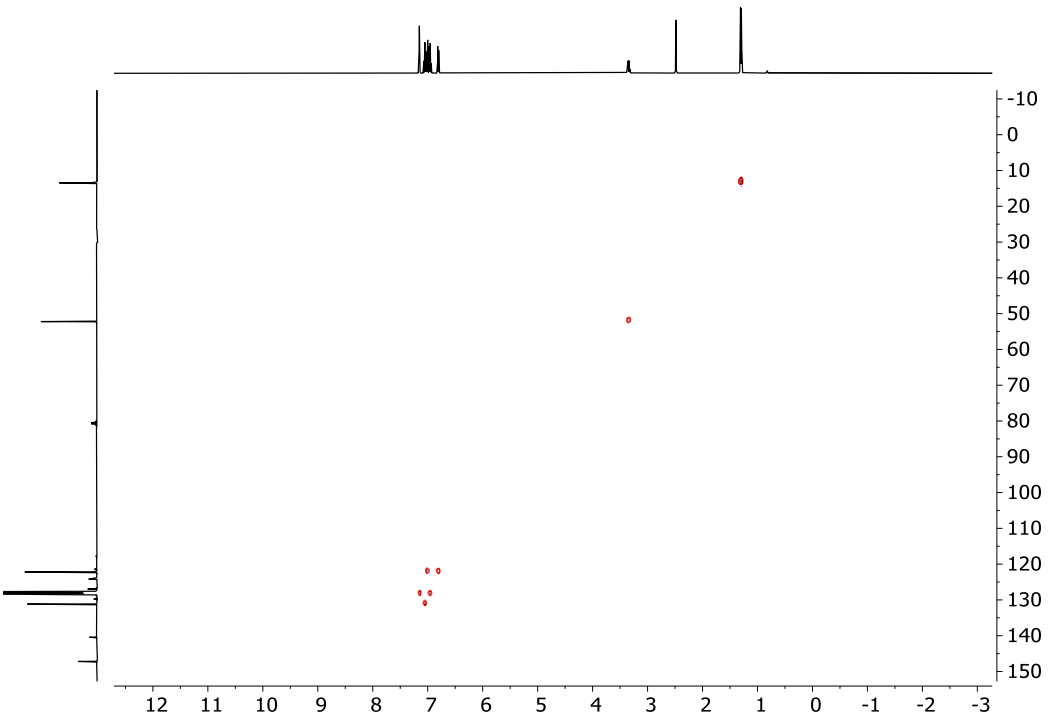

Figure 42: HSQC spectrum of 3.40 in C_6D_6.

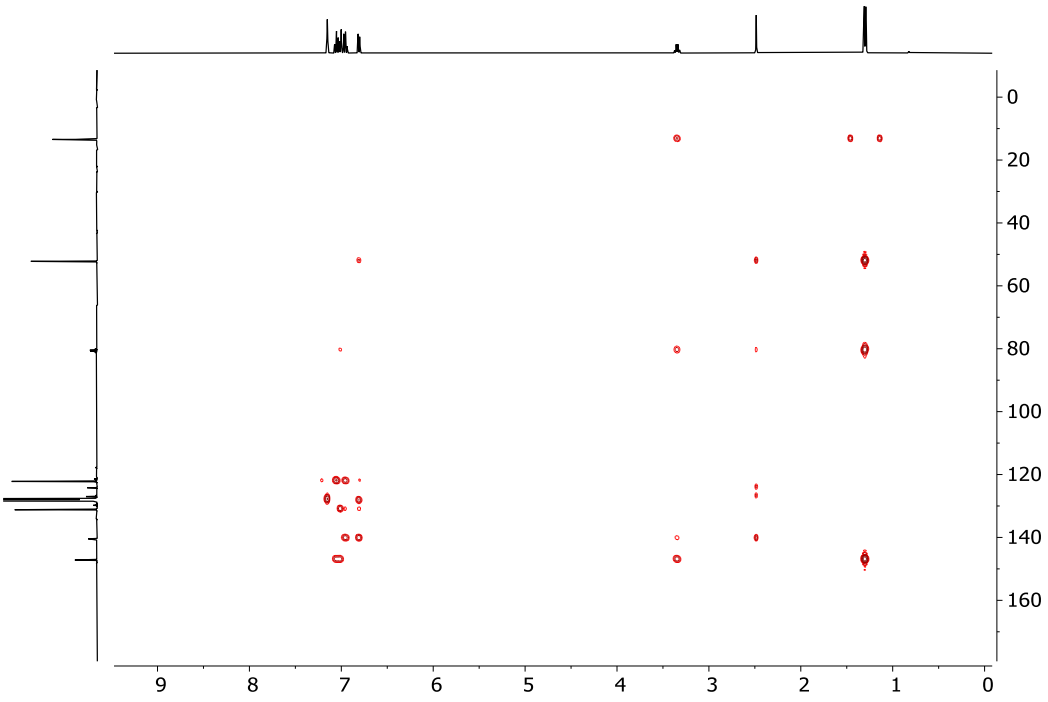

Figure 43: HMBC spectrum of 3.40 in C_6D_6.

(7S,8R)-3-Chloro-8-methyl-7-(trifluoromethyl)bicyclo[4.2.0]octa-1,3,5-trien-7-ol (3.42)

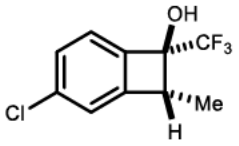

Following **GP-I**, using **3.15** (78 mg, 0.33 mmol) in benzene (16.5 mL, 20 mM), with 10 8 Watt LZC-UVA (355 nm) lamps for 16 h at rt. The product was isolated after automated FC (pentane : Et_2O, 100:0 to 50:50) as a colourless solid (66 mg, 0.28 mmol, 85%). A sample suitable for X-ray analysis was obtained and its configuration proven unambiguously.

M.P.: 44.4 – 53.5 °C. **IR (neat)**: $\tilde{\nu}$ = 3359 (w), 2995 (w), 2941 (w), 2884 (w), 1588 (w), 1455 (w), 1414 (w), 1339 (w), 1279 (m), 1248 (w), 1227 (w), 1162 (s), 1112 (s), 1081 (w), 1057 (s), 1013 (w), 942 (m), 896 (w), 876 (w), 820 (m), 757 (w), 740 (w), 709 (w), 653 (w), 597 (w), 535 (w), 505 (w), 454 (w), 433 (w). **^{1}H NMR (400 MHz, C_6D_6):** δ = 6.93 (dt, J = 7.8, 1.3 Hz, 1H), 6.75 (q, J = 1.1 Hz, 1H), 6.67 (d, J = 7.9 Hz, 1H), 3.30 – 3.02 (m, 1H), 2.01 (d, J = 2.4 Hz, 1H), 1.16 (dq, J = 7.4, 1.7 Hz, 3H). **^{13}C NMR (101 MHz, C_6D_6):** δ = 148.4, 138.4 (q, J = 2.3 Hz), 137.0, 129.1, 125.2 (q, J = 283.5 Hz), 123.8, 123.1, 79.9 (q, J = 31.1 Hz), 52.0, 13.1 (q, J = 2.3 Hz). **^{19}F NMR (282 MHz, C_6D_6):** δ = -75.94 (s, 3F). **HRMS (ESI)**: Calculated for $C_{10}H_7ClF_3O$ $[M-H]^-$: 235.0143, found: 235.0152.

Chemotion ELN sample number: HMA-4-482.

(3aS,4S,9aS)-4-Hydroxy-2-methyl-4-(trifluoromethyl)-3a,4,9,9a-tetrahydro-1H-benzo[f]isoindole-1,3(2H)-dione (3.45)

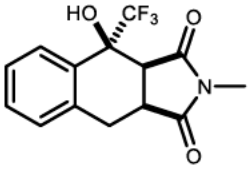

3.8 (47.0 mg, 250 µmol, 1.00 eq.) and N-methylmaleimide (139 mg, 1.25 mmol, 5.00 eq.) were dissolved in benzene (6.00 mL) in an oven-dried Schlenk-flask and

the solution was degassed *via* freeze-pump-thaw cycles (3×). The solution was irradiated using a Kessil 45W PR160L 370nm Gen2 LED for 8 h (see chapter 4.1 for set-up). The solvent was removed under reduced pressure, the sample was dissolved in $CDCl_3$ and CH_2Br_2 (43.5 mg, 17.5 µL, 250 µmol, 1.00 eq. was added. The mixture was analyzed *via* NMR (92% NMR yield). The sample was purified *via* automated FC (CyH:EtOAc, 100:0 to 60:40, then C18-RP column: H_2O/CD_3CN (90:10 to 10:90) and the product was obtained as a colourless oil (27 mg, 90 µmol, 36%). The diminished isolated yield is due to a difficult separation from N-methylmaleimide, that eludes together with the product. Relative configuration was assigned in analogy to **3.46** CCDC 2371854, synthesised by [redacted]

IR (neat): $\tilde{\nu}$ = 3391 (w), 1778 (w), 1684 (s), 1442 (m), 1388 (m), 1287 (m), 1245 (s), 1164 (s), 1127 (s), 1029 (m), 978 (m), 948 (w), 908 (m), 845 (w), 766 (m), 729 (s), 650 (w), 520 (w). **^{1}H NMR (400 MHz, $CDCl_3$):** δ = 7.88 (dd, J = 7.3, 2.0 Hz, 1H), 7.41 – 7.28 (m, 2H), 7.18 – 7.09 (m, 1H), 6.04 (q, J = 0.9 Hz, 1H), 3.66 (d, J = 9.1 Hz, 1H), 3.47 (td, J = 9.4, 8.9, 1.2 Hz, 1H), 3.32 (ddq, J = 16.5, 9.9, 1.1 Hz, 1H), 3.16 (dp, J = 16.5, 2.0 Hz, 1H), 2.89 (s, 3H). **^{13}C NMR (101 MHz, $CDCl_3$):** δ = 179.0, 178.8, 133.8, 132.4, 130.0, 128.8, 127.9, 127.8, 125.0 (q, J = 285.5 Hz), 73.6 (q, J = 30.7 Hz), 42.4, 37.9, 29.1 (q, J = 4.3 Hz), 25.6. **^{19}F NMR (282 MHz, $CDCl_3$):** δ = -80.09 (d, J = 1.6 Hz, 3F). **HRMS (ESI):** Calculated for $C_{14}H_{11}F_3NO_3$ $[M-H]^-$: 298.0697, found: 298.0694.

Chemotion ELN sample number: HMA-4-433.

4.3.3.4 Mechanism of the peroxide formation

A stock solution was prepared by dissolving **3.8** (94.1 mg, 500 µmol, 1.00 eq.) in benzene (10 mL, 20 mM) and adding $PhCF_3$ as an internal standard (60.9 µL, 500 µmol, 1.00 eq.) The solution was divided into 5 × 10 mL vial, of which three contained TPP (0.6 mg, 1 µM, 1mol%). Afterwards the solutions were saturated with oxygen and irradiated under oxygen atmosphere for 4 h with a combination of two different lamps, namely a 355 nm UV lamp and/or a LCW (cool-white, for emission spectrum cf. chapter 4.1, Figure 23). The results are depicted in (Table 11).

Table 30: Control experiments for a potential reaction of singlet oxygen generated from 3.47, reactions performed on 500 µmol scale in C_6D_6 [20 mM] under oxygen atmosphere for 4 h at 22 °C, yield determined *via* ^{19}F NMR with $PhCF_3$ as internal standard.

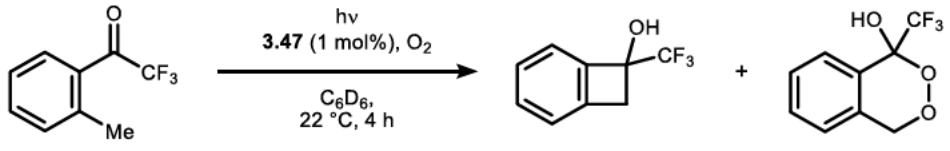

3.8 **3.26** **3.27**

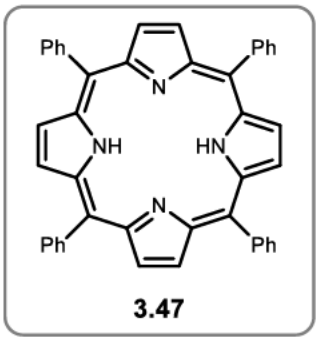

3.47

Entry	Irradiation source	addition of **3.47**	Yield **3.26**	Yield **3.27**
1	CW-LED	yes	0	0
2	CW-LED + 355 nm	-	5%	7%
3	CW-LED + 355 nm	yes	1%	3%
4	355 nm	-	3%	6%
5	355 nm	yes	1%	2%

4.3.4 Scope

3-Chloro-7-(trifluoromethyl)bicyclo[4.2.0]octa-1,3,5-trien-7-ol (3.29)

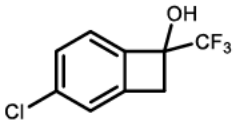

Following **GP-I**, using **3.14** (22.7mg, 0.10 mmol) in benzene (6 mL, 20 mM). The product was obtained after automated FC (pentane : Et_2O, 100:0 to 50:50) as a colourless solid (12 mg, 0.054 mmol, 53%).

M.P.: 70 – 77 °C. **IR (neat)**: $\tilde{\nu}$ = 3361 (w), 2945 (w), 1591 (w), 1458 (w), 1426 (w), 1301 (m), 1230 (w), 1167 (s), 1134 (m), 1104 (w), 1072 (m), 1049 (w), 1020 (m), 954 (w), 854 (w), 819 (m), 758 (w), 715 (w), 595 (w), 505 (w), 424 (w). **^{1}H NMR (400 MHz, C_6D_6):** δ = 6.90 (ddt, J = 7.9, 1.7, 0.9 Hz, 1H), 6.72 – 6.69 (m, 1H), 6.63 (d, J = 7.9 Hz, 1H), 3.18 (dt, J = 14.7, 0.9 Hz, 1H), 2.54 (dd, J = 14.7, 1.1 Hz, 1H), 2.00 (s, 1H). **^{13}C NMR (101 MHz, C_6D_6):** δ = 143.5, 140.0, 140.0 (q, J = 1.9 Hz), 137.0, 128.9, 125.2 (q, J = 281.7 Hz), 124.4, 123.7, 77.6 (q, J = 32.9 Hz), 41.5 (q, J = 1.9 Hz). **^{19}F NMR (282 MHz, C_6D_6):** δ = -81.20 (s, 3F). **HRMS (ESI)**: Calculated for $C_9H_5ClF_3O$ $[M\text{-}H]^-$: 220.9995, found: 220.9987.

Chemotion ELN sample number: HMA-4-299 and HMA-4-481.

7-(Fluoromethyl)bicyclo[4.2.0]octa-1,3,5-trien-7-ol (3.37)

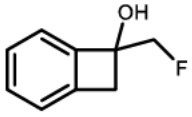

Following **GP-I**, using **3.18** (112 mg, 0.74 mmol) in acetonitrile (50 mL) for 6 h. The desired product was obtained after FC (pentane : Et_2O, 80:20) and bulb-to-bulb distillation (150 °C, 1.1 mbar) as a colourless oil (14 mg, 0.09 mmol, 12%).

IR (neat): $\tilde{\nu}$ = 3551 (w), 3387 (m), 3346 (m), 3069 (w), 2928 (m), 1459 (m), 1423 (w), 1364 (m), 1331 (w), 1266 (m), 1201 (s), 1155 (m), 1111 (m), 1067 (m),

1044 (m), 1018 (s), 994 (s), 966 (m), 918 (m), 758 (s), 734 (s), 715 (s), 644 (m), 601 (w), 583 (w), 572 (w), 541 (w), 478 (w), 422 (w), 415 (w). **^{1}H NMR (400 MHz, C_6D_6):** δ = 7.08 (td, J = 7.2, 1.6 Hz, 1H), 7.05 – 6.97 (m, 2H), 6.88 (dt, J = 7.3, 1.0 Hz, 1H), 4.33 – 4.24 (m, 1H), 4.21 – 4.10 (m, 1H), 2.99 (d, J = 14.2 Hz, 1H), 2.82 (dd, J = 14.2, 3.3 Hz, 1H), 2.03 (s, 1H). **^{13}C NMR (101 MHz, C_6D_6):** δ = 147.2 (d, J = 7.4 Hz), 141.7, 130.0, 127.6, 123.9, 122.0, 87.3 (d, J = 174.7 Hz), 78.7 (d, J = 19.4 Hz), 42.9 (d, J = 6.5 Hz). **^{19}F NMR (377 MHz, C_6D_6):** δ = -225.74 (t, J = 47.2 Hz, 1F). **HRMS (ESI)**: Calculated for C_9H_8FO $[M-H]^-$: 151.0565, found: 151.0526.

Chemotion ELN sample number: HMA-4-464.

7-(Difluoromethyl)bicyclo[4.2.0]octa-1,3,5-trien-7-ol (3.36)

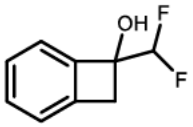

Following **GP-I**, using **3.21** (21.4 mg, 0.126 mmol) in benzene (6 mL, 20 mM). The product was obtained after automated FC (pentane : Et_2O, 100:0 to 50:50) as a colourless oil (13.0 mg, 0.076 mmol, 61%).

IR (neat): $\tilde{\nu}$ = 3363 (w), 2935 (w), 1460 (w), 1425 (w), 1347 (w), 1277 (w), 1239 (m), 1192 (w), 1157 (w), 1113 (m), 1094 (m), 1062 (s), 982 (w), 952 (w), 889 (w), 818 (w), 758 (m), 735 (w), 715 (w), 673 (w), 657 (w), 621 (w), 567 (w), 552 (w), 516 (w), 464 (w), 449 (w), 414 (w). **^{1}H NMR (400 MHz, C_6D_6):** δ =7.10 – 6.91 (m, 3H), 6.82 (d, J = 7.3 Hz, 1H), 5.42 (t, J = 54.8 Hz, 1H), 3.19 (dd, J = 14.4, 2.4 Hz, 1H), 2.73 (d, J = 14.3 Hz, 1H), 1.98 (s, 1H). **^{13}C {^{1}H, ^{19}F} NMR (101 MHz, C_6D_6):** δ = 143.7, 142.1, 130.6, 127.9, 123.6, 122.5, 115.9, 78.8, 41.3. **^{19}F NMR (377 MHz, C_6D_6):** δ = -126.79 – -132.30 (m, 2F). **HRMS (ESI)**: Calculated for $C_9H_7F_2O$ $[M-H]^-$: 169.0470, found: 169.0475.

Chemotion ELN sample number: HMA-4-344 and HMA-4-484.

8-Methoxy-7-(trifluoromethyl)bicyclo[4.2.0]octa-1,3,5-trien-7-ol (3.49)

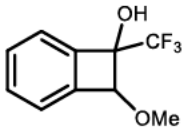

Following **GP-I**, using **3.11** (26.5 mg, 0.122 mmol) in benzene (6 mL, 20 mM). The product was obtained after automated FC (pentane : Et_2O, 100:0 to 50:50) as a colourless oil (18.0 mg, 0.083 mmol, 68%).

M.P.: 40.0 – 46.5 °C. **IR (neat)**: $\tilde{\nu}$ = 3389 (w), 2942 (w), 2841 (w), 1463 (w), 1361 (m), 1298 (m), 1208 (m), 1177 (s), 1151 (s), 1115 (s), 1063 (s), 1013 (w), 986 (m), 905 (m), 802 (w), 760 (m), 736 (m), 685 (w), 660 (m), 624 (w), 592 (w), 519 (w), 468 (w). **^{1}H NMR (400 MHz, C_6D_6):** δ = 7.08 – 6.93 (m, 4H), 4.52 (s, 1H), 3.29 (s, 3H), 2.31 (br s, 1H). **^{13}C NMR (101 MHz, C_6D_6):** δ = 143.9, 138.9 (q, J = 2.4 Hz), 131.4, 130.4, 125.28 (q, J = 280.6 Hz), 123.7, 122.8, 88.4, 82.9 (q, J = 30.6 Hz), 58.7. **^{19}F NMR (282 MHz, C_6D_6):** δ = –75.7 (s, 3F). **HRMS (APCI)**: Calculated for $C_{10}H_8F_3O_2$ $[M\text{-}H]^-$: 217.0482, found: 217.0452.

Chemotion ELN sample number: HMA-4-335 and HMA-4-478.

3-Methoxy-7-(trifluoromethyl)bicyclo[4.2.0]octa-1,3,5-trien-7-ol (3.50)

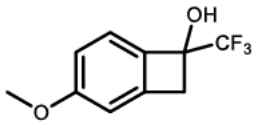

Following **GP-I**, using **3.12** (27.2mg, 0.125 mmol) in benzene (6 mL, 20 mM). The product was obtained after automated FC (pentane : Et_2O, 100:0 to 50:50) as a colourless oil (4.0 mg, 0.018 mmol, 15%).

IR (neat): $\tilde{\nu}$ = 3413 (w), 2943 (w), 1605 (w), 1481 (m), 1314 (w), 1275 (m), 1257 (m), 1238 (m), 1162 (s), 1127 (s), 1090 (s), 1017 (m), 955 (w), 822 (w), 733 (w), 602 (w), 589 (w), 549 (w), 503 (w), 473 (w), 464 (w), 453 (w), 426 (w), 413 (w). **^{1}H NMR (400 MHz, C_6D_6):** δ = 6.90 (d, J = 8.2 Hz, 1H), 6.62 (dd, J = 8.3, 2.1 Hz, 1H), 6.46 – 6.32 (m, 1H), 3.38 (d, J = 14.3 Hz, 1H), 3.21 (s, 3H), 2.75 (d, J

= 14.3 Hz, 1H), 2.10 (s, 1H). **^{13}C NMR (101 MHz, C_6D_6):** δ = 162.7, 143.3, 133.6, 125.7 (q, J = 281.6 Hz), 123.6, 115.4, 108.9, 77.6 (q, J = 32.8 Hz), 55.0, 41.4 (q, J = 2.4 Hz). **^{19}F NMR (282 MHz, C_6D_6):** δ = –81.1 (s, 3F). **HRMS (ESI)**: Calculated for $C_{10}H_8F_3O_3$ [M-H]$^-$: 217.0482, found: 217.0486.

Chemotion ELN sample number: HMA-4-208 and HMA-4-479.

3-Fluoro-7-(trifluoromethyl)bicyclo[4.2.0]octa-1,3,5-trien-7-ol (3.51)

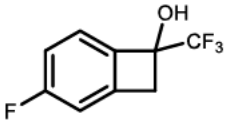

Following **GP-I**, using **3.13** (24.8mg, 0.12 mmol) in benzene (6 mL, 20 mM). The product was obtained after automated FC (pentane : Et_2O, 100:0 to 50:50) as a colourless oil (16 mg, 0.078 mmol, 65%).

IR (neat): $\tilde{\nu}$ = 3375 (w), 2946 (w), 1598 (w), 1471 (m), 1427 (w), 1311 (m), 1243 (m), 1158 (s), 1127 (s), 1083 (s), 1018 (m), 960 (m), 899 (w), 879 (w), 849 (m), 820 (m), 787 (w), 734 (w), 650 (w), 597 (m), 580 (m), 541 (w), 511 (w), 469 (w), 412 (w). **^{1}H NMR (400 MHz, C_6D_6):** δ = 6.71 (dd, J = 8.2, 4.6 Hz, 1H), 6.59 (ddd, J = 10.5, 8.2, 2.4 Hz, 1H), 6.42 (dd, J = 7.7, 2.1 Hz, 1H), 3.19 (d, J = 14.6 Hz, 1H), 2.56 (dt, J = 14.7, 1.2 Hz, 1H), 2.03 (s, 1H). **^{13}C NMR (101 MHz, C_6D_6):** δ = 165.0 (d, J = 248.6 Hz), 143.8 (d, J = 8.6 Hz), 137.3 – 137.2 (m), 125.3 (q, J = 281.8 Hz), 124.4 (d, J = 9.4 Hz), 116.0 (d, J = 24.3 Hz), 111.56 (d, J = 23.1 Hz), 77.3 (q, J = 32.9 Hz), 41.4 – 41.1 (m) **^{19}F NMR (282 MHz, C_6D_6):** δ = -81.27 (s, 3F), -107.45 – -107.55 (m, 1F). **HRMS (APCI)**: Calculated for $C_9H_5F_4O$ [M-H]$^-$: 205.0282, found: 205.0281.

Chemotion ELN sample number: HMA-4-290 and HMA-4-480.

7-Hydroxy-7-(trifluoromethyl)bicyclo[4.2.0]octa-1,3,5-triene-3-carbonitrile (3.52)

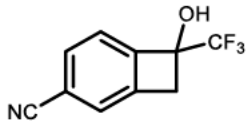

Following **GP-I**, using **3.16** (25.6 mg, 0.12 mmol) in benzene (6 mL, 20 mM). The product was obtained after automated FC (pentane : Et_2O, 100:0 to 50:50) as a colourless solid (11.0 mg, 0.052 mmol, 43%).

M.P.: 142.0 – 146.5 °C. **IR (neat)**: $\tilde{\nu}$ = 3384 (w), 2235 (w), 1427 (w), 1305 (w), 1239 (w), 1166 (s), 1144 (s), 1121 (w), 1092 (w), 1073 (w), 1019 (w), 959 (w), 831 (w), 727 (w), 654 (w), 604 (w), 536 (w), 506 (w), 465 (w), 431 (w). **^{1}H NMR (400 MHz, C_6D_6):** δ = 6.78 (dd, J = 7.8, 1.2 Hz, 1H), 6.54 (d, J = 7.7 Hz, 1H), 6.53 – 6.49 (m, 1H), 3.08 (d, J = 14.9 Hz, 1H), 2.46 (d, J = 14.9 Hz, 1H), 2.12 (s, 1H). **^{13}C NMR (101 MHz, C_6D_6):** δ = 145.9 – 145.8 (m), 142.7, 132.3, 127.2, 124.8 (q, J = 281.9 Hz), 122.8, 118.5, 115.1, 78.0 (d, J = 33.2 Hz), 41.4 (q, J = 2.0 Hz). **^{19}F NMR (282 MHz, C_6D_6):** δ = -81.11 (s, 3F). **HRMS (ESI)**: Calculated for $C_{10}H_5F_3NO$ $[M-H]^-$: 212.0329, found 212.0336.

Chemotion ELN sample number: HMA-4-334 and HMA-4-483.

Methyl 7-hydroxybicyclo[4.2.0]octa-1,3,5-triene-7-carboxylate (3.53)

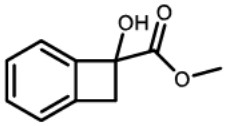

Following **GP-I**, using **3.23** (21.4 mg, 0.12 mmol) in benzene (6 mL, 20 mM). The product was obtained after automated FC (pentane : Et_2O, 100:0 to 50:50) as a colourless solid (13.0 mg, 0.084 mmol, 70%).

M.P.: 53 – 58 °C. **IR (neat)**: $\tilde{\nu}$ = 3477 (w), 3392 (w), 2953 (w), 1732 (s), 1459 (w), 1438 (w), 1319 (w), 1276 (m), 1203 (m), 1159 (s), 1133 (m), 1097 (w), 1069 (w), 1029 (w), 765 (w), 734 (m), 710 (w), 666 (w), 595 (w), 482 (w), 473 (w), 458 (w), 430 (w), 423 (w), 413 (m). **^{1}H NMR (400 MHz, C_6D_6):** δ = 7.09 – 7.02

(m, 1H), 7.01 – 6.95 (m, 2H), 6.90 (dt, *J* = 7.2, 1.0 Hz, 1H), 3.92 (s, 1H), 3.60 (d, *J* = 13.7 Hz, 1H), 3.26 (d, *J* = 13.7 Hz, 1H), 3.11 (s, 3H). **^{13}C NMR (101 MHz, C_6D_6):** δ = 175.1, 146.5, 143.4, 130.1, 127.9, 123.6, 121.4, 78.5, 52.4, 45.8. **HRMS (APCI)**: Calculated for $C_{10}H_{10}O_3$ $[M]^{\cdot+}$: 178.0624, found 178.0602.

Chemotion ELN sample number: HMA-4-314 and HMA-4-485.

4.3.4.1 Effect of substitution on reactivity

Following **GP-H,** using acetophenones (10 µM) in degassed C_6D_6 (0.5 mL; 20 mM) at 355 nm for 3 h at 20 °C. Conversion and yield were determined by ^{1}H NMR with mesitylene as internal standard or ^{19}F NMR with $PhCF_3$ as internal standard as mean value of three experiments (Table 31).

Table 31: Substrate scope and selectivity, reactions performed on 10 µM scale in 0.5 mL C_6D_6 [20 mM] at 20 °C in the *Luzchem* photoreactor with 355 nm lamps, conversion and yield based on ^{1}H NMR with mesitylene as internal standard or ^{19}F NMR with $PhCF_3$ as internal standard as mean value of three experiments.

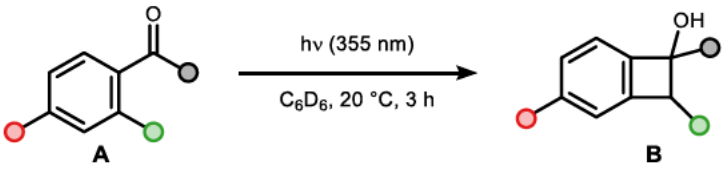

Entry	A	B	NMR standard	Conversion	Yield	Side reactions
1	**3.8**	**3.26**	$PhCF_3$	66.0% ± 0.4%	66.0% ± 0.4%	-
2	**3.9**	**3.40**	$PhCF_3$	33.0% ± 0.3%	27.4% ± 0.1%[a]	~6%
3	**3.10**	**3.48**	$PhCF_3$	8.0% ± 1.75%	0%	8%
4	**3.11**	**3.49**	$PhCF_3$	37.2% ± 0.8%	29.9% ± 1.9% [a]	7%
5	**3.12**	**3.50**	$PhCF_3$	90.9% ± 1.4%	63.0% ± 0.5%	28%
6	**3.13**	**3.51**	$PhCF_3$	68.7% ± 0.2%	59.6% ± 0.4%	9%
7	**3.16**	**3.52**	$PhCF_3$	48.4% ± 4.5%	42.2% ± 3.1%	6%
8	**3.14**	**3.29**	$PhCF_3$	79.3% ± 0.7%	73.9% ± 0.7%	5%
9	**3.15**	**3.42**	$PhCF_3$	41.2% ± 0.8%	36.3% ± 0.3% [a]	5%
10	**3.23**	**3.53**	mesitylene	82.0% ± 2.0%	79.3% ± 1.0%	3%
11	**3.21**	**3.36**	mesitylene	55.2% ± 1.3%	47.5% ± 0.6%	7%
12	**3.18**	**3.37**	mesitylene	7.7% ± 0.7%	~1%	7%[c]
13	**1.9**	**1.10**	mesitylene	~4%[b]	~1%	3%

[a] Formation of a single diastereomer. [b] Conversion not precisely determined due to signal overlap. [c] Formation of enol.

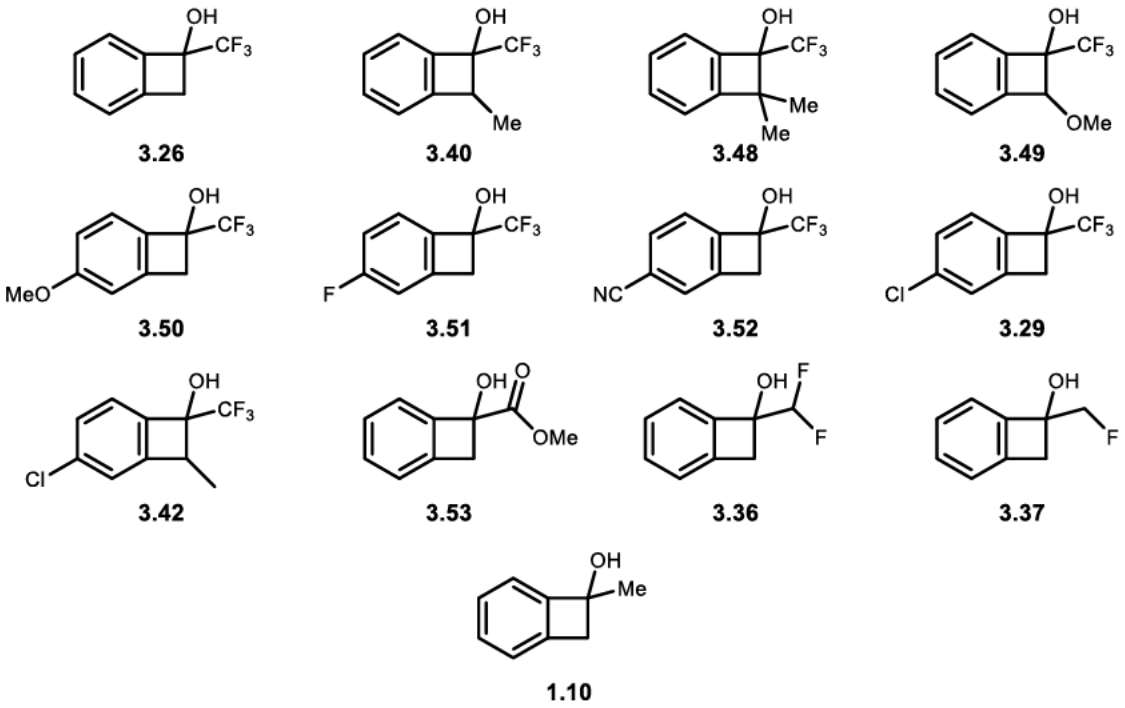

Scheme 59: Formed products after irradiation, corresponding to Table 31.

A visualisation of the relative reaction rates of the employed substrates to the standard pair **3.8** ⇄ **3.26** is depicted in a bubble diagram in Figure 20. The energy storage density of benzocyclobutenol **3.26** (311 J/g, cf. chapter 3.6.3) was used to calculate the energy densities of the different derivatives (Figure 44).

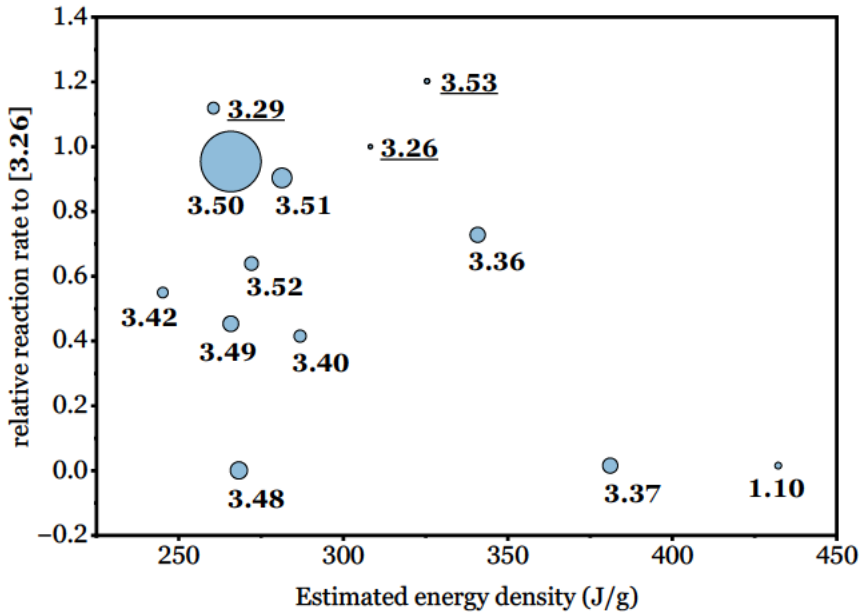

Figure 44: Visualization of the relative rates of the photocyclisation relative to the standard product 3.26. The size of the bubbles indicates the difference between conversion and yield of product, where bigger bubbles correspond to a larger amount of side reactions.

The standard product **3.26** and the benzocyclobutenol **3.29** and **3.53** were formed with the highest reaction (Figure 44, top). Several of the synthesised benzocyclobutenols show higher potential energy densities (*e.g.* **1.10** and **3.37**), but

their low synthetic accessibility excludes them as potential MOST candidates. The selected visualisation neglects the potential influence of molecular substitution on the absolute energetic properties of the molecule, which would in turn alter the achievable values of the potential energy density of the different benzocyclobutenols. Fortunately, this effect can be assumed to be small for *para*-substituted examples (*e.g.* **3.50**, **3.52**) or substrates with H/F displacements (*e.g.* **3.37** and **3.36**). Larger effects can be assumed for substrates bearing direct ring-substituents, exemplary benzocyclobutenol **3.40**, **3.48** and **3.49**. An ideal MOST system is characterised by high energy density and a high reaction rate, hence it would be displayed in the upper right corner of the diagram.

4.3.5 Ring-opening reaction

4.3.5.1 Thermal ring-opening

The thermal stability of **3.26** in different high-boiling solvents was investigated. Samples of **3.26** (3.8 mg, 20 µM) were dissolved in solvents (0.5 mL, 40 mM) and heated. $PhCF_3$ was added as an internal standard and the mixture was analysed by ^{19}F NMR (Table 32).

Table 32: Investigation of the electrocyclic ring-opening in different solvents, reactions were performed on 20 µmol scale in different solvents [40 mM], yield based on ^{19}F NMR with $PhCF_3$ as internal standard.

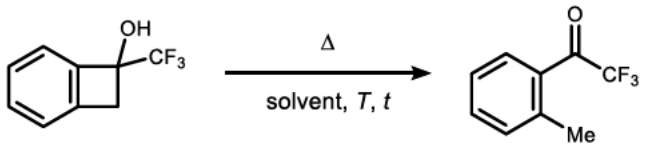

3.26 **3.8**

Entry	Solvent	*T*	*t*	Yield
1	PhMe	120 °C	16 h	0%
2	mesitylene	150 °C	16 h	0%
3	1,3,5-triethylbenzene	210 °C	1 h	~20%[a]
4	dodecane	210 °C	2 h	~9%[a]
5	diphenyl ether	220 °C	1 h	25%

[a] Evaporation of material observed by ^{19}F NMR against internal standard.

Still, achieving reproducible results was found challenging and another method was employed. Herein, samples of **3.26** (9.4 mg, 50 µM) were sealed neat in

NMR tubes under nitrogen atmosphere, to eliminate the risk of evaporation and full submerged in a metal heating block to guarantee uniform reactivity (Figure 45).

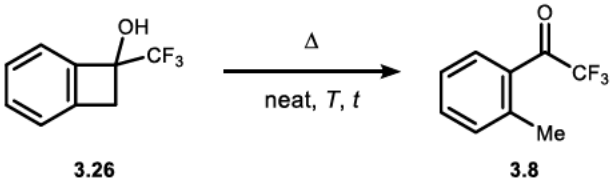

3.26 **3.8**

Entry	*T*	*t*	Yield
1	200 °C	1 h	1%
2	220 °C	1 h	16%
3	250 °C	1 h	49%[a]

[a] Mean value of three experiments.

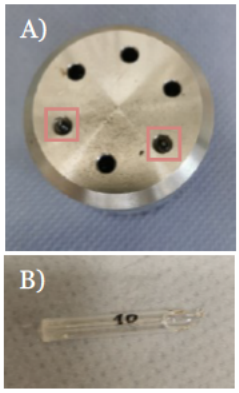

Figure 45: Neat electrocyclic ring-opening in fused NMR tubes, reactions performed on 50 µM scale, with the vials fully submerged into a fully equilibrated metal heating block. Yield based on ^{19}F NMR with $PhCF_3$ as internal standard. A) Metal heating block with fully submerged vials. B) Fused NMR tube containing a solid sample of 3.26.

The thermal half-life of **3.26** was determined by following reported procedures [76,173]. From these experiments, the preparation and measurement of the data for 503.15 K was performed by [redacted] (Figure 46, B). Samples of solid **3.26** (5.64 mg, 30.0 µmol, 1.00 eq.) were added to NMR tubes, that were fused to a closed vial under inert-gas-atmosphere using a propane torch. The tubes were placed in a metal heating block at 220 °C and removed after 1 to 32 hours. The tubes were opened with a glass cutter and rinsed with $CDCl_3$. $PhCF_3$ (5 µL, 41µmol, 1.37 eq.) was added as an internal standard and the progress of the thermal isomerization was measured by ^{1}H and ^{19}F NMR. As the MOST system is unimolecular, first order kinetics apply for the modelling of the thermal rate of back conversion [90b]. The rate law is therefore defined as

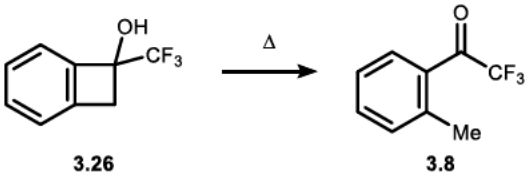

3.26 **3.8**

$$\frac{d[\mathbf{3.8}]}{dt} = -\frac{d[\mathbf{3.26}]}{dt} = k[\mathbf{3.26}] \quad (1)$$

where *k* is the rate constant, *t* is the time in seconds and the concentrations of **3.8** and **3.26**. The integrated rate law is given in equation (2) and can be written as (3) and (4)

$$\frac{d[\mathbf{3.26}]}{[\mathbf{3d}]} = -kdt \quad (2)$$

$$\ln[\mathbf{3.26}] = \ln[\mathbf{3.26}]_0 - kt \quad (3)$$

$$[\mathbf{3.26}] = [\mathbf{3.26}]_0 \, e^{-kt} \quad (4)$$

With $[\mathbf{3.26}]_0$ being the starting concentration of **3.26**. The concentration-time plots are depicted in Figure 46. By plotting $-\ln[\mathbf{3.26}]$ vs t and fitting the data to a straight line, the rate constant can be obtained as the slope of the line.

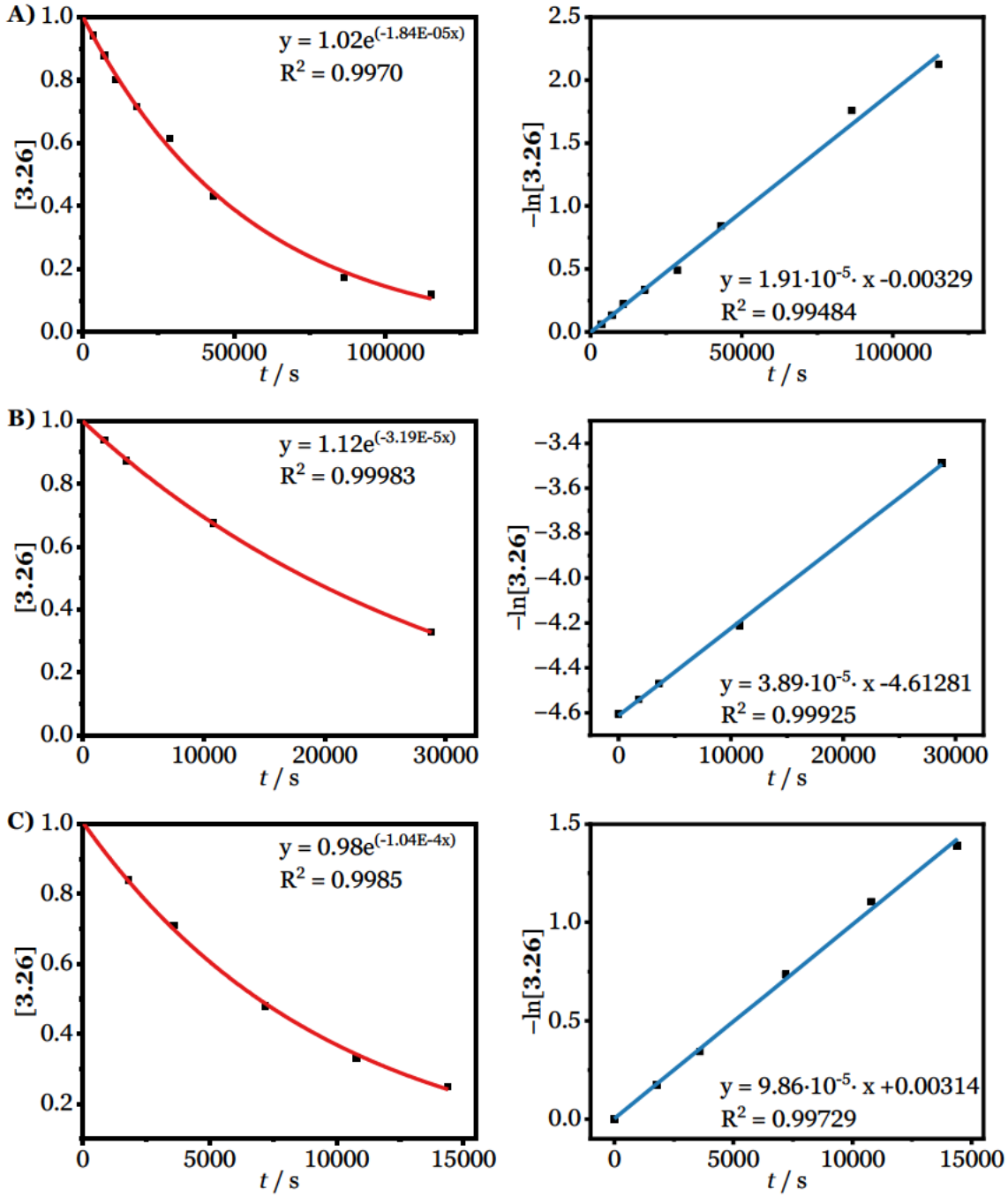

Figure 46: Concentration-time plots of the thermal electrocyclic ring-opening reaction (left) and plot of –ln[3.26] vs. time (right). Temperature = 493.15 K (A), 503.15 K (B), 513.15 K (C).

Table 33: Calculated reaction rates corresponding to Figure 46.

Value	493.15 K	503.15 K	513.15 K
k (1/s)	$k_1 = 1.91 \times 10^{-5}$	$k_2 = 3.89 \times 10^{-5}$	$k_3 = 9.86 \times 10^{-5}$

Using this data, the activation energy E_a can be calculated using the Arrhenius rate law (5).

$$k = Ae^{\left(-\frac{E_a}{RT}\right)} \tag{5}$$

with the preexponential factor A. Equation (5) can be rewritten as:

$$\ln(k) = -\left(\frac{E_a}{R}\right)\left(\frac{1}{T}\right) + \ln(A) \tag{6}$$

By plotting $\ln(k)$ vs $\left(\frac{1}{T}\right)$, E_a and A can be obtained (Figure 47).

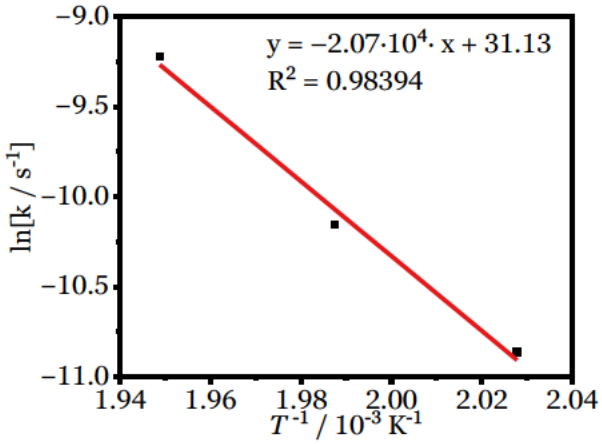

Figure 47: Arrhenius plot of the temperature dependent reaction rates.

The obtained values from Figure 47 are:

$$A = e^{31.130036} = 3.31 \times 10^{13}\ \frac{1}{\mathrm{s}}$$

$$E_a = -\mathrm{Slope} \times R = 20730 \times R = 172\ \frac{\mathrm{kJ}}{\mathrm{mol}}.$$

The thermal half-life of **3.26** was determined by following reported procedures (*70–75*). With the rate constant, the half-life $\tau_{1/2}$ at a given temperature can be calculated using equation (7).

$$\tau_{1/2} = \frac{\ln 2}{k} \tag{7}$$

To extrapolate the thermal half-life at room temperature, the Arrhenius equation (8) can be used.

$$\ln\frac{k_4}{k_3} = \frac{E_a}{R}\left(\frac{1}{T_3} - \frac{1}{T_4}\right) \tag{8}$$

With k_4 being the rate constant at room temperature, k_3 being the rate constant at T_3 = 503.15 K, R being the ideal gas constant in $JK^{-1}mol^{-1}$, and T_4 being room

temperature (298.15 K). Using equation (7), the thermal half-life can be calculated from k_4.

This concludes:

$$k_4\ (298.15\ \mathrm{K}) = \ 4.02 \times 10^{-17}\ \frac{1}{\mathrm{s}}$$

$$\tau_{1/2} = 5.47\ \times 10^{8}\ \text{years.}$$

4.3.5.2 Base-accelerated ring-opening

Samples of benzocyclobutenol **3.26** (9.41 mg, 50.0 µmol) were dissolved in C_6D_6 (0.5 mL) in an NMR tube and base (25 µmol, 0.5 eq.) was added. The reaction progress was monitored by ^{1}H NMR and ^{19}F NMR with $PhCF_3$ as internal standard.

Table 34: Base catalysed ring opening of benzocyclobutenol 3.26, Reactions run on 0.05 mmol scale in C_6D_6 under inert gas atmosphere. Yields determined by ^{1}H NMR and ^{19}F NMR with $PhCF_3$ as internal standard.

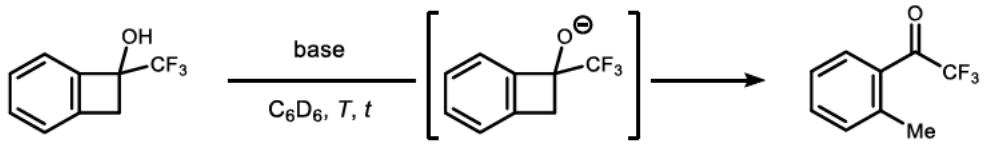

3.26 **3.54** **3.8**

Entry	Base	Equivalents	*T*	*t*	Yield
1	NBu_4OH	0.50	80 °C	96 h	0%[a]
2	KO*t*Bu	0.50	80 °C	96 h	49%[a]
3	DBU	0.50	80 °C	96 h	93%
4	DBU	0.50	30 °C	16 h	7%
5	TBD	0.50	30 °C	16 h	89%
6	TBD	0.20	30 °C	23 h	81%
7	*N*-Me-TBD	0.50	30 °C	16 h	34%
8	*N*-Me-TBD	0.50	30 °C	44 h	75%
9	*N*-Me-TBD	0.50	30 °C	120 h	97%
10	PS-TBD	0.50	30 °C	16 h	72%
11	BTPP	0.43	30 °C	16 h	99%

[a]HCF_3 detected in ^{19}F NMR.

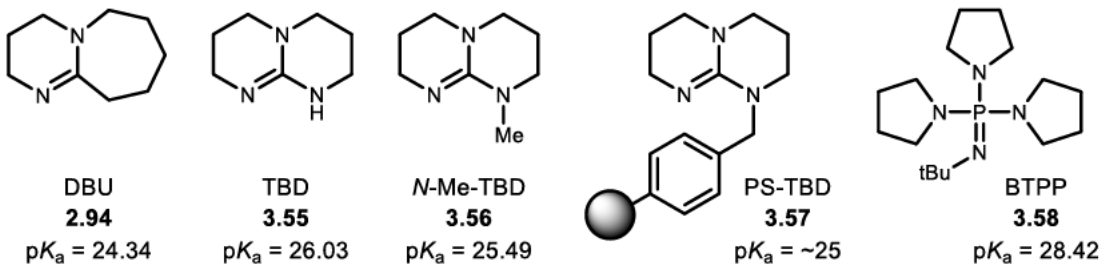

Figure 48: Employed bases in the ring-opening reaction (Table 14), basicity in acetonitrile according to *Kaljurand et. al.*[132] Basicity of 3.57 of estimated compared to 3.56.

Evolution of HCF_3 was evident from ^{1}H and ^{19}F NMR with the distinct coupling pattern according to literature [174]. Exemplary spectra from Entry 3 (Table 34) are shown in Figure 49 and Figure 50.

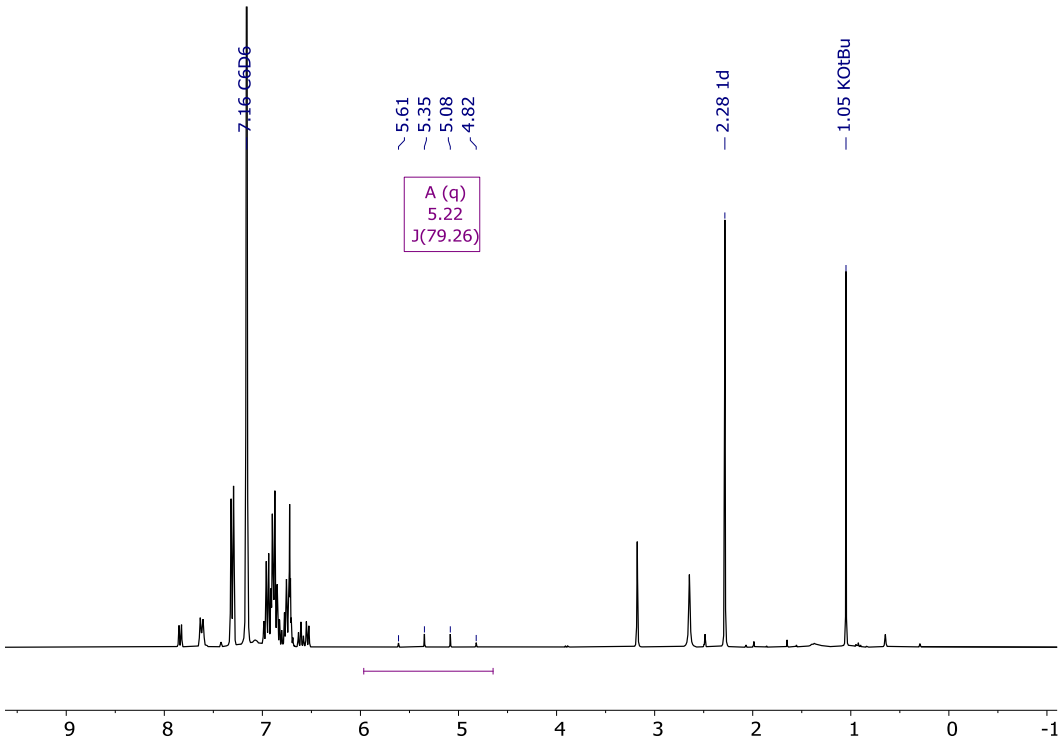

Figure 49: ^{1}H NMR corresponding to Table 34, Entry 2.

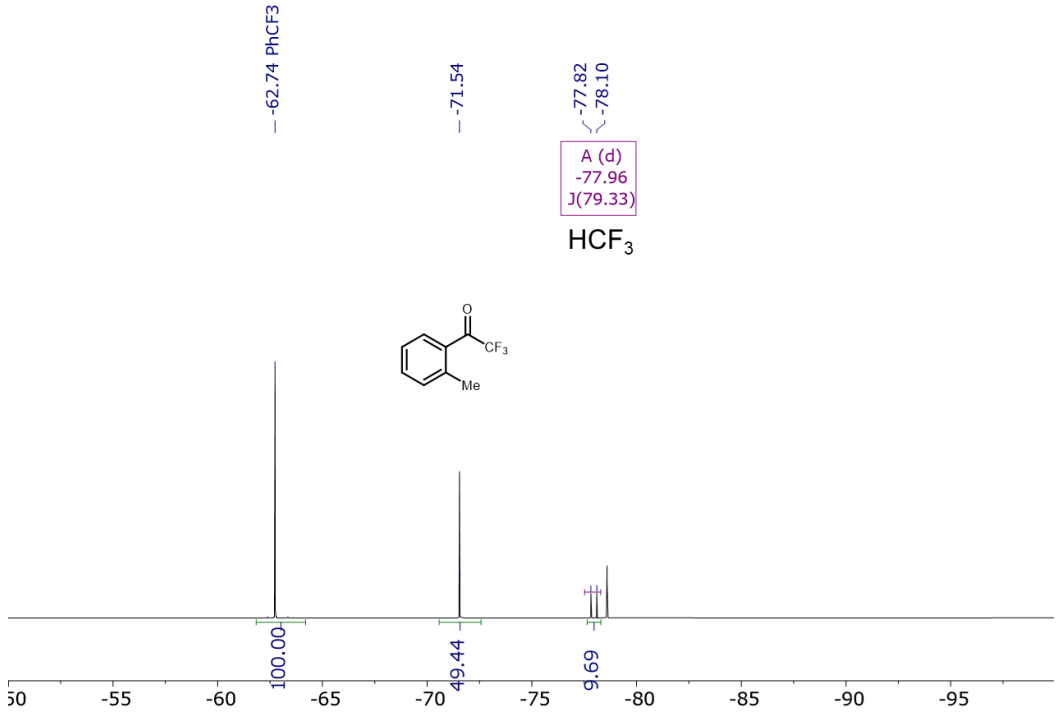

Figure 50: ^{19}F NMR corresponding to Table 34, Entry 2.

With the established bases, the ring-opening reaction under base catalysis of the three previously determined candidates **3.26**, **3.29** and **3.53** was compared (Table 15). Samples of benzocyclobutenols (50.0 µmol) were dissolved in C_6D_6 (0.5 mL) in an NMR tube and base (25 µmol, 0.5 eq.) was added. The samples were placed in a metal heating block and the reaction progress was monitored by ^{1}H NMR and ^{19}F NMR with $PhCF_3$ as internal standard after 16 h at 30 °C.

Table 35: Reaction of the three MOST candidates with organic bases, reactions performed on 0.05 mmol scale in C_6D_6 under inert gas atmosphere. Yields determined by ^1H NMR with mesitylene and ^{19}F NMR with $PhCF_3$ as internal standard.

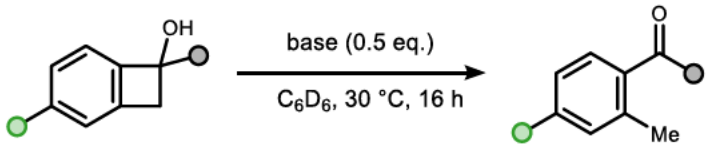

Entry		DBU **2.94**	TBD **3.55**	*N*-Me-TBD **3.56**
1	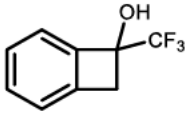 **3.26**	7% yield	89% yield	34% yield
2	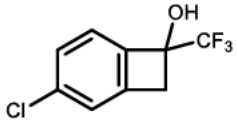 **3.29**	22% yield [a]	78% yield [a]	93% yield [a]
3	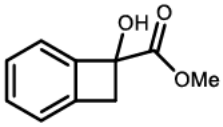 **3.53**	38% yield [a]	38% yield [a]	78% yield [a]

[a] Solution changes colour upon addition of base.

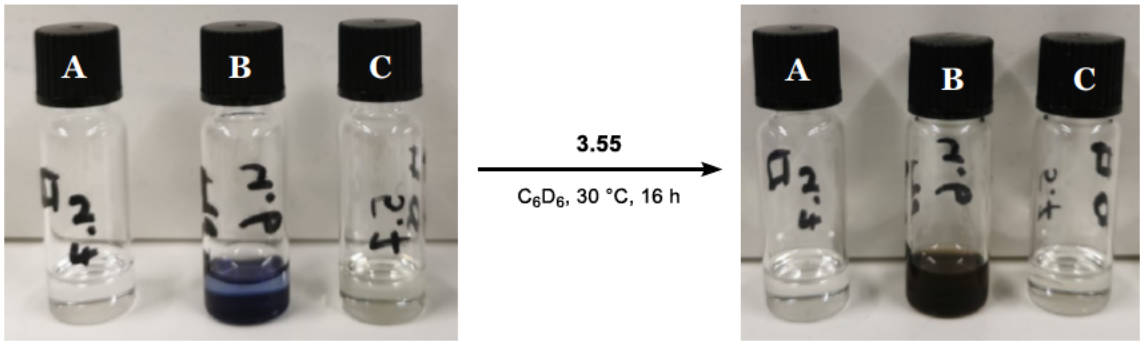

Figure 51: Visual colour change of a colourless solution after addition of 3.55, corresponding to Table 15. Left: Picture taken 30 s after injection of base, right: after 16 h. A) Reaction of 3.26, B) 3.53, C) 3.29.

4.3.5.3 Determination of the energy storage density

DSC studies were performed on a *μRC*® micro Reaction Calorimeter (Figure 52) which uses standard HPLC vials. For each measurement, two identical samples were added to the sample and reference chamber. The mixture in the sample chamber was stirred using 8 x 1.5 mm *VWR* PTFE Micro Stirrer Bars (Cat No. 442-0364) at 400 rpm unless stated otherwise. The *μRC*® micro Reaction

Calorimeter features a syringe holder, that can be loaded with precision syringes and allows the controlled release of substance *via* a motorized piston. For a sample volume around or above 1 mL, the syringe will reach into solution to achieve a good distribution of the added substance without impeding the stirring function.

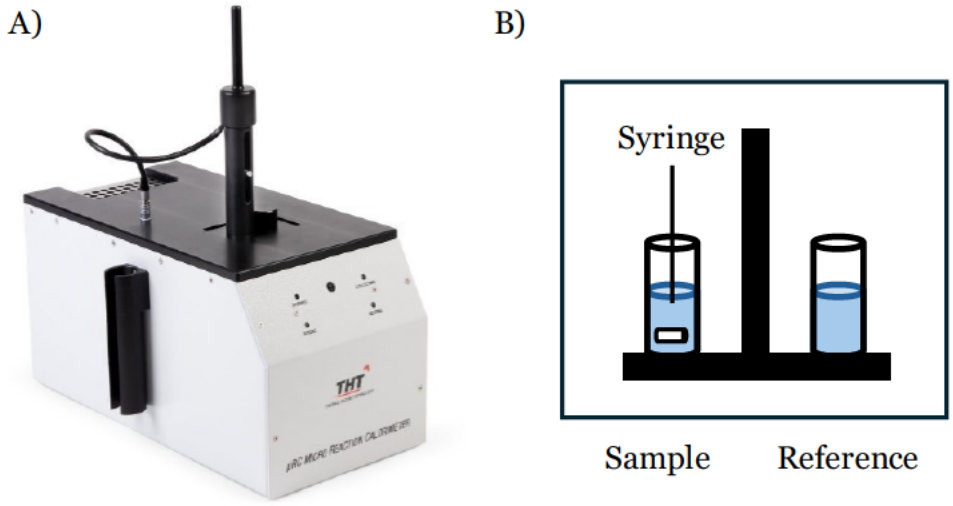

Figure 52: A) *µRC*® micro Reaction Calorimeter with syringe holder attached. B) Illustration of sample and reference chamber. The syringe is submerged in the measuring solution for a sample volume ≥ 1 mL and will not impede the stir bar.

An exemplary measurement is shown in Figure 53. The syringe was equilibrated with the sample chamber to achieve isothermal addition of substances (Figure 53, A). Heating and titration experiments were performed automatically *via* the software (*URC* Control 3.3.8). The software detects a baseline by a moving average calculation, where the baseline will be monitored for 200 s. If the baseline variation is within 0.005 mW/s power gradient threshold, an action can be perfomed, *e.g.* the programmed addition of a selected volume from the syringe (Figure 53, B). After the action has been performed, the baseline is monitored again (Figure 53, C) and the next programmed action will be performed once the baseline is found to be stable.

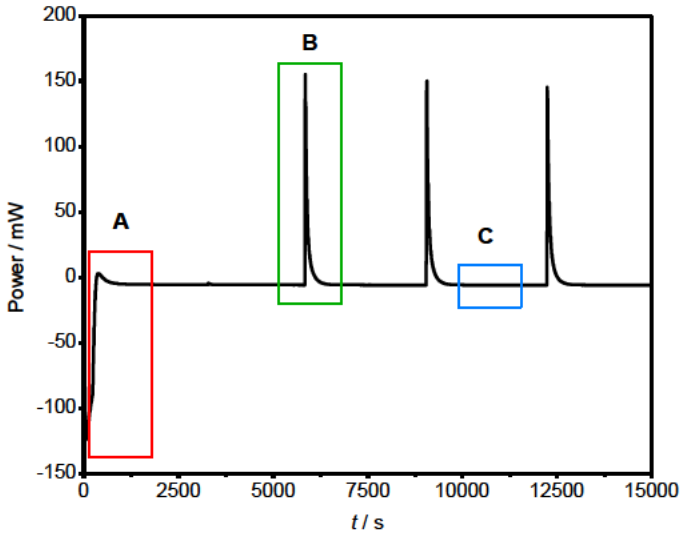

Figure 53: Exemplary DSC measurement with the different action modes highlighted. A) Equilibration of the measurement cell and syringe. B) Example of an exothermic reaction after syringe movement. Here: addition of 3d into MeTBD toluene. C) Selected example of a baseline interval. After reaching the desired specification, another injection is performed.

Addition of substrate 3.26

Base **3.56** (104 mg, 97.0 µL, 676 µmol, 0.96 eq.) was dissolved in toluene (1 mL) and placed in the sample holder. A sample of benzocyclobutenol **3.26** (132 mg, 100 µL, 700 µmol, 1.00 eq.) was taken up in a weighed precision syringe and loaded into the syringe holder at 90° C. The sample was stirred at 90 °C to equilibrate and **3.26** was injected (5 µL, 30 µL, 30 µL, 30 µL, 5µl). The first injection is measured to ensure that no bubbles developed during the equilibration period as substance could leach out of the syringe into the sample (Table 36, entries 1-4). To evaluate the transformation under catalytic conditions, the same experiment was performed using base **3.56** (10.7 mg, 10.0 µL, 69.6 µmol, 0.10 eq.), toluene (1mL) and benzocyclobutenol **3.26** (131 mg, 100 µL, 696 µmol, 1.00 eq.). The data is listed in Table 36 (entries 5-8)

Table 36: DSC measurements of the addition of 3.26 into a solution of 3.56 in toluene at 90 °C, reaction completion confirmed by ^{19}F NMR with $PhCF_3$ as internal standard.

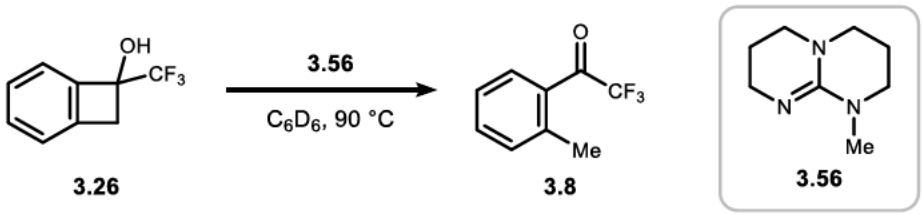

3.26 **3.8** **3.56**

Entry	Added amount of **3.26**	Equivalents base	Energy
1	5 µL (35 µmol)	1.00 eq.	0.090 J
2	30 µL (210 µmol)	1.00 eq.	11.187 J
3	30 µL (210 µmol)	1.00 eq.	11.214 J
4	30 µL (210 µmol)	1.00 eq.	11.343 J
5	5 µL (35 µmol)	0.30 eq.	0.606 J
6	30 µL (209 µmol)	0.30 eq	10.827 J
7	30 µL (209 µmol)	0.30 eq	10.828 J
8	30 µL (209 µmol)	0.30 eq	10.931 J

To evaluate the effect of the heat of mixing of benzocyclobutenol **3.26** into toluene, substrate **3.26** (128 mg, 98µL, 678 µmol) was added to toluene (1 mL). The data is listed in Table 37.

Table 37: Measurement parameters and calculations for the addition of 3.26 to toluene.

Entry	*T* (°C)	*V* (µL)	Integration value (J)	Integration value (J/g)	Integration value (kJ/mol)
1	90	5	–0.021833	–3.34	–0.63
2	90	30	–1.196477	–30.47	–5.73
3	90	30	–1.114938	–28.39	–5.34
4	90	30	–1.025931	–26.13	–4.92

The heat of mixing decreases for each injection, as the amount of benzocyclobutenol **3.26** in solution increases. As the titration shows full conversion per injection, the heat of mixing for 3.26 and toluene can be estimated at –30.5 J/g or –5.7 kJ/mol. The combined averaged results are listed in Table 38.

Table 38: Average values from 6 injections (Table 36) of 3.26 into toluene and 3.56.

Average energy density (J/g)	Average energy density (kJ/mol)	Factor of heat of mixing (J/g)	Factor of heat of mixing (kJ/mol)	Corrected heat release (J/g)	Corrected heat release (kJ/mol)
280.3 ± 3.7	52.7 ± 0.7	–30.5	–5.7	310.8	58.4

Addition of base 3.56

To verify these findings, a second approach was taken to establish the heat release by inverting the addition of base and substrate. The desired substance is diluted with a suitable solvent and a catalytic amount of base is added. The sequence was programmed to consist of two injections of 50 µL, one for the reaction and one to control the success of the transformation. Leaching of catalytic amounts of base in the equilibration period of the measurement must be prevented to ensure correct measurement of the induced heat release. Therefore, smaller volumes are used to minimize possible contact between syringe and sample before measurement.

Base **3.56** (16.0 mg, 15.0 µL, 104 µmol, 0.19 eq.) was dissolved in toluene (135 µL) and the precision syringe was filled with the mixture. The syringe was equilibrated in measuring position with an empty vial at 90 °C for 10 min. In a separate vial, substrate **3.26** (103 mg, 545 µmol, 1.00 eq.) was dissolved in toluene (0.2 mL). The syringe holder was removed briefly, cleaned with a paper cloth and the sample vial was added to the sample holder. After equilibration, the base **3.56** mixture in toluene was added as a drop (50 µL, 0.06 eq. base) to the sample solution, which was stirred at 400 rpm. The measurement was repeated with different concentrations of base and **3.26** to confirm the robustness of the measured values. First base **3.56** (21.3 mg, 20.0 µL, 139 µmol, 0.51 eq.), toluene (200 µL) and substrate **3.26** (103 mg, 545 µmol, 1.00 eq.) in toluene (0.2 mL) were used in the same procedure with two injections (2 x 25 µL, each 0.05 eq. base). It was also repeated with base **3.56** (21.3 mg, 20.0 µL, 140 µmol, 0.25 eq.), toluene (120 µl) and cyclobutanol **3.26** (104 mg, 550 µmol, 1.00 eq.) in toluene (0.2 mL) in one injection of base (75 µL, 0.13 eq. base). To measure the heat of mixing, the same procedure was repeated with base **3.56** (16.0 mg, 15.0 µL, 104 µmol) in

toluene (135µl) and a sample vial filled with toluene (330 µL). The combined data is listed in Table 39.

Table 39: DSC measurements of the dropwise addition of 3.56 in toluene into a solution of 3.26 in toluene (0.2 mL), reactions performed at 90 °C.

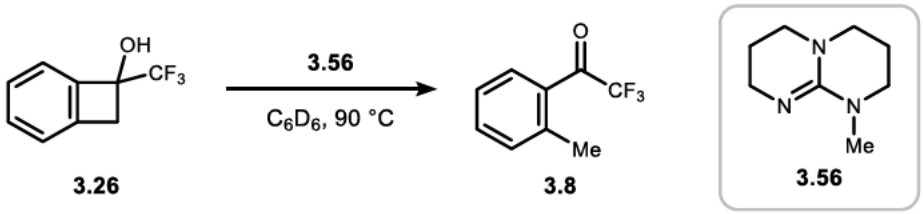

3.26 **3.8** **3.56**

Entry	Amount of **3.26**	Equivalents of added base	Energy
1	550 µmol	0.06 eq. (50 µL)	32.442 J
2	271 µmol	0.05 eq. (25 µL)	15.337 J
3	550 µmol	0.13 eq (75 µL)	32.214 J
4	-	50 µL	–0.092 J

4.3.6 Cyclability of the system

The isomerization process was studied using ^{19}F NMR. A sample of acetophenone **3.8** (99.6 mg, 492 µmol, 1.00 eq.) was dissolved in benzene (5 mL, 100 mM) in an oven dried Schlenk-flask under inert gas atmosphere and the mixture was degassed (3 × freeze-pump-thaw, liquid nitrogen). The solution was irradiated for 3 h with a 40 W 370 nm Gen 2 KSPR160L Kessil LED from 1 cm distance. $PhCF_3$ (18.0 mg, 15.0 µL, 123 µmol, 0.25 eq.) was added using a Hamilton syringe as an internal reference. The reaction yield in both transformations, that is photocyclization and opening was found to be unchanged upon addition of $PhCF_3$ and mesitylene as internal reference compounds for NMR analysis. A sample (0.1 mL) was taken, diluted with C_6D_6 (0.4 mL) and subjected to ^{19}F NMR analysis. Base **3.57** (*Biotage*® PS-TBD, 1.3 mmol/g, 196 mg, 255 µmol, 0.518 eq.) was added to a 10 mL flask and the mixture was transferred along with the sample taken for NMR analysis. The NMR tube was washed with benzene (2 x 0.5 mL), then the flask (3 x 1 mL). The mixture was placed in a heating block and stirred for 24 h at 30 °C. $PhCF_3$ (18.0 mg, 15.0 µL, 123 µmol, 0.25 eq.) was added, the mixture was stirred for 5 minutes, sonicated for 3 minutes and another sample was taken for NMR analysis (0.1 mL diluted with 0.4 mL C_6D_6). The mixture was filtered over a 2 cm thick celite pad with 0.5 cm sand on top, the NMR tube was transferred over the filter and washed (2 x 0.5 mL benzene) and the flask was

rinsed (3 x 1mL benzene). Then the filter was washed with portions of benzene (25 mL total), $PhCF_3$ (18.0 mg, 15.0 µL, 123 µmol, 0.25 eq.) was added and another NMR sample (0.3 mL, diluted with 0.2 mL C_6D_6) was taken. The sample was transferred back (2 x 0.5mL benzene), degassed (3 × freeze-pump-thaw, liquid nitrogen) and irradiated for 3 h with a 40 W 370 nm Gen 2 KSPR160L Kessil LED from 1 cm distance. $PhCF_3$ (18.0 mg, 15.0 µL, 123 µmol, 0.25 eq.) was added and the final NMR sample was taken (0.3 mL, diluted with 0.2 mL C_6D_6). A second run was performed using acetophenone **3.8** (101 mg, 498 µmol, 1.00 eq.), PS-TBD **3.57** (173 mg, 224 µmol, 0.451 eq.) and benzene (5 mL, 100 mM). The combined data is summarized in Table 40.

Table 40: Charge/Discharge experiments for the system 3.8⇄3.26. Reaction performed on 0.5 mmol scale in degassed benzene (100 mM) at 30 °C, yields determined by ^{19}F NMR with $PhCF_3$ as internal standard as the mean value of two experiments. hυ= 370 nm Kessil LED, base = 3.57 (0.50 eq.). [a] 98% recovered 3.8 by amount of substance from filter cake.

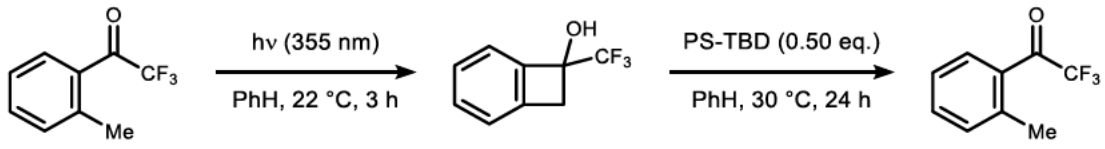

3.8 **3.26** **3.8**

1st irradiation	99.8% ± 0.1% yield[a]
Base opening	90.1% ± 0.5% yield[a]
Recovery	98.1% ± 1.3% yield
2nd irradiation	98.8% ± 0.6% yield[a]

4.3.7 Crystallographic Data

All X-ray measurements and structure refinements were performed by [redacted]

X-ray crystal structure analysis of 3.26 (hma4217)

A colourless plate of $C_9H_7F_3O$, approximate dimensions 0.050 mm × 0.120 mm × 0.210 mm, was used for the X-ray crystallographic analysis. The X-ray intensity data were measured on a STOE IPDS-2T Diffractometer system. CCDC number: 2371853.

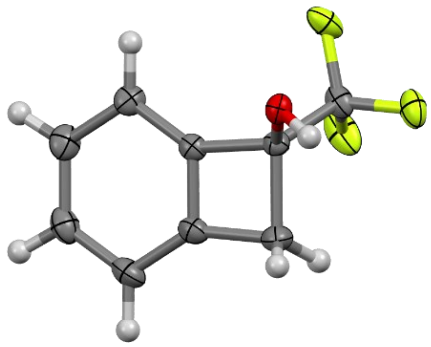

Figure 54: Graphical representation of the X-Ray structure of 3.26.

Table 41: Crystal data and structure refinement for 3.26 (hma4217)

Identification code	hma4217
Empirical formula	$C_9H_7F_3O$
moiety formula	$C_9H_7F_3O$
Formula weight	188.15
Temperature	120(2) K
Wavelength, radiation type	0.71073Å, MoKα
Diffractometer	STOE IPDS 2T
Crystal system	Monoclinic
Space group name, number	P 2_1/n, (14)
Unit cell dimensions	a = 11.1506(5) Å
	b = 12.4828(3) Å
	c = 18.7500(8) Å
Volume	2575.06(17) $Å^3$
Number of reflections	30640
and range used for lattice parameters	2.47° <=θ<= 28.51°
Z	12
Density (calculated)	1.456 Mg/m3
Absorption coefficient	0.137 mm-1
Absorption correction	Integration
Max. and min. transmission	0.9930 and 0.9743
F(000)	1152
Crystal size, colour and form	0.050 x 0.120 x 0.210 mm3, colourless plate
Theta range for data collection	2.468 to 28.165°.
Index ranges	-14<=h<=14, -16<=k<=14, -24<=l<=24
Number of reflections:	
collected	31080
independent	6251 [R(int) = 0.0290]
observed [I>2sigma(I)]	4579
Completeness to theta = 25.2°	99.9 %
Refinement method	Full-matrix least-squares on F2
Data / restraints / parameters	6251 / 57 / 442
Goodness-of-fit on F2	1.133
Final R indices [I>2sigma(I)]	R1 = 0.0579, wR2 = 0.1198
R indices (all data)	R1 = 0.0857, wR2 = 0.1396
Largest diff. peak and hole	0.475 and -0.265 $eÅ^{-3}$
Remark	OH's localized and refined, three independent molecules, one is disordered

X-ray crystal structure analysis of 3.28 (hma4218)

A colourless block of $C_9H_7F_3O_3$, approximate dimensions 0.340 mm × 0.460 mm × 0.460 mm, was used for the X-ray crystallographic analysis. The X-ray intensity data were measured on a STOE IPDS-2T Diffractometer system. CCDC number: 2371855.

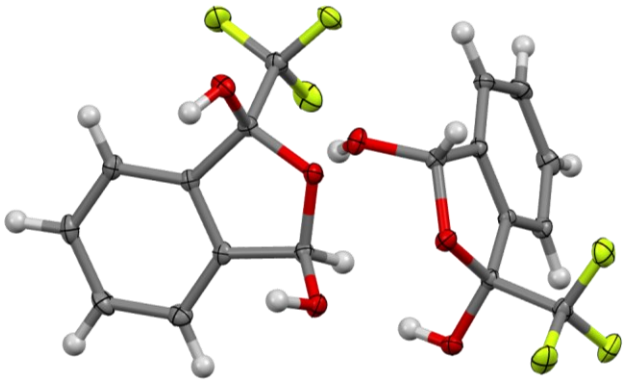

Figure 55: Graphical representation of the X-Ray structure of 3.28.

Table 42: Crystal data and structure refinement for 3.28 (hma4218)

Identification code	hma4218
Empirical formula	$C_9H_7F_3O_3$
moiety formula	$C_9H_7F_3O_3$
Formula weight	220.15
Temperature	120(2) K
Wavelength, radiation type	0.71073Å, MoKα
Diffractometer	STOE IPDS 2T
Crystal system	Triclinic
Space group name, number	P -1, (2)
Unit cell dimensions	a = 8.2210(5) Å
	b = 10.0720(6) Å
	c = 11.6095(7) Å
Volume	908.38(10) Å3
Number of reflections	12284
and range used for lattice parameters	2.88° <=θ<= 28.36°
Z	4
Density (calculated)	1.610 Mg/m3
Absorption coefficient	0.158 mm-1
Absorption correction	Integration
Max. and min. transmission	0.9688 and 0.9058
F(000)	448
Crystal size, colour and form	0.340 x 0.460 x 0.460 mm3, colourless block
Theta range for data collection	2.878 to 27.956°.
Index ranges	-9<=h<=10, -13<=k<=13, -15<=l<=15
Number of reflections:	
collected	8300
independent	4302 [R(int) = 0.0228]
observed [I>2sigma(I)]	3700
Completeness to theta = 25.2°	99.7 %
Refinement method	Full-matrix least-squares on F2
Data / restraints / parameters	4302 / 0 / 325
Goodness-of-fit on F2	1.070
Final R indices [I>2sigma(I)]	R1 = 0.0433, wR2 = 0.1057
R indices (all data)	R1 = 0.0527, wR2 = 0.1119
Largest diff. peak and hole	0.472 and -0.253 eÅ-3
Remark	isotropic refinement for H-atoms

X-ray crystal structure analysis of 3.30 (hma4316)

A colourless block of $C_9H_6ClF_3O_3$, approximate dimensions 0.110 mm × 0.310 mm × 0.540 mm, was used for the X-ray crystallographic analysis. The X-ray intensity data were measured on a STOE IPDS-2T Diffractometer system. CCDC number: 2371857.

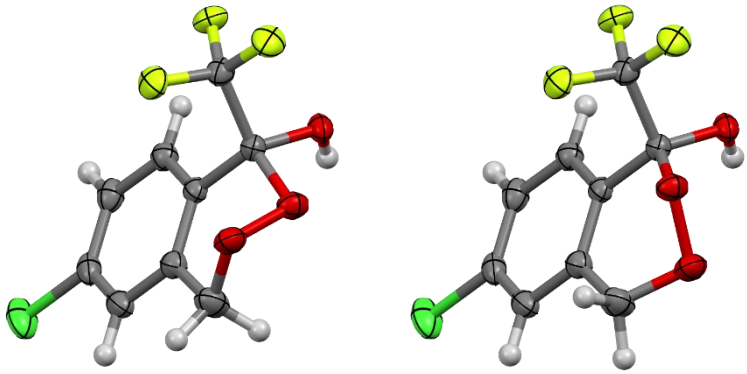

Figure 56: Graphical representation of the X-Ray structure of 3.30. Two conformers of the 6-membered ring containing the cyclic peroxide crystallized together and are depicted separately.

Table 43: Crystal data and structure refinement for 3.30 (hma4316)

Identification code	hma4316
Empirical formula	$C_9H_6ClF_3O_3$
moiety formula	$C_9H_6ClF_3O_3$
Formula weight	254.59
Temperature	120(2) K
Wavelength, radiation type	0.71073Å, MoKα
Diffractometer	STOE IPDS 2T
Crystal system	Monoclinic
Space group name, number	P 2_1/c, (14)
Unit cell dimensions	a = 7.1493(6) Å
	b = 7.7680(6) Å
	c = 17.9137(15) Å
Volume	974.87(14) Å3
Number of reflections	9880
and range used for lattice parameters	2.62° <=θ<= 28.42°
Z	4
Density (calculated)	1.735 Mg/m3
Absorption coefficient	0.426 mm-1
Absorption correction	Integration
Max. and min. transmission	0.9595 and 0.7963
F(000)	512
Crystal size, colour and form	0.110 x 0.310 x 0.540 mm3, colourless plate
Theta range for data collection	2.867 to 27.934°.
Index ranges	-9<=h<=9, -9<=k<=10, -23<=l<=23
Number of reflections:	
collected	5169
independent	2313 [R(int) = 0.0207]
observed [I>2sigma(I)]	2011
Completeness to theta = 25.2°	99.8 %
Refinement method	Full-matrix least-squares on F2
Data / restraints / parameters	2313 / 3 / 155
Goodness-of-fit on F2	1.117
Final R indices [I>2sigma(I)]	R1 = 0.0412, wR2 = 0.1008
R indices (all data)	R1 = 0.0493, wR2 = 0.1081
Largest diff. peak and hole	0.514 and -0.240 eÅ-3
Remark	O8/O9 disordered, H11 was localized and refined with isotropic displacement parameters

X-ray crystal structure analysis of 3.42 (hma4347)

A colourless needle of $C_{10}H_8ClF_3O$, approximate dimensions 0.030 mm × 0.040 mm × 1.300 mm, was used for the X-ray crystallographic analysis. The X-ray intensity data were measured on a STOE IPDS-2T Diffractometer system. CCDC number: 2371856.

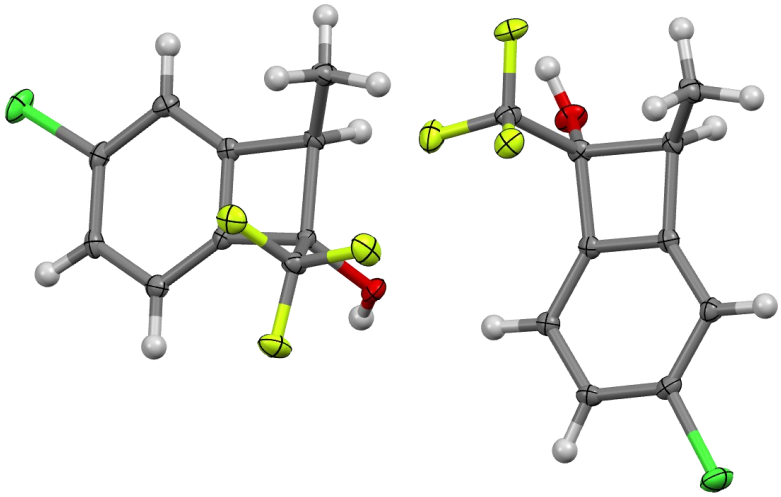

Figure 57: Graphical representation of the X-Ray structure of 3.42.

Table 44: Crystal data and structure refinement for 3.42 (hma4316)

Identification code	hma4347
Empirical formula	$C_{10}H_8ClF_3O$
moiety formula	$C_{10}H_8ClF_3O$
Formula weight	236.61
Temperature	120(2) K
Wavelength, radiation type	0.71073Å, MoKα
Diffractometer	STOE IPDS 2T
Crystal system	Monoclinic
Space group name, number	P 2_1/c, (14)
Unit cell dimensions	a = 11.6109(7) Å
	b = 9.4108(5) Å
	c = 18.7097(12) Å
Volume	2009.1(2) $Å^3$
Number of reflections	7425
and range used for lattice parameters	2.43° <=θ<= 28.52°
Z	8
Density (calculated)	1.564 Mg/m^3
Absorption coefficient	0.392 mm^{-1}
Absorption correction	None
F(000)	960
Crystal size, colour and form	0.030 x 0.040 x 1.300 mm^3, colourless needle
Theta range for data collection	2.431 to 28.040°.
Index ranges	-15<=h<=15, -12<=k<=12, -24<=l<=22
Number of reflections:	
collected	10422
independent	4857 [R(int) = 0.0506]
observed [I>2sigma(I)]	3304
Completeness to theta = 25.2°	99.8 %
Refinement method	Full-matrix least-squares on F^2
Data / restraints / parameters	4857 / 2 / 277
Goodness-of-fit on F^2	1.127
Final R indices [I>2sigma(I)]	R1 = 0.0700, wR2 = 0.1362
R indices (all data)	R1 = 0.1171, wR2 = 0.1623
Largest diff. peak and hole	0.435 and -0.447 $eÅ^{-3}$
Remark	Structure contains two independent molecules

4.4 UV-Spectra

Measurement of all UV-spectra was conducted in collaboration with [redacted].

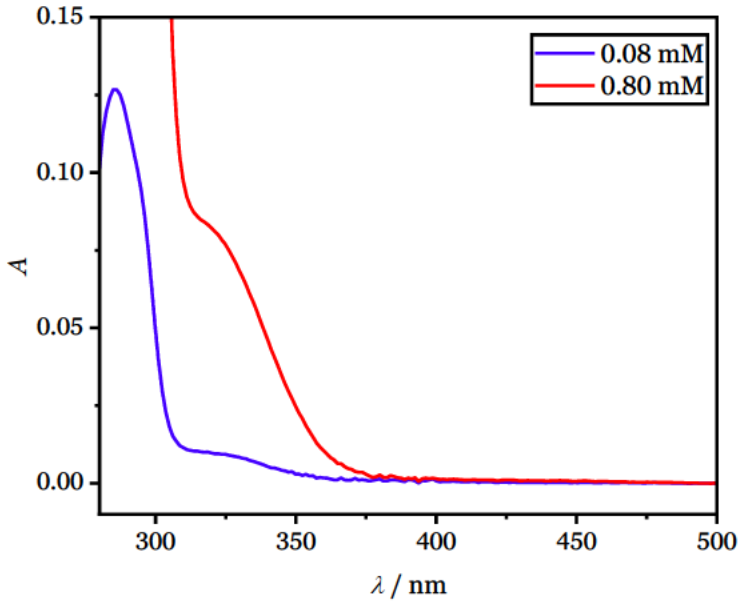

Figure 58: Concentration dependent UV-vis absorption spectrum of 1.9 in benzene at 0.80 ± 0.15 mM (red) and 0.08 ± 0.13 mM (blue).

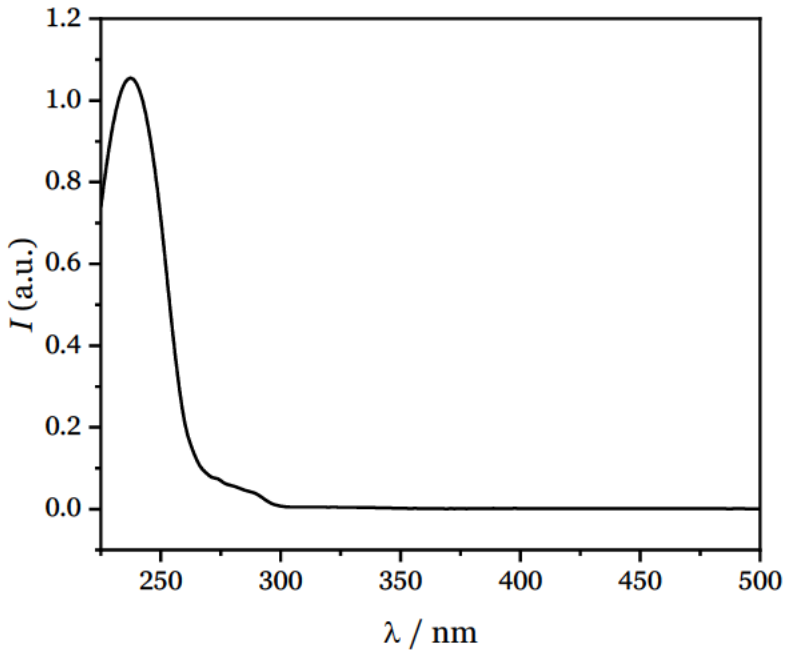

Figure 59: UV Spectrum of 2.5 in acetonitrile at ca. 7 x 10^{-5} mol/l.

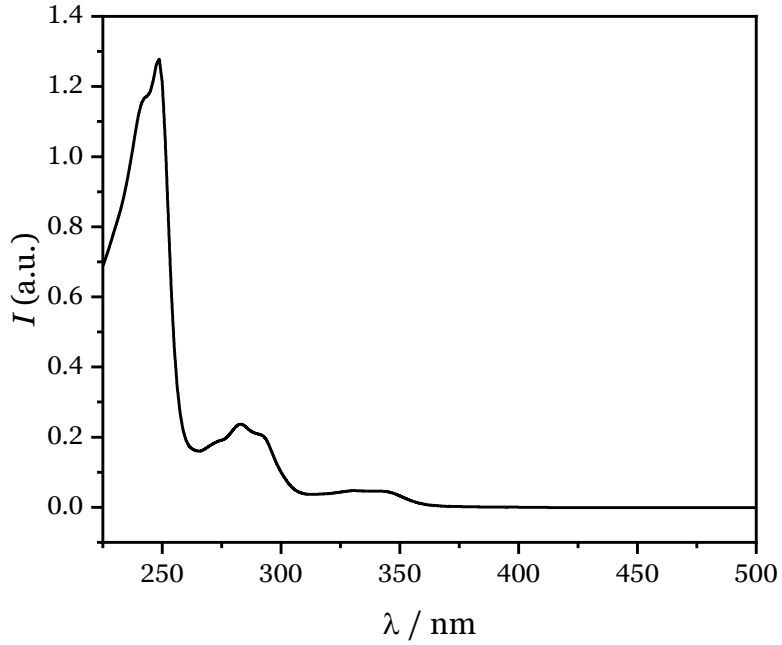

Figure 60: UV Spectrum of 2.45 in acetonitrile at ca. 2 x 10^{-5} mol/l.

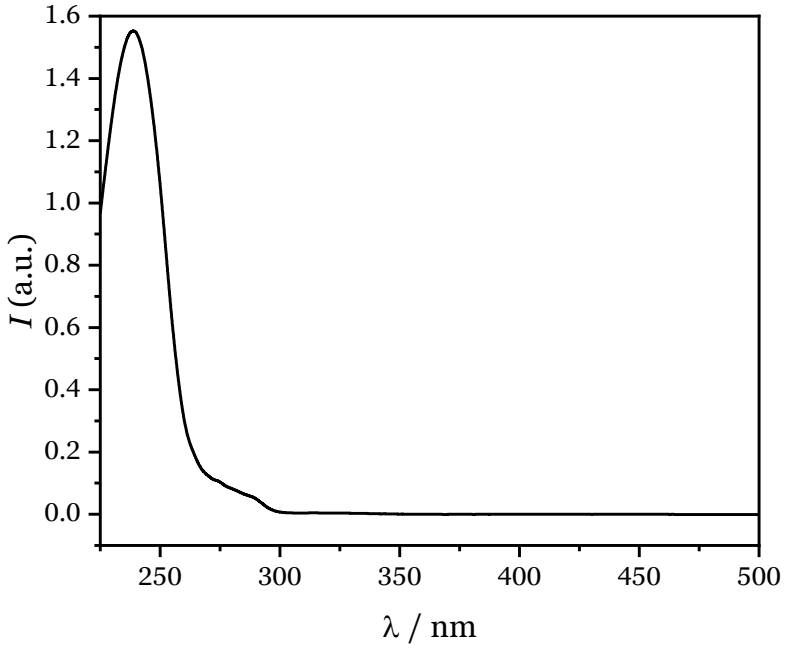

Figure 61: UV Spectrum of 2.38 in acetonitrile at ca. 7 x 10^{-5} mol/l.

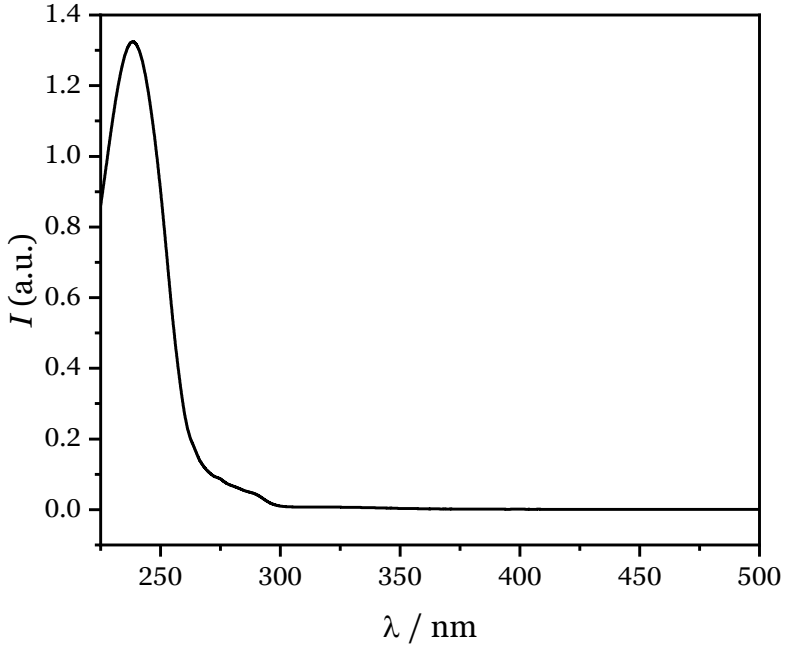

Figure 62: UV Spectrum of 2.39 in acetonitrile at ca. 6 x 10^{-5} mol/l.

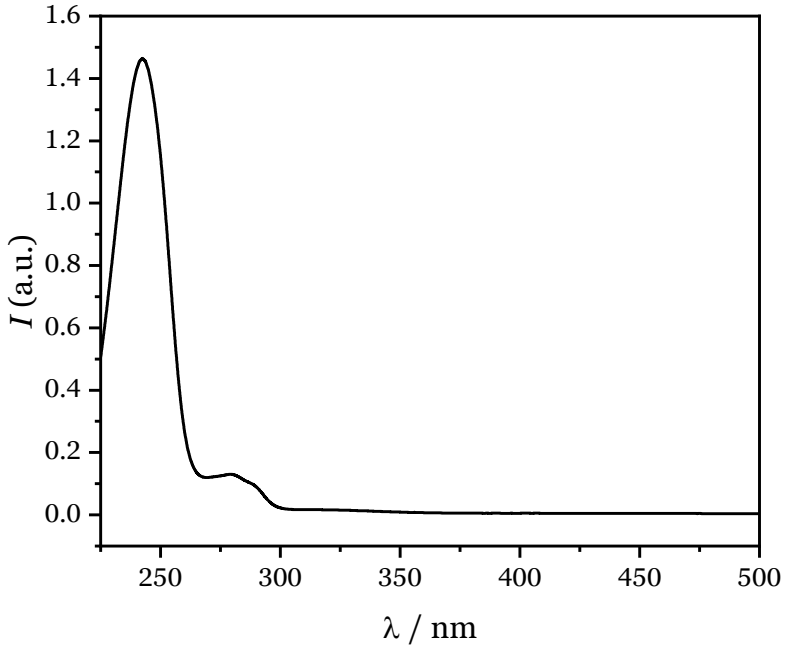

Figure 63: UV Spectrum of 2.40 in acetonitrile at ca. 1 x 10^{-4} mol/l.

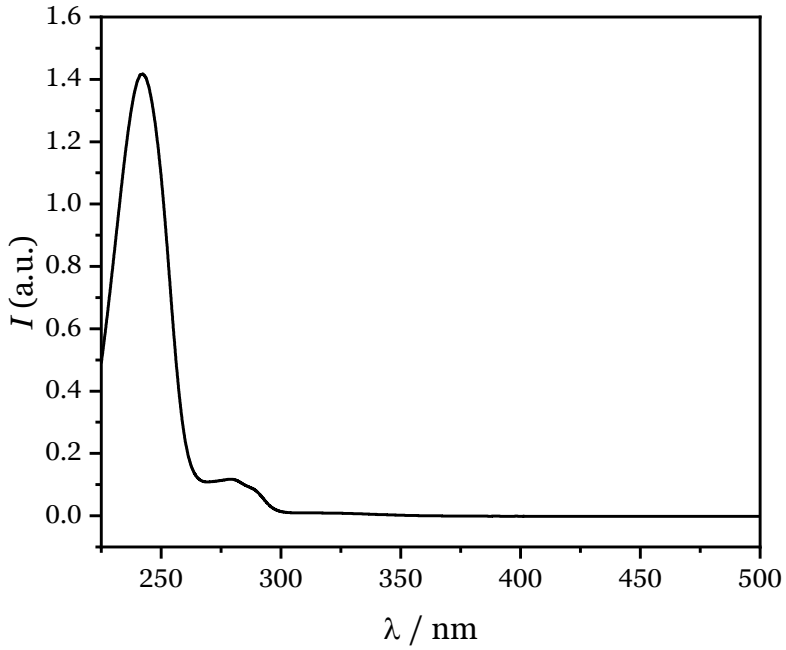

Figure 64: UV Spectrum of 2.41 in acetonitrile at ca. 1 x 10^{-4} mol/l.

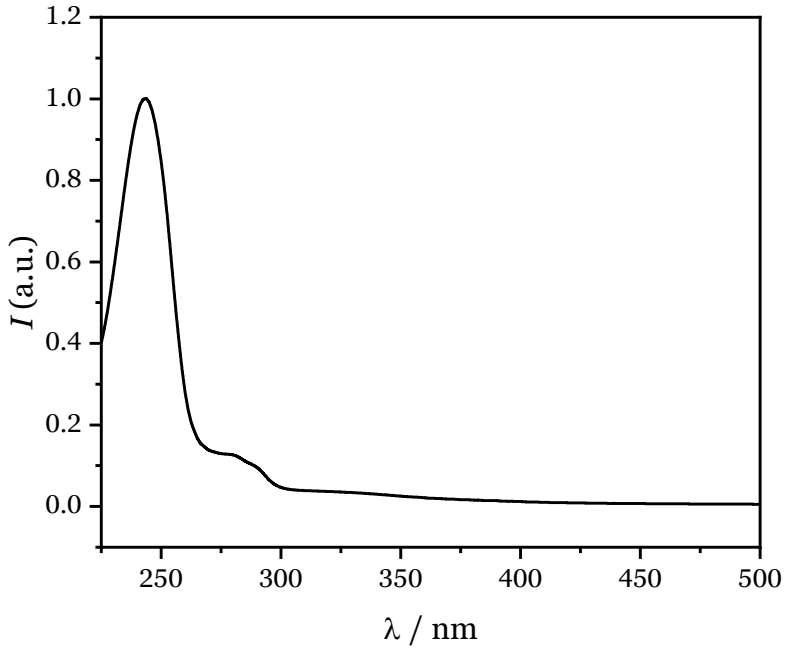

Figure 65: UV Spectrum of 2.42 in acetonitrile at ca. 6 x 10^{-5} mol/l.

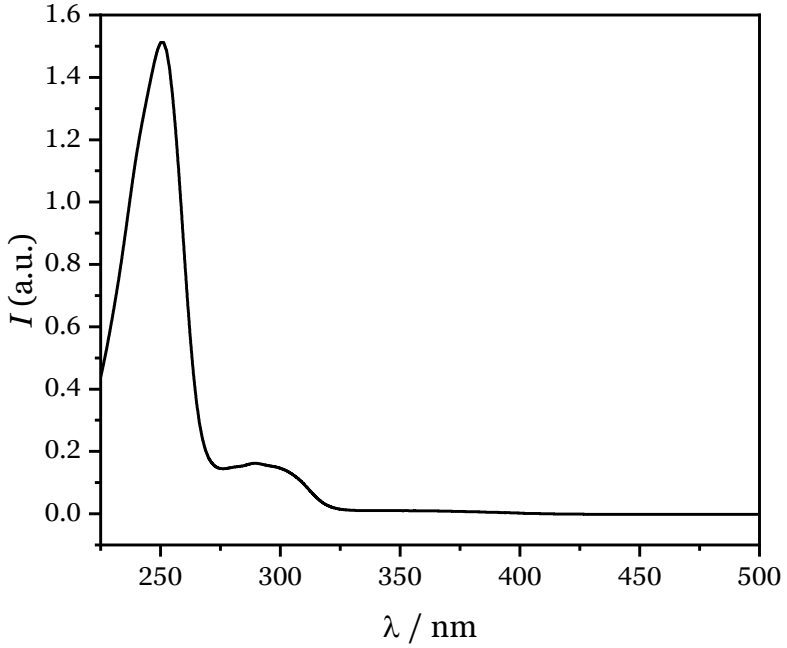

Figure 66: UV Spectrum of 2.43 in acetonitrile at ca. 5 x 10^{-5} mol/l.

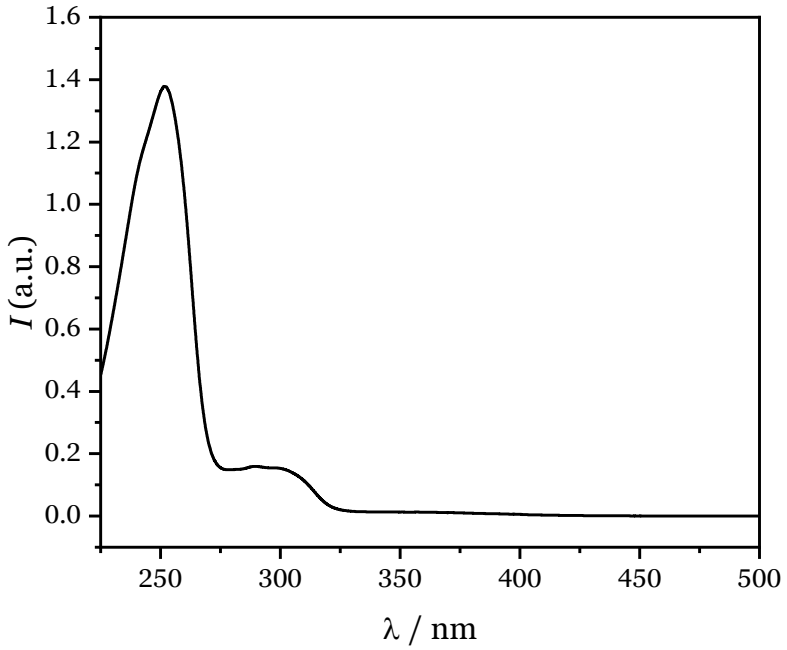

Figure 67: UV Spectrum of 2.44 in acetonitrile at ca. 4 x 10^{-5} mol/l.

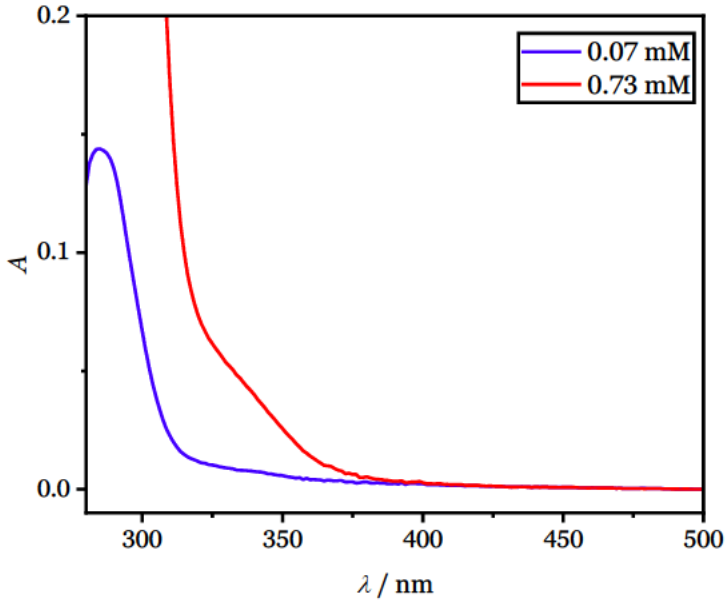

Figure 68: Concentration dependent UV-vis absorption spectrum of *α*-methoxyacetophenone 2.47 in benzene at 0.73 ± 0.15 mM (red) and 0.07 ± 0.13 mM (blue).

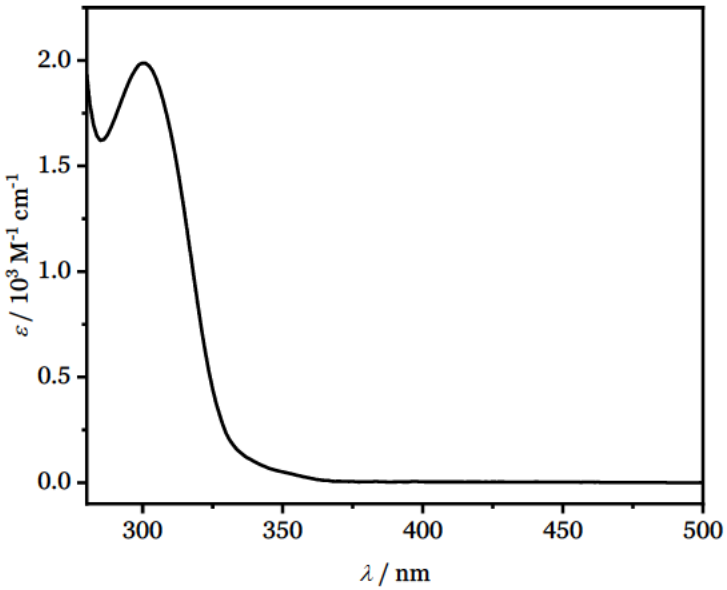

Figure 69: Extinction coefficient of 3.8 in benzene.

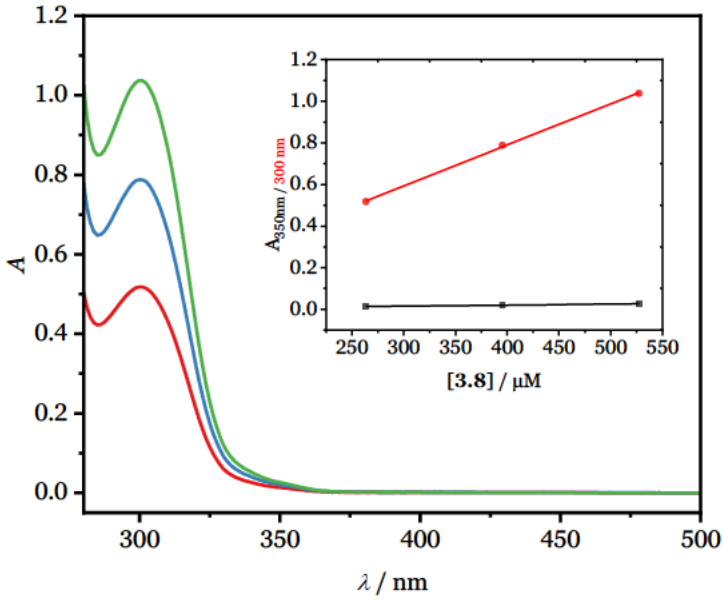

Figure 70: Concentration dependent UV-vis absorption spectrum of 3.8 in benzene. Exact values are summarised in Table 45.

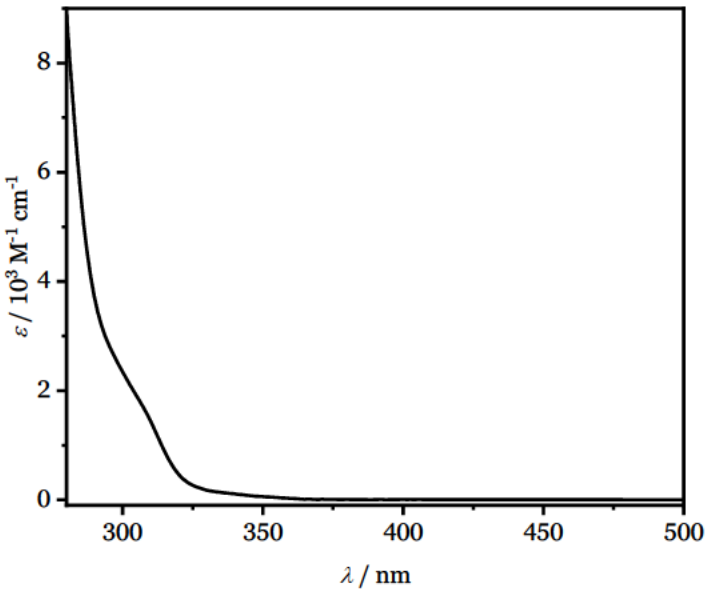

Figure 71: Extinction coefficient of 3.14 in benzene.

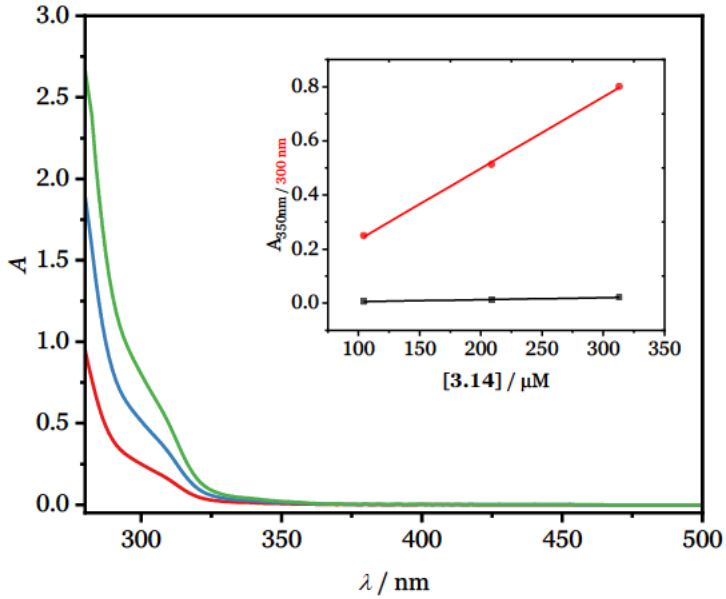

Figure 72: Concentration dependent UV-vis absorption spectrum of 3.14 in benzene. Exact values are summarised in Table 45.

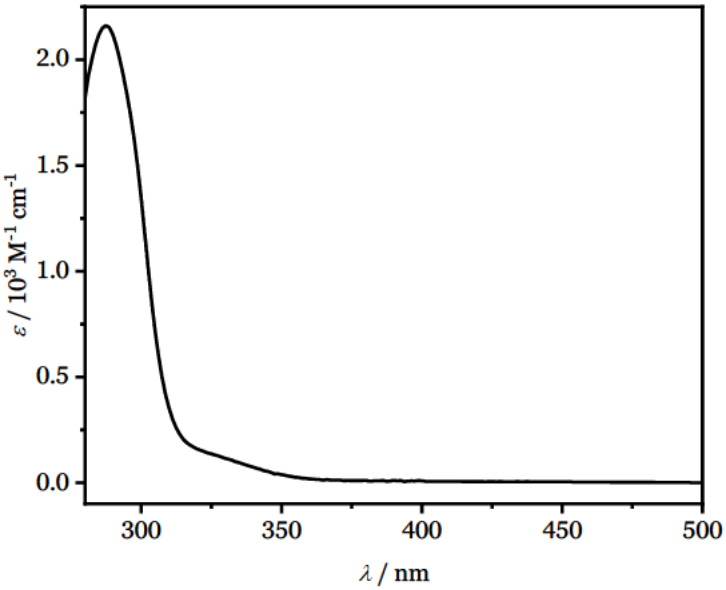

Figure 73: Extinction coefficient of 3.18 in benzene.

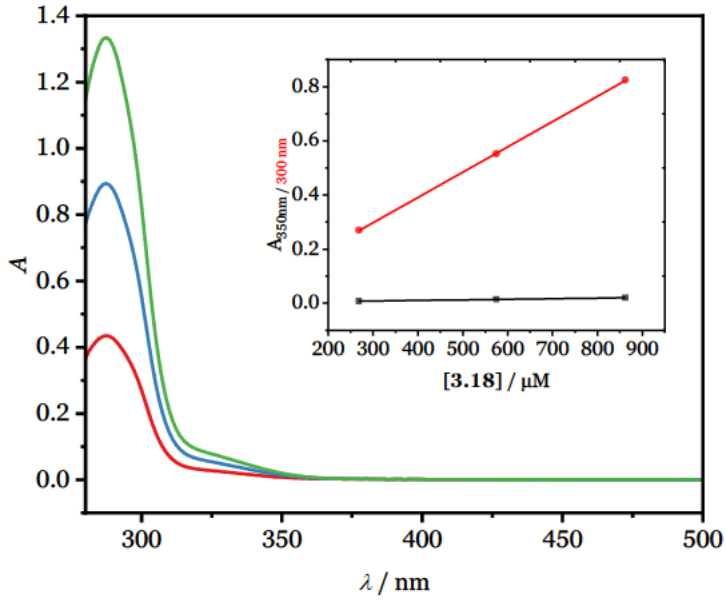

Figure 74: Concentration dependent UV-vis absorption spectrum of 3.18 in benzene. Exact values are summarised in Table 45.

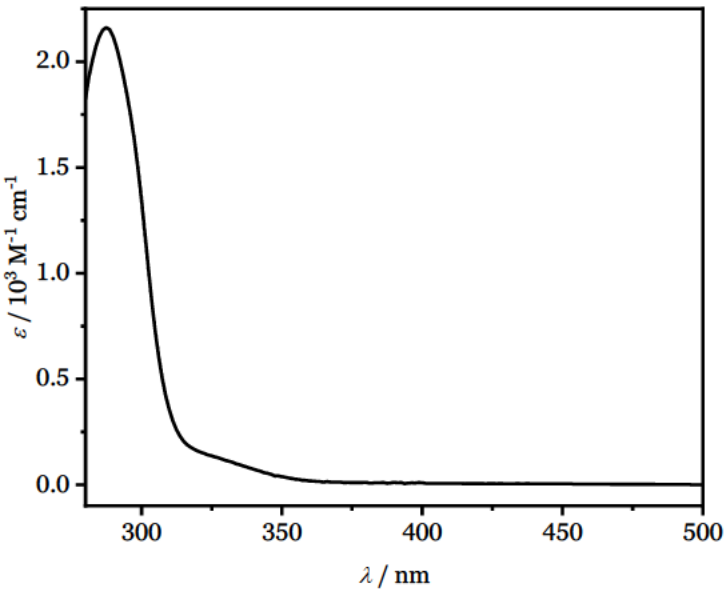

Figure 75: Extinction coefficient of 3.21 in benzene.

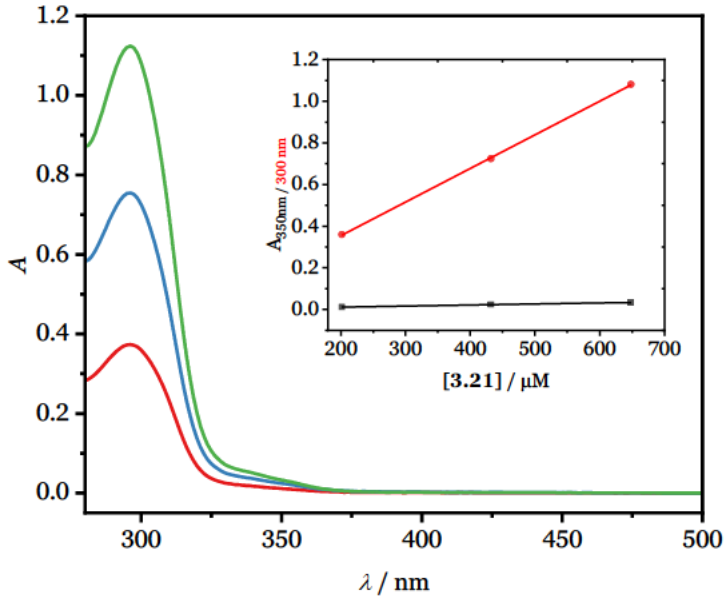

Figure 76: Concentration dependent UV-vis absorption spectrum of 3.21 in benzene. Exact values are summarised in Table 45.

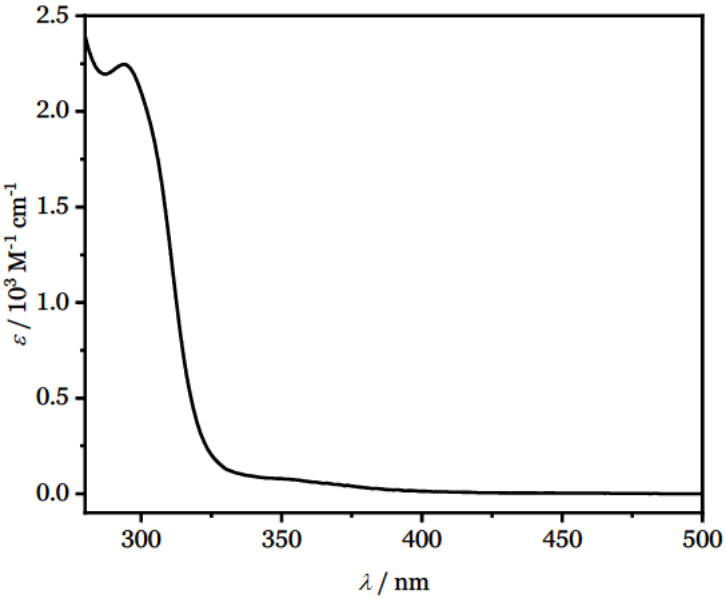

Figure 77: Extinction coefficient of 3.23 in benzene.

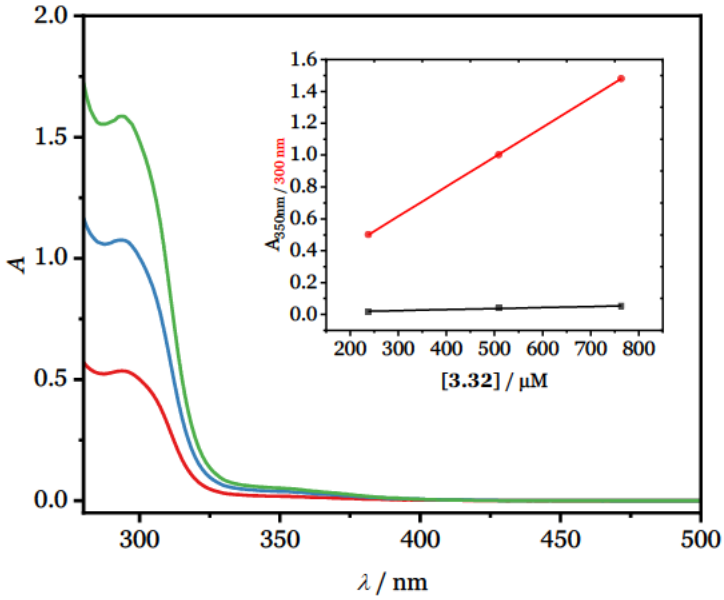

Figure 78: Concentration dependent UV-vis absorption spectrum of 3.23 in benzene. Exact values are summarised in Table 45.

Table 45: Overview of extinction coefficients at 20 °C in benzene.

Entry	Substrate	λ_{abs} / nm	ε / 10^3 M^{-1} s^{-1}
1	**3.8**	300	1.99
		350	0.05
2	**3.14**	300	2.34
		350	0.06
3	**3.18**	300	1.34
		350	0.04
4	**3.21**	300	1.77
		350	0.06
5	**3.23**	300	2.10
		350	0.08

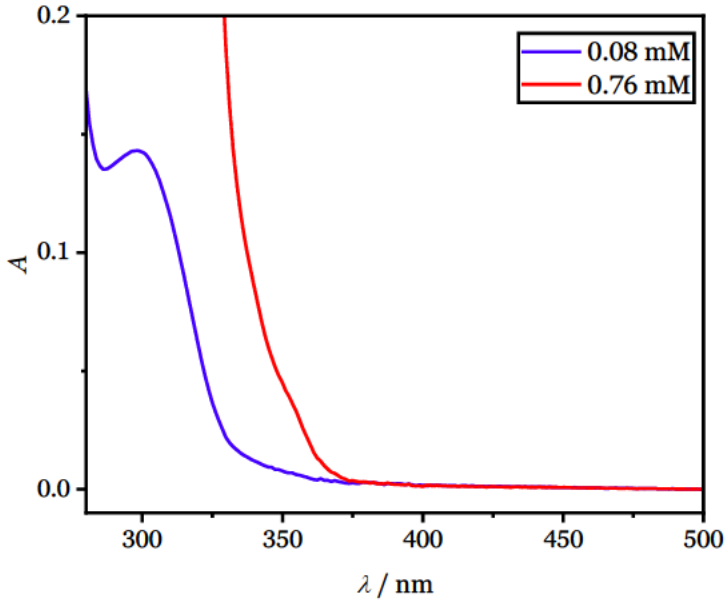

Figure 79: Concentration dependent UV-vis absorption spectrum of 3.9 in benzene at 0.76 ± 0.13 mM (red) and 0.08 ± 0.19 mM (blue).

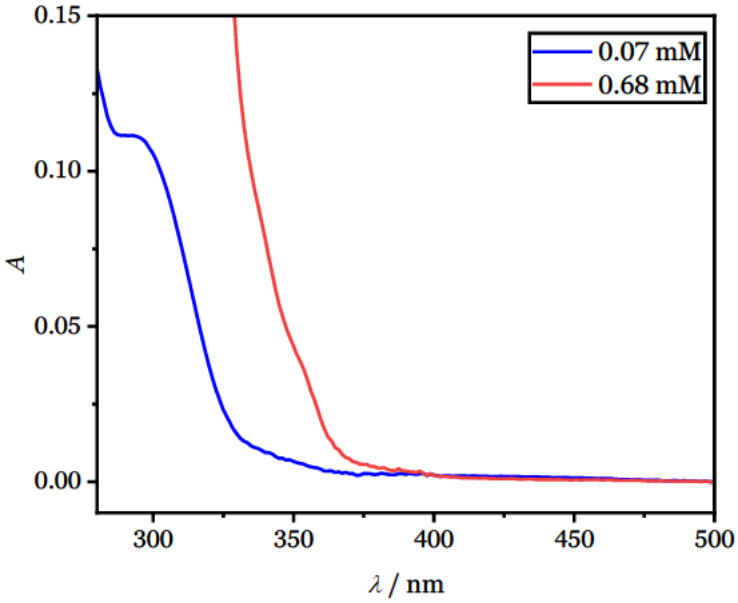

Figure 80: Concentration dependent UV-vis absorption spectrum of 3.10 in benzene at 0.68 ± 0.16 mM (red) and 0.07 ± 0.25 mM (blue).

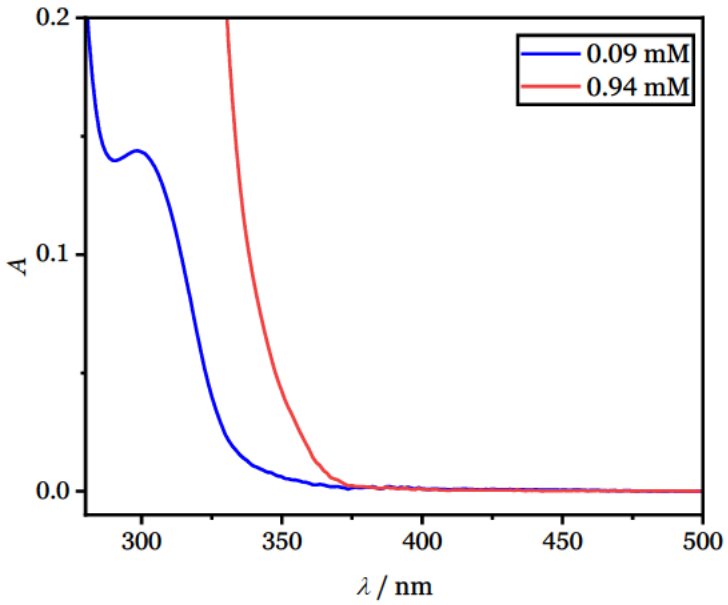

Figure 81: Concentration dependent UV-vis absorption spectrum of 3.11 in benzene at 0.94 ± 0.14 mM (red) and 0.09 ± 0.13 mM (blue).

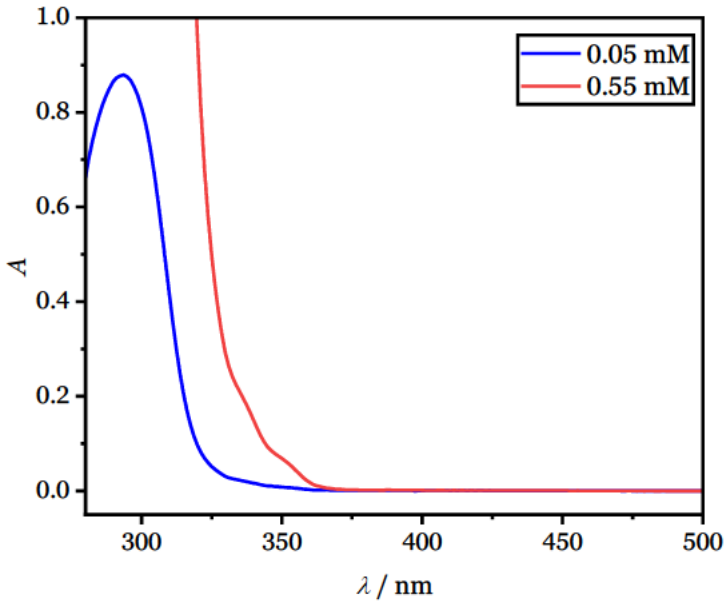

Figure 82: Concentration dependent UV-vis absorption spectrum of 3.12 in benzene at 0.55 ± 0.15 mM (red) and 0.05 ± 0.13 mM (blue).

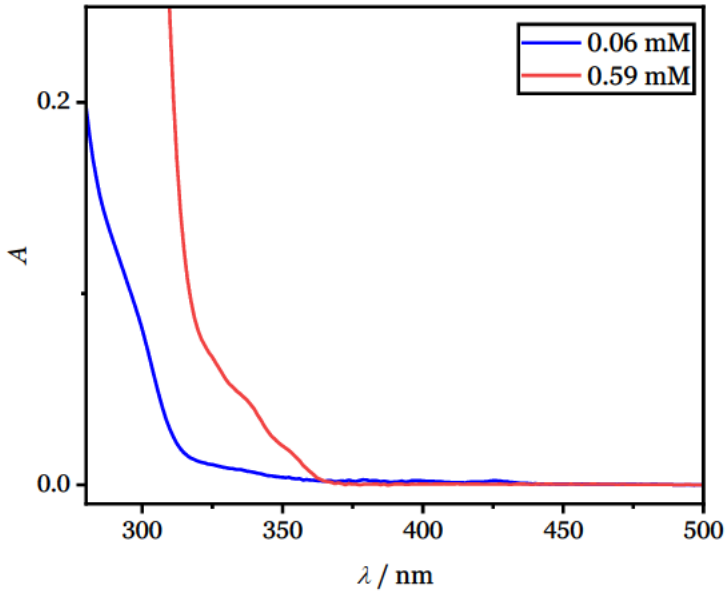

Figure 83: Concentration dependent UV-vis absorption spectrum of 3.13 in benzene at 0.59 ± 0.15 mM (red) and 0.06 ± 0.13 mM (blue).

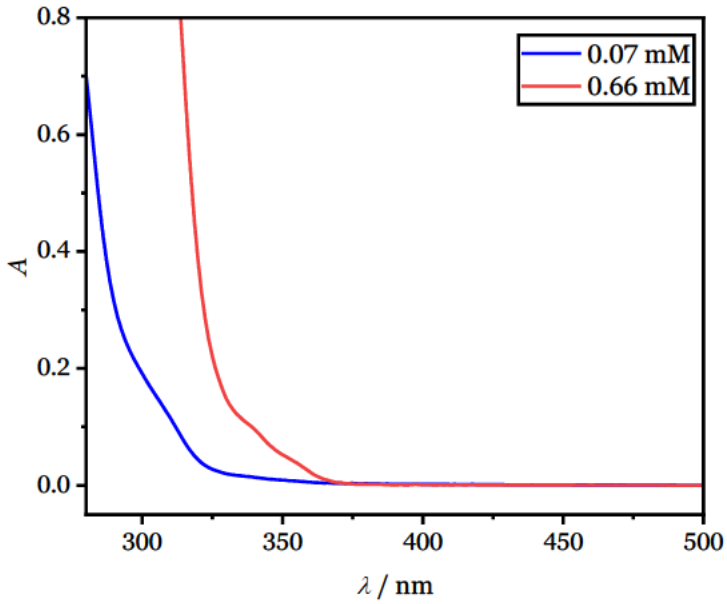

Figure 84: Concentration dependent UV-vis absorption spectrum of 3.15 in benzene at 0.66 ± 0.15 mM (red) and 0.07 ± 0.13 mM (blue).

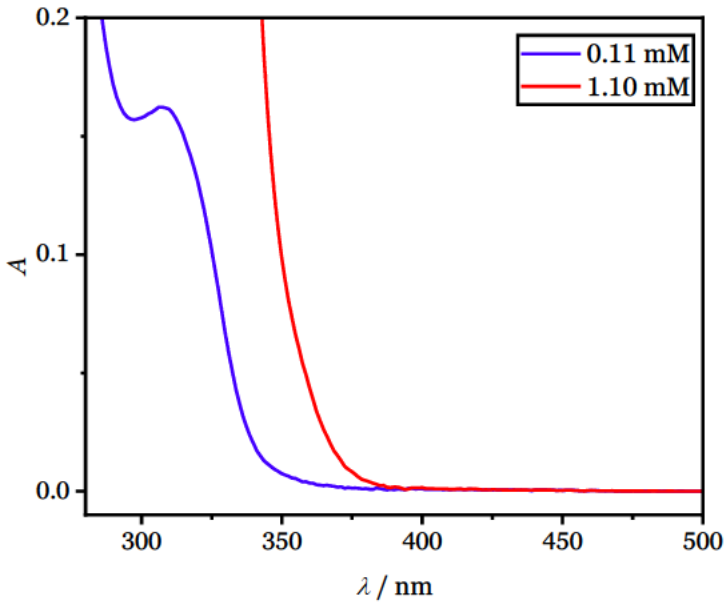

Figure 85: Concentration dependent UV-vis absorption spectrum of 3.16 in benzene at 1.10 ± 0.14 mM (red) and 0.11 ± 0.12 mM (blue).

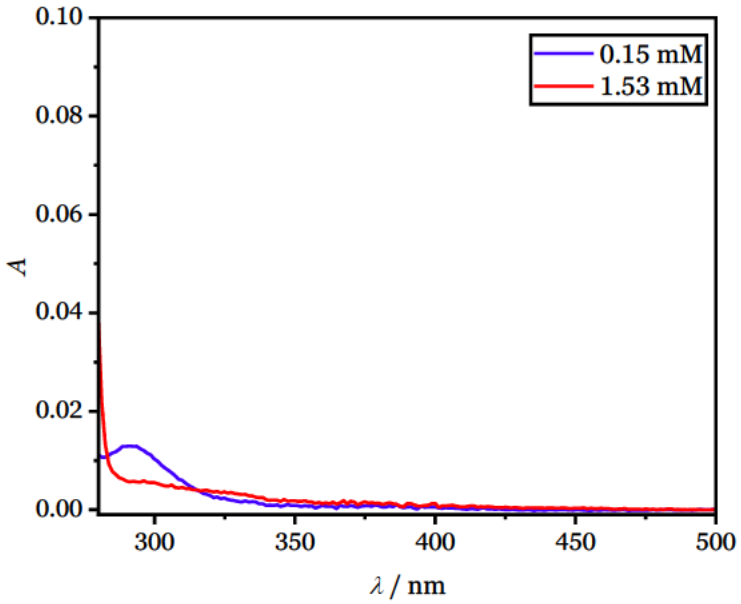

Figure 86: Concentration dependent UV-vis absorption spectrum of 3.26 in benzene at 1.53 ± 0.14 mM (red) and 0.15 ± 0.12 mM (blue).

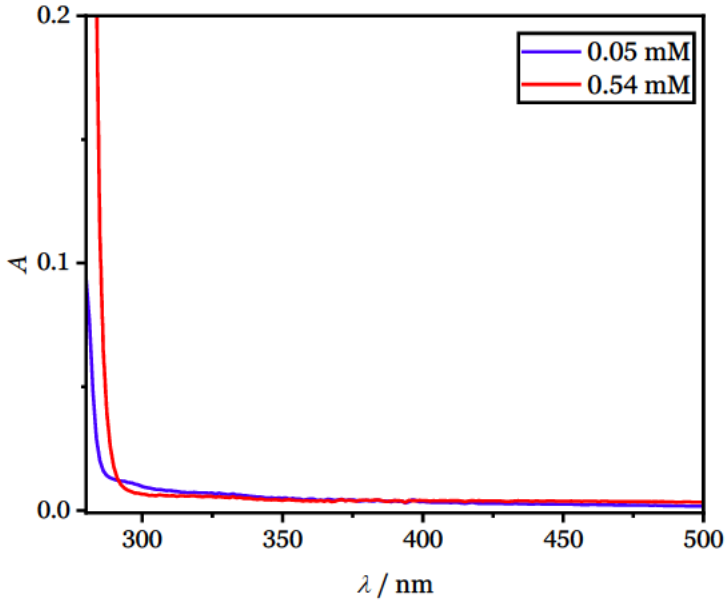

Figure 87: Concentration dependent UV-vis absorption spectrum of 3.29 in benzene at 0.54 ± 0.15 mM (red) and 0.05 ± 0.13 mM (blue).

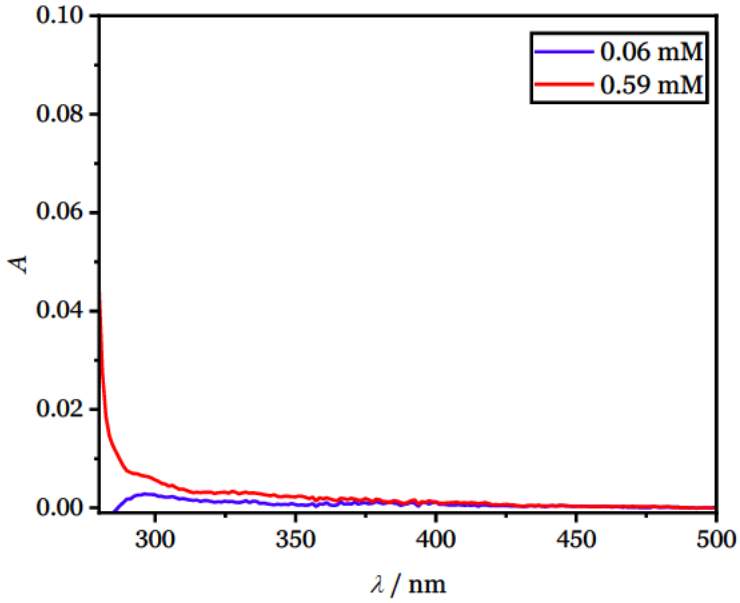

Figure 88: Concentration dependent UV-vis absorption spectrum of 3.53 in benzene at 0.59 ± 0.15 mM (red) and 0.06 ± 0.13 mM (blue).

References

[1] V. M. Canuto, J. S. Levine, T. R. Augustsson, C. L. Imhoff, M. S. Giampapa, *Nature* **1983**, *305*, 281–286.

[2] H. D. Roth, *Angew. Chem. Int. Ed.* **1989**, *28*, 1193–1207.

[3] J. S. Levine, P. B. Hays, J. C. Walker, *Icarus* **1979**, *39*, 295–309.

[4] H.-D. Scharf, J. Fleischhauer, H. Leismann, I. Ressler, W. Schleker, R. Weitz, *Angew. Chem. Int. Ed.* **1979**, *18*, 652–662.

[5] G. Ciamician, *Science* **1912**, *36*, 385–394.

[6] N. Armaroli, V. Balzani, *Angew. Chem. Int. Ed.* **2007**, *46*, 52–66.

[7] S. Berardi, S. Drouet, L. Francàs, C. Gimbert-Suriñach, M. Guttentag, C. Richmond, T. Stoll, A. Llobet, *Chem. Soc. Rev.* **2014**, *43*, 7501–7519.

[8] H. C. Kolb, M. G. Finn, K. B. Sharpless, *Angew. Chem. Int. Ed.* **2001**, *40*, 2004–2021.

[9] a) C. H. U. Gregson, A. Noble, V. K. Aggarwal, *Angew. Chem.* **2021**, *133*, 7436–7441; b) A. Fawcett, A. Murtaza, C. H. U. Gregson, V. K. Aggarwal, *J. Am. Chem. Soc.* **2019**, *141*, 4573–4578; c) R. I. Rodríguez, V. Corti, L. Rizzo, S. Visentini, M. Bortolus, A. Amati, M. Natali, G. Pelosi, P. Costa, L. Dell'Amico, *Nat. Catal,* **2024.** https://doi.org/10.1038/s41929-024-01206-4; d) A. Fawcett, T. Biberger, V. K. Aggarwal, *Nat. Chem.* **2019**, *11*, 117–122; e) S. M. Anthony, L. G. Wonilowicz, M. S. McVeigh, N. K. Garg, *JACS Au* **2021**, *1*, 897–912.

[10] a) J. Turkowska, J. Durka, D. Gryko, *Chem. Commun.* **2020**, *56*, 5718–5734; b) W. Huang, S. Keess, G. A. Molander, *J. Am. Chem. Soc* **2022**, *144*, 12961–12969; c) J. M. Lopchuk, K. Fjelbye, Y. Kawamata, L. R. Malins, C.-M. Pan, R. Gianatassio, J. Wang, L. Prieto, J. Bradow, T. A. Brandt, M. R. Collins, J. Elleraas, J. Ewanicki, W. Farrell, O. O. Fadeyi, G. M. Gallego, J. J. Mousseau, R. Oliver, N. W. Sach, J. K. Smith, J. E. Spangler, H. Zhu, J. Zhu, P. S. Baran, *J. Am. Chem. Soc* **2017**, *139*, 3209–3226; d) R. Gianatassio, J. M. Lopchuk, J. Wang, C.-M. Pan, L. R. Malins, L. Prieto, T. A. Brandt, M. R. Collins, G. M. Gallego, N. W. Sach, J. E. Spangler, H. Zhu, J. Zhu, P. S. Baran, *Science* **2016**, *351*, 241–246.

[11] A. Baeyer, *Ber. Dtsch. Chem. Ges.* **1885**, *18*, 2269–2281.

[12] K. B. Wiberg, *Angew. Chem. Int. Ed.* **1986**, *25*, 312–322.

[13] K. B. Wiberg, *Acc. Chem. Res.* **1984**, *17*, 379–386.

[14] a) T. Dudev, C. Lim, *J. Am. Chem. Soc* **1998**, *120*, 4450–4458; b) P. R. Khoury, J. D. Goddard, W. Tam, *Tetrahedron* **2004**, *60*, 8103–8112.

[15] A. Brandi, S. Cicchi, F. M. Cordero, *Chem. Rev.* **2008**, *108*, 3988–4035.

[16] A. Luque, J. Paternoga, T. Opatz, *Chem. Eur. J.* **2021**, *27*, 4500–4516.

[17] P. Kaszynski, J. Michl, *J. Am. Chem. Soc* **1988**, *110*, 5225–5226.

[18] C. J. M. Stirling, *Pure Appl. Chem.* **1984**, *56*, 1781–1796.

[19] a) J. A. Bull, R. A. Croft, O. A. Davis, R. Doran, K. F. Morgan, *Chem. Rev.* **2016**, *116*, 12150–12233; b) J. A. Moore, R. S. Ayers in *Chemistry of Heterocyclic Compounds*, *Chemistry of Heterocyclic Compounds: A Series Of Monographs*; (Ed. A. Hassner), Wiley, **1983**, pp. 1–217; c) M. Murakami, N. Ishida, *Chem. Rev.* **2021**, *121*, 264–299.

[20] a) A. Sella, H. Basch, S. Hoz, *J. Am. Chem. Soc* **1996**, *118*, 416–420; b) D. Sawicka, S. Wilsey, K. N. Houk, *J. Am. Chem. Soc* **1999**, *121*, 864–865; c) K. B. Wiberg, *J. Am. Chem. Soc* **1983**, *105*, 1227–1233.

[21] A. J. Sterling, R. C. Smith, E. A. Anderson, F. Duarte, *J. Org. Chem.* **2024**, *89*, 9979–9989.

[22] H. Wang, Y.-M. Tian, B. König, *Nat. Rev. Chem.* **2022**, *6*, 745–755.

[23] M. A. M. Subbaiah, N. A. Meanwell, *J. Med. Chem.* **2021**, *64*, 14046–14128.

[24] K. B. Wiberg, F. H. Walker, *J. Am. Chem. Soc* **1982**, *104*, 5239–5240.

[25] J. Belzner, U. Bunz, K. Semmler, G. Szeimies, K. Opitz, A.-D. Schlüter, *Chem. Ber.* **1989**, *122*, 397–398.

[26] J. D. Daniel Rehm, B. Ziemer, G. Szeimies, *Justus Liebigs Ann. Chem.* **1999**, *1999*, 2079–2085.

[27] P. Bellotti, F. Glorius, *J. Am. Chem. Soc* **2023**, *145*, 20716–20732.

[28] N. Ishida, S. Sawano, M. Murakami, *Nat. Commun.* **2014**, *5*, 3111.

[29] B. M. Trost, *Science* **1991**, *254*, 1471–1477.

[30] A. Sandvoß, J. M. Wahl, *Org. Lett.* **2023**, *25*, 5795–5799.

[31] S. Poplata, A. Tröster, Y.-Q. Zou, T. Bach, *Chem. Rev.* **2016**, *116*, 9748–9815.

[32] a) D. M. Flores, V. A. Schmidt, *J. Am. Chem. Soc* **2019**, *141*, 8741–8745; b) D. R. Arnold, R. L. Hinman, A. H. Glick, *Tetrahedron Lett.* **1964**, *5*, 1425–1430.

[33] N. C. Yang, D.-D. H. Yang, *J. Am. Chem. Soc* **1958**, *80*, 2913–2914.

[34] E. H. Gold, *J. Am. Chem. Soc* **1971**, *93*, 2793–2795.

[35] a) P. J. Wagner, *Acc. Chem. Res.* **1971**, *4*, 168–177; b) P. J. Wagner, *Top. Curr. Chem.* **1976**, 1–52.

[36] A. G. Griesbeck, A. Henz, W. Kramer, P. Wamser, K. Peters, E.-M. Peters, *Tetrahedron Lett.* **1998**, *39*, 1549–1552.

[37] H.-G. Henning, *Z. Chem.* **1982**, *22*, 77–86.

[38] R. Pedrosa, C. Andrés, J. Nieto, S. Del Pozo, *J. Org. Chem.* **2005**, *70*, 1408–1416.

[39] H.-G. Henning, J. Fuhrmann, U. Krippendorf, *Z. Chem.* **1981**, *21*, 36.

[40] a) S. V. Evans, M. Garcia-Garibay, N. Omkaram, J. R. Scheffer, J. Trotter, F. Wireko, *J. Am. Chem. Soc* **1986**, *108*, 5648–5650; b) H. Aoyama, K.-I. Miyazaki, M. Sakamoto, Y. Omote, *Tetrahedron* **1987**, *43*, 1513–1518.

[41] J. Fuhrmann, M. Haupt, H.-G. Henning, *J. Prakt. Chem.* **1984**, *326*, 177–186.

[42] H. Ihmels, J. R. Scheffer, *Tetrahedron* **1999**, *55*, 885–907.

[43] A. G. Griesbeck, H. Heckroth, *J. Am. Chem. Soc* **2002**, *124*, 396–403.

[44] F. Toda, K. Tanaka, O. Kakinoki, T. Kawakami, *J. Org. Chem.* **1993**, *58*, 3783–3784.

[45] J. N. Gamlin, R. Jones, M. Leibovitch, B. Patrick, J. R. Scheffer, J. Trotter, *Acc. Chem. Res.* **1996**, *29*, 203–209.

[46] N. Ishida, Y. Shimamoto, M. Murakami, *Angew. Chem. Int. Ed.* **2012**, *51*, 11750–11752.

[47] M. Ruggeri, A. W. Dombrowski, S. W. Djuric, I. R. Baxendale, *J. Org. Chem.* **2020**, *85*, 7276–7286.

[48] P. Wessig in *CRC handbook of organic photochemistry and photobiology*; (Ed. W. M. Horspool), CRC Press, Boca Raton, Fla, **2004**, 57-1–57-20.

[49] a) R. A. Croft, J. J. Mousseau, C. Choi, J. A. Bull, *Chem. Eur. J.* **2016**, *22*, 16271–16276; b) S. Ahmad, M. Yousaf, A. Mansha, N. Rasool, A. F. Zahoor, F. Hafeez, S. M. A. Rizvi, *Synth. Commun.* **2016**, *46*, 1397–1416; c) J. Anaya, R. M. Sánchez in , *Progress in Heterocyclic Chemistry*, Elsevier, **2017**, pp. 115–145.

[50] a) J. Xiao, S. W. Wright, *Tetrahedron Lett.* **2013**, *54*, 2502–2505; b) H. Mughal, M. Szostak, *Org. Biomol. Chem.* **2021**, *19*, 3274–3286.

[51] N. Cramer, T. Seiser, *Synlett* **2011**, *2011*, 449–460.

[52] R. Crossley, *Tetrahedron* **1992**, *48*, 8155–8178.

[53] a) C. Nájera, F. Foubelo, J. M. Sansano, M. Yus, *Tetrahedron* **2022**, *106-107*, 132629; b) M. C. Willis, *J. Chem. Soc, Perkin Trans. 1* **1999**, 1765–1784; c) M. Wang, M. Feng, B. Tang, X. Jiang, *Tetrahedron Lett.* **2014**, *55*, 7147–7155; d) K. S. Petersen, *Tetrahedron Lett.* **2015**, *56*, 6523–6535; e) X.-P. Zeng, Z.-Y. Cao, Y.-H. Wang, F. Zhou, J. Zhou, *Chem. Rev.* **2016**, *116*, 7330–7396; f) A. Borissov, T. Q. Davies, S. R. Ellis, T. A. Fleming, M. S. W. Richardson, D. J. Dixon, *Chem. Soc. Rev.* **2016**, *45*, 5474–5540; g) J. Merad, M. Candy, J.-M. Pons, C. Bressy, *Synthesis* **2017**, *49*, 1938–1954.

[54] R. N. Loy, E. N. Jacobsen, *J. Am. Chem. Soc* **2009**, *131*, 2786–2787.

[55] R. Zhang, W. Guo, M. Duan, K. N. Houk, J. Sun, *Angew. Chem. Int. Ed.* **2019**, *58*, 18055–18060.

[56] a) W. Yang, J. Sun, *Angew. Chem. Int. Ed.* **2016**, *55*, 1868–1871; b) H. Huang, W. Yang, Z. Chen, Z. Lai, J. Sun, *Chem. Sci.* **2019**, *10*, 9586–9590; c) X. Zou, G. Sun, H. Huang, J. Wang, W. Yang, J. Sun, *Org. Lett.* **2020**, *22*, 249–252.

[57] Z. Wang, Z. Chen, J. Sun, *Angew. Chem. Int. Ed.* **2013**, *52*, 6685–6688.

[58] R. Zhang, M. Sun, Q. Yan, X. Lin, X. Li, X. Fang, H. H. Y. Sung, I. D. Williams, J. Sun, *Org. Lett.* **2022**, *24*, 2359–2364.

[59] W. Yang, Z. Wang, J. Sun, *Angew. Chem. Int. Ed.* **2016**, *55*, 6954–6958.

[60] a) T. Zhang, H. Zhuang, L. Tang, Z. Han, W. Guo, H. Huang, J. Sun, *Org. Lett.* **2022**, *24*, 207–212; b) H. Huang, T. Zhang, J. Sun, *Angew. Chem. Int. Ed.* **2021**, *60*, 2668–2673; c) M. Mizuno, M. Kanai, A. Iida, K. Tomioka, *Tetrahedron* **1997**, *53*, 10699–10708; d) M. Mizuno, M. Kanai, A. Iida, K. Tomioka, *Tetrahedron: Asymmetry* **1996**, *7*, 2483–2484; e) M. Yamaguchi, Y. Nobayashi, I. Hirao, *Tetrahedron* **1984**, *40*, 4261–4266; f) M. Yamaguchi, Y. Nobayashi, I. Hirao, *Tetrahedron Lett.* **1983**, *24*, 5121–5122.

[61] a) A. Jeziorna, B. Krawiecka, *Tetrahedron: Asymmetry* **2005**, *16*, 1577–1581; b) Y. Hata, M. Watanabe, *Tetrahedron* **1987**, *43*, 3881–3888.

[62] M. Raulin, B. Drouillat, J. Marrot, F. Couty, K. Wright, *Tetrahedron Lett.* **2022**, *94*, 153710.

[63] a) Z. Li, Y. Wang, D. Liu, L. Ning, M. Pu, L. Lin, X. Feng, *Org. Lett.* **2023**, *25*, 7612–7616; b) G. Masson, D. Gomez Pardo, J. Cossy, *Chirality* **2021**, *33*, 5–21.

[64] Z. Wang, F. K. Sheong, H. H. Y. Sung, I. D. Williams, Z. Lin, J. Sun, *J. Am. Chem. Soc.* **2015**, *137*, 5895–5898.

[65] D. Qian, M. Chen, A. C. Bissember, J. Sun, *Angew. Chem. Int. Ed.* **2018**, *57*, 3763–3766.

[66] M. Murakami, N. Ishida, *J. Am. Chem. Soc* **2016**, *138*, 13759–13769.

[67] T. Matsuda in *Cleavage of Carbon-Carbon Single Bonds by Transition Metals*; (Eds. M. Murakami, M. Murakami), Wiley, **2015**, pp. 89–118.

[68] a) S. Matsumura, Y. Maeda, T. Nishimura, S. Uemura, *J. Am. Chem. Soc* **2003**, *125*, 8862–8869; b) T. Nishimura, S. Matsumura, Y. Maeda, S. Uemura, *Chem. Commun.* **2002**, 50–51; c) T. Nishimura, S. Uemura, *J. Am. Chem. Soc* **1999**, *121*, 11010–11011.

[69] N. Ishida, S. Sawano, Y. Masuda, M. Murakami, *J. Am. Chem. Soc.* **2012**, *134*, 17502–17504.

[70] A. F. Abdel-Magid, K. G. Carson, B. D. Harris, C. A. Maryanoff, R. D. Shah, *J. Org. Chem.* **1996**, *61*, 3849–3862.

[71] E. F. DiMauro, M. C. Kozlowski, *Org. Lett.* **2001**, *3*, 1641–1644.

[72] H. Sasaki, R. Irie, T. Hamada, K. Suzuki, T. Katsuki, *Tetrahedron* **1994**, *50*, 11827–11838.

[73] K. Ebisawa, K. Izumi, Y. Ooka, H. Kato, S. Kanazawa, S. Komatsu, E. Nishi, H. Shigehisa, *J. Am. Chem. Soc* **2020**, *142*, 13481–13490.

[74] M. Ruggeri, A. W. Dombrowski, S. W. Djuric, I. R. Baxendale, *ChemPhotoChem* **2019**, *3*, 1212–1218.

[75] a) Sigma-Aldrich, "Acetonitrile-d3". to be found under https://www.sigmaaldrich.com/DE/en/product/aldrich/151807 (accessed Apr 27, 2024); b) Sigma-Aldrich, "N,N-Dimethylformamid-d7". to be found under https://www.sigmaaldrich.com/DE/en/product/aldrich/189979 (accessed Jul 27, 2024).

[76] E. V. Anslyn, D. A. Dougherty, *Modern physical organic chemistry;* University Science Books, Mill Valley, California, **2006.**

[77] K. L. Allworth, A. A. El-Hamamy, M. M. Hesabi, J. Hill, *J. Chem. Soc, Perkin Trans. 1* **1980**, 1671.

[78] F. D. Lewis, N. J. Turro, *J. Am. Chem. Soc* **1970**, *92*, 311–320.

[79] a) L.-Z. Sun, J.-B. Xie, *Synlett* **2023**, *34*, 14–22; b) M. M. Claffey, C. J. Helal, P. R. Verhoest, Z. Kang, K. S. Fors, S. Jung, J. Zhong, M. W. Bundesmann, X. Hou, S. Lui, R. J. Kleiman, M. Vanase-Frawley, A. W. Schmidt, F. Menniti, C. J. Schmidt, W. E. Hoffman, M. Hajos, L. McDowell, R. E. O'Connor, M. Macdougall-Murphy, K. R. Fonseca, S. L. Becker, F. R. Nelson, S.

Liras, *J. Med. Chem.* **2012**, *55*, 9055–9068; c) V. Krishna Reddy, H. Ramamohan, A. Ganesh, K. Srinivas, K. Mukkanti, G. Madhusudhan, *Asian J. Chem.* **2012**, *24*, 3468–3472.

[80] R. G. Laughlin, *J. Am. Chem. Soc* **1967**, *89*, 4268–4271.

[81] a) R. Blaauw, I. E. Kingma, J. H. Laan, J. L. van der Baan, S. Balt, M. W. G. de Bolster, G. W. Klumpp, W. J. J. Smeets, A. L. Spek, *J. Chem. Soc, Perkin Trans. 1* **2000**, 1199–1210; b) J. M. Ready, E. N. Jacobsen, *J. Am. Chem. Soc* **1999**, *121*, 6086–6087.

[82] H. Maag, D. J. Lemcke, J. M. Wahl, *Beilstein J. Org. Chem.* **2024**, *20*, 1671–1676.

[83] A. Sandvoß, H. Maag, C. G. Daniliuc, D. Schollmeyer, J. M. Wahl, *Chem. Sci.* **2022**, *13*, 6297–6302.

[84] A. K. Yudin, *Chem. Sci.* **2020**, *11*, 12423–12427.

[85] F. Weigert, *Eder's Jahrbuch* **1909**, *23*, 122–127.

[86] a) J. Fritzsche, *J. Prakt. Chem.* **1866**, *97*, 30–37; b) J. Fritzsche, *J. Prakt. Chem.* **1869**, *106*, 274–293.

[87] a) R. Luther, F. Weigert, *Z. Phys. Chem.* **1905**, *51U*, 297–328; b) R. Luther, F. Weigert, *Z. Phys. Chem.* **1905**, *53U*, 385–427.

[88] Z. Yoshida, *J. Photochem.* **1985**, *29*, 27–40.

[89] a) Z. Wang, P. Erhart, T. Li, Z.-Y. Zhang, D. Sampedro, Z. Hu, H. A. Wegner, O. Brummel, J. Libuda, M. B. Nielsen, K. Moth-Poulsen, *Joule* **2021**, *5*, 3116–3136; b) V. A. Bren', A. D. Dubonosov, V. I. Minkin, V. A. Chernoivanov, *Russian Chemical Reviews* **1991**, *60*, 451–469.

[90] a) C. Philippopoulos, J. Marangozis, *Ind. Eng. Chem. Prod. Res. Dev.* **1984**, *23*, 458–466; b) K. Börjesson, A. Lennartson, K. Moth-Poulsen, *ACS Sustainable Chem. Eng.* **2013**, *1*, 585–590.

[91] I. Gur, K. Sawyer, R. Prasher, *Science* **2012**, *335*, 1454–1455.

[92] S. J. Cristol, R. L. Snell, *J. Am. Chem. Soc* **1958**, *80*, 1950–1952.

[93] a) X. An, Y. Xie, *Thermochim. Acta* **1993**, *220*, 17–25; b) A. Gimenez-Gomez, B. Rollins, A. Steele, H. Hölzel, N. Baggi, K. Moth-Poulsen, I. Funes-Ardoiz, D. Sampedro, *Chem. Eur. J.* **2024**, *30*, e202303230.

[94] W. G. Dauben, R. L. Cargill, *Tetrahedron* **1961**, *15*, 197–201.

[95] Y. Harel, A. W. Adamson, C. Kutal, P. A. Grutsch, K. Yasufuku, *J. Phys. Chem.* **1987**, *91*, 901–904.

[96] A. D. Dubonosov, V. A. Bren, V. A. Chernoivanov, *Russian Chemical Reviews* **2002**, *71*, 917–927.

[97] B. Zhang, Y. Feng, W. Feng, *Nano Micro Lett.* **2022**, *14*, 138.

[98] Z. Wang, R. Losantos, D. Sampedro, M. Morikawa, K. Börjesson, N. Kimizuka, K. Moth-Poulsen, *J. Mater. Chem. A* **2019**, *7*, 15042–15047.

[99] A. Kunz, A. H. Heindl, A. Dreos, Z. Wang, K. Moth-Poulsen, J. Becker, H. A. Wegner, *ChemPlusChem* **2019**, *84*, 1145–1148.

[100] M. A. Strauss, H. A. Wegner, *Angew. Chem. Int. Ed.* **2019**, *58*, 18552–18556.

[101] V. Gray, A. Lennartson, P. Ratanalert, K. Börjesson, K. Moth-Poulsen, *Chem. Commun.* **2014**, *50*, 5330–5332.

[102] a) D. Bléger, S. Hecht, *Angew. Chem. Int. Ed.* **2015**, *54*, 11338–11349; b) A. Goulet-Hanssens, T. C. Corkery, A. Priimagi, C. J. Barrett, *J. Mater. Chem. C* **2014**, *2*, 7505–7512.

[103] M. J. Kuisma, A. M. Lundin, K. Moth-Poulsen, P. Hyldgaard, P. Erhart, *J. Phys. Chem. C* **2016**, *120*, 3635–3645.

[104] M. Mansø, A. U. Petersen, Z. Wang, P. Erhart, M. B. Nielsen, K. Moth-Poulsen, *Nat. Commun.* **2018**, *9*, 1945.

[105] S. P. Jeong, L. A. Renna, C. J. Boyle, H. S. Kwak, E. Harder, W. Damm, D. Venkataraman, *Sci. Rep.* **2017**, *7*, 17773.

[106] M. D. Kilde, M. Mansø, N. Ree, A. U. Petersen, K. Moth-Poulsen, K. V. Mikkelsen, M. B. Nielsen, *Org. Biomol. Chem.* **2019**, *17*, 7735–7746.

[107] K. Masutani, M. Morikawa, N. Kimizuka, *Chem. Commun.* **2014**, *50*, 15803–15806.

[108] A. Dreos, Z. Wang, J. Udmark, A. Ström, P. Erhart, K. Börjesson, M. B. Nielsen, K. Moth-Poulsen, *Adv. Energy Mater.* **2018**, *8*.

[109] Z. Wang, A. Roffey, R. Losantos, A. Lennartson, M. Jevric, A. U. Petersen, M. Quant, A. Dreos, X. Wen, D. Sampedro, K. Börjesson, K. Moth-Poulsen, *Energy Environ. Sci.* **2019**, *12*, 187–193.

[110] a) S. Miki, T. Maruyama, T. Ohno, T. Tohma, S. Toyama, Z. Yoshida, *Chem. Lett.* **1988**, *17*, 861–864; b) S. Miki, Y. Asako, M. Morimoto, T. Ohno, Z. Yoshida, T. Maruyama, M. Fukuoka, T. Takada, *BCSJ* **1988**, *61*, 973–981.

[111] A. Dreos, K. Börjesson, Z. Wang, A. Roffey, Z. Norwood, D. Kushnir, K. Moth-Poulsen, *Energy Environ. Sci.* **2017**, *10*, 728–734.

[112] P. J. Wagner, A. E. Kemppainen, H. N. Schott, *J. Am. Chem. Soc.* **1973**, *95*, 5604–5614.

[113] J. M. Chong, E. K. Mar, *J. Org. Chem.* **1991**, *56*, 893–896.

[114] Q. Yang, L.-L. Mao, B. Yang, S.-D. Yang, *Org. Lett.* **2014**, *16*, 3460–3463.

[115] a) G. Surya Prakash, J. Hu, G. A. Olah, *J. Fluorine Chem.* **2001**, *112*, 355–360; b) H. Amii, T. Kobayashi, Y. Hatamoto, K. Uneyama, *Chem. Commun.* **1999**, 1323–1324.

[116] Y. Liang, R. Kleinmans, C. G. Daniliuc, F. Glorius, *J. Am. Chem. Soc.* **2022**, *144*, 20207–20213.

[117] L. Pitzer, F. Schäfers, F. Glorius, *Angew. Chem. Int. Ed.* **2019**, *58*, 8572–8576.

[118] T. Sato, Y. Hamada, M. Sumikawa, S. Araki, H. Yamamoto, *Ind. Eng. Chem. Res.* **2014**, *53*, 19331–19337.

[119] a) P. G. Sammes, *Tetrahedron* **1976**, *32*, 405–422; b) P. Klán, J. Wirz, A. Gudmundsdottir in *CRC Handbook of Organic Photochemistry and Photobiology, Third Edition - Two Volume Set*; (Eds. A. Griesbeck, M. Oelgemöller, F. Ghetti), CRC Press, **2012**, pp. 627–652.

[120] a) R. Haag, J. Wirz, P. J. Wagner, *HCA* **1977**, *60*, 2595–2607; b) R. D. Small, JR, J. C. Scaiano, *J. Am. Chem. Soc* **1977**, *99*, 7713–7714.

[121] P. J. Wagner, D. Subrahmanyam, B. S. Park, *J. Am. Chem. Soc* **1991**, *113*, 709–710.

[122] R. B. Woodward, R. Hoffmann, *J. Am. Chem. Soc* **1965**, *87*, 395–397.

[123] N. C. Yang, C. Rivas, *J. Am. Chem. Soc* **1961**, *83*, 2213.

[124] L. Dell'Amico, A. Vega-Peñaloza, S. Cuadros, P. Melchiorre, *Angew. Chem. Int. Ed.* **2016**, *55*, 3313–3317.

[125] J. Y. J. Wang, M. T. Blyth, M. S. Sherburn, M. L. Coote, *J. Am. Chem. Soc* **2022**, *144*, 1023–1033.

[126] H. Lutz, E. Bréhéret, L. Lindqvist, *J. Chem. Soc, Faraday Trans. 1* **1973**, *69*, 2096.

[127] R. W. Redmond, J. C. Scaiano, *J. Phys. Chem.* **1989**, *93*, 5347–5349.

[128] E. D. Mihelich, D. J. Eickhoff, *J. Org. Chem.* **1983**, *48*, 4135–4137.

[129] a) B. J. Arnold, P. G. Sammes, T. W. Wallace, *J. Chem. Soc, Perkin Trans. 1* **1974**, 415; b) K. Iida, K. Komada, M. Saito, M. Yoshioka, *J. Org. Chem.* **1999**, *64*, 7407–7411.

[130] a) M. P. Cava, K. Muth, *J. Am. Chem. Soc* **1960**, *82*, 652–654; b) W. Choy, H. Yang, *J. Org. Chem.* **1988**, *53*, 5796–5798.

[131] A. Delgado, J. Clardy, *Tetrahedron Lett.* **1992**, *33*, 2789–2790.

[132] I. Kaljurand, R. Lilleorg, A. Murumaa, M. Mishima, P. Burk, I. Koppel, I. A. Koppel, I. Leito, *J. Phys. Org. Chem.* **2013**, *26*, 171–181.

[133] M. K. Kiesewetter, M. D. Scholten, N. Kirn, R. L. Weber, J. L. Hedrick, R. M. Waymouth, *J. Org. Chem.* **2009**, *74*, 9490–9496.

[134] J. Orrego-Hernández, A. Dreos, K. Moth-Poulsen, *Acc. Chem. Res.* **2020**, *53*, 1478–1487.

[135] a) O. Faye, J. Szpunar, U. Eduok, *Int. J. Hydrogen Energy* **2022**, *47*, 13771–13802; b) A. M. Abdalla, S. Hossain, O. B. Nisfindy, A. T. Azad, M. Dawood, A. K. Azad, *Energy Convers. Manage.* **2018**, *165*, 602–627.

[136] I. Hadjipaschalis, A. Poullikkas, V. Efthimiou, *Renewable Sustainable Energy Rev.* **2009**, *13*, 1513–1522.

[137] D. A. Strubbe, J. C. Grossman, *J. Phys. Condens. Matter.* **2019**, *31*, 34002.

[138] A. U. Petersen, A. I. Hofmann, M. Fillols, M. Mansø, M. Jevric, Z. Wang, C. J. Sumby, C. Müller, K. Moth-Poulsen, *Adv. Sci.* **2019**, *6*, 1900367.

[139] C. P. Rosenau, B. J. Jelier, A. D. Gossert, A. Togni, *Angew. Chem. Int. Ed.* **2018**, *57*, 9528–9533.

[140] *X-RED and X-AREA*; Stoe & Cie, Darmstadt, Germany, **2019.**

[141] G. M. Sheldrick, *Acta. Cryst.* **2015**, *A71*, 3–8.

[142] G. M. Sheldrick, *Acta. Cryst.* **2015**, *C71*, 3–8.

[143] A. L. Spek, *Acta. Cryst.* **2009**, *D65*, 148–155.

[144] Luzchem, "Luzchem Exposure Standards". to be found under https://luzchem.com/pages/exposure-standards (accessed Aug 3, 2024).

[145] Kessil, "PR160L-370nm Gen 2". to be found under https://kessil.com/products/science_PR160L.php (accessed Jun 25, 2024).

[146] a) B. L. Dick, S. M. Cohen, *Inorg. Chem.* **2018**, *57*, 9538–9543; b) R. A. Croft, M. A. J. Dubois, A. J. Boddy, C. Denis, A. Lazaridou, A. S. Voisin-Chiret, R. Bureau, C. Choi, J. J. Mousseau, J. A. Bull, *Justus Liebigs Ann. Chem.* **2019**, *2019*, 5385–5395; c) M. Haerter, H. Beck, P. Ellinghaus, K. Berhoerster, S. Greschat, K. H. Thierauch, F. Suessmeier. HETEROAROMATIC COMPOUNDS FOR USE AS HIF INHIBITORS. US2011301122 (A1), December 8, 2011.

[147] A. Saxena, N. Ghosh, *J. Org. Chem.* **2023**, *88*, 300–309.

[148] W. Chen, H. Xu, R. Wu, Y. Chen, P. Yu, Y. Jin, *Org. Biomol. Chem.* **2023**, *21*, 5547–5552.

[149] S. J. Heffernan, J. M. Beddoes, M. F. Mahon, A. J. Hennessy, D. R. Carbery, *Chem. Commun.* **2013**, *49*, 2314–2316.

[150] F. Bai, N. Wang, Y. Bai, X. Ma, C. Gu, B. Dai, J. Chen, *J. Org. Chem.* **2023**, *88*, 2985–2998.

[151] J. Fuhrmann, H. Haber, M. Haupt, H.-G. Henning, *J. Prakt. Chem.* **1982**, *324*, 1055–1059.

[152] S. Lachhein, K. Dehmer. Process for the preparation of N-alkyl sulfonamides. EP0504873 (A1), September 23, 1992.

[153] D. C. Johnson, T. S. Widlanski, *J. Org. Chem.* **2003**, *68*, 5300–5309.

[154] L. Andna, L. Miesch, *Org. Biomol. Chem.* **2019**, *17*, 5688–5692.

[155] J. K. Laha, P. Gupta, A. Hazra, *Beilstein J. Org. Chem.* **2023**, *19*, 771–777.

[156] W. Li, Y. Duan, M. Zhang, J. Cheng, C. Zhu, *Chem. Commun.* **2016**, *52*, 7596–7599.

[157] M. R. Bodireddy, R. S. Mahla, P. M. Khaja Mohinuddin, G. T. Reddy, D. V. Raghava Prasad, H. Kumar, N. C. G. Reddy, *RSC Adv.* **2016**, *6*, 75651–75663.

[158] Y.-M. Chai, Q. Zou, Z.-X. Guo, Y.-J. Qin, P. Zhang, *Tetrahedron Lett.* **2023**, *122*, 154517.

[159] R. B. Mohan, N. C. G. Reddy, *Synth. Commun.* **2013**, *43*, 2603–2614.

[160] T. A. Schmidt, B. Ciszek, P. Kathe, I. Fleischer, *Chem. Eur. J.* **2020**, *26*, 3641–3646.

[161] M. Nigríni, V. A. Bhosale, I. Císařová, J. Veselý, *J. Org. Chem.* **2023**, *88*, 17024–17036.

[162] M. Ichinose, H. Suematsu, Y. Yasutomi, Y. Nishioka, T. Uchida, T. Katsuki, *Angew. Chem. Int. Ed.* **2011**, *50*, 9884–9887.

[163] S. Tai, T. S. Maskrey, P. R. Nyalapatla, P. Wipf, *Chirality* **2019**, *31*, 1014–1027.

[164] T. Honjo, R. J. Phipps, V. Rauniyar, F. D. Toste, *Angew. Chem. Int. Ed.* **2012**, *51*, 9684–9688.

[165] J. F. Larrow, E. N. Jacobsen, *Org. Synth.* **1998**, *75*, 1.

[166] a) D. D. Miller, J. Fowble, P. N. Patil, *J. Med. Chem.* **1973**, *16*, 177–178; b) N. Ishida, Y. Shimamoto, T. Yano, M. Murakami, *J. Am. Chem. Soc.* **2013**, *135*, 19103–19106.

[167] S. S. Chatterjee, A. Shoeb, *Synthesis* **1973**, 153–154.

[168] J. Wang, W.-G. Kong, F. Li, J. Liu, Q. Shen, L. Liu, W.-X. Zhao, *Org. Biomol. Chem.* **2015**, *13*, 5399–5406.

[169] L. C. Finney, L. J. Mitchell, C. J. Moody, *Green Chem.* **2018**, *20*, 2242–2249.

[170] X. Liu, L. Liu, T. Huang, J. Zhang, Z. Tang, C. Li, T. Chen, *Org. Lett.* **2021**, *23*, 4930–4934.

[171] A. Messara, A. Panossian, K. Mikami, G. Hanquet, F. R. Leroux, *Angew. Chem. Int. Ed.* **2023**, *62*, e202215899.

[172] J. Saadi, H. Yamamoto, *Chem. Eur. J.* **2013**, *19*, 3842–3845.

[173] a) M. J. Moran, M. Magrini, D. M. Walba, I. Aprahamian, *J. Am. Chem. Soc* **2018**, *140*, 13623–13627; b) L.-Q. Zheng, S. Yang, J. Lan, L. Gyr, G. Goubert, H. Qian, I. Aprahamian, R. Zenobi, *J. Am. Chem. Soc* **2019**, *141*, 17637–17645; c) M. Guentner, E. Uhl, P. Mayer, H. Dube, *Chem. Eur. J.* **2016**, *22*, 16433–16436; d) B. Maerz, S. Wiedbrauk, S. Oesterling, E. Samoylova, A. Nenov, P. Mayer, R. de Vivie-Riedle, W. Zinth, H. Dube, *Chem. Eur. J.* **2014**, *20*, 13984–13992; e) S. Wiedbrauk, B. Maerz, E. Samoylova, A. Reiner, F. Trommer, P. Mayer, W. Zinth, H. Dube, *J. Am. Chem. Soc* **2016**, *138*, 12219–12227.

[174] G. Meißner, M. Feist, T. Braun, E. Kemnitz, *J. Organomet. Chem.* **2017**, *847*, 234–241.

Declaration of academic integrity

I hereby confirm that this thesis, entitled *Build and release of molecular strain as a tool in organic synthesis* was prepared independently and no sources or aids other than the ones stated were used. All passages in my thesis for which other sources, including electronic media, have been used, be it direct quotes or content references, have been acknowledged as such and the sources cited. I assure, that any ideas taken over, verbatim or in spirit, have been clearly stated.

Place, Date

Henning Maag

Curriculum Vitae

Personal data

[redacted]

Education

[redacted]

[redacted]

[redacted]